Queen Mary
University of London

Investigating early events in HIV-1 replication: the role of envelope signalling and PAF1 restriction factor

Ana Guerrero Alonso

A thesis submitted in partial fulfillment of the requirements of the Degree of Doctor of Philosophy

2015

Centre for Immunology and Infectious Disease
The Blizard Institute
Barts and The London School of Medicine and Dentistry
Queen Mary, University of London

Abstract

To enter cells, HIV utilises the envelope (Env) protein to engage the CD4 receptor and a co-receptor, CXCR4 or CCR5. In addition to its role in HIV entry, the Env protein also triggers intracellular signalling events. Expression of the HIV-1 and HIV-2 Env gp41 cytoplasmic tails triggered a significant decrease in microtubule acetylation at the single cell level. Since microtubule stability is controlled by Rac1, the role of Rac1 in HIV-1 infection was investigated. Treatment of TZM-bl cells with a Rac1 inhibitor that blocks its upstream activators, Tiam1 and TrioN, inhibited HIV-1 NL4.3 (X4-tropic) but not HIV-1 BaL (R5-tropic) suggesting a role for these activators which is possibly, co-receptor dependent. Subsequently, an siRNA screen including 145 upstream regulators of Rac1, cdc42 and RhoA were investigated in their role in HIV-1 NL4.3 and HIV-1 BaL infection. As a result, 39 upstream regulators of Rho-GTPases were identified of which 5 proteins had effects on both HIV-1 BaL and HIV-1 NL4.3 infection which suggests a novel role of Rho-GTPase upstream regulators in HIV-1 infection. Early in infection, HIV-1 also encounters restriction factors such as RNA polymerase II-Associated Factor 1 (PAF1). The possible cytoplasmic or nuclear role of PAF1 in HIV-1 infection was investigated. Confocal imaging and cellular fractionation suggested that endogenous PAF1 is localised mostly in the nuclei but also in the cytoplasm. Overexpression of a murine PAF1 cytoplasm-localised mutant decreased HIV-1 infection similarly to wild-type overexpression. On the other hand, overexpression of a nuclear PAF1 construct decreased infection better than the wild-type. This suggests that PAF1 restricts HIV-1 via a nuclear function. In addition, infection time-course experiments revealed that HIV-1 counteracts the effect of PAF1 within 30 minutes of infection. Overall, the evidence presented, suggests that PAF1 has a nuclear mechanism and that its downregulation could take place in the cytoplasm.

Acknowledgments

Firstly, I'd like to give special thanks to Patricia Costa, Francesca Ammoscato and Aneta Kucik for their support and for our friendship during these hard four years. I couldn't have made it without you and I'll never forget it. I'd like to thank Deseada Camuesco, Nidia Oliveira, Ainhoa Lucia and Julieta Díaz-Delfín for their encouragement, their example and for their beautiful smiles during these years, I learnt so much from you guys and I feel gifted! I would also like to thank all the people I met at the Blizard for their support and laughs we shared, especially to Paolo Giuffrida, Margarida Rei, Renata Curciarello, Paolo Biancheri, Supatra Marsh, Filipe Almeida, Vera Cabeços, Capucine Grandjean, Tania Garcia, Dario Ceric, Simona Mazza, Valentina DiFoggia, Silvia Dibenedetto, Barbara Ricci and Dan Pennington. I'd like to thank Marjolein Snippe for her friendship, for her useful input in the FRET experiments and for counting with me for co-organising the All on Board science sessions, I really enjoyed them, thanks! I'd also like to thank Martha Wildemann for teaming up with me in the organization of the All on Board science sessions, many thanks! I'd like to thank Aysegul Tosun for her contribution to my thesis and her great enthusiasm in the lab! I'd like to thank Alex Poll, Marie Marsden and Ben Hockman for their support and love during these and previous years. I'd like to thank Alexander Ashall-Kelly and the Ashall-Kelly's for making me feel at home during my UK years, I'll never forget it! I'd like to thank my friends from home: Berto Arranz, Marta Hernández, Belén Jorquera, Sergio Castro, Jorge Ruiz, Rodri González, Laura Ruiz, Ana Alonso, Blanca Gil, Edu Pardo, Virginia Murialdo, Jesús Ruiz, Enrique Sánchez Bautista, Carlos Gómez and César García for showing me during years that distance does not matter. Many thanks to my girls, Irene Solís and Sara Nieto Fernández, for all the love and strength during this process. I'd like to thank my Lola for her company during the long nights in which I wrote this thesis and for her unconditional love.

Thank you too to the Samba da Rua family for the strength and love during the writing of this thesis!

I'd also like to thank Áine McKnight for the supervision of my PhD. I'd like to thank Professor Denise Sheer for kindly accepting to be my second PhD supervisor. I'd like to thank Kelly Marno for all of her help in the lab and in the writing of my PhD thesis. I'm very grateful too for William Ogunkolade's help in the lab. I'd also like to thank Paul Allen for his support during these tough years. I'd like to thank the BALM facility staff including Ann Wheeler, Isma Ali and Amanda Wilson for always ensuring the microscopes were ready for my experiments and for my questions. Similarly, I'd like to thank Gary Warnes for guiding me through the use of the flow cytometers and for his useful input. I'd like to thank Corina Pade and Hanna Dreja for their help at the start of my PhD. I would like to thank Cleo Bishop for all of her help during the siRNA screen. I would like to thank Eithne O'Sullivan for providing me the reagents I required and for taking care of my health and safety in the lab. I'd like to thank Jaya Rajamanie and Mary Martins for their help in the office and also the Blizard Institute's lab managers Jeff Maskell and Chris Pelling.

Bizitzari eskertu nahi diot Asier Jaio oparitu izana. Zu gabe, hau ez litzateke posible izango, mila esker, maite zaitut.

Me gustaría agradecerle y dedicarle esta tesis a mi familia, que tanto me han apoyado en mis sueños, toda mi vida. Nunca lo olvidaré.

A mis padres, Ana y Carlos y a mis abuelos Antonio, Antonia, Pepe y Blanca.

Table of contents

Abbreviations

AIDS Acquired Immunodeficiency Syndrome

APOBEC3G Apolipoprotein B mRNA-Editing enzyme, Catalytic polypeptide-like 3G

BCA Bicinchoninic Acid

CA Constitutively Active

CA Capsid

CB Cyclophilin B

CCL3 CC-chemokine ligand-3

CCL4 CC-chemokine ligand-4

CCL5 CC-chemokine ligand-5

CCR5 C-C Chemokine Receptor type 5

CD4 Cluster of Differentiation 4

CD8 Cluster of Differentiation 8

CDC73 Cell Division Cycle 73

CDK9 Cyclin-Dependent Kinase 9

CFP Cyan Fluorescent Protein

CHIP Chromatin Immunoprecipitation

CPSF Cleavage and Polyadenylation Specificity Factor

CT HIV-1 envelope gp41 Cytoplasmic Tail

CTD C-Terminal Domain

CTS Central Termination Sequence

CXCR4 CXC Chemokine Receptor type 4

DAPI 4',6-Diamidino-2-phenylindole

DCCR DharmaFECT Cell Culture Reagent

DMEM Dulbecco's Modified Eagle Medium

DMF Dimethylformamide

DMSO Dimethylsulfoxide

dsDNA Double-stranded DNA

dsDNA-RT Double-stranded DNA -Reverse Transcription

dsRNA Double-stranded RNA

E1A Human Adenovirus Early Region 1A viral protein

EACS European AIDS Clinical Society

EDTA Ethylenediaminetetraacetic acid

EHT EHT1864

Env Envelope glycoprotein

Env Envelope gene

FBS Fetal Bovine Serum

FDA US Food and Drug Administration

FRET Fluorescence Resonance Energy Transfer

Gag Group-specific Antigen Gene

Gag Group-specific Antigen Gene

GAP GTPase Activating Protein

GAPDH Glyceraldehyde 3-Phosphate Dehydrogenase

GDI Guanine Dissociation Inhibitor

GDP Guanine Nucleotide Diphosphate

GEF Guanine Nucleotide Exchange factor

GPCR G-Protein-Coupled Receptor

GTP Guanine Nucleotide Triphosphate

HA Hemagglutinin

HAART Highly Antiretroviral Therapy

HAdV Human Adenovirus

HIV Human Immunodeficiency Virus

HRP Horseradish Peroxidase

HTLV Human T-Lymphotropic Virus

ICTV International Committee on Taxonomy of Viruses

IFN Interferon

IL-1β interleukin 1β

IL-2 interleukin-2

INSTI Integrase Strand Transfer Inhibitor

INT Integrase protein

LB Luria Bertani

Lck Lymphocyte-specific *Kinase*

LIMK1 LIM Kinase 1

LTR Long Terminal Repeat

MA Matrix protein

MHC-I Major Histocompatibility Class I

MIP-1α Macrophage Inflammatory Protein 1α

NC Nucleocapsid protein

Nef Negative factor protein

NIH United States National Institutes of Health

NLS Nuclear Localization Signal

NNRTI Non-Nucleoside Reverse Transcriptase Inhibitors

NRTI Nucleoside Reverse Transcription Inhibitors

NS1 Influenza Non-Structural protein 1

NSC NSC23766

PAF1 Polymerase II-Associated Factor 1

PBMC Peripheral Blood Mononuclear Cell

PBS Phosphate Buffer Saline

PBS Primer Binding Site

PEI Polyethylenimine

Pol Polymerase gene

PPT Polypurine Tract

PR Protease

RNAPII RNA polymerase II

ROI Region Of Interest

RRE Rev-Responsive Element

RT Reverse Transcriptase

RTC Reverse Transcription Complex

SDS Sodium Dodecyl Sulphate

SEM Standard Error of the Mean

siRNA small interfering RNA

SIV Simian Immunodeficiency Virus

SKIc Superkiller Complex

snoRNA Small Nucleolar RNA

ssDNA Single-stranded DNA

(-) ssRNA Negative single-stranded RNA

(+)ssRNA Positive single-stranded RNA

ssRNA-RT Single-stranded reverse transcribing

STDEV Standard Deviation

TAR Transactivation response Region

Tat Transactivator of Transcription

TMD Transmembrane Domain

Vif Viral Infectivity Factor

Vpr Viral Protein R

VSV-G Vesicular Stomatitis Virus

WHO World Health Organisation

WT Wild Type

X-gal 5-bromo-4-chloro-indolyl-β-D- galactopyranoside

YFP Yellow Fluorescent Protein

Chapter 1. Introduction

1. Introduction

This thesis describes new evidence on the signaling pathways triggered by Human Immunodeficiency Virus 1 (HIV-1) envelope (Env) (chapter 3 and 4) and on the possible mechanism of RNA Polymerase II-Associated Factor 1 complex (PAF1c) restriction factor in HIV-1 infection (chapter 5).

1.1 Viral taxonomy

Since Dimitri Ivanovsky, one of the founders of virology, described an infectious agent that was smaller than bacteria, the Tobacco Mosaic Virus, our knowledge on viruses has widely broadened [1]. For instance, virus classification can be performed according to the nucleic acid as defined by Nobel prize-winner biologist, David Baltimore. Baltimore classification comprises seven groups which include: double-stranded DNA (dsDNA), single-stranded DNA (ssDNA), double-stranded RNA (dsRNA), positive single-stranded RNA ((+)ssRNA), negative single-stranded RNA ((-) ssRNA), single-stranded reverse transcribing (ssRNA-RT) and double-stranded reverse transcribing (dsDNA-RT) viruses (Table 1.1) [2, 3]. According to the Baltimore classification, retroviruses belong to group six of single-stranded RNA-reverse transcribing viruses because their genome consists of two copies of single- stranded RNA which is reverse transcribed [3].

Group	Nucleic acid type	Examples
I	dsDNA	Adenoviruses, Herpesviruses, Poxviruses
II	ssDNA	Parvoviruses
III	dsRNA	Reoviruses
IV	(+)ssRNA	Picornaviruses
V	(-) ssRNA	Orthomyxoviruses, Rhabdoviruses
VI	ssRNA-RT	Retroviruses
VII	dsDNA-RT	Hepadnaviruses

Table 1.1. Baltimore classification of viruses according to viral nucleic acid. Viruses can have dsDNA, ssDNA, dsRNA, (+)ssRNA, (-) ssRNA, ssRNA-RT and dsDNA-RT. Nucleic acid type dictates the replication mechanism by which viruses amplify their genome to produce novel virus progeny. Adapted from Sharma et al., [4]

1.2 Retroviruses

This thesis describes studies on HIV-1 which is a retrovirus. According to the International Committee on Taxonomy of Viruses (ICTV), retroviruses are part of the *Retroviridae* family which includes the subfamilies of *Orthoretrovirinae* and *Spumavinirae* [5]. The *Orthoretrovirinae* subfamily is divided into six genera which include: *Alpharetrovirus*, *Betaretrovirus, Deltaretrovirus, Epsilonretrovirus, Gammaretrovirus* and *Lentivirus* (Table 1.2) [5]. The first five genera fall into the classification of oncoviruses which further divide morphologically into B-, C- and D-type particles [6]. The *Spumaretrovirinae* subfamily is divided into the Spumavirus genus [5]. All viruses from the *Retroviridae* family share in common a single-stranded RNA genome which is reverse transcribed by the virally-encoded reverse transcriptase enzyme and then, integrated into the host's genome. However, their genomes vary in complexity. For instance, Alpharetrovirus, Betaretrovirus, Epsilonretrovirus and Gammaretroviruses have a simple genome which is composed of three major coding domains*: gag* (for group-specific antigen, encodes capsid (CA), nucleocapsid (NC) and matrix (MA), *pol* (for *polymerase,* encodes reverse transcriptase (RT), protease (PR) and integrase (IN) enzymes) and *env* (which encodes the viral surface and transmembrane Env glycoproteins) [6, 7]. On the other hand, complex retroviruses such as Lentiviruses, Spumaviruses and Deltaretroviruses additionally encode a series of accessory proteins which are multiply spliced [6-8].

Genera	Examples	Genome type
Alpharetrovirus	Avian leukosis virus Rous sarcoma virus	Simple
Betaretrovirus	Mouse mammary tumour virus Mazon-Pfizer monkey virus	Simple
Deltaretrovirus	Human T-Lymphotropic virus Bovine leukaemia virus	Complex
Epsilonretrovirus	Walladee dermal sarcoma virus	Simple
Gammaretrovirus	Murine leukaemia virus Feline leukaemia virus	Simple
Lentivirus	Human immunodeficiency virus 1 Human immunodeficiency virus 2 Simian immunodeficiency virus Equine infectious anemia virus Feline immunodeficiency virus	Complex
Spumavirus	Human foamy virus	Complex

Table 1.2. Classification of retroviruses by genera and genome type. Simple retroviruses have *gag*, *pol* and *env* genes which encode matrix, capsid, nucleoprotein, integrase, protease, reverse transcriptase and Env proteins. Complex retroviruses additionally have regulatory proteins that enhance their infection and replication abilities. Adapted from Fields Virology [9].

Within the *Retroviridae* family of viruses and *Orthoretrovinae* subfamily, HIV-1 is part of the Lentivirus genera. HIV-1 is further classified into four lineages: group M (main), group O (outlier), group N (non M/non O) and group P. These four lineages are a result of four cross-species transmission events, being M the most prevalent [10]; the M lineage is further divided into 9 subtypes or clades (A,B, C, D, F, G, H, J and K) [11]. Similarly, HIV-2 is also subclassified into groups A-H [10]. Even though HIV is the best known retrovirus as the causative agent of Acquired Immunodeficiency Syndrome (AIDS) in humans, retroviruses can infect many other species such as monkeys, fish, and cats [12, 13]. Retroviruses have an important economic and agricultural impact causing for example leukoencephalomyelitis in goats or leukosis in chickens [6, 14, 15].

1.3 Discovery and origin of Human Immunodeficiency Virus

HIV was first isolated by two independent teams lead by Luc Montagnier's and Robert Gallo [16, 17]. Both teams described a novel retrovirus with great similarity in shape to human T-lymphotropic virus (HTLV) which was later confirmed as the causative agent of AIDS [18]. HIV-1 arose from cross-species transmission events from a chimpanzee SIV in Southeastern Cameroon and HIV-2 from Sooty Mangabey [19, 20], suggesting that AIDS had resulted from inter-species infections with related lentiviruses [10]. Exactly how the zoonosis emerged is unknown but several studies suggest that it could have been through hunters being exposed to ape blood in the context of bush meat hunting [21]. A recently published evolutionary study suggests that the HIV epidemic originated in the 1920s in Kinshasha, Democratic Republic of Congo, reaching south cities, Lubumbashi and Mbuji-Mayi in the late 1930s. Interestingly, the authors believe that it was not until 1960s that AIDS started to spread in the general African population far from the local initial hotspots due to migration changes triggered as a consequence of the Congo Republic independence.

1.3.1 Genetic variability and epidemiology

HIV-1 presents extensive genetic diversity for four reasons. Firstly, the HIV genome has high replication rates which result in 10^9 virions produced per day in an infected individual [22]. Secondly, reverse transcriptase is highly error-prone because it lacks proofreading mechanisms (unlike other DNA polymerases); the reverse transcription mutation rate has been estimated to be 1-10 errors per replication cycle [23]. The HIV-1 genome undergoes recombination events which also contribute to a wide genetic variability [24]. These recombination events give rise to genetic forms of the virus known as Circulating Recombinant Forms (CRFs) which arise from single patients infected with multiple subtypes [25]. Additionally, the host immune pressure also plays a role in the high rate of

mutation that causes the wide genetic variability of HIV-1 [26]. Altogether this gives rise to virus quasispecies which present different phenotypes and antigenic responses within an infected person [22, 27]. Mutations that are beneficial for the virus under specific environmental pressures are termed escape mutants since they are resistant to immune and antiretroviral suppression [28].

Whilst in sub-Saharan Africa nearly all subtypes of HIV-1 are present, the pattern of HIV-1 infection is more specific worldwide [29]. The most prevalent group of HIV-1 worldwide is the M or main group which is further divided into clades A,B, C, D, F, G, H, J and K [11] . Most HIV-1 infections worldwide belong to clades A, B and C; for instance, clade C alone accounts for at least 50% of the cases [25]. Clade A HIV-1 infections concentrate mostly in eastern Europe and countries in central and eastern Africa [25]. Subtype B is most prevalent in USA, Australia, central and western Europe; this form is also prevalent in some Southeast Asian countries, Northern Africa and the Middle East. Clade C HIV-1 infection concentrate in India and Southern Africa [25]. In Senegal, Guinea Bissau, Ivory Coast, Burkina Faso, Ghana and Gambia, HIV-2 is prevalent and within the 9 HIV-2 clades, clade A is the most predominant [30].

1.4 Clinical aspects of HIV infection

1.4.1 HIV transmission

Report of the first cases of AIDS in the USA were found to be clustered in male homosexual that had had high-risk sexual encounters, intravenous drug users or within hemophiliac populations which suggested that AIDS was a blood-transmitted disease that is transmitted horizontally [31]. The link between HIV and AIDS caused public interventions by which blood banks were screened to prevent further infections through blood-transfusions. HIV-antibody screening decreased the incidence from 1 in 1000 infected units to 1 in 40000 infected units

at high risk areas [31, 32]. Apart from being transmitted horizontally from cell-free virus or cell-associated [33], HIV can be transmitted vertically from mother to child [6]. Vertical transmission of HIV can occur *in utero*, post-natally through breast-feeding and during birth, the latter being the most common mode of vertical transmission [34]. Vertical transmission *in utero* can be reduced by treatment of the mother with antiretrovirals to reduce viral load [35]. In addition, discouragement of breast-feeding and recommendation of cesarean section during birth have also contributed to decrease the chances of vertical transmission [36].

1.4.2 Clinical manifestations of AIDS

Between 1980 and 1981, five patients in Los Angeles were treated for *Pneumocistis carinii* and had Cytomegalovirus infection and Candida mucosal infection [37]. Three out of five patients had low T-cell numbers. The others were not tested. This was the first documentation of patients with what was later defined as AIDS.

The World Health Organization (WHO) has defined four clinical stages: asymptomatic, mild, advanced and severe which are symptomatically well-defined [38]:

- The *initial* asymptomatic period which varies in time is characterized by the absence of symptoms but enlarged lymph nodes.
- The *mild* stage of infection is characterized by diarrhoea, recurrent respiratory upper tract infections, herpes zoster, recurrent oral ulceration, dermatitis, fungal nail infections, weight loss and fever.
- The *advanced* stage is defined by recurring weight loss, chronic diarrhea episodes that last longer than a month, oral candidiasis, pulmonary tuberculosis, severe bacterial infection (pneumonia, meningitis, bone or joint infection bacteraemia), acute necrotizing ulcerative gingivitis or periodontitis, unexplained anemia (decrease in red blood cells),

neutropenia (low number of neutrophils) or chronic thrombocytopenia (decrease of platelet numbers).

- The *severe* stage is defined by an HIV wasting syndrome (constant loss of weight), recurrent bacterial pneumonia, chronic herpes simplex virus infection, oesophagial candidiasis, extrapulmonary tuberculosis, Kaposi sarcoma, Cytomegalovirus infection, HIV encephalopathy, mycosis, septicaemia, cardiopathies, and invasive cervical carcinoma.

The common laboratory markers that are used to estimate patient prognosis include depletion of cluster of differentiation 4 (CD4)+ T-lymphocyte (T-cell) counts [39], elevated serum b2-microglobulin which marks immune activation [40] and neopterin (a catalytic product of GTP which marks immune activation) [41].

1.5 Cell tropism

HIV infects cells from both the innate and the adaptive immune system. The fastest immune response, the innate immunity, comprises: macrophages, dendritic cells, mast cells, natural killer cells, basophils, eosinophils, neutrophils and granulocytes [42]. The slowest immune response, the adaptive immunity is comprised by B cells, T cells (CD4+ T-cells and cluster of differentiation 8 (CD8)+ T-cells) and γδ-T cells[42]. HIV is able to infect cells that express CD4 [43] and either C-C chemokine receptor type 5 (CCR5) [44, 45] or CXC-chemokine receptor type 4 (CXCR4) [46] because these are the main entry receptors to which HIV binds in order to access the cell [47]. These includes T-cells, macrophages and dendritic cells [48]. Whilst in T-cells and macrophages, it is able to productively infect cells, in dendritic cells the current consensus is that they are the initial cells that transfer HIV from the mucosal barriers to T-cells in lymph nodes [49]. Since these cell types are at the center of the innate and adaptive immune responses, an HIV-infected patient is no longer able to fight opportunistic infections giving rise to AIDS.

Apart from immune cells, HIV-1 is also able to infect cells from other tissues. For instance, HIV-1 crosses the blood-brain barrier and infects microglia and

perivascular macrophages [50]. This is why HIV-1 patients present cognitive impairment which can range in severity from mild to severe [51].

1.6 The HIV-1 genome

Two copies of positive sense unspliced single-stranded and non-covalently linked RNAs are found in the viral particles of HIV-1 [52]. They are identical and they are able to dimerise through their dimer initiation sites [53]. As shown in figure 1.1A, the HIV-1 genome encodes the *gag*, *pol* (for polymerase) and *env* (for envelope) genes. The gag polyprotein, also referred to as $pr55^{Gag}$, due to its total molecular weight, is cleaved by protease (PR) to give rise to MA (p17), CA (p24), NC (p7) and p6 [54]. The *pol* gene is synthesized during a rare frameshifting event from $p160^{GagPol}$ which encodes the viral enzymes: RT (p51), RNAse H (p15) and INT (p31) [55]. Each individual enzyme is cleaved from $p160^{GagPol}$ by PR [56]. Similarly the *env* gene is synthesized as a polyprotein precursor (gp160) which once synthesized, is cleaved by the viral PR to produce, gp120 and g41, the two components of the viral Env protein [56].

In addition to *env, gag* and *pol* genes, HIV also synthesizes a range of accessory proteins which allow HIV to replicate more efficiently. For instance, Tat (for transactivator of transcription) increases RNA synthesis rate from the 5' Long terminal repeat (LTR) HIV-1 promoter; tat is synthesized as a two exon RNA [57, 58]. Rev is also synthesized as a two exon RNA and is required for transport of unspliced and partially spliced viral RNAs out of the nuclei into the cytoplasm [59]. These RNA species have specific packaging signals which, together with the other protein components, allow them to be packaged efficiently into infectious viral particles [60]. In addition, Nef (for negative factor) plays a wide range of functions which enhance viral infectivity: 1) it downregulates CD4 surface expression which in turn allows HIV to be released from the membrane upon assembly [61], 2) it

downregulates major histocompatibility class I proteins (MHC-I) from the cell surface [62] and 3) activates signaling pathways [63-65]. Vpr (for viral protein R) is a multifunction protein which not only contributes to transport of the preintegration complex to the nuclei but is also a co-activator of Tat-mediated transcription and exerts G2-cycle arrest [66]. HIV-2 strains lack Vpr but encode Vpx which is genetically similar to Vpr [67]. Vpx is packaged into virions and upon release, it downregulates SAMHD1, a restriction factor that downregulates the pool of dNTPs required for DNA synthesis during reverse transcription. Vpx also contributes to nuclear import of the preintegration complex. Vpu (for Viral Protein Unique) is also a multifunctional protein that is synthesized from a Rev-dependent bicistronic mRNA molecule that also encodes *env* [68]. Vpu degrades CD4+ in the endoplasmic degradation to facilitate release of virion particles and additionally degrades tetherin, a cellular protein that anchors exiting virion particles, to avoid release of new particles [68, 69]. In addition, viral infectivity factor (vif)-mutant HIV strains were shown to have low infectivity rates [70, 71]. It was later shown that Vif antagonizes the human cytidine deaminase, apolipoprotein B mRNA-editing enzyme, catalytic polypeptide-like 3G (APOBEC3G) to overcome its antiviral function [72]. As shown by Stopak *et al*., Vif physically interacts with APOBEC3G. Vif forms a Vif-CBF-β-ElonginB-ElonginC-Cullin5-Rbx (Vif-CBF-β-EloB-EloC-Cul5-Rbx) E3 complex which tethers APOBEC3G resulting in proteasomal degradation [73].

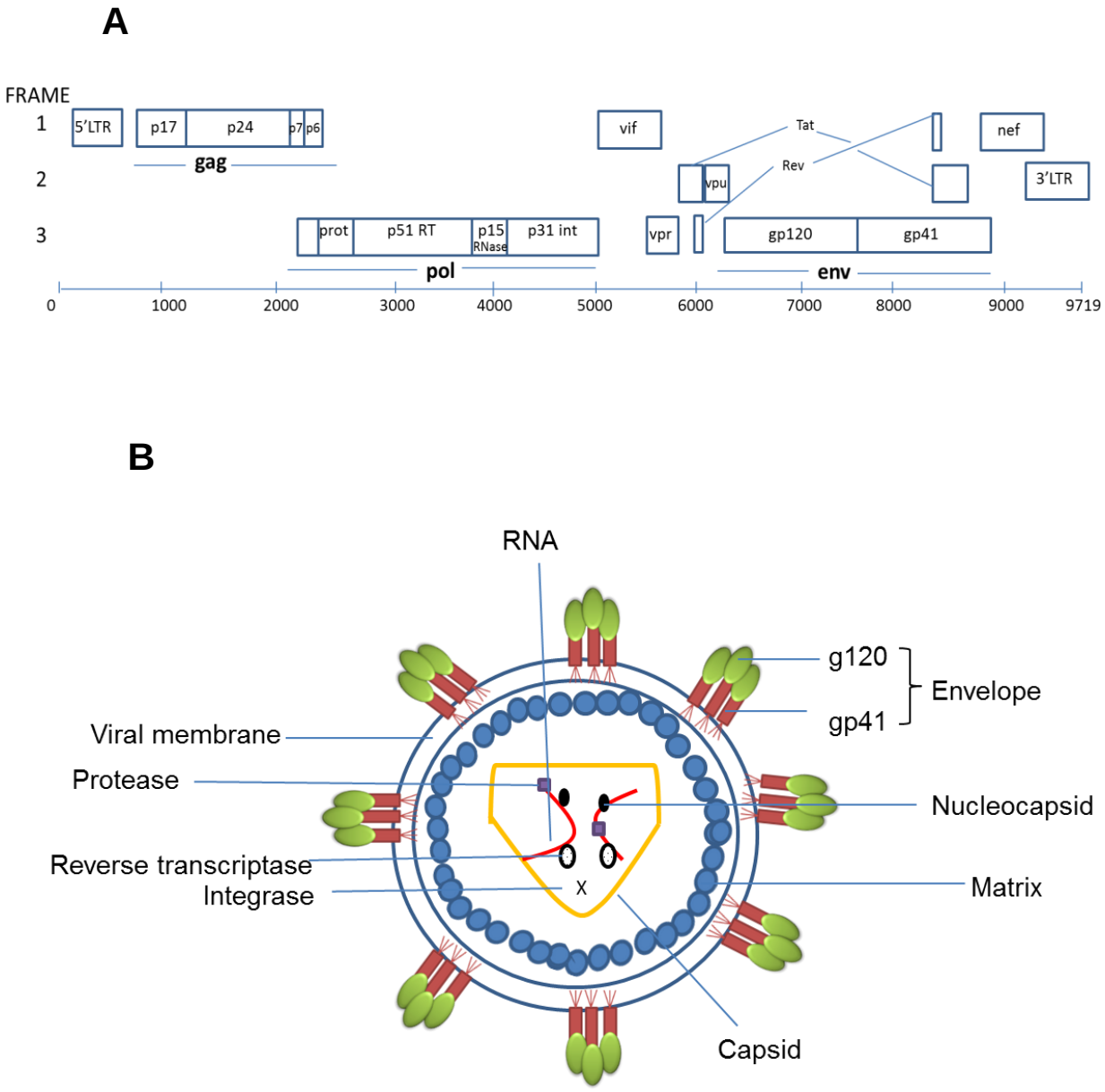

Figure 1.1 The HIV-1 genome and viral proteins. (A) Schematic representation of the HIV-1 genome. The HIV genome is 9,7 Kbp in length and the relative locations of each open reading frames are described. The *gag* gene comprises MA (p17), CA (p24), NC (p7) and p6. The *pol* gene comprises RT (p51), RNAse H (p15) and IN (p31). The *env* gene comprises gp120 and g41, the two components of viral Env protein. (B) Schematic representation of the HIV-1 viral particle. Each HIV-1 viral particle has a viral membrane lined with matrix protein. Inside the matrix protein is the capsid protein which contains the viral RNA genomes associated with nucleocapsid, integrase, protease and reverse transcriptase. Adapted from Freed O., [56].

1.7 HIV-1 replication cycle

Initially, HIV enters the cells by engaging the CD4 [43] receptor and either CXCR4 [46] or CCR5 [44, 45]. This engagements trigger fusion with the cell membrane (Figure 1.2) [74, 75]. Alternatively, HIV is also able to enter cells via clathrin-mediated endocytosis though this entry route has been lessl characterized [76]. Clustering of receptors/co-receptors at the plasma membrane is a crucial step to trigger membrane fusion upon Env binding, and for that instance, HIV utilizes actin cytoskeleton [77]. This process also involves filamin, an actin-binding protein which links the CD4+ receptor cytoplasmic tails to actin [78, 79]. After receptor binding, HIV has to overcome the cortical-actin barrier and to do so, HIV has been shown to upregulate cofilin, a cellular protein which severes actin filaments [80]. Reverse transcriptase then transcribes the positive, single-stranded RNA molecule to a double-stranded DNA molecule [81]. The double-stranded DNA molecule is then transported to the nuclei as part of the preintegration complex; the pre-integration complex is composed of viral DNA, MA, RT, Vpr , nucleocapsid and protease [82]. In the nuclei, the double-stranded viral DNA integrates in the hosts' genome. Transcription produces a mix of partially spliced and unspliced RNA species which are transported into the cytoplasm by the viral protein Rev [56]. The polyprotein precursors, Gag and Gag-Pol are synthesized and packaged into the virions, where they are cleaved by PR shortly after or during virus release from the plasma membrane giving rise to their encoded mature proteins [56]. In addition, at the plasma membrane, the RNA viral genomes are packaged into new particles which bud out of the cells [83].

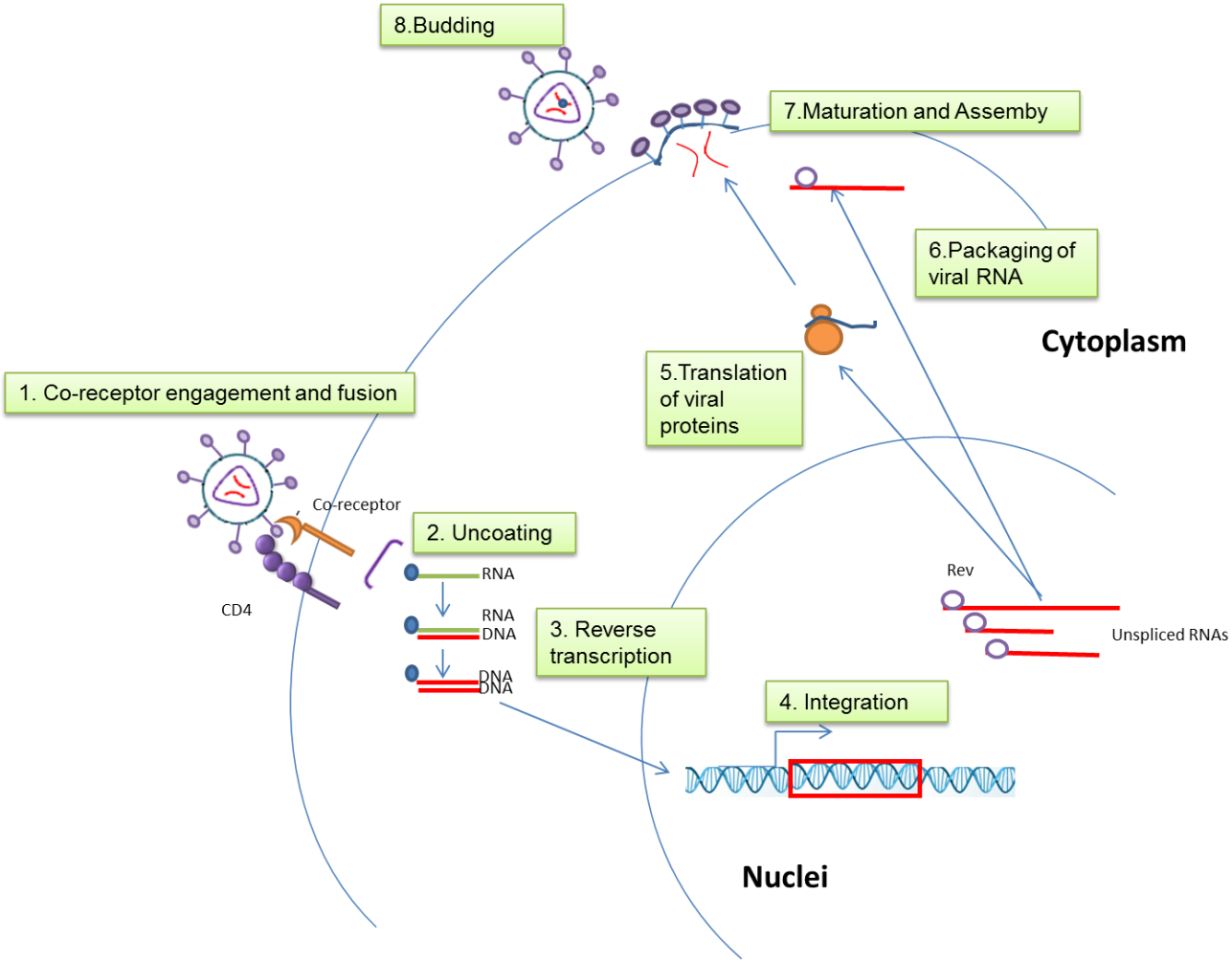

Figure 1.2 HIV-1 replication cycle. Schematic representation of HIV-1 infection. HIV fuses with cells via CD4 and CXCR4 or CCR5 co-receptor engagement and/or clathrin-mediated endocytosis. Once in the cell, CA uncoats to release the viral genome. The viral genome is then reverse transcribed to give rise to double-stranded DNA. This DNA is integrated in the cell's genome where it is transcribed. With the aid of Rev, the partially spliced and spliced RNA species are imported to the cytoplasm. Unspliced RNAs are packaged into viral particles after protein synthesis of viral components. At the plasma membrane, new viral particles are assembled which then bud out of the cell, ready to infect new cells. Adapted from Frankel, [84].

1.7.1. HIV entry and receptor engagement

HIV enters the target cell via plasma membrane fusion and/or clathrin-mediated endocytosis mediated by receptor/co-receptor binding of viral Env [76]. To enter cells gp120, a component of the Env glycoprotein, must interact with CD4 [43]. The Env glycoprotein also binds to a secondary co-receptor, CXC-chemokine receptor-4 (CXCR4) [46] or CC-chemokine receptor-5 (CCR5)) [44, 45, 48]. HIV-1 strains that enter via CXCR4 are named X4-tropic whilst HIV-1 strains that enter via CCR5 are termed R5-tropic. In addition to viral entry, engagement of Env to cellular receptors also induces signaling events which are the subject of chapter 3 and 4. The importance of the co-receptor for HIV-1 infection is highlighted by the findings that patients with mutant CCR5 alleles are resistant to infection [85].

The HIV Env protein is a multimeric protein that consists of two components: gp120 and gp41, which form homotrimers that are non-covalently associated to form heterodimers that can be visualized by electron microscopy as spikes (Figure 1.3) [86, 87]. HIV gp120 has five conserved (C1-C5) regions which form the core of the protein and interact with gp41 [88]. The constant domains are interspersed with five highly glycosylated variable protein domains (V1-V5) which lie at the surface of the protein [89]. The third variable loop (V3) determines co-receptor usage [47]. In its native or pre-fusion state, HIV gp41 has three domains: an external, a transmembrane and an intracellular domain. The extracellular or ectodomain has three marked regions, two heptad repeats located next to the C- and N-terminal regions of the extracellular domain and a fusion peptide located at the N-terminus [90]. Binding of HIV gp120 to the target cell's CD4 causes a conformational change in gp120 that enable it's binding to the co-receptor [91]. This double interaction exposes the gp41 fusion peptide and triggers a series of conformational changes which result in the formation of a gp41 pre-hairpin

intermediate that anchors the virus membrane to the cell membrane [92]. These conformational changes generate a highly thermostable gp41 conformation which is thought to trigger the fusion event between viral and cellular membranes [93].

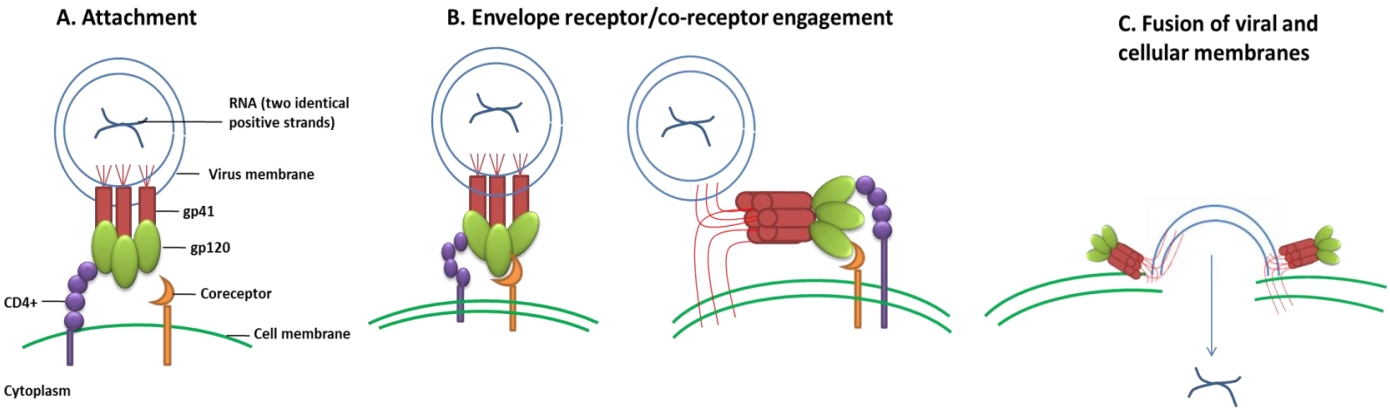

Figure 1.3. HIV fusion. A. HIV attachment to the cell membrane. HIV anchors the Env protein (composed of gp120 and gp41) to the primary receptor, CD4+, and a co-receptor, CXCR4 or CCR5. B. Co-receptor engagement. Attachment of the Env protein triggers a conformational change in the gp41 portion of the Env protein which brings into close proximity the viral and cellular membranes. C. Fusion. The viral and cellular membranes fuse to release the viral genome into the cell's cytoplasm, initiating the replication cycle. Adapted from Tomkowicz et al., [94].

After receptor/co-receptor engagement, the viral core is released into the cytoplasm. The viral core is composed of the CA protein which encases the viral genome and associated proteins including reverse transcriptase, nucleocapsid and integrase [95]. Following release into the cytoplasm, the CA protein disassembles in a multistep process which requires host factors such as cyclophillin A, a peptidyl propyl isomerase [96, 97]. Lack of detection of CA in preintegration complexes and reverse transcription complexes initially suggested that uncoating takes place prior to or during reverse transcription [95]. However,

more recent *in vivo* imaging studies suggest that CA uncoating is coupled to reverse transcription [98, 99].

1.7.2 Reverse transcription

Reverse transcription of a single-stranded RNA molecule into a double-stranded DNA molecule is a unique feature of retroviruses and hepadnaviruses [100]. The process of reverse transcription is catalyzed by virally-encoded RT and takes place in several steps which involves viral RNA cis-acting sequences; namely primer binding site (PBS), short regions of homology or R sequences, polypurine tract (PPT), the central termination sequence (CTS) and U3/U5 sequences (Figure 1.4) [56]. The U3, R and U5 sequences are part of the 5'/3' LTR HIV-1 promoter which binds to Tat to initiate transcription of DNA into RNA after integration [56].

Reverse transcription is a multistep process (Figure 1.4) [56, 95, 101]:

1. Initiation of reverse transcription takes place by binding of a tRNA to the 5' PBS site. DNA synthesis starts from 3' and results in the generation of a DNA/RNA hybrid.
2. The RNA fragment of the generated hybrid is degraded by virally-encoded RNase H which is part of the RT enzyme. The resulting DNA fragment is referred to as the minus-strand strong stop DNA.
3. The minus-strand strong stop DNA "jumps" from the 5' end to the 3' ends using the R sequences and this constitutes the first strand transfer.
4. The minus-strand strong stop DNA serves as a primer for DNA synthesis from 3'.
5. DNA synthesis takes places from other sites including the central PPT site, this generates the plus-strand DNA fragment.

6. Once PPT-initiated DNA synthesis stops, the tRNA is removed by RNAse H giving rise to the plus-strand strong stop product.
7. Generation of the plus-strand strong stop product allows a second jump to take place by annealing to the PBS on the minus-strand DNA. DNA synthesis continues.
8. After generation of the plus-strand strong stop, DNA synthesis continues.
9. The RT then synthesizes from the PBS and PPT sites. Repair and ligation of the generated circular intermediate results in a linear DNA duplex which has 5'/3' LTRs.

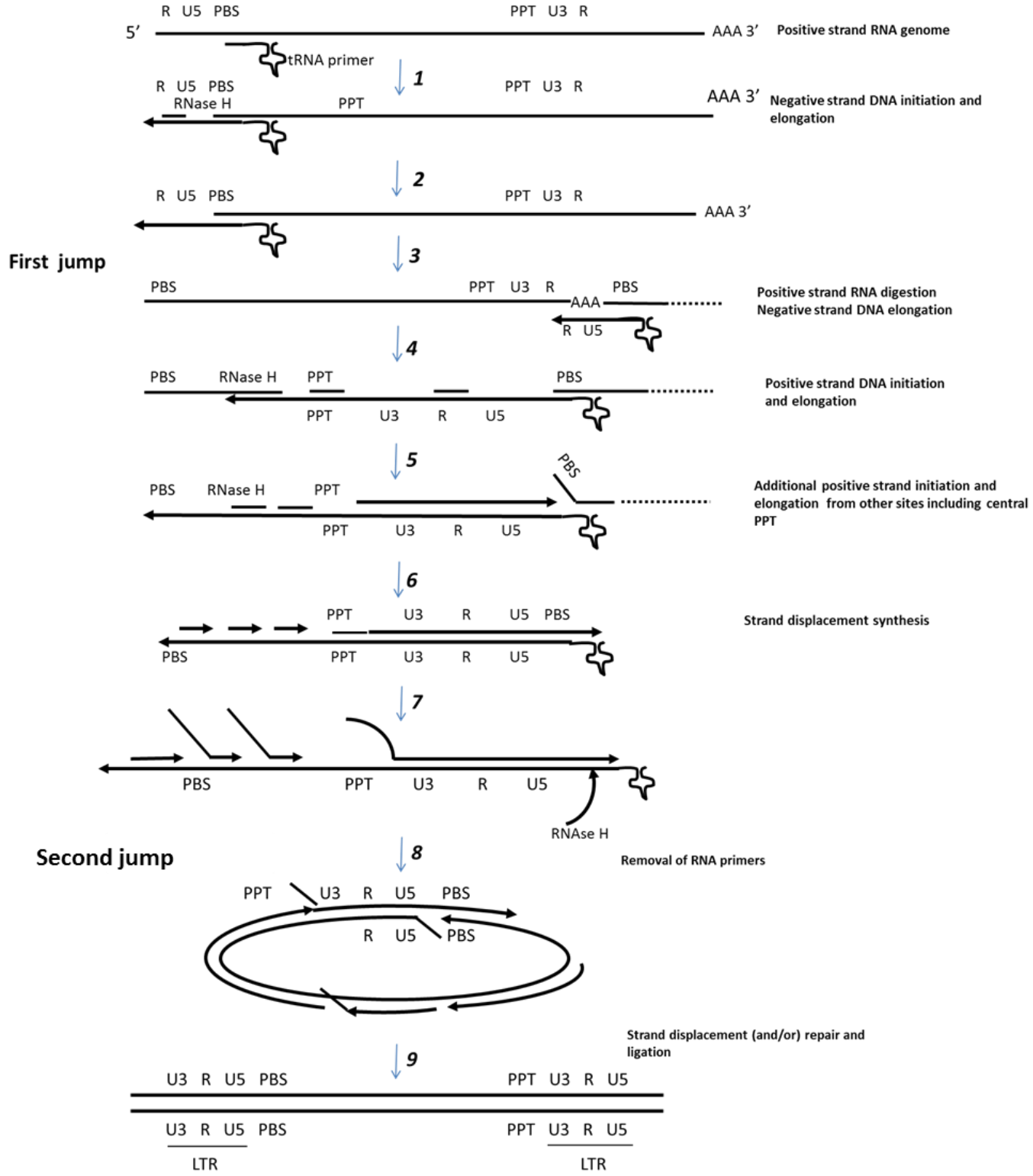

Figure 1.4 Reverse transcription of the HIV genome. Reverse transcription is a multistep process which involves: 1) Binding of a molecule of tRNA to the PBS. 2) Negative strand DNA initiation and elongation. 3) First strand transfer or "jump", negative strand elongation and degradation of positive RNA strand. 4) Positive strand DNA initiation and elongation. 5) Additional positive strand initiation and elongation from central PPT. 6) Strand synthesis. 7) Removal of RNA primers. 8) Second strand transfer or "jump". 9) Strand displacement and/or repair and ligation to produce a linear double DNA molecule. Adapted from Sarafianos et al., [101].

1.7.3 Integration

Following reverse transcription, the reverse transcription complex (RTC) composed of the double-stranded DNA viral genome, NC, IN, Vpr and MA, is imported into the host's nucleus [102]. Various proteins involved in cellular import pathways have been linked to nuclear import of the RTC including importin 7 [102], karyopherin α2 Rch1 [103], transportin SR-2 [104] and nucleoporins Nup98 [105], Nup358/RANBP2, and Nup153 [106]. In addition, MA, Vpr and IN have nuclear localization signals (NLS) [102]. The elements involved in nuclear import of the RTC are numerous although the exact mechanism is still not clear.

Once in the nucleus the IN enzyme catalyses integration of the viral genome into a cell's chromosome. IN has two catalytic activities: a 3' processing activity and a DNA strand transfer activity [81]. Using the 3' processing activity, IN cleaves the ends of the LTRs of both viral DNA strands using water a nucleophile [107]. The 3' resulting hydroxyl groups are then used by IN to cut and join the viral DNA strands to the opposing host DNA strands [107].

1.7.4 Gene expression, nuclear RNA export and viral protein translation

Upon integration of the viral genome into the host chromosome, transcription is initiated from the LTR HIV-1 promoter; transcription starts from the U3/R junction sequence which contains several elements that form a platform to which transcription initiator factors bind to [56]. For instance, the viral DNA sequence has regulator sequences that include, a TATA element, three tandem Sp1 binding sites and an initiator sequence [108]; these sequences contribute efficiently to cooperative binding of transcription initiator TFIID and other factors to TATA [109]. Additionally, viral DNA also contains two NF-κB binding sites which act as enhancers of transcription upon binding of NF-κB [110]. However, basal transcription from the HIV-1 promoter is low which suggested that

additional factor(s) were required [56]. Subsequent studies showed that the transcription activation of the HIV genome required the viral accessory protein, Tat [111, 112]. The mechanism by which Tat transactivates LTR-driven transcription is via binding to an RNA element at the 5′ ends of HIV-1 transcripts, the transactivation response region (TAR) [112] and recruits cyclin T1 which in turn binds to cyclin-dependent kinase 9 (CDK9) forming a heterodimer [113]. The cyclinT1/CDK9 heterodimer recruits human P-TEFb to Tat [114] and this results in phosphorylation of the C-terminal domain of RNA polymerase II (RNAPII) which is required for transcription elongation [115]. Following transcription, the transcription products undergo alternative splicing in the nucleus which gives rise to a complex and extensive range of transcripts to produce the complete set of mRNAs that encode the viral proteins [109]. In addition, unspliced transcripts are also produced. To evade cellular surveillance mechanisms that normally degrade unspliced transcripts, HIV-1 utilises the virally encoded accessory protein, Rev; Rev binds to an RNA element located in the Env-encoding region, the Rev-responsive element (RRE), a 350 nt highly-structured cis-acting RNA, which enables unspliced mRNAs to be transported to the cytoplasm [109, 116, 117]. Rev contains both a nuclear export signal element and a nuclear localization signal that enables shutting from the nuclei to the cytoplasm and viceversa. In this manner, unspliced and partially-spliced transcripts are transported from the nuclei to the cytoplasm by binding of Rev to the RRE (Figure 1.5) where transcripts are translated [117] (Figure 1.5).

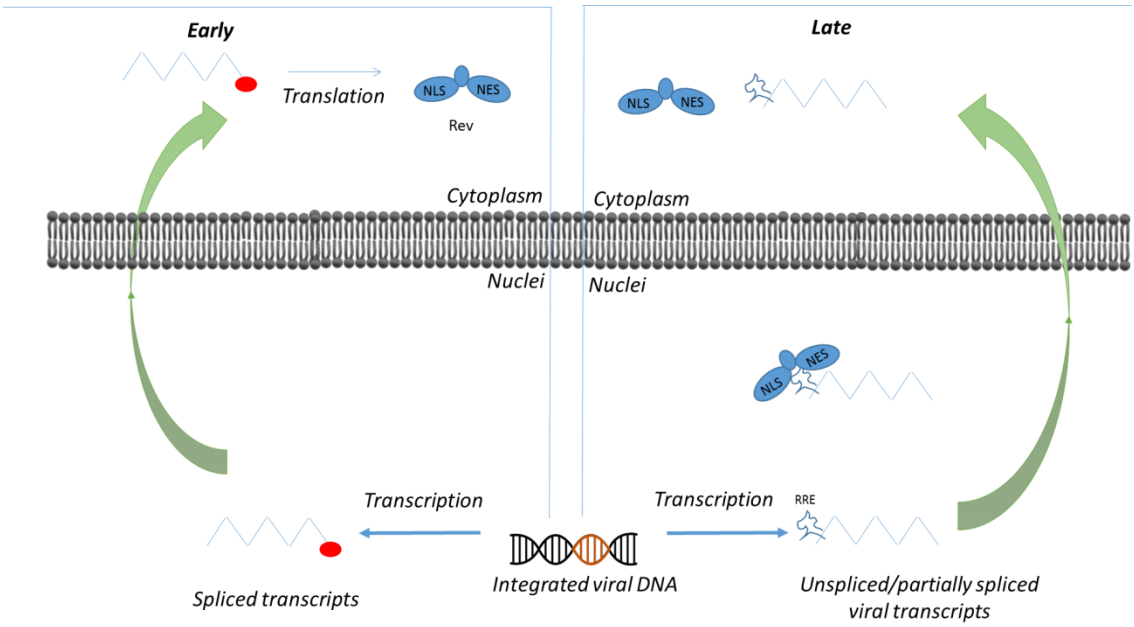

Figure 1.5 Transport of HIV-1 spliced and unspliced/partially spliced transcripts. Early in the replication cycle, spliced transcripts are transported from the nuclei to the cytoplasm similarly to cellular mRNAs. On the other hand, Rev enters the nucleus via an Arg-rich nuclear localization signal to then bind to the RRE of unspliced and partially spliced transcripts, which then are transported to the cytoplasm where they are then translated (Adapted from [117]).

1.7.5 Viral assembly, budding and maturation

The viral components required to assemble a fully infectious HIV virus particle are two copies of positive single-stranded RNAs which constitute the viral genome, the viral Env protein, the $tRNA^{Lys,3}$ that initiates reverse transcription and the Gag-pol polyprotein which encodes PR, IN and RT and that is translated via rare frameshift[56] event [83, 118]. In addition, the Gag polyprotein which encodes MA, CA, NC and p6 is synthesized from an unspliced viral mRNA and orchestrates assembly at the plasma membrane by recruiting two copies of the viral RNA which constitutes the genomic viral RNA. The MA domain of Gag is responsible for binding to the plasma membrane where assembly takes place [118]. The viral mRNA unspliced transcripts to be packaged in the virions, are targeted to the plasma membrane where assembly of new virion particles takes places via a packaging sequence located in the 5' end between the LTR and the

gag initiation codon [60]. To package and assemble novel virus particles the virus hijacks the ESCRT pathway which is normally involved in production of vesicles that are then released into multivesicular bodies and abcission cytokinesis [119-121].

1.8 Highly Active Antiretroviral Therapy

Highly Antiretroviral Therapy (HAART) has proven to be efficient at reducing morbidity and mortality by suppressing viral RNA and blood viral load; this in turn, decreases the risks of transmission [122]. According to the United States National Institutes of Health (NIH) and the European AIDS Clinical Society (EACS) guidelines, patients presenting less than 350 CD4-T-cells per mm^3 are strongly recommended to start HAART. However, HAART does not eradicate HIV infection completely as it does not eliminate viral DNA reservoirs or immune dysregulation as a result of chronic immune activation [123]. Since HIV-1 mutates at very high rates, the success of this therapy relies on the use of a combination of drugs that target different steps of the virus replication cycle [23]. Based on their targets, antiretroviral drugs are classified into 5 different groups: fusion, co-receptor, nucleoside reverse transcription, non-nucleoside reverse transcription, integrase and protease inhibitors (Figure 1.6).

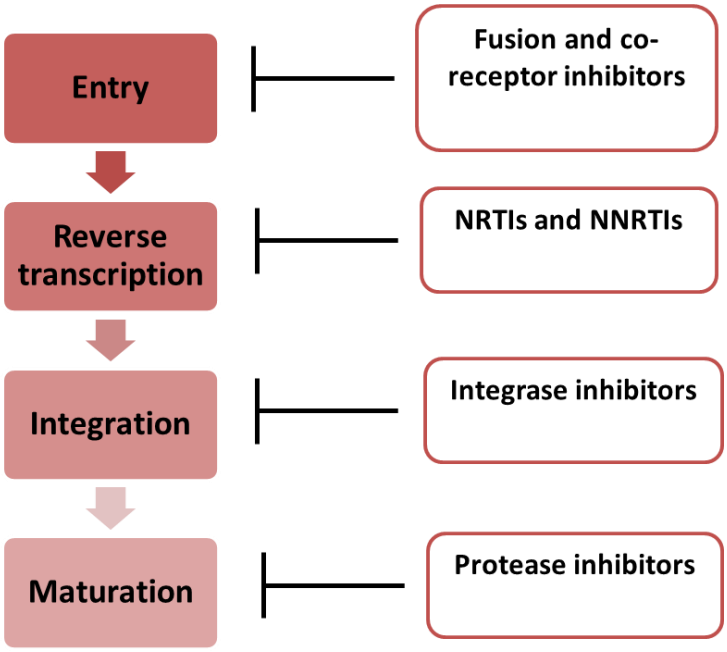

Figure 1.6 Viral replication steps targeted by five different antiretroviral groups. There are currently five types of antiretrovirals which have different mechanisms. Fusion and co-receptor inhibitors, interfere with the Env-receptor/co-co-receptor interactions. Reverse transcription inhibitors block reverse transcriptase. Integrase inhibitors block viral DNA integration into the host genome. Protease inhibitors block the cleavage of polyprotein precursors which give rise to the different viral proteins. Adapted from La Bonte et al., [124].

1.8.1. Nucleoside reverse transcription inhibitors (NRTIs)

Nucleoside reverse transcription inhibitors (NRTIs) were the first class of antiretrovirals approved by the US Food and Drug Administration (FDA) [125]; NRTIs are prodrugs that require phosphorylation by cellular kinases to be activated [126]. NRTIs are analogues of nucleoside substrates that lack a 5' hydroxyl group and which substitute nucleoside 3' triphosphates during reverse transcription. This causes premature termination of viral DNA synthesis [126].

1.8.2 Non-nucleoside reverse transcriptase inhibitors (NNRTIs)

NNRTIs bind non-competitively to a region proximal to the catalytic pocket of RT which triggers changes in the conformation of RT, reducing its catalytic activity [127]. Importantly, NNRTIs are highly specific compared to NRTIs which can interfere with normal cellular processes by binding to DNA polymerases and

unlike NRTIs they do not need to be activated to exert their function [128]. NNRTIs and NRTIs account for nearly half of the antiretrovirals approved [23].

1.8.3 Fusion and co-receptor inhibitors

Since HIV requires gp120 to interact with CD4 to gain access to the cells, this interaction has been an extensively investigated drug target. As a result, BMS-378806 and TNX-355, have shown clinical promise [23]. BMS-378806 is a small molecule inhibitor that binds to gp120 and inhibits binding to CD4 [129]. TNX-355 is an antibody that binds to CD4 and thus, prevents gp120 attachment [130]. Current available fusion inhibitors are a peptide-like inhibitor that targets the gp41 fusion peptide (fuzeon) [131] and a small molecule inhibitor that targets the CCR5 co-receptor (maraviroc) [132].

1.8.4 Integrase inhibitors

As described in section 1.7.3, the HIV-1 IN enzyme has two catalytic activities: a 3' processing activity and a strand transfer activity [81]. Raltegravir, the first approved integrase inhibitor, targets the strand transfer activity and most molecules investigated so far target this IN activity and so, are referred to as integrase strand transfer inhibitors (INSTIs) [133]. However raltegravir has to be taken twice a day and resistance has been reported [134, 135] which prompted for the development of alternative IN inhibitors. As a result, elvitegravir was approved in a daily single tablet format but with a similar resistance profile to raltegravir [134]. Most recently dolutegravir, a novel INSTI being reviewed by the FDA for marketing, shows an improved resistance profile compared to raltegravir and elvitegravir and can be taken once a day [136].

1.8.5 Protease inhibitors

As described in section 1.7.5, PR is responsible of cleaving $p160^{GagPol}$ and $pr55^{Gag}$ polyproteins into the individual viral proteins [137]. Protease polyprotein processing is essential for viral replication and so, it has been object of numerous studies which resulted in the development and approval of a 10 protease inhibitors which are commonly used in conjunction to other inhibitors [138]. Apart from tripanavir, all of the protease inhibitors mimic protein binding and include saquinavir, ritonavir,or darunavir, the latter being the latest approved [139].

1.9 Prevention strategies and vaccine attempts

Currently, various strategies are being studied to prevent HIV infection; these include microbicides, pre/post-exposure prophylaxis of high-risk populations (such as sex workers and injecting drug users) and male circumcision.

There are various types of microbicides available with different mechanisms of action. For instance, some microbicides such as Cyanovirin® act as a barrier against incoming virus by blocking the Env glycoprotein which prevents CD4 engagement and thus, viral entry [140]. Other microbicides aim to acidify the pH thus enhancing the mucosal defences such as cellulose sulphate or Acidform®. Tenofovir is an antiretroviral formulated in gel form which acts by inhibiting HIV replication which is currently being tested in a South African Phase III clinical trial [141]. Another antiretroviral drug being currently being tested as a microbicide is dapivirine which innovatively, is being marketed as a vaginal ring [142].

In addition, three phase III randomized clinical trials showed that male circumcision has a protective effect against heterosexual HIV transmission of 60% [143-145] and so, the WHO has recommended its implementation for prevention in high-risk areas [146].

Despite huge efforts to develop a vaccine that broadly neutralizes HIV, to date there are no vaccines against HIV. The main strategies being currently investigated are to produce a preventive vaccine and a therapeutic vaccine that intensifies the effect of ART, delays treatment initiation or clears viral reservoirs [123, 147]. However, numerous attempts have proven unsuccessful due to: genetic variability of target epitopes as a result of high mutation rates and the structural biology of the Env glycoprotein which includes conserved glycan motifs and receptor/co-receptor binding sites [148]. The most recent trials (Figure 1.7) include efficacy evaluation of two recombinant vaccines of gp120 in USA [149] and in Thailand [150], VAX 004 and VAX003, which showed no efficacy. Another strategy attempted has been using adenoviral vectors as systems for delivery of genes. The MRKAd5® HIV-1gag/pol/nef vaccine is an adenovirus-5 based vector that delivers *gag, pol* and *nef* genes which was trialled in the STEP trial but even though it showed promising immunogenicity and safety [151] it was halted due to reviews that suggested it was not effective [152]. Similarly, in the HVTN505 trial, evaluated the efficacy of an adenoviral vector delivery to deliver DNAs encoding HIV-1 clade B *gag* and *pol* and *env* derived from clade A, B and C [153]. Unfortunately the trial had to be halted after results showed that it failed to prevent infection [152]. Out of the 6 trials so far, only one has showed a modest efficacy, the RV144 trial in which the vaccine trialled showed a 31.2% efficacy at preventing HIV-1 infection [154]. The trial evaluated the efficacy of a combination of ALVAC® (incorporating a canarypox vector, vCP1521) and AIDSVAX® B/E vaccine, including the gp120 constructs assayed in the VAX trials. Currently, a clinical trial in South Africa is being conducted to improve the RV144 vaccine in which HIV-1 clade specificity has been modified to clade C because in South Africa HIV-1 clade C is the most prevalent [155].

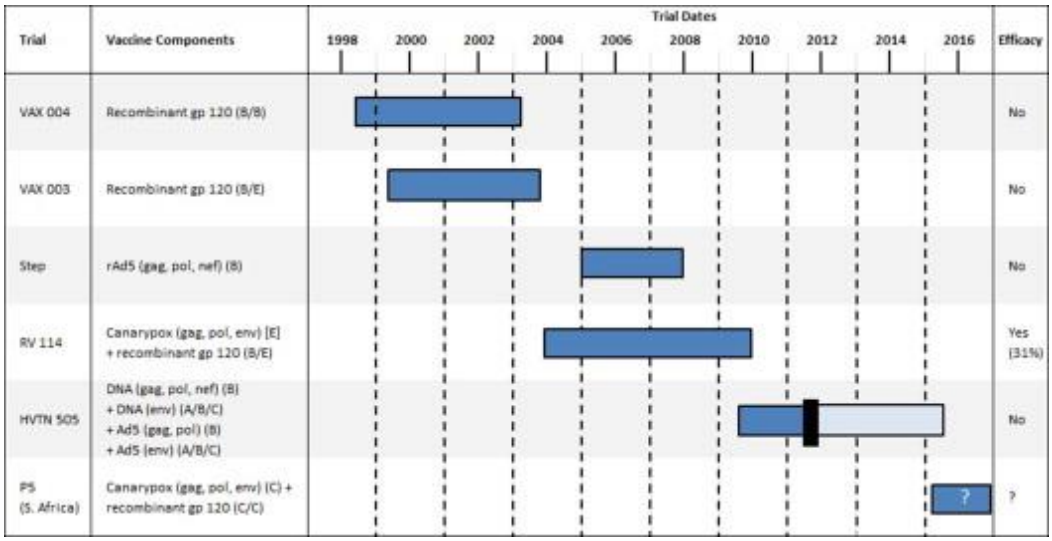

Figure 1.7 HIV efficacy vaccine trials including vaccine components, name of trial and trial dates. From Esparza et al, [152]

Despite the efforts in education prevention strategies, the WHO estimates that in 2013, 2 million people newly enrolled in antiretroviral therapy, the largest annual increase ever [156].

1.10 HIV restriction

Host cells have evolved a wide diversity of proteins termed restriction factors that constitute a first line of defence against incoming virus. The first evidence of restriction factors came from studies with the murine *Friend Virus susceptibility 1* gene (*Fv1*) [157]. The authors showed that mice cells that encode the $Fv1^n$ allelic form were susceptible to infection by N-tropic MLV but resistant to B-tropic MLV infection [157]. Since then, a number of proteins that inhibit HIV-1 infection have been described which vary in potency and mechanism. In an effort to identify other proteins that are involved in HIV-1 restriction, Liu et al., performed a whole genome screen which identified additional 114 proteins which significantly inhibit HIV-1 infection [158]. I will give a brief overview of the restriction factors that are best characterized which differ in the step of the replication cycle they target (Figure 1.8).

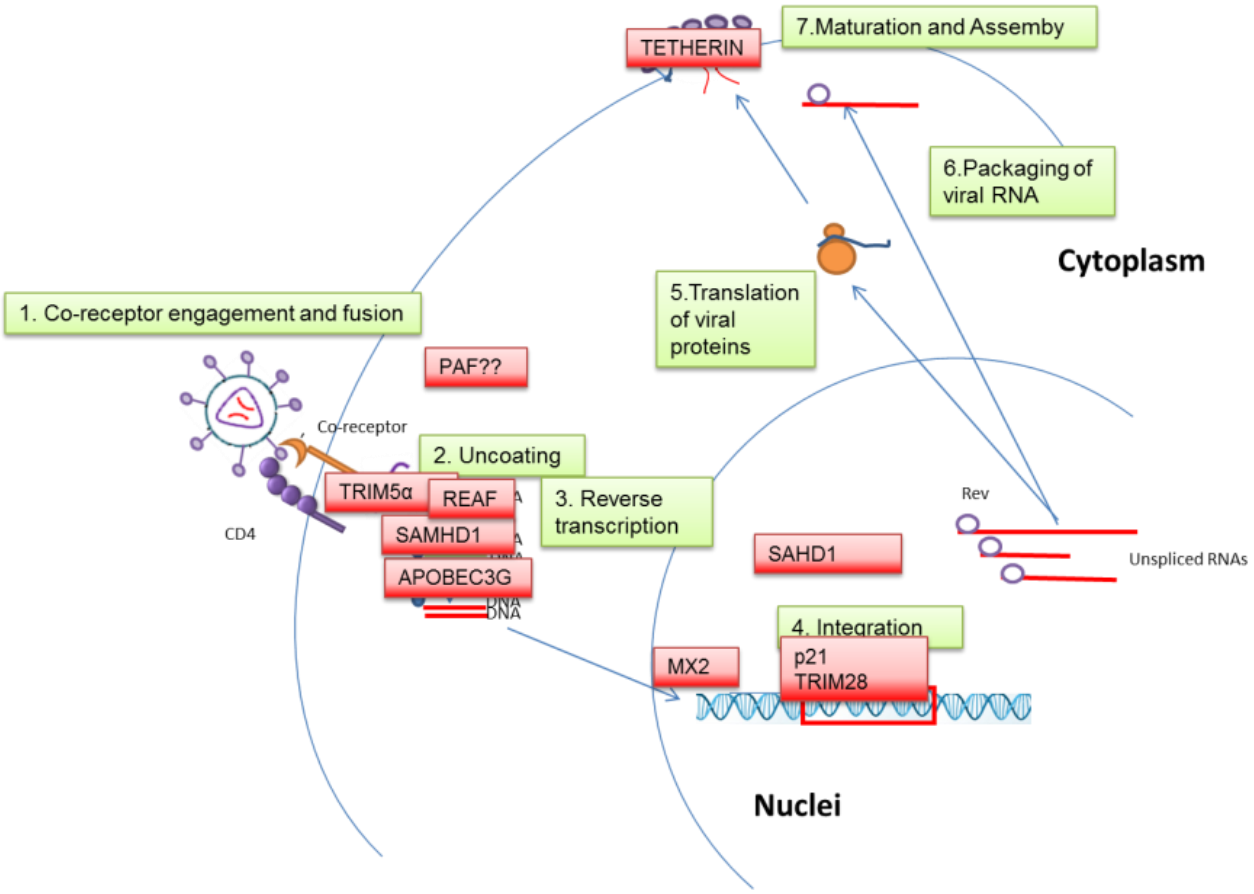

Figure 1.8. Known restriction factors and their viral step targets in the HIV replication cycle. Restriction factors that target early steps in the replication cycle include TRIM5α, REAF, SAMHD1 and APOBEC3G whilst MX2, SAMHD1, p21 and Tetherin all target later stages of the viral replication cycle.

1.10.1 Apolipoprotein B mRNA-editing, enzyme-catalytic, polypeptide-like: APOBEC3G.

Apolipoprotein B mRNA-editing, enzyme-catalytic, polypeptide-like (APOBEC3G) was discovered upon characterisation of the HIV-1 virally encoded Vif accessory protein. Initially, Vif was shown to be required for viral DNA synthesis [159] and for stabilisation of viral nucleocapsid protein complexes [160, 161]. Following studies to try and understand the function of Vif showed that in non-permissive cells, Vif was absolutely required for HIV-1 replication but in permissive cells, Vif was not essential [160]. This supported the hypothesis that there was an innate defence mechanism that Vif could overcome, the cellular gene responsible for

this defence was *APOBEC3G*, also known as *CEM15* [161]. APOBEC3G restricts HIV-1 infection in T-lymphocytes during reverse transcription through its deaminase activity that mutates G-A in nascent retroviral DNA and it is also effective against other retroviruses such as MLV or SIV [162]. Interestingly, in MLV, APOBEC3G is packed into virions where it deaminates the viral genome in a destruction mechanism, a strategy overcome by Vif [163]. It was later confirmed that APOBEC3G can also mutate viral RNA [164].

1.10.2 Tripartite-motif-containing 5α (TRIM5α)

HIV is able to readily enter Old World Monkey cells but upon doing so, it encounters a block which happens earlier than reverse transcription[165]. The restriction block was found to be Tripartite-motif-containing 5α protein which recognises incoming capsid [165]. Owl monkey cells are resistant to TRIM5α restriction because a cellular protein, Cyclophillin A, binds to CA and protects HIV from TRIM5α [166]. The human equivalent of TRIM5α encodes the human restriction factor Ref1 [167].

1.10.3 The TRIM28 (KAP1)/SETDB1 complex

Another restriction factor within the TRIM family of proteins, TRIM28, has been described to target HIV-1 replication [168]. TRIM28 targets acetylated INT which is required to efficiently integrate the viral DNA into the host genome. TRIM28 forms a complex with HDAC1 which allows deacetylation of integrase [168].

1.10.4 Tetherin.

Upon release, virus particles encounter another restriction factor named tetherin. Tetherin, also known as BST2 or HM1.24 is a membrane protein that anchors budding virus particles and targets them for degradation [69]; it is constitutively expressed and interferon (IFN) induced [69]. Tetherin-enriched filaments physically link virions to the surface of the plasma membrane as shown by

immune-electron microscopy [169]. Unfortunately, tetherin is counteracted by Vpu, an accessory HIV protein [69]. It was later shown that Vpu binds to tetherin and targets it to the ER-associated degradation (ERAD) pathway and lysosomal degradation pathway [170, 171]. As well as HIV-1, tetherin is able to restrict other retroviruses such as equine anemia virus (which interestingly counteracts it via the viral Env) [172], foamy virus [173] as well as filoviruses such as Ebola virus [174].

1.10.5 SAM domain and HD domain-containing protein 1: SAMHD1.

Even though dendritic cells play an important role in viral persistence, HIV-1 is not able to replicate efficiently in dendritic cells [175]. The explanation could be partly due to the restriction exerted by SAM domain and HD domain-containing protein 1 (SAMHD1) [176]. Soon after the discovery, Lahouassa et al., showed that the mechanism by which SAMHD1 restricts HIV-1 is by depleting the pool of deoxynucleosides triphosphates (dNTPs) required for DNA synthesis during reverse transcription and can be counteracted by the virion-packed SIV/HIV-2 accessory protein Vpx [177, 178]. Interestingly, SAMDH1 must be in the nucleus to be degraded by Vpx even though its main antiviral function takes place in the cytoplasm [179]. The antiviral activity of SAMHD1 is regulated by phosphorylation by Cyclin A2/CDK1 [180].

1.10.6 Cyclin-dependent kinase inhibitor: p21

The Cyclin-Dependent Kinase 1 inhibitors, (CKI) $p21^{Cip1/Waf1}$ is known as p21 and restricts HIV-1, SIV and HIV-2 infection in macrophages. Importantly, p21 restricts infection in haematopoietic stem cells [181]. A novel function of p21 has recently been described as part of its HIV antiviral mechanism by which p21 also depletes the pool of dNTPs impairing reverse transcription [182].

1.10.7 Myxovirus resistance 2 (MX2 or MxB) protein

A recently discovered restriction factor is the human dynamin-like, myxovirus resistance 2 (MX2 or MxB) protein [183]. MX2 is interferon-induced and potently inhibits X4 and R5 HIV-1 strains, modestly inhibits SIV and has no effect on MLV, E1AV or FIV[183]. Specificity of action is determined by CA and causes nuclear accumulation and integration defects of viral cDNA [183, 184]. HIV-1 is able to escape MX2 restriction through an Alanine mutation in CA which abolishes the ability of CA to binding by Cyclophillin A, suggesting a role of Cyclophillin A in MX2 restriction [184]. Most recently, Fricke et al., showed that MX2 binds to core and prevents uncoating[185].

1.10.8 RNA-associated Early-stage Anti-viral Factor: REAF.

One of the most potent restriction factors discovered recently is the RNA-associated Early-stage Anti-viral Factor, also known as RPRD2 [186]. RPRD2 is a cellular protein with unknown function that is potent against HIV-1, HIV-2 and different SIV strains with a restriction potency of >50 fold that occurs during reverse transcription. Interestingly, REAF was shown to interact with viral RNA and/or DNA so it could be that this is the first restriction factor that actually targets the viral genome *per se* [186]. Viral challenge decreases REAF protein expression so it could be that it is counteracted by an HIV viral protein similar to Vif against APOBEC3G or Vpu against tetherin [186].

1.10.9 The Polymerase II-Associated Factor 1 Complex

The Polymerase-Associated Factor 1 (PAF1) was identified as a potent restriction factor against HIV-1 in the same siRNA screen that identified REAF [158]. Since PAF1 is subject of chapter 5, a review of the current knowledge on the discovery and cellular functions of PAF1 and its involvement in viral infection will be outlined here.

1.10.9.1 Discovery of Polymerase II-Associated Factor 1 in humans

During gene transcription, initiation factors that recognize gene promoters bind to the C-terminal domain (CTD) of RNAPII. The RNAPII CTD has a $Y_1S_2P_3T_4S_5P_6S_7$ repeat where the Ser5 and Ser7 become phosphorylated by Kin28 which is part of the TFIIH initiation factor [187]. As elongation proceeds, Ser2 becomes phosphorylated by Ctk1 and Bur1 kinases to allow association of other elongation factors with RNAPII [188]. Phosphorylation of Ser2 allows association of RNA splicing factors and polyadenylation enzymes which causes the nascent RNA to be spliced, polyadenylated and cleaved.

To understand if additional proteins associate with RNAPII during transcription, an antibody directed against the C-terminal domain (CTD) of the *Saccharomyces cerevisiae* RNAPII and the complex was affinity purified [189]. These studies revealed that PAF1 (Polymerase-Associated Factor 1) and CDC73 (Cell Division Cycle73), two proteins involved in gene expression, interact with RNAPII [190]. Subsequent studies showed that in addition, LEO1, CTR9 and RTF1 are part of the yeast Polymerase-Associated Factor 1 complex (PAF1c) [191]. CTR9 was first described through its link to cell cycle regulation by regulation of G1 cyclin genes [192] and RTF1 was shown to be involved in TATA-box site selection and transcription elongation [193, 194].

The PAF1c has also been shown to bind to RNAPII in higher eukaryotes including human, *Drosophila*, mouse and plants such as *Arabidopsis thaliana* [195]. The human PAF1c has an additional component, SKI8/WDR61, which together with SKIV2L and TTC37 constitutes the trimeric Superkiller complex (SKIc) [196, 197]. The human SKIc is directs RNAs to the exosome which plays a role in mRNA surveillance and degradation [198]. Within the PAF1c, chromatin immunoprecipitation (CHIP) experiments show that SKI8 is present at transcriptionally active genes and that recruitment is PAF1c-dependent

suggesting a new role for PAF1 downstream of transcription, in mRNA quality control and surveillance [196]. However, there is still no additional structural or functional information of the role of SKI8 in the PAF1c functions. Indeed, the structural information regarding PAF1c assembly is limited. The crystal structure of the C-terminal domain of CDC73 revealed a Ras-like domain that promotes recruitment of the PAF1c to chromatin [199]. In addition, Amrich. et al., showed that mutations in the C-terminal domain of CDC73 and RTF1, caused a defect in transcription elongation suggesting that CDC73 might be the scaffold protein that interacts with RTF1 to promote RNAPII association [199]. RTF1 has also been shown to have a central domain, the ORF-Association Region also referred to as Plus3 domain, which promotes recruitment of PAF1 complex to the chromatin [200]. In addition, NMR studies showed that the RTF1 Plus3 domain has a DNA binding domain similar to the domain of DNA which unwinds during transcription [201] which further reinforces the central role of RTF1 in DNA binding of the PAF1c. As to inter-subunit interactions, a recent study mapped the minimal regions of direct interaction of PAF1 and LEO1 and resolved the crystal structure of these regions [202]. Through CHIP strategies using human Myc-tagged constructs of the PAF1c subunits, Chu. et al., showed that Myc-LEO1 only co-precipitated with PAF1 suggesting that LEO1 binds to the PAF1c through PAF1 [202]. In addition, the authors showed that PAF1 co-precipitated with CTR9, SKI8 and cdcd73 and that the scaffold linking protein was CTR9. The interaction studies obtained thus far allows the following model of PAF1c (Figure 1.9).

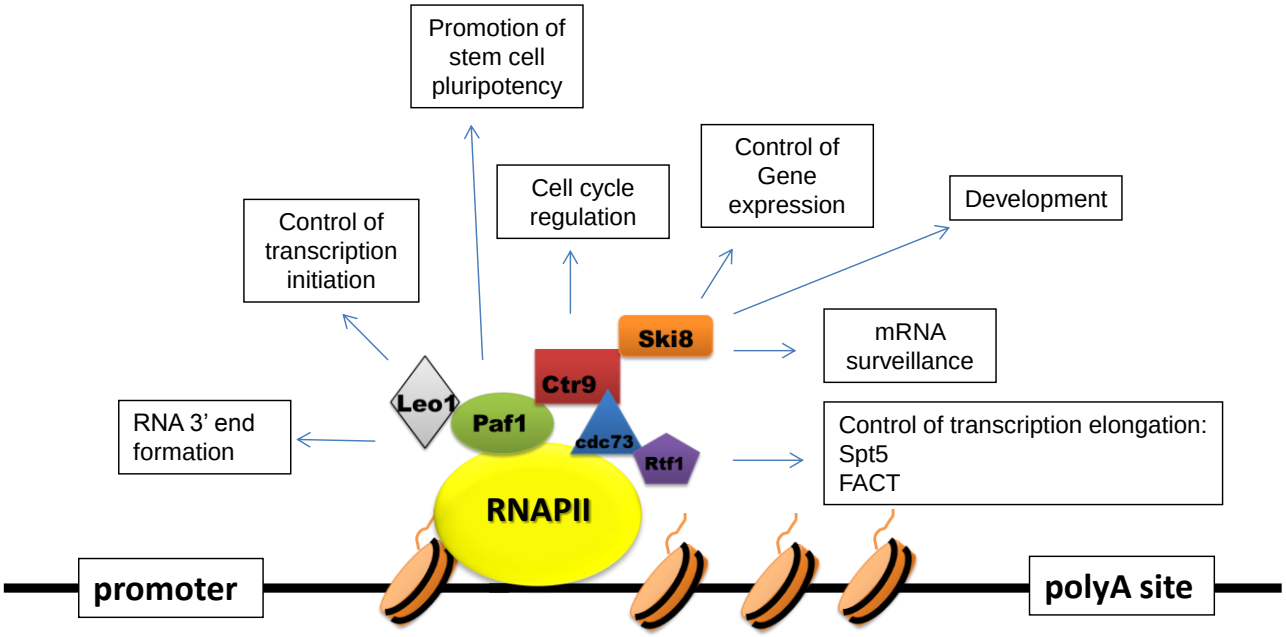

Figure 1.9 Model of human PAF1c and known cellular functions. Schematic representation of the PAF1c which binds to RNAPII. RNAPII is shown bound to DNA (black) which is packaged around histones (orange). The known PAF1 function are outlined according to the current knowledge**.** Adapted from [195].

The FACT complex (Facilitates Chromatin Transcription), which has a role in transcription elongation, also interacts with PAF1c [203] and in doing so, it monoubiquitinates histone H2B, important in displacement of the nucleosomal barrier [204]. Apart from histone ubiquitination, PAF1 has also been shown to have an influence on other histone modifications which regulate gene expression, for example CDC73 is required for H3K36-Me3 and H3K4-Me3 [205] Furthermore, PAF1C has a role in RNA 3' formation. Both yeast and human PAF1 component depletions have been shown to decrease polyA mRNA length [206, 207]. In addition the hPAF1C has been shown to interact with factors involved in RNA processing such as the homologous CPSF (Cleavage and Polyadenylation Specificity Factors) [205]. The yeast PAF1C has roles not only in processing of polyA mRNA transcripts but also in 3'-end processing of non-polyadenylated RNAs such as small nucleolar RNAs (snoRNAs) [208].

1.10.9.2 The role of PAF1 in viral infection

As obligate intracellular parasites, viruses have evolved to hijack the cell's machinery in order to replicate. Given the fine mechanisms by which PAF1c regulates transcription and gene expression, a role of PAF1c in control of viral gene expression has also been reported.

For instance, to efficiently transcribe the viral genome once integrated, HIV-1 requires the viral protein, Tat which, according to Sobhian *et al*., interacts with PAF1c and enhances transactivation [209]. Sobhian *et al*., purified Tat complexes and showed that Tat forms two functionally distinct complexes, Tatcom1 and Tatcom2. Tatcom1, the complex found to have enhanced CTD-kinase activity, was found to bind to PAF1, suggesting that it is directly involved in transcription elongation. Indeed, knockdown of PAF1 decreased Tat transactivation by 2- 5 fold. Importantly, CHIP showed that Tat recruits PAF1 and the additional components of the Tatcom1 complex to the TAR promoter region and these travel along with RNAPII. This therefore constitutes a first example of how HIV-1 may appropriate the transcription elongation function of PAF1c to enhance viral transcription. Most recently, in addition to HIV, human adenovirus (HAdV) Early Region 1A viral protein (E1A) has also been shown to recruit PAF1 to stimulate transcription and to regulate transcription-coupled histone modifications of HAdV early genes [210, 211]. Interestingly, influenza virus has been shown to usurp PAF1 activity [212]. In the search for proteins that bind to the influenza non-structural protein 1 (NS1) tail, Marazzi et al., identified a direct interaction of PAF1 with methylated and unmethylated NS1 tail. Importantly, PAF1 was shown to increase the expression levels of an array of genes involved in antiviral and pro-inflammatory responses upon influenza virus infection and IFN-β stimulation suggesting that NS1 might bind to PAF1 in order to halt this process.

The functions of PAF1 in viral infection so far described here, focus on viral hijacking of PAF1 to favour viral replication at late stages of infection. My group described the role of PAF1c in restriction of HIV-1 infection [158]. To identify novel restriction factors that may be involved in HIV-1 infection, Liu *et al*., performed a genome wide siRNA knockdown screen of 19,121 genes and identified 114 factors that significantly decrease HIV-1 infection [158]. Amongst the proteins identified were PAF1, LEO1, CDC73, RTF1 and CTR9. Knockdown of any of the five components of PAF1c rescued HIV-1 infection. Interestingly, knockdown of PAF1 also rescued infection of HIV-2 and SIV virus isolates, suggesting that PAF1 is a broad-acting antiviral factor against lentiviruses. In addition, overexpression of a PAF1-HA construct inhibited HIV-1 infection further confirming the antiviral function of PAF1. Importantly, PAF1 was shown to be expressed in primary macrophages and CD4+ T-cells, two of the main cellular targets of HIV-1 [47]. Most recently, PAF1, CTR9 and RTF1 have been shown to be upregulated upon Peripheral Blood Mononuclear Cell (PBMC) activation [213]. Increased levels of PAF1 and RTF1 in activated PBMCs correlated with decreased HIV-1 infection which further supports a role of PAF1 as a HIV-1 restriction factor in primary cells [213].

Elite controllers are defined as untreated HIV-1 infected patients that control viremia to undetectable levels in blood [214]. The mechanisms underlying why elite controllers sustain a virological response have been the subject of extensive study [215]. A recent comparative study of the expression levels of known restriction factors from elite controllers and ART-supressed patients, showed that CTR9 is elevated in elite controllers further supporting the role of the PAF1 complex in control of HIV-1 infection [216]. However the mechanism by which it inhibits HIV and other retroviruses is still unknown.

Chapter 2. Materials & Methods

2.1 Materials: Reagents and antibodies

Table 2.1. List of reagents employed classified by protocol and brand.

Reagent	Protocol	Brand
Agarose	DNA preparation	Sigma
Ampicillin	Bacterial culture	Sigma
AZT	Drug-virus assay	Sigma
CellTiter 96® Aqueous One Solution Cell Proliferation Assay (MTS)	Cytotoxicity assay	Promega
DharmaFECT cell culture reagent	Transfection	Dharmacon, Thermoscientific
DharmaFECT reagent 1 and reagent 4	siRNA screen	Dharmacon, Thermoscientific
DMF	p24 staining/β-gal staining	Acros Organics
DMSO	Drug diluent	Sigma
Dulbecco's Modified Eagle Medium	Cell culture	Sigma
ECL Prime	Western-blot	GEHealthcare
EDTA	Transfection	Life Technologies
EHT1864	Drug-virus assay	Tocris
Fetal Bovine Serum	Cell culture	Biosera Laboratories International
G418	Cell culture	Fisher Scientific
Hiperfect	Transfection	Qiagen
Kanamycin	Bacterial culture	Sigma
Lipofectamine 2000	Transfection	Invitrogen
Luria Bertani buffer	Bacterial culture	Fisher Scientific
Maxiprep kit	DNA preparation	Qiagen
Methanol	Imaging	Fisher Scientific
MG132	Drug-virus assay	Sigma
Nitrocellulose membranes	Western-blot	Life Technologies
NP40	Cellular fractionation	Pierce
NSC23766	Drug-virus assay	Tocris
Optimem-I	Transfection	Life Technologies
Paraformaldehyde	Imaging	Acros Organics
Penicillin-Streptomycin	Cell culture	Sigma
Phosphate Buffer Saline	Cell culture	Sigma
Polyethylenimine, JetPEI	Transfection	Polyplus
Pre-plated siRNA screen plates	siRNA screen	Dharmacon, Thermoscientific
Protease inhibitors	Western-blot	Complete, Roche Applied Sciences
Restriction enzymes	DNA preparation	New England Biolabs
RNAse-free water	siRNA screen	Qiagen
RPMI(+)L-glutamine	Cell culture	Gibco, Invitrogen
Running buffer	Western-blot	Life Technologies
SDS	Cellular fractionation	Pierce
siGLO-red	siRNA screen	Dharmacon, Thermoscientific
Sucrose	Cellular fractionation	Pierce
Transfer buffer	Western-blot	Life Technologies
8%-Tris-Bis NuPage gel	Western-blot	Life Technologies
Triton X-100	Imaging	Sigma
Trypsin-EDTA (0.05%), phenol red	Cell culture	Life Technologies
Vectashield-DAPI	Imaging	Vectorlab
X-gal	p24 staining/β-gal staining	Melford
X-gal buffer	p24 staining/β-gal staining	Melford

Table 2.2. List of antibodies employed.

Target	Antibody brand	Number
Acetylated α-tubulin	SCBT	23950
IgG Alexa Fluor®555	Abcam	ab150110
IgG DyLight®488	Abcam	ab98488
GAPDH	Abcam	128915
Hemagglutinin	Abcam	1208
Histone3	Abcam	1791
p24	NIBSC, UK	EVA365 and 366
PAF1	Abcam	20662
Recombinant Soluble Human CD4 (sCD4)	NIH AIDS Reagent Program, Division of AIDS, NIAID, NIH: Soluble Human CD4 from Progenics	#4615
α-Tubulin	SCBT	H-300

2.2. Methods

2.2.1 DNA preparations.

2.2.1.1. DNA production

DNA was amplified by heat shock transformation of *E.Coli* DH5-α cells[217]. An aliquot of *E.Coli* DH5-α cells (kindly provided by Kelly Marno) were thawed on ice for 5 minutes. 1 ng of DNA (quantified using a NanoDrop 1000 spectrophotometer) was incubated with 40 µl of *E.Coli* DH5-α cells on ice for 10 minutes. Cells were then heat shocked at 42°C for 110 seconds and incubated for 10 minutes on ice. The transformed cells were then incubated with 300µl of Luria-Bertani (LB) (Fisher Scientific) media at 37°C shaking in an automatic shaker for one hour. 150 µl of transformed cells were then plated onto agar

plates containing ampicillin at 100 µg/ml for antibiotic resistance selection. Plates were incubated overnight at 37°C. Colonies were then picked and incubated in 5ml of LB-antibiotic and incubated for 8 hours in a room at 37°C. The cultures were then diluted into 200ml of LB-antibiotic and incubated overnight in a room at 37ºC. DNA was extracted using a QIAGEN Maxiprep Kit according to manufacturer's instructions.

2.2.1.2. Agarose gel electrophoresis and restriction digest of DNA

Size of DNA was analysed by restriction enzyme digestion using 10 units of restriction enzyme (NEB) per reaction with appropriate buffer and Bovine Serum Albumin if required, followed by incubation in a water bath at 37°C for 1hr. Digest products were visualized on a 0.8% agarose (Sigma) gel which was run for 1 hour at 100V.

2.2.2. Cellular fractionation

To purify the nuclear and cytoplasmic fractions of HeLa-CD4+ cells, cells were seeded at $2x10^5$ cells/ml in 6-well dishes (ThermoScientific, Nunclon). 24 hours after seeding, cells were washed with Phosphate Buffer Saline (PBS) (Sigma) and harvested from the plate using a cell scraper (three wells/fraction). Cells were pelleted at 1000 rpm for 5 minutes. Cells were pipette-resuspended and put on ice to avoid protein degradation in cold swelling buffer (see table 1) and incubated for 5 minutes. 0.1% NP40 (Pierce) was added to lyse the cell membrane without lysing the nuclei and incubated on ice for one minute. Lysates were then centrifuged at 1000 rpm, 4ºC for 5 minutes.

The supernatant, containing the cytoplasmic fraction, was then transferred to a new Eppendorf tube. The cytoplasmic fraction was centrifuged for 5 minutes at 1500 rpm to pellet nuclei contamination. 1% sodium dodecyl sulphate (SDS)-PBS was added to solubilize cytoplasmic membranes (such as Golgi or endoplasmic

reticulum (ER) membranes) and incubated for 5 minutes at room temperature. The cytoplasmic fraction was then pelleted and the supernatant was transferred to a new Eppendorf and stored at -80ºC until required.

The pellet of nuclear fraction was resuspended in 1ml of solution 1 (Table 2.3). It was then layered onto 1 ml of solution 2. As shown in table 1, solution 2 has a higher concentration of sucrose than solution 1 and so together, both solutions form a concentration gradient. The purpose of the sucrose gradient is to purify the nuclear fraction which is high in molecular weight from the cytoplasmic fraction which is lower in molecular weight (Figure 2.1). Cells were then centrifuged for 10 minutes at 3500 rpm at 4ºC. Upon centrifugation, the nuclear fraction migrates and is pelleted, whilst the cytoplasmic fraction, which is lighter, migrates to solution 1. After centrifugation, solutions 1 and 2 were discarded and the pellet with nuclei was resuspended in 1x RIPA buffer (described in section 2.2.10.) with protease inhibitors (Complete, Roche). Lysates were then centrifuged to pellet nuclear membranes and the supernatant was transferred to a new Eppendorf before being stored at -80ºC prior to Western-blot analysis (described in section 2.2.10).

SWELLING BUFFER		
Stock	**Volume/ml**	**Final concentration/mM**
1M HEPES, pH 7.9	0.1	10
1M $MgCl_2$	0.015	1.5
2.5M KCl	0.04	10
1M DTT	0.005	0.5
dH2O	up to 10ml	
SUCROSE GRADIENT SOLUTION 1		
Stock	**Volume/ml**	**Final concentration/mM**
2.5M sucrose	1.96	0.25
1M $MgCl_2$	0.2	10
dH_2O	up to 20ml	
SUCROSE GRADIENT SOLUTION 2		
Stock	**Volume/ml**	**Final concentration/mM**
2.5M sucrose	5.5	0.35
1M $MgCl_2$	0.02	0.5
dH_2O	up to 40ml	

Table 2.3. Buffers used in the cellular fractionation protocol to purify cytoplasmic and nuclear fractions.

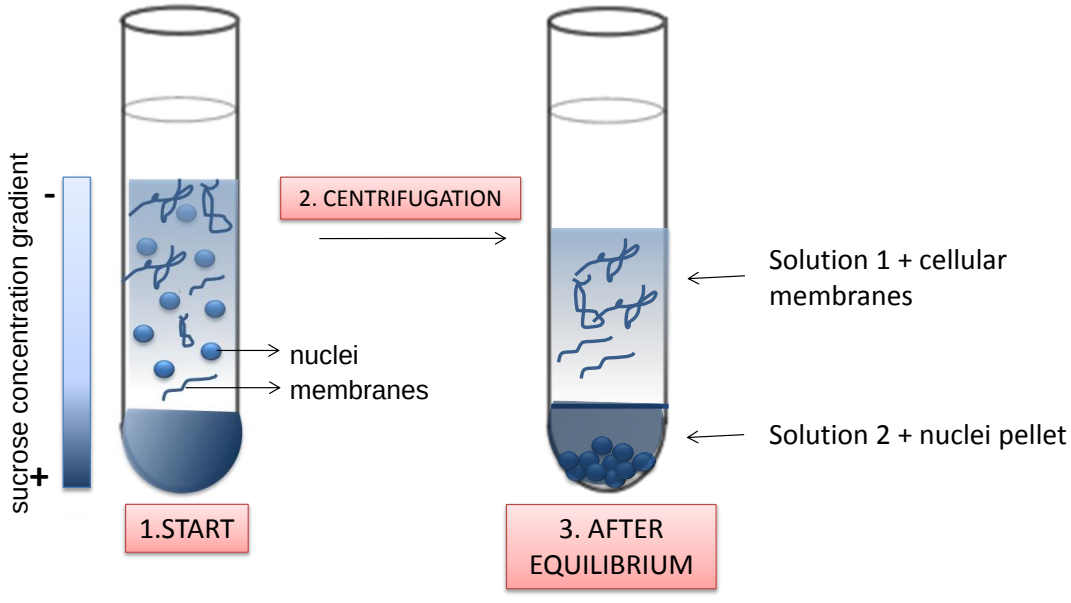

Figure 2.1. Sucrose gradient to purify nuclei from cellular membranes. A sucrose gradient is established with the heavier and most concentrated solution lying at the bottom of the falcon tube and the lighter and most diluted solution lying at the top portion of the falcon tube. After centrifugation, heavy nuclei remain in the most concentrated sucrose gradient forming a pellet and the lighter cellular membranes remain at the top within the most diluted solution.

2.2.3 Cells

The adherent cell lines that were employed consist of HeLa-CD4$^+$ [218], TZM-bl [219] and 293T cells[220]. Cells were grown in Dulbecco's Modified Eagle Medium (DMEM) (Sigma) with 1% penicillin-streptomycin (PAA), 10% fetal bovine serum (FBS) (Biosera Laboratories International) at 37ºC and 5% CO_2 conditions. HeLa-CD4$^+$ and TZM-bl cells are derivatives of the HeLa cervical cancer cell line. HeLa-CD4+ cells are a derivative of HeLa cells which stably express CD4+ after infection with a retroviral vector [221]; HeLa-CD4$^+$ cells express CD4 under the control of HIV-1 long terminal repeat and are grown in the presence of 1mg/ml of G418 (32). They also express naturally CXCR4 and CCR5 and since these are the receptors and co-receptors for entry of HIV, they are a widely used cell line in the HIV field. TZM-bl express cell surface CD4, CXCR4 and CCR5 and in addition, have Tat-inducible luciferase and β-galactosidase reporter genes.

The suspension cell lines used in this project were Jurkat,[222] and PM1[223, 224] cell lines. Jurkat and PM1 cells are derived from T-cells and naturally express CXCR4 and CXCR4/CCR5 respectively. Cells were grown in RPMI(+)L-glutamine (Gibco, Invitrogen) supplemented with 1% penicillin-streptomycin (PAA) and 10% FBS (Biosera Laboratories International).

2.2.4 MTS cytotoxicity assays

EHT1864 (EHT) and NSC23766 (NSC) were diluted to 10mM in dimethylsulfoxide (DMSO) (Sigma), aliquoted and stored in dark conditions at -20°C.

To characterise the cytotoxic profile of these inhibitors, a cytotoxic assay was performed in Jurkat and PM1 cells. For this purpose, 4x10^3 cells/well were seeded in 96-well plates (ThermoFischer, Nunclon). Cells were incubated

overnight at 37ºC. Serial dilutions of EHT and NSC from 50µM to 3.125 µM were prepared in in RPMI(+)L-glutamine (Gibco, Invitrogen) supplemented with 1% penicillin-streptomycin (PAA) and 10% FBS (Biosera Laboratories International) . Similarly, in parallel, as a control, serial dilutions of DMSO were prepared. The purpose was to assess the toxicity effect of DMSO since the compounds had been diluted in 100% DMSO. Cells were incubated at 37ºC for 48 hours post-addition of drugs/DMSO dilutions. A cytotoxic assay was performed using the colorimetric assay, CellTiter 96® Aqueous One Solution Cell Proliferation Assay (MTS) (Promega). In this assay, cell viability is proportional to the ability of cells of metabolically processing a tetrazolium salt, MTS to formazan, a purple compound which can be measured at 490nm [225] using a BMG FLUOstar OPTIMA Microplate Reader. Thus, after incubation of cells with DMSO, EHT and NSC for 48 hours, 20 µl of Aqueous One solution (Promega) were added to each well. Cells were incubated for one hour at 37ºC in dark conditions and absorbance was read at 490nm. Previously, the cytotoxic profile of EHT and NSC in TZM-bl cells had been characterised (Appendix 2).

2.2.5 Virus production and HIV-1 detection of infection

2.2.5.1 Production of single round infectious pseudovirus stocks in 293T cells

Single round infectious pseudovirus particles were produced by transfection of 293T cells with a plasmid encoding HIV-1 NL4.3 or HIV-1 BaL envelopes and a genomic plasmid, TN6stop [226], which encodes a GFP reporter gene. For this purpose, $4x10^6$ cells were seeded in 10-cm dishes. Cells were incubated overnight at 37ºC. A total of 1.5 µg of the envelope and the genomic plasmid were transfected using polyethylenimine (PEI, Polyplus) in a 1:3 ratio in a total transfection volume of 100µl in media. Each transfection reaction was incubated at room temperature for 20 minutes and then added to each 10-cm dish. Cells were incubated at 37ºC for 48 hours post-transfection. The supernatant was then

pelleted at 1,500 rpm, room temperature, aliquoted in cryovials and frozen at -80ºC. Replication competent HIV virus stocks were prepared using the same protocol. Virus titres obtained by this method ranged from $5x10^3$ to $7x10^5$ focus forming units per ml (ffu/ml) measured as described in section 2.2.5.3.

2.2.5.2. Production of replication-competent HIV-1 in C8166 cells

The human umbilical cord blood lymphocyte cell line, C8166, was used to produce HIV-1 89.6 full length, replication competent virus. For this purpose, $2x10^6$ cells were pelleted at 1000 rpm for 5 minutes. Cells were resuspended at $1x10^5$ ffu/ml of HIV-1 89.6 virus kindly provided by Kelly Marno and originally obtained from the Centre for AIDS Research (NIBSC, UK). Cells and virus were incubated at 37ºC for 2 hours, at which time they were seeded upright in a T25 flask with an extra 5ml of RPMI-10%FCS. Two days after infection, upon visualization of syncytia (indicates high titer virus), $2x10^7$ cells were added. 24 hours after incubation at 37ºC, cells were pelleted in a 50ml falcon at 3,500 rpm. The supernatant was aliquoted into 0.5ml aliquots and frozen in liquid nitrogen.

Full replication-competent HIV-1 NL4.3 and BaL (chapter 5) were kindly provided by Kelly Marno. The production protocol was the same as described above in PM1 cells.

2.2.5.3. Detection of infection by *in situ* staining for β- galactosidase in TZM-bl cells

TZM-bl cells have a HIV Tat-inducible β-galactosidase gene, which provide a convenient method to calculate the number of virus particles/ml in a virus stock solution. When TZM-bl cells are infected by a single round infectious virus β-galactosidase expression is induced by HIV Tat and by reaction with its substrate, 5-bromo-4-chloro-indolyl-β-D- galactopyranoside (X-gal), β-galactosidase hydrolyses X-gal into galactosidase (colourless) and 4-chloro-3-

brom-indigo which forms a blue precipitate [227], thus allowing the count of infected cells.

A total of $4x10^3$ cells/well were plated in 96-well plates and incubated overnight at 37ºC. An aliquot of each virus stock was thawed for 5 minutes in a water bath at 37ºC. Serial dilutions (1:5) were performed and 100 µl of each virus dilution were added per well. Cells were then incubated at 37ºC for 48 hours.

To fix and stain TZM-bl cells, media was discarded from each well. Cells were then washed twice with 100 µl 1x PBS (PAA) and fixed with 50µl/well of 3.7% formaldehyde for 5 minutes at room temperature. The formaldehyde was discarded and cells were washed twice with 100 µl 1x PBS. A 1 mg/ml solution of X-gal (Melford, MB1001;) in X-gal buffer (consisting of 5mM Potassium Ferricyanide Crystalline, 5mM Potassium Ferricyanide Trihydrate and 2mM Magnesium Chloride in PBS) was prepared from a 80 mg/ml stock solution in dimethylformamide (DMF) and 100µl/well was added. Cells were incubated for 4 hours at 37ºC. Foci of cells were counted and focus forming units/ml were calculated for each virus stock.

2.2.5.4. Detection of infection in Jurkat and PM1 cells

Pseudovirus stocks have a GFP reporter gene so infection of Jurkats and PM1 cells is monitored by flow cytometry through the detection of GFP-positive cells. Jurkat and PM1 cells were fixed 48 hours-post infection by overlaying cells onto 2ml of 3.7% formaldehyde, incubating at room temperature for 5 minutes in 10ml falcon tubes (BDBiosciences). Cells were then pelleted at 1,500 rpm for 5 minutes at room temperature, the supernatant discarded and cells resuspended in 250µl of 1x PBS. Cells were then analysed by flow cytometry using a Becton Dickinson FACScan Analyser fitted with an Argon laser (488nm) and CellQuest software, (Becton Dickinson, San Jose, USA).

2.2.5.5. Determination of focus forming units by *in situ* immunostaining for p24 antigen

To calculate the virus infectivity of the HIV-1 89.6 virus stocks HeLa-CD4+ cells were seeded at 7x104 cells/ml in 48-well plates. Cells were infected, in duplicate, by addition of neat virus and successive 1:5 virus dilutions in DMEM-10% FCS (with no antibiotic added). Cells were incubated with the virus dilutions for two hours at 37ºC, after which media was replaced with DMEM- 10%FCS. Infected cells were incubated for 48 hours at 37ºC. At 48 hours post-infection, cells were fixed with a cold 1:1 acetone:methanol solution (stored at -20ºC) for 10 minutes. Cells were quickly washed twice with PBS to remove any acetone-methanol excess and cells were then incubated with anti-p24 antibody. The monoclonal antibodies to p24 (EVA365 and 366) were provided by the EU Programme EVA Centre for AIDS Reagents, NIBSC, UK (AVIP Contract Number LSHP-CT-2004-503487). at 1:50 in 1%FCS-PBS for 1 hour. Cells were then washed three times with PBS. Cells were then incubated with anti-mouse β-galactosidase antibody at 1:400 in 1%FCS-PBS for 45 minutes. Cells were then washed three times with PBS. Cells were then incubated with X-galactosidase substrate at 1:80 in dimethylformamide (DMF, Acros Organics), overnight at 37ºC. 24 hours post-incubation, blue focus forming units were counted and virus infectivity per ml of virus was calculated. Viruses produced by the method described in section 2.2.5.2 ranged from 1x104 to 9x104 ffu/ml.

2.2.6. Drug-virus inhibition assays

2.2.6.1. Drug-virus assay in TZM-bl cells

TZM-bl cells were seeded at $4x10^3$ cells/well in 96-well plates and incubated for 24 hours at 37ºC. EHT and NSC were diluted in DMEM supplemented with 1% penicillin-streptomycin (PAA) and 10% fetal bovine serum (FBS) (Biosera

Laboratories International) according to the concentrations found not to be significantly toxic in the cytotoxic assay (described in section 2.2.4.) Similarly, as a control, DMSO was diluted in media. Each drug/DMSO dilution was then added in triplicate (100µl/well). Treated cells were incubated for 24 hours. Virus dilutions of pseudovirus stocks HIV-1 NL4.3 and BaL (produced as described in 2.2.5.1) were prepared in DMEM supplemented with 1% penicillin-streptomycin (PAA) and 10% fetal bovine serum (FBS), according to the results of the virus titrations (described in 2.2.5.3) to achieve an infection rate of 1000 ffu/ml (50µl/well). Cells were incubated for 48 hours at 37ºC. Cells were then fixed and an X-gal staining was performed as described in section 2.2.5.3.

2.2.6.2. Drug-virus assays in Jurkat and PM1 cells

Jurkat and PM1 cells were seeded at $4x10^3$ cells/well in 96-well plates and incubated for 24 hours at 37ºC. EHT and NSC were diluted in RPMI supplemented with 1% penicillin-streptomycin (PAA) and 10% fetal bovine serum (FBS) (Biosera Laboratories International) according to the concentrations found not to be significantly toxic in the cytotoxic assay (described in section 2.2.4) and added in duplicate (50µl/well). Cells were incubated at 37ºC for 24 hours. Neat HIV-1 NL4.3 and BaL was added (100µl/well). Cells were incubated for 48 hours, pelleted at 1,500 rpm, resuspended in PBS and analysed by flow cytometry in a Becton Dickinson FACScan instrument.

2.2.6.3. Virus infection time-course.

HeLa-CD4+ cells for imaging were seeded directly onto microscope coverslides (12mm diameter, VWR), at $7x10^4$ cells/ml. To prepare the microscope coverslides before cell seeding, slides were sterilised by immersion in 100% industrial methylated spirit (Ranson) and sterile water (Fisher) and placed into wells of a 24 well dish (Nunclon). In parallel, cells were seeded for Western-blot

analysis at 4x 10^5 cells/ ml in 6-well dishes. Cells were incubated for 24 hours at 37ºC. After incubation, cells seeded on coverslides and on 6-well trays, were incubated with DMEM media or anti-CD4 antibody (recombinant soluble human CD4 (sCD4), #4615**) for one hour. Cells were then infected with full-length replication competent HIV-1 89.6 for 30 minutes, 1 hour and 5 hours. To fix cells after infection, each time point coverslip was immersed into a 4% PFA for 30 minutes, after which they were washed with PBS ready for staining as described in section 2.2.9.3.

** Recombinant soluble human CD4 was obtained through the NIH AIDS Reagent Program, Division of AIDS, NIAID, NIH: Soluble Human CD4 from Progenics.

2.2.7. Transfections

2.2.7.1 JetPEI DNA transfections of HeLa-$CD4^+$ cells

HeLa-$CD4^+$ cells were seeded at 3.0x 10^4 cells/well in a final volume of 0.5ml per well, in 8-chamber microscope slides (BDFalcon). Cells were incubated overnight at 37ºC. Media was discarded and replaced with 200 µl/well of fresh media. Cells were transfected at a 1:3 ratio of DNA:PEI (JetPEI, Polyplus). Transfection of 320 ng DNA/ transfection was performed in a final volume of 4 µl. Cells were incubated for 48 hours, at which time cells were fixed and stained as described in section 2.2.9.2.

2.2.7.2. Lipofectamine DNA transfections of HeLa-$CD4^+$ cells and HIV-1 infection.

HeLa-$CD4^+$ cells were also transfected with Lipofectamine (Invitrogen). For this purpose, a 3µl of Lipofectamine was diluted in 50µl of Opti-MEM I (Life Techonologies) in an Eppendorf. In parallel, 1µg DNA was diluted in 50 µl of

Optimem-1. After 20 minutes the Lipofectamine and DNA dilutions were combined and incubated for 20 minutes at room temperature. HeLa-$CD4^+$ cells were plated at 4 x 10^5 cells/ml in 12-well dishes, a high concentration because Lipofectamine is highly toxic. After incubation, the DNA-Lipofectamine complexes were added to the cells dropwise and incubated for 4 hours at 37ºC. Cells were incubated with 5mM Ethylenediaminetetraacetic acid (EDTA)-PBS to harvest them from the plate at 4 hours post transfection and diluted 1:2 into a new 12-well to avoid over confluence. Cells were incubated for 24 hours at 37ºC and 5% CO_2 conditions. After incubation, cells were infected with HIV-1 89.6 (100 FFU/well) with stocks that had been previously titrated (as described in section 2.2.5.5.). Cells were incubated for 4 hours at 37ºC, at which time media was changed. Cells were then incubated for 48 hours, before being fixed and p24-immunostained as described in 2.2.5.5.

2.2.7.3 Transient PAF1-siRNA knockdown

PAF1-small interfering RNA (siRNA) (QIAGEN, cat number 5105107606) was diluted in 0.57µl HiPerfect (QIAGEN) and 14.2 µl OPTImem (Life Technologies) at a final siRNA concentration of 0.15 µM. The lipid/siRNA mix was incubated at room temperature for 30 minutes. Meanwhile HeLa-CD4+ cells were counted and diluted to a final concentration of 2.2 x 10^4 cells/ml. Cells were plated in a 48-well plate, 0.2ml/well in DMEM-1%FCS media (Biosera Laboratories International, Sigma). The lipid/siRNA mix was added dropwise. Cells were incubated for 4 hours, at which time media was replaced with DMEM-10%FCS-1%penicillin-streptomycin. Cells were incubated at 37ºC for 72 hours, when they were fixed and stained as described in section 2.2.9.3.

2.2.8 siRNA screen

2.2.8.1. Optimisation of siRNA screen

To assess the transfection efficiency of siRNA in TZM-bl cells, siGLO Red was transfected using two candidate transfection reagents: Dharmafect tranfection reagent 1 and Dharmafect transfection reagent 4 (Dharmacon, Thermo Scientific). Since siGLO-Red has been modified to have a 557 (excitation wavelength) fluorophore attached, detection of fluorescence emission wavelength at 570 nm allows it to be conveniently visualized using a fluorescent microscope such as the Zeiss 510 confocal microscope. In this manner the internalized siRNA is detected and approximate transfection efficiencies can be calculated.

For this purpose, TZM-bl cells were counted and diluted to a cell density of 5 x 10^4 cells/ml. siGLO was diluted initially in RNase-free water (QIAGEN) to a concentration of 10µM and further diluted to 500nM in antibiotic-free media. Transfection reagents were diluted (1:200) in antibiotic-free media. A volume of 10µl of 500nM siGLO was combined with 10 µl of diluted transfection reagent per transfection, mixed gently and incubated for 20 minutes at room temperature. After incubation, addition of 80 µl of media per transfection further diluted siGLO to 50nM. The combination of siGLO and transfection reagent (100µl) was added per well in a 96-well plate and cells were incubated for 48 hours at 37ºC. Cells were then fixed as described in 2.2.9.2 ready for confocal imaging. Images were performed in a Zeiss 510 microscope using 40x/63x lenses and a 561 multi-beam splitter (to excite siGLO red) and 405 multi-beam splitter (to excite nuclear staining, 4',6-diamidino-2-phenylindole, (DAPI)).

2.2.8.2. siRNA knockdown of GAPs and GEFs

To investigate the role of GTPase Activating Proteins (GAPs) and Guanine Nucleotide Exchange Factors (GEFs) in HIV-1 NL4.3 and HIV-1 BaL infection, an infectivity assay was performed in TZM-bl cells with individual knockdowns of 145 genes encoding the Rho GTPase GAPs and GEFs modulators (targets included are listed in Appendix 3 and individual sequences of each siRNA employed can be found as supplementary material in the electronic version). For this purpose custom-made 96-well plates were purchased from Dharmacon Thermo Scientific. The plates included 4 single siRNAs per gene screened, pre-seeded into each well. In addition, four Dharmacon ON-TARGETplus® Non-Targeting siRNA control pools and one Dharmacon ON-TARGETplus® Cyclophilin B siRNA control pool were included. Moreover, four single siRNAs against CD4, CCR5 and CXCR4 were included as positive controls. Initially, the plates were equilibrated at room temperature for 20 minutes. Each siRNA was resuspended in DharmaFECT Cell Culture Reagent (DCCR) (Dharmacon, Thermoscientific) and reagent 1 (50 µl of reagent 1 was diluted in 6 ml of DCCR, 25µl/well). siRNA was left to rehydrate for 60 minutes at 4ºC. TZM-bl cells were counted and diluted to 5 x 10^4 cells/ml. 100 µl of the cell dilution were added per well. Cells were incubated for 48 hours at 37ºC. For each screen, viruses were diluted to 1ffu/µl and added into each well (50 ffu/well). HIV-1 NL4.3 HIV-1 NL4.3 was obtained from the Centre for AIDS Research (NIBSC, UK) and HIV-1 BaL was obtained from For this purpose, viruses had been titrated as described in 2.6.3. Cells were incubated for 48 hours post-infection at 37ºC. Cells were then fixed and stained using the X-gal assay as described in section 2.2.5.3. Blue cells were imaged using INCell machine Analyzer 1000 (GEHealthcare).

2.2.9 Imaging techniques

2.2.9.1. Transfection and imaging of Rac1 and Rac1 CA Raichu probes.

One of the methods by which spatio-temporal changes in Rho GTPase activity can be monitored at the single cell level is through the use of Raichu probes. Raichu probes encode the GTPase subject of study, a GTPase binding domain and two fluorochromes, yellow fluorescent protein (YFP) and cyan fluorescent protein (CFP) (see chapter 3, figure 3.5) [228]. After transfection of Rac1 into HeLaCD4+ cells by the method described in 2.2.7.1., cells were fixed by adding 100 µl of methanol at -20°C for 10 minutes. Cells were then washed twice in 1x PBS and mounted on coverslides with Vectashield (Vectorlab). Cells to be analysed were chosen on the basis of a normal elongated cytoplasm and intact nuclei. Only cells that displayed a strong signal in the YFP channel were analysed to avoid false positives. Bleaching parameters were adjusted to achieve a 90% bleach using a Zeiss 710 confocal microscope and images pre- and post-bleach were taken in the CFP and YFP channels using a 405 diode laser line and a 488nm Argon laser line respectively. Image analysis was performed with the AccPbFRET plugin v.3.16 [229] in the ImageJ MacBiophotonics (MBF) version (Rasband, W.S., ImageJ, U. S.NIH Maryland, USA, http://imagej.nih.gov/ij/, 1997-2011).

2.2.9.2. Immunostaining of HIV gp41 constructs and microtubules.

After transfection of constructs using JetPEI as described in 2.2.7.1, media was discarded and cells were washed once with 1x PBS. Cells were incubated anti-HA-FITC antibody (100µl/well) (Abcam1208) for 30 minutes at 4ºC at 1:100 in 1x PBS-1%FCS. Anti-rabbit FITC conjugated antibody at 1:500 (Abcam, 98488), 100µl/well was added. Cells were then incubated with the secondary antibody at 4ºC for 30 minutes. Cells were fixed and permeabilised with 100% methanol for 10 minutes at -20ºC. Cells were then washed once with 1x PBS-1%FCS. Cells

were then incubated with anti-tubulin (1:100), 100 µl/well at 4ºC for 30 minutes. Cells were then washed twice with 1x PBS-1%FCS and incubated with anti-mouse-Alexa 555 conjugated secondary antibody (1:500) for 30 minutes at 4ºC. Cells were then washed twice with 1x PBS-1%FCS. Chambers were removed from slides and mounted using Vectashield-DAPI stain diluted 1:2 in distilled water and sealed with nail varnish. Imaging was performed using a Leica DM5000B epi-fluorescence upright microscope keeping exposure and gain parameters constant in each experiment. Filter cubes included Rhodamine - Band Pass 560nM +/-20nM and DAPI – BandPass 400nM+/-20nM and FITC - Band Pass 490nM +/- 20nM. For each experiment, image acquisition settings were set with the lowest expression construct to avoid pixel saturation of the higher expressing constructs. Image analysis was performed with ImageJ MBF version (Rasband, W.S., ImageJ, U. S.NIH Maryland, USA, http://imagej.nih.gov/ij/, 1997-2011) using an automated threshold method to avoid bias. The cell perimeter of each cell analysed was selected using the free-hand drawing application of ImageJ MBF and mean integrated density of the acetylated tubulin was quantified in untransfected cells and in cells expressing the anchor, full length and truncated versions of the cytoplasmic tail constructs.

2.2.9.3. PAF1 and HIV-1 capsid immunostaining

Media was initially removed from seeded HeLa-CD4+ cells. Cells were washed with 500 µl 1% FBS/PBS. Cells were fixed with 200 µl 4% Paraformaldehyde for 30 mins at room temperature. Cells were then washed with 500 µl 1% FBS/PBS. Cells were then permeabilised with 100 µl 0.1% Triton X-100/PBS for 5 min at room temperature. Triton x-100 was then removed and washed with 100 µl 1%FBS/PBS. Cells were then blocked with 100 µl 0.25% BSA/PBS for 20 minutes at room temperature. Anti-PAF1 primary antibody was added at 1:80 (rabbit). Cells were then incubated at 4ºC for 1 hour with the primary antibody.

Cells were then washed twice with 1x PBS-1%FCS. Secondary antibody was added at 1:500 (anti-rabbit FITC conjugate) for 30 minutes at 4°C. For experiments in which double staining was performed including p24, cells were then incubated with anti-p24 (1:50) (EVA 365 and EVA366) for 1 hour at 4ºC. Cells were then washed three times with 1x PBS-1%FCS. Cells were then incubated with anti-mouse 555 (Abcam, 150110) for 30 minutes. Cells were then washed twice with 1x PBS-1%FCS and mounted on a slide using Vectashield-DAPI. Imaging was performed using a Zeiss 710 confocal microscope using the same exposure, gain and pinhole settings for each experiment. Lasers employed were a 405 diode laser line for DAPI, a 543 Helium/Neon laser line and a 488nm Argon laser line.

2.2.10. Western-Blot analysis

Cells to be analysed were harvested using a cell scraper into an Eppendorf. Cells were pelleted at 1,100 rpm for 5 minutes at room temperature. Cells were then lysed by addition of 100 µM per sample of 1x RIPA buffer (20 mM Tris-HCl (pH 7.5), 150 mM NaCl, 1% NP-40, 1% sodium deoxycholate, 2.5 mM sodium pyrophosphate, 1 mM β-glycerophosphate, 1 mM Na_3VO_4 with added protease inhibitors (Complete, Roche). Cells were incubated for 30 minutes on ice. Cells were then shaken in an automatic shaker for 1 hour in a room at 4ºC to ensure complete lysis. Lysates were centrifuged at 13000 rpm at 4ºC to pellet cellular membranes. Supernatants were then transferred to new Eppendorfs. Protein quantification was performed by Bicinchonic acid (BCA) (Pierce) according to manufacturer's instructions. Per well, 20 µg of protein was incubated with 4xloading buffer (4% SDS, 10% 2-mercaptoethanol, 20% glycerol, 0.0004% bromophenol blue and 0.125M Tris-HCl). Lysates in loading buffer were incubated at 70ºC for 10 minutes. Meanwhile, a 10-well 8%-Tris-Bis NuPage gel was rinsed with distilled water. The pre-cast gel was positioned into the running

tank with 1x MOPS-SDS running buffer (Lifetechnologies). Samples were loaded and run for 1.5 hours at 110V after which time the gel was set for transfer. The gel was positioned between two nitrocellulose membranes (Life technologies). Transfer was performed at 40V for 3 hours. The nitrocellulose membrane was then washed with 1x TBST (137 mM Tris-HCl, 2.7 mM KCl and 19mM Tris base, 1% Tween-20). The membrane was then blocked with 5% skimmed milk in 1x TBST. Membranes were then washed four times with 1x TBST for 15 minutes each at room temperature. The membrane was then incubated with anti-PAF1 (1:1000) (Abcam 20662) or anti-Glyceraldehyde 3-phosphate dehydrogenase (GAPDH) (Abcam 128915) antibodies in 5% milk overnight at 4ºC. Membranes were then washed four times with 1x TBST for 15 minutes each at room temperature. The membrane was then incubated with anti-rabbit-Horseradish Peroxidase (HRP) (Abcam 6721) for 1 hour in 5% milk. Membranes were then washed four times with 1x TBST for 15 minutes each at room temperature. The membrane was then developed using ECL Prime blocking reagent (Amersham) which reacts with HRP from the secondary antibody. This reaction between the secondary HRP antibody and the ECL reagent is a chemiluminiscent reaction which produces light. The light from this reaction is recorded onto a film using a CCD camera.

Band densitometry was measured using ImageJ MBF and results are presented as a ratio of integrated density normalized to loading control.

2.2.11 Statistical analysis

Each data population was assessed to understand if data points had a normal distribution using SPPS IBM software. When the data population followed a normal distribution, the statistical test applied to understand whether the differences observed were significant was the parametric Student t-test. When

the population did not follow a normal distribution, the statistical test employed was the non-parametric Wilcoxon Man-Whitney test.

Chapter 3. Investigating the role of HIV envelope signalling during cellular entry

3.1. Introduction

HIV entry: Env signaling pathways

To gain access into the cell, HIV-1 utilises the Env protein to bind to a primary receptor, CD4 [43] and a co-receptor either CXCR4 [46] or CCR5 [45, 230] (as described in section 1.7.1). HIV-1 strains that utilize CXCR4 as co-receptor for entry are named X4-tropic and those that utilize CCR5 are termed R5-tropic viruses [47]. Apart from binding to CD4 and a co-receptor for entry, the HIV Env-receptor/co-receptor interaction also serves to trigger signaling cascades that benefit the virus at early stages of infection [80, 231-233]. Env signaling can be triggered by various mechanisms.

Firstly, signaling can be induced via the Env protein interacting with CD4. CD4 has a central role in T-cell mediated immune responses. For instance, CD4 interacts with regions of class II Major Histocompatibility Complex and the T-cell receptor which in turn increases the interaction between the antigen presenting cell and the T-cell [78]. In addition, CD4 mediates T-cell receptor activation via phosphorylation of the src-tyrosine kinase, Lymphocyte-specific Kinase (Lck) [234]; this non-covalent interaction between CD4 and Lck, results in signaling pathways that promote T-cell proliferation, interleukin-2 (IL-2) transcription and calcium mobilization amongst other pathways (Figure 3.1) [235]. On the other hand, incubation of HIV gp120 with T-lymphocytes decreases the amount of Lck bound to CD4, impairing T-cell signaling [236, 237]. In addition, to study the signaling events triggered upon ligand binding to CD4, Jabado et al., directed an antibody against CD4 and found that antibody binding to CD4 and HIV-1 gp120 interaction with CD4 both trigger a decrease of the DNA-binding ability of transcription factors such as NF-kB which in turn, regulate interleukin-2 transcription [238]. Furthermore, apart from virion-associated and cell-expressed

gp120, gp120 complexed with anti-gp120 is found cell-free in serum plasma and in lymphoid tissue; binding of these complexes to CD4 negatively affects T-cell activation [237, 239]. T-cell signaling impairment and decrease of CD4 T-cell count by HIV-1 infection leads to AIDS disease progression [240].

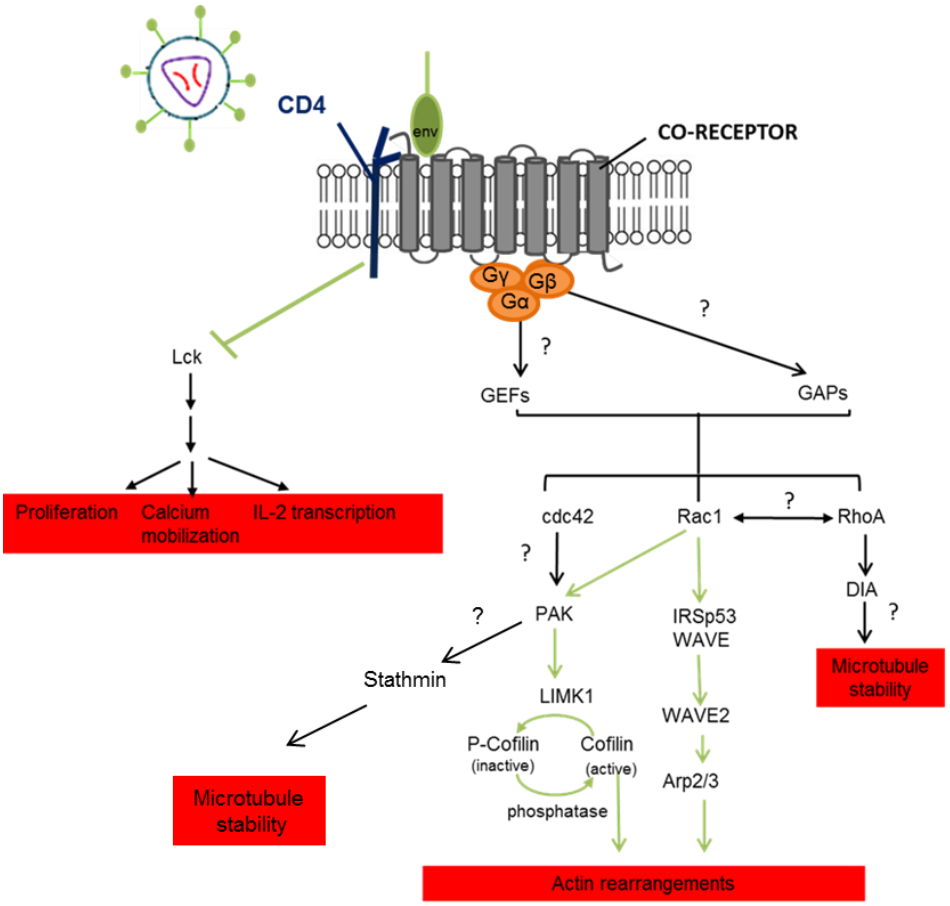

Figure 3.1. Signalling events upon HIV Env binding to its primary receptor, CD4 and co-receptor. HIV-1 Env interacts with CD4, blocking the CD4-Lck interaction that results in T-cell proliferation, calcium mobilization and IL-2 transcription [235-237]. In addition, HIV-1 triggers actin rearrangements via the Rac1-PAK-LIMK1 pathway that results in actin depolymerisation [80]. Furthermore, actin rearrangements are triggered via Env signal transduction of the WAVE2-Arp2/3 pathway [241]. Env-triggered signal pathways are depicted in green whilst pathways in black are normal cellular pathways whose role is still not well-understood in Env signalling. These include for example the involvement of Rho-GTPase upstream regulators, GAPs and GEFs or the role of Env signalling in microtubule dynamics. Adapted from [242].

Secondly, Env signaling can be induced via the Env-co-receptor interaction. CXCR4 and CCR5 are part of the G-protein-coupled receptor family (GPCRs)

which are integral membrane proteins that share in common a seven transmembrane alpha-helix spanning domain [243]. This transmembrane architecture serves as a cell signaling platform that coordinates many cellular functions. Importantly, GPCRs represent 3% of genes found in the human genome amongst which include, receptors responsible for smell, taste, metabolism, chemotaxis and blood pressure regulation [243, 244]. Since they are involved in many key cellular processes, 30%-60% of the present drugs target GPCRs [244]. Activation of GPCRs is triggered by external binding of a small molecule, a protein or a photon of light which triggers conformational changes in the cytoplasmic domains of the GPCR (Figure 3.2)[245]. GPCRs, as their name indicates, are coupled to a G-protein. G-proteins are heterotrimeric proteins which have: α, β and γ subunits. Upon activation of a GPCR, the GPCR catalyses GTP-GDP exchange in the α- subunit [245].

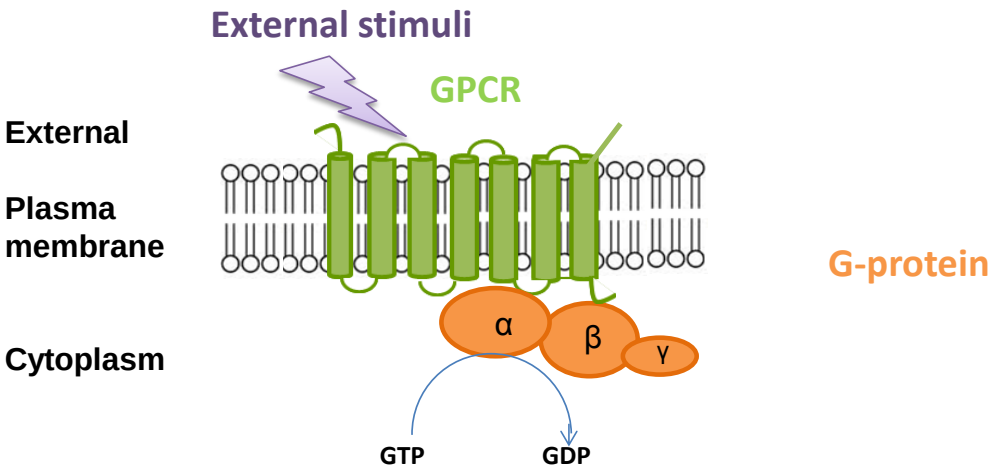

Figure 3.2. GPCR activation mechanism, structure and localization. GPCRs are activated by an external stimuli which can be a photon of light or a protein ligand which in turn, causes hydrolysis of GTP to GDP in the alpha subunit. Adapted from Cattaneo et al., [246].

The natural ligands for CCR5 include CC-chemokine ligand-3 (CCL3) or macrophage inflammatory protein (MIP-1α), CCL4 (termed also MIP-1β) and

CCL5 (or RANTES) [247]. Addition of the natural ligands to CCR5-expressing cells blocks entry of R5-tropic HIV strains [230]. Similarly, binding of the CXCR4 agonist, the lymphocyte chemoattractant CXCL12/SDF1, prevents entry of X4-tropic HIV strains but does not prevent infection with R5-tropic strains or dual tropic strains [248]. Primary isolates of HIV-2 utilize CCR5 and CXCR4 as well as other co-receptors including CCR1, CCR2b, CCR3 and CCR4 [249]. The first evidence for signaling events triggered by Env-co-receptor interaction came from experiments that showed that cells incubated with recombinant Env, signal through CCR5 enhancing T-cell chemotaxis towards HIV Env [250]. In addition, Kroemer et al., later described that when HIV-1 Env interacts with CXCR4, the interaction mediates ATP release which in turn stimulates HIV-1 fusion [251].

The cortical actin barrier poses an obstacle for HIV entry. Cofilin is an F-actin-severing protein which is inactivated in the cell through phosphorylation by LIM kinase 1 (LIMK1) (Figure 3.1) [231]. Initial clues to the role of cofilin in HIV entry came from Yoder et al., who found that HIV activates cofilin by Env-CXCR4-mediated signal transduction [80]. Importantly, the amount of active cofilin was found to be significantly higher in cells isolated from peripheral blood of HIV-infected patients compared to non-infected cells [252]. As shown in Figure 3.1, LIMK1 is downstream of cdc42, Rac1 and indirectly of RhoA since RhoA and Rac1 regulate each other [253]. In addition to mediating cofilin activation, the HIV Env binding has been shown to activate Rac1 specifically [254, 255] and to signal through the Gαq signalling pathway which is essential for virus entry in order to trigger rearrangements of cortical actin necessary for fusion with the plasma membrane [256]. Actin rearrangements by Env-co-receptor signaling are also mediated by the WAVE2 complex through Arp2/3 [241].

Thirdly, upon viral fusion, the Env gp41 cytoplasmic tail (CT) is thought to be inserted into the cell's cytoplasm [257], being therefore a third possible way by

which the Env protein induces cell signaling. For instance, Malinowsky et al. described that expression of the HIV-1 and HIV-2 Env gp41 CTs, reduces tubulin acetylation which is a marker of microtubule stability [258, 259], ie. expression of the gp41 CTs, decreases microtubule stability. The signaling mechanism by which the gp41 CT reduces tubulin acetylation is unknown. On the other hand, HIV-1 utilises microtubules for nuclear import of the preintegration complex [260] and for uncoating [261, 262] and for this purpose, it requires stable microtubules. Microtubule acetylation has been shown to be upregulated by gp120 [263]. Overall this suggests that Env signaling could be involved in regulation of microtubule dynamics during HIV-1 infection. Microtubule stability is mediated by RhoA through the DIA pathway and by Rac1 via PAK and stathmin [264-266].

Apart from the importance of Env signaling in T-cell activation via CD4, the evidence described, also suggests a role for Rho-GTPases in Env signaling through interaction with the co-receptor and possibly through signaling via expression of the gp41 CT which modifies the cell's cytoskeleton. Rac1, RhoA and cdc42 are the best characterized members of the Rho family of GTPases (Rho GTPases) which have a central role in control of cell cytoplasm dynamics including regulation of cell motility, cytoskeleton and vesicular traffic [267]. Rho-GTPases are controlled upstream by GTPase Activating Proteins (GAPs) and Guanine Nucleotide Exchange Factors (GEFs) [267]. However, the role of the upstream regulators of Rho-GTPases in HIV-1 Env signaling is largely unknown. Since the role of GAPs and GEFs in HIV-1 infection is the focus of chapter 4, upstream control of Rho-GTPases will be described in more detail in chapter 4.

3.2 Aims

Since Env signaling events are suspected to be essential for HIV-1 replication at early steps, my study focuses on enhancing the current understanding on HIV

Env signaling. I hypothesized that expression of the HIV-1 and HIV-2 gp41 CTs reduce tubulin acetylation at the single cell level and that HIV-1 Env-co-receptor signal transduction might control Rac1 through its upstream effectors. The proposed aims of this chapter are to:

- Investigate whether expression of the HIV-1 and HIV-2 gp41 CTs, interferes with tubulin acetylation at the single cell level.
- Determine whether using Raichu probes are an appropriate method to measure GTPase activity.
- Study of the impact of treatment with Rac1 inhibitors EHT and NSC in HIV-1 NL4.3 (X4-tropic) and HIV-1 BaL (R5-tropic) infection.

3.3. Results

3.3.1. Expression of HIV-1 and HIV-2 full length gp41 CTs reduces levels of acetylated tubulin.

Microtubules undergo post-translational modifications at the C-terminus that produce microtubule subpopulations specific for different functions; these post-translational modifications enable microtubule-Associated Proteins (MAPs) or motors to bind or unbind [268]. Post-translational modifications include detyrosination, glutamylation, glycylation, acetylation, phosphorylation, and palmitoylation [269]. In particular, tubulin acetylation has been shown to be present in microtubules which are less stable and thus, it is a marker for stability[259]. Malinowsky et al., described by Western-Blot quantitation that expression of Env tail constructs induced a reduction of acetylated tubulin in HeLa-CD4+ cell lysates [258]. The control construct (anchor) comprised a transmembrane domain (TMD) derived from the platelet-derived growth factor receptor (amino acids 687-841) and a Myc/HA-tag (HA for hemagglutinin) (Figure 3.2A). The full length constructs consisted of the full length HIV-1 (HIV-1 FL) and HIV-2 (HIV-2 FL) gp41 CTs fused to the same TMD and a Myc/HA-tag. Two additional constructs were included in the study which consist of two truncated versions of the HIV-1 and HIV-2 CTs (HIV-1 tr and HIV-2 tr respectively) which also are fused to the same TMD and a Myc/HA-tag and which incorporate C-terminal deletions (amino acids 687-731 and aminoacids 687-741 respectively [258].

To characterize further the reduction of acetylated tubulin upon expression of HIV-1 and HIV-2 Env tails, these results were confirmed at the single cell level. Single cell analysis gives more information about the localization of the

constructs in the cell and their expression levels. This can later be useful for the interpretation of the biological process.

To confirm the reduction of acetylated tubulin in HeLa-CD4+, I examined this by epifluorescent imaging at the single cell level transfecting the HIV-1 and HIV-2 CT constructs into HeLa-CD4+ cells (Figure 3.3A). After transfection, cells were fixed and stained against HA (to visualize constructs since they express an HA-tag) and against anti-acetylated tubulin. As expected, since all constructs have transmembrane domains, the HIV-1 and HIV-2 gp41 CT constructs localize most abundantly in the cell membrane but also in the cytoplasm (Figure 3.3B). The anchor and truncated constructs are expressed at higher levels than the full-length construct. Cells that express the full-length constructs and the truncated construct have less acetylated tubulin than anchor-control cells. However, quantification is required to confirm this visual result.

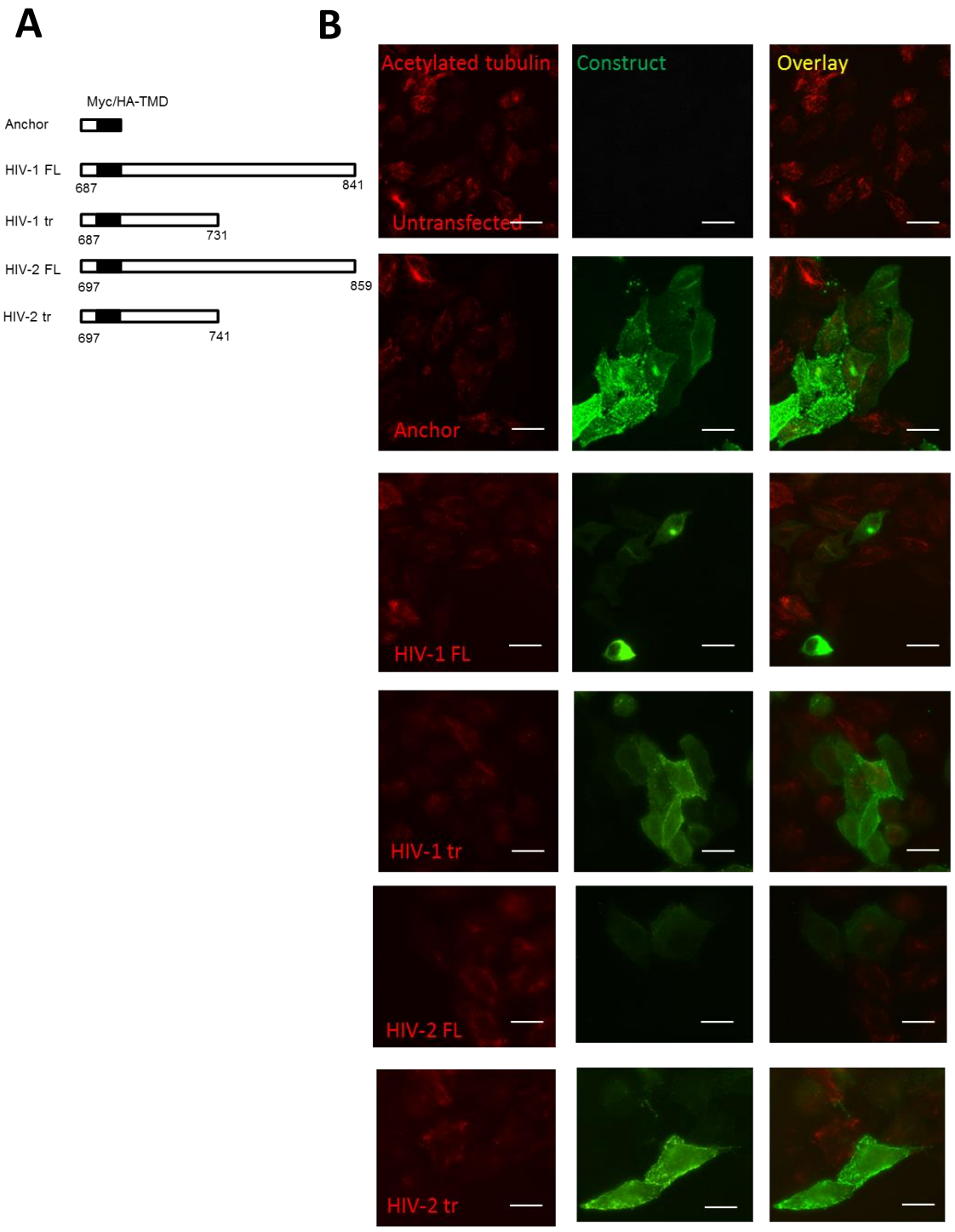

Figure 3.3. HIV-1 and HIV-2 Env CT constructs. (A) Schematic representation of anchor-only construct, HIV-1 full length (HIV-1 FL, aa 687-841) and HIV-1 truncated version (HIV-1 tr, Δ687-731). The same constructs were used with the HIV-2 sequence, an HIV-2 full length CT (HIV-2 FL, aa 697-859) and HIV-2 truncated (HIV-2 tr, aa 697-741). B) Examples of epifluorescent images of the HIV-1 and HIV-2 CT constructs transfected into HeLa-CD4+ cells, stained using an anti-HA-488 antibody for the gp41 constructs (green) and anti- acetylated tubulin (red). Controls included were untransfected cells, immunostained with acetylated tubulin and anti-HA-488 and anchor-transfected cells. Scale bar is representative of 10μM. N=3.

Quantitative epifluorescent imaging was then performed to measure the levels of acetylated tubulin in single cells expressing the HIV-1 and HIV-2 CT constructs using ImageJ MBF. Acetylated tubulin levels per cell were quantified as described in chapter 2, section 2.2.9.2. Quantitative results show that upon expression of HIV-1 FL there is a significant decrease of acetylated tubulin compared to anchor control ($p=0.033$) (Figure 3.4A). A decrease in acetylated tubulin was also observed upon expression of the HIV-1 tr construct although it was not significant ($p=0.06$). In the same fashion, expression of HIV-2 FL reduced the amount of acetylated tubulin significantly ($p=0.046$) suggesting that reduction of acetylated tubulin is a shared feature of lentiviral gp41 CTs (Figure 3.4B). Expression of the truncated HIV-2 CT did not reduce tubulin acetylation significantly ($p=0.07$) although a decreasing tendency is observed if compared to anchor control. Both these findings concur with those described by Malinowsky et al.,[258]. Interestingly, as can be seen in Figure 3.3B, even though the full-length tail was expressed at lower levels than the truncated construct, the effect on reduction of tubulin acetylation is stronger upon expression of the full-length than upon expression of the truncated tail construct.

A

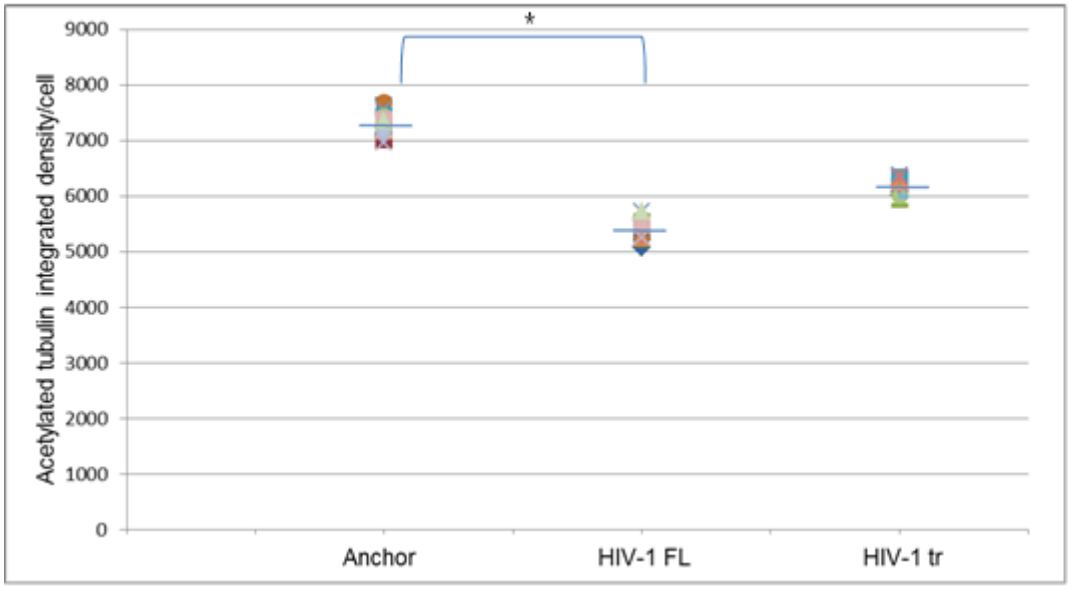

B

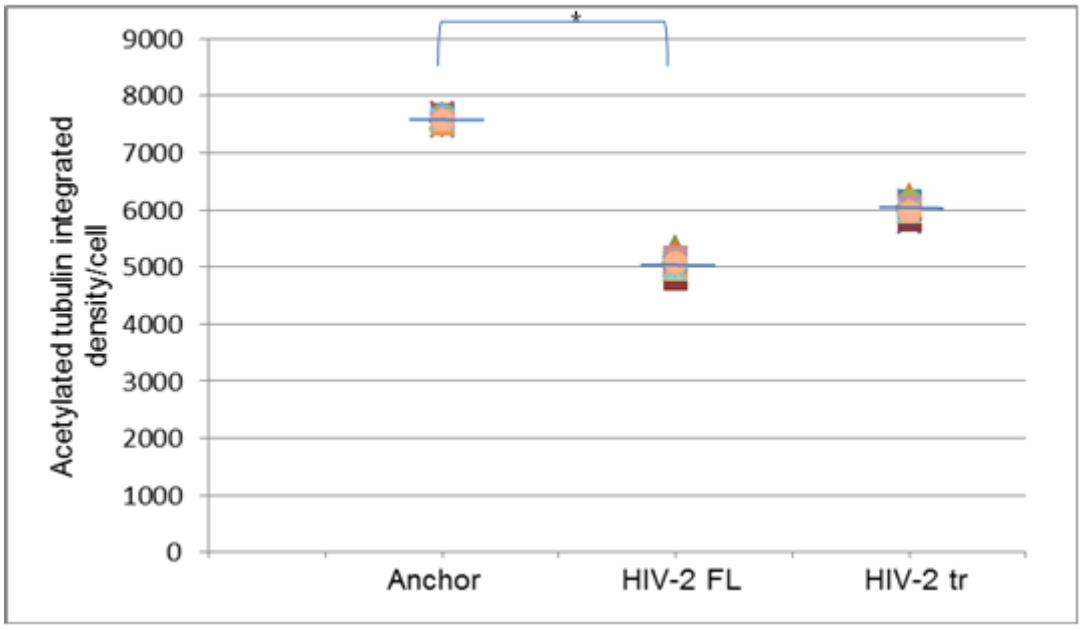

Figure 3.4. Expression of HIV-1 and HIV-2 CTs but not truncated, decrease the levels of acetylated tubulin in HeLa-CD4+ cells. HeLa-CD4+ cells were transfected with A)HIV-1 and B) HIV-2 FL and tr gp41 CT constructs. Cells were then fixed and double stained for acetylated tubulin and HA (to visualize the constructs). Single cell quantititative image analysis of the integrated mean density of the acetylated tubulin staining was performed with ImageJ MBF of cells expressing the tails. Results show a representative of 3 experiments; 300 cells in total were analysed. Significance was assessed by Wilcoxon Man-Whitney test*p<0.05.

3.3.2. Investigating Raichu probes as GTPase activity biosensors

So far in this chapter, my results and those of Malinowsky et al., [258] suggest that expression of the HIV-1 and HIV-2 full length Env CTs, reduces acetylation of tubulin, which is a marker of microtubule stability [259]. Microtubule stability is promoted through activation of RhoA which in turn activates DIA [264]. Downstream of DIA, End-binding protein 1 and adenomatous polyposis coli bind to the end of the microtubules and promote their stability possibly by forming a complex at stable microtubule ends [270]. Microtubule stability is also controlled by Rac1 via stathmin which is a downstream effector of Rac1 [265] (see figure 3.1). Stathmin is a microtubule depolimerising protein that regulates microtubule dynamics by changes in phosphorylation; this dynamic regulation allows stathmin to, for example, regulate microtubule stability during cell cycle progression[271]. In addition, Rac1 and RhoA regulate each other [272] . It could be that HIV modulates the activity of Rac1 or RhoA to achieve this reduction of acetylated tubulin. Therefore, being able to measure the effect of gp41 cytoplasmic expression on the activity of Rho GTPases could shed light on the signaling mechanism that HIV Env orchestrates to modulate the cytoskeleton.

Raichu probes are GTPase activity biosensors that have been described as reporters of GTPase activity at the single cell level by confocal microscopy [228]. Classical methods to measure GTPase activity include biochemical pull down of active form (GTP-loaded) with known GTPase effector domains tagged to GTP (Glutathion S-transferase) [273]. This method does not give information about the localization of the active GTPase. Nor is it sensitive enough to detect small changes. On the other hand, Raichu probes have proven to be useful in the understanding of spatio-temporal regulation of Rho GTPases [274-276]. This

method in turn, could serve to understand if Rho GTPases are activated upon expression of the HIV gp41 CT.

The chosen method to measure Fluorescence Resonance Energy Transfer (FRET) was acceptor photobleaching (Figure 3.5). The Raichu probe, encoding Rac1 wild-type (Rac1 WT) or Rac1 constitutively active (Rac1 CA), consisted of: the GTPase protein, two fluorochromes: an acceptor, yellow fluorescent protein (YFP) (514/527) and a donor, cyan fluorescent protein (CFP) (433/475) and a GTP binding domain. GTPase activation brings the YFP and CFP fluorochromes into close proximity by a conformational change. Upon acceptor photobleaching, if the GTPase is active, YFP and CFP are within 5nm and there is an energy transfer which results in the excitation of YFP and very low excitation of CFP (Figure 3.5A) [277]. On the contrary, if the GTPase is not active, the two fluorochromes are more than 5nm from each other and the energy transfer upon bleaching does not occur (Figure 3.5B). In this case, the fluorochrome CFP is strongly excited. In acceptor photobleaching FRET efficiency is measured as the ratio of CFP before and after photobleaching.

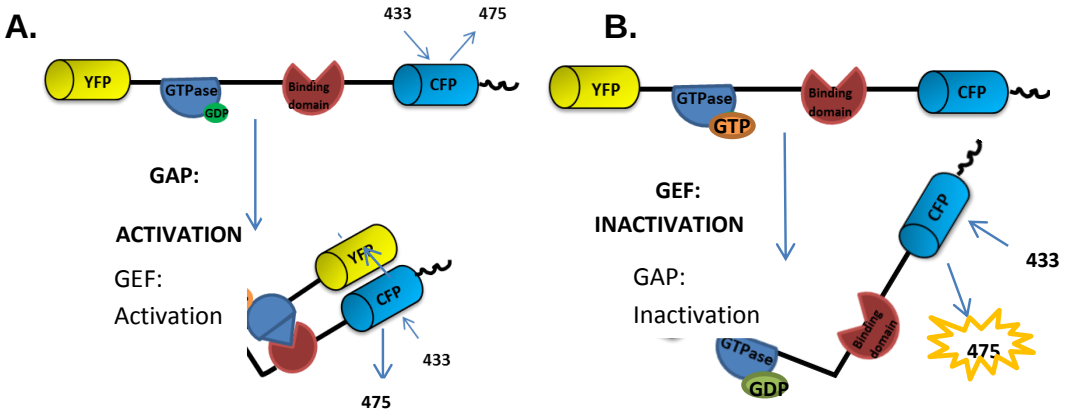

Figure 3.5. Schematic representation of the structure and mechanism of Raichu probes for the measurement of intracellular Rho GTPase activity. The Raichu probe encodes a small Rho GTPase, two fluorophores: YFP and CFP and a GTPase binding domain. A. If the Rho GTPAse is active (GTP-bound), upon bleaching, there is a Fluorescent Resonance Energy Transfer (FRET) that results in excitation of YFP. B. If the GTPase is not active (GDP-bound), upon bleaching, there is no energy transfer and the YFP fluorochrome is not excited; the CFP is the fluorochrome excited.

I first tested the validity of using Raichu probes to measure GTPase activity. Rac1 WT and Rac1 CA Raichu probes were transfected into HeLa-CD4+ cells, to optimize photobleaching conditions.

Images show that Rac1 WT (Figure 3.6A) and CA (Figure 3.6B) are expressed in HeLa-CD4+ cells as shown by the YFP expression. Pre-bleach, YFP is bright and post-bleach, YFP is not detectable, which suggests that bleaching parameters were set correctly. Their activity is shown in images where upon photobleaching, YFP is excited and CFP is detected (FRET efficiency). Importantly, activity of both Rac1 WT (Figure 3.6A FRET efficiency panel) and CA (Figure 3.6B FRET efficiency panel) is at its highest at the cell membrane which is where GTPases are mostly active. This suggests that Raichu probes are functional in HeLa-CD4+ cells.

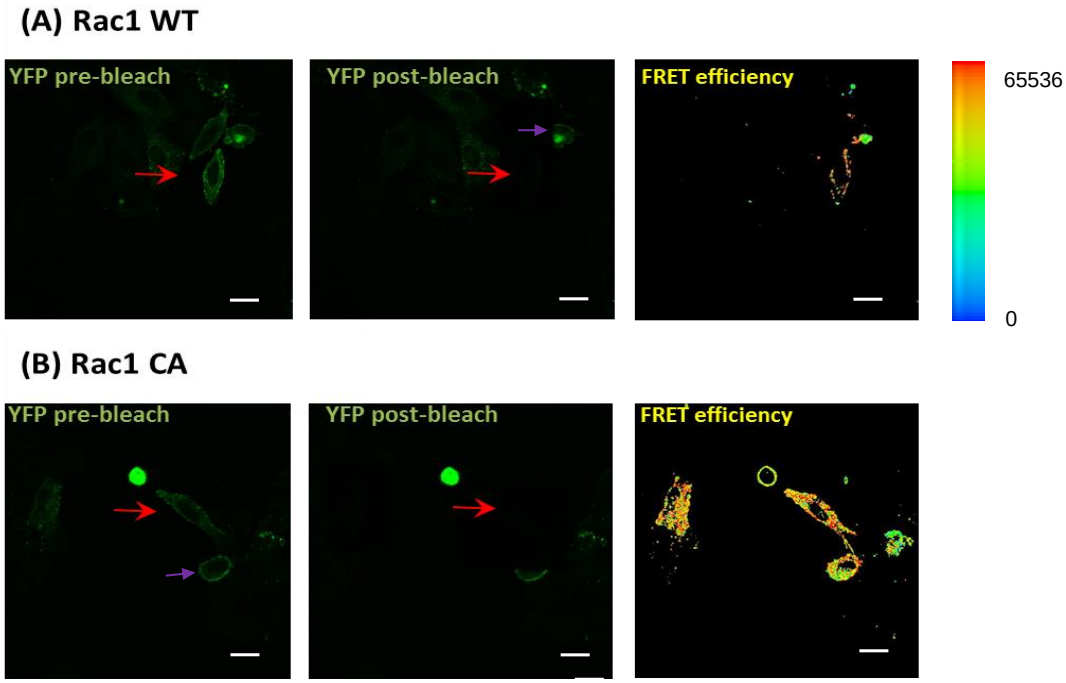

Figure 3.6. Confocal imaging of Rac1 WT and Rac1 CA Raichu probes during FRET. Confocal images show HeLa-CD4+ cells transfected with (A) Rac1 WT and (B) Rac1 CA Raichu probes. FRET efficiency or GTPase activity, which is the ratio of CFP emission pre and post-bleach, is represented in (orange/yellow) mostly at the cell membranes.YFP in green channel is bright pre-bleaching and is absent post-bleach. Red arrows indicate cells that were bleached with the parameters set. Purple arrows indicate cells that have lost the characteristic HeLa-CD4+ morphology. Image scale bar is representative of 10µM. Pseudocolor 16-bit grayscale gradient where warm colours indicate high FRET efficiency.

Once the photobleaching parameters were optimized (chapter 2, section 2.2.9.1), HeLa-CD4+ cells were transfected with Rac1WT or Rac1 CA. The purpose was to assess whether the Raichu probes were sensitive enough to measure Rac1 WT and Rac1 CA changes in activity. Additionally, as a control, cells transfected with Rac1WT were treated with a Rac1 inhibitor, EHT. EHT is an inhibitor that binds directly to Rac1 [278] (Figure 3.7A). The cytotoxicity of both EHT and NSC23766 (NSC) (another Rac1 inhibitor employed further on as described in section 3.3.3) was assessed (Figure 3.7B and 3.7C). EHT and NSC showed no significant cytotoxicity upon treatment at 25µM and 12.5µM respectively.

(A)

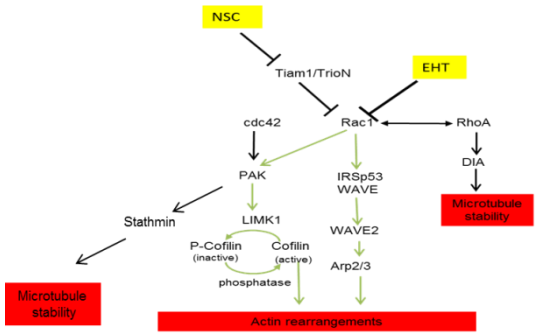

(B)

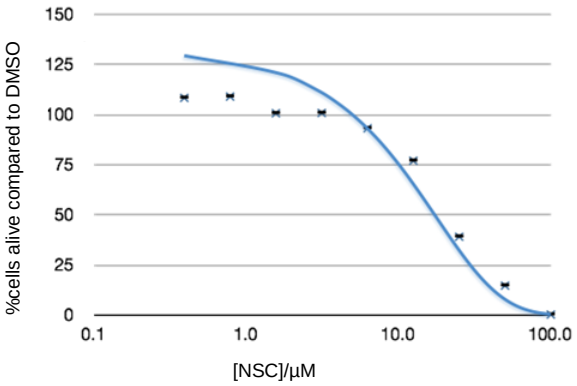

(C)

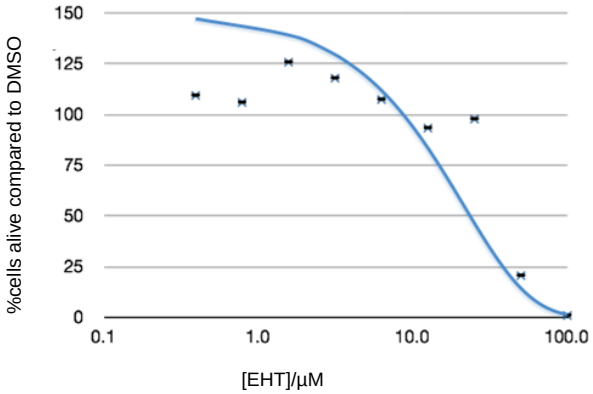

(D)

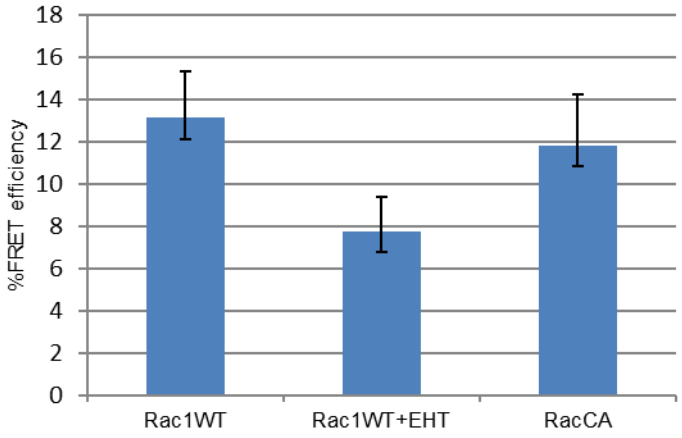

Figure 3.7. Mode of action of EHT and NSC Rac1 inhibitors and FRET efficiency of Rac1 WT, Rac1 WT in EHT-treated cells and Rac1 CA. (A) Schematic representation of inhibition targets of NSC and EHT. (B) Cytotoxic profile of TZM-bl cells treated with NSC for 48 hours as measured by MTT cytotoxicity assay. (C) Cytotoxic profile of TZM-bl cells treated with EHT for 48 hours as measured by MTT cytotoxicity assay. (D) Cells were transfected with Rac1 WT and Rac1 CA constructs and treated or non-treated for 48 hours, time at which they were photobleached and readings of CFP before and after photobleaching were taken from the images in Figure 3.5 to calculate the ratio or %FRET efficiency using the AccPbFRET plugin from ImageJ MBF. In total, 21 cells were analysed, n=1. Error bars represent Standard Deviation, STDEV. Cytotoxicity assays were performed by Dr. Aysegul Tosun.

Quantification of 15 cells of the ratio of CFP before and after photobleaching (Figure 3.7D) pre- and post-bleach showed that Rac1 WT has a FRET efficiency (GTPase activity) of 13% and Rac1 CA of 12%. In EHT-treated cells, FRET efficiency decreased to 9% which is only 4% and 3% compared with untreated Rac1 WT and Rac1 CA. Typically, Rac1 WT and Rac1 CA differ in a 2-fold FRET efficiency difference [274]. Since the differences were not very strong compared to what others have reported, it was agreed that acceptor photobleaching of Raichu probes was not suitable for measuring changes in GTPase activity in HeLa-CD4+ cells. In addition, it was observed that Raichu probes were toxic since transfected cells did not look very healthy; for example cell cytoplasm was rounded and had lost the HeLa-CD4+-characteristic elongated cytoplasm (see cells with purple arrows in Figure 3.6). Since the objective was to double transfect the gp41 constructs and the Raichu probes, it was thought that this could additionally affect cell viability and so, the use of the probes was discontinued.

3.3.3. Treatment with Rac1 inhibitor, NSC, decreases infection of HIV-1 NL4.3 but not HIV-1 BaL.

Results in section 3.3.1 indicate that expression of the HIV-1 and HIV-2 gp41 FL CT in HeLa-CD4+ cells reduces acetylated tubulin. Tubulin acetylation is a marker of microtubule stability [259]; apart from RhoA, microtubule stability is also regulated by Rac1 via PAK and stathmin [265, 266]. It could be that, to modulate the cytoskeleton via Env, HIV requires Rac1. I therefore hypothesized that Rac1 could have a role in HIV-1 infection.

Two Rac1 inhibitors, EHT [278] and NSC [279], were employed to investigate their effect on HIV-1 infection. These inhibitors target Rac1 through different mechanisms (Figure 3.7A). For instance, EHT targets Rac1 by binding directly to

Rac1 [278] whilst NSC targets Rac1 by specifically binding to its GEF upstream activators, Tiam1 and TrioN [280].

Rac1 has been shown to promote microtubule stability through PAK and stathmin (Figure 3.1) [265, 266]; it is therefore expected that inhibiting Rac1 decreases microtubule stability. Previously, others have shown that EHT and NSC treatment causes alterations in normal microtubule organization [281]. To determine if treatment with EHT and NSC have an effect on microtubule stability of TZM-bl cells as an indirect measure of Rac1 inhibition, cells were treated with EHT and NSC at 25 µM and 12.5µM respectively for 24 hours and microtubules were immunostained. Results (Figure 3.8), show that upon DMSO treatment, microtubules have a fibrous morphology characteristic of microtubules. However, upon treatment with EHT, the microtubules morphology and organisation is diffuse and microtubule length is disturbed as would be expected upon inhibition of Rac1 since it controls microtubule stability. In addition, treatment with NSC, also disrupts microtubule organization and length as can be seen by the uneven, diffuse and irregular shape of the microtubules compared to untreated control. Altogether, results therefore suggest that treatment with EHT and NSC affect microtubule structure and since Rac1 has been shown to promote microtubule stability [265, 266], this could be an indirect measure of inhibition of Rac1 by EHT and NSC.

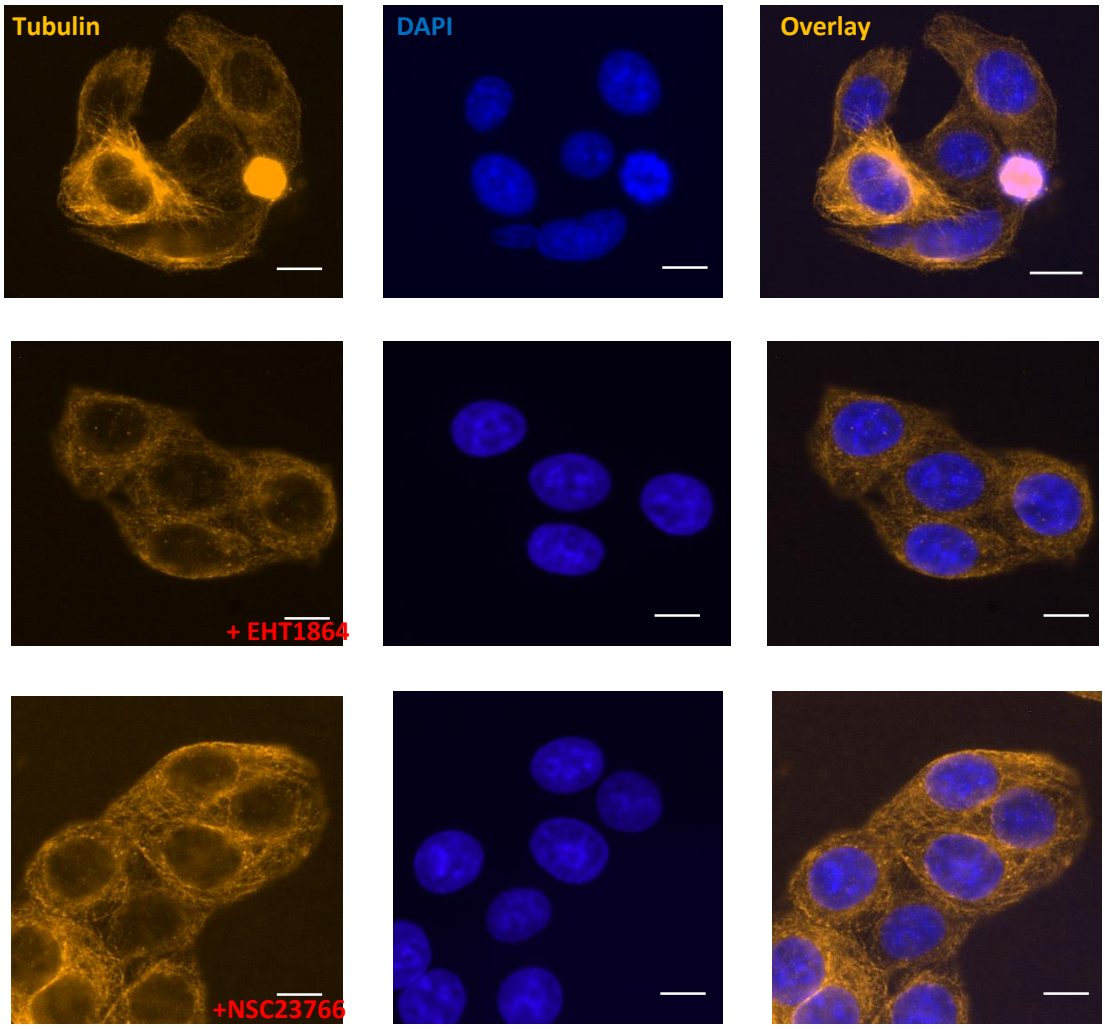

Figure 3.8 Microtubule disassembly after treatment with EHT and NSC. TZM-bl cells were treated with EHT and NSC at 25µM and 12.5µM for 24 hours, time at which they were fixed and stained with anti-tubulin-555 (orange) and DAPI (blue) to visualize nuclei. Scale bar represents 10 µM, n=1.

I then assessed the effect of treating cells with EHT and NSC on infection of HIV-1 NL4.3 (X4-tropic) and HIV-1 BaL (R5-tropic) which differ in co-receptor usage. I therefore hypothesized that the effect of treatment with EHT and NSC on infection could differ on the virus strain employed and so, that the effect could be co-receptor dependent. TZM-bl cells were pre-incubated with EHT and NSC at decreasing concentrations from 25µM and 12.5µM respectively and challenged with HIV-1 NL4.3 and HIV-1 BaL pseudotype virus. β-gal staining was performed to detect infected cells as described in section 2.2.5.3. Results show that

treatment with EHT did not have an effect on HIV-1 BaL or HIV-1 NL4.3 infection in TZM-bl cells compared to DMSO-treated infected cells (Figure 3.9A). On the other hand, treatment of TZM-bl cells with 12.5µM of NSC inhibited 99% of HIV-1 NL4.3 (Figure 3.9B) in a dose-dependent manner. Treatment with NSC had no effect on HIV-1 BaL infection suggesting that the effect observed is strain-dependent and could depend on co-receptor usage.

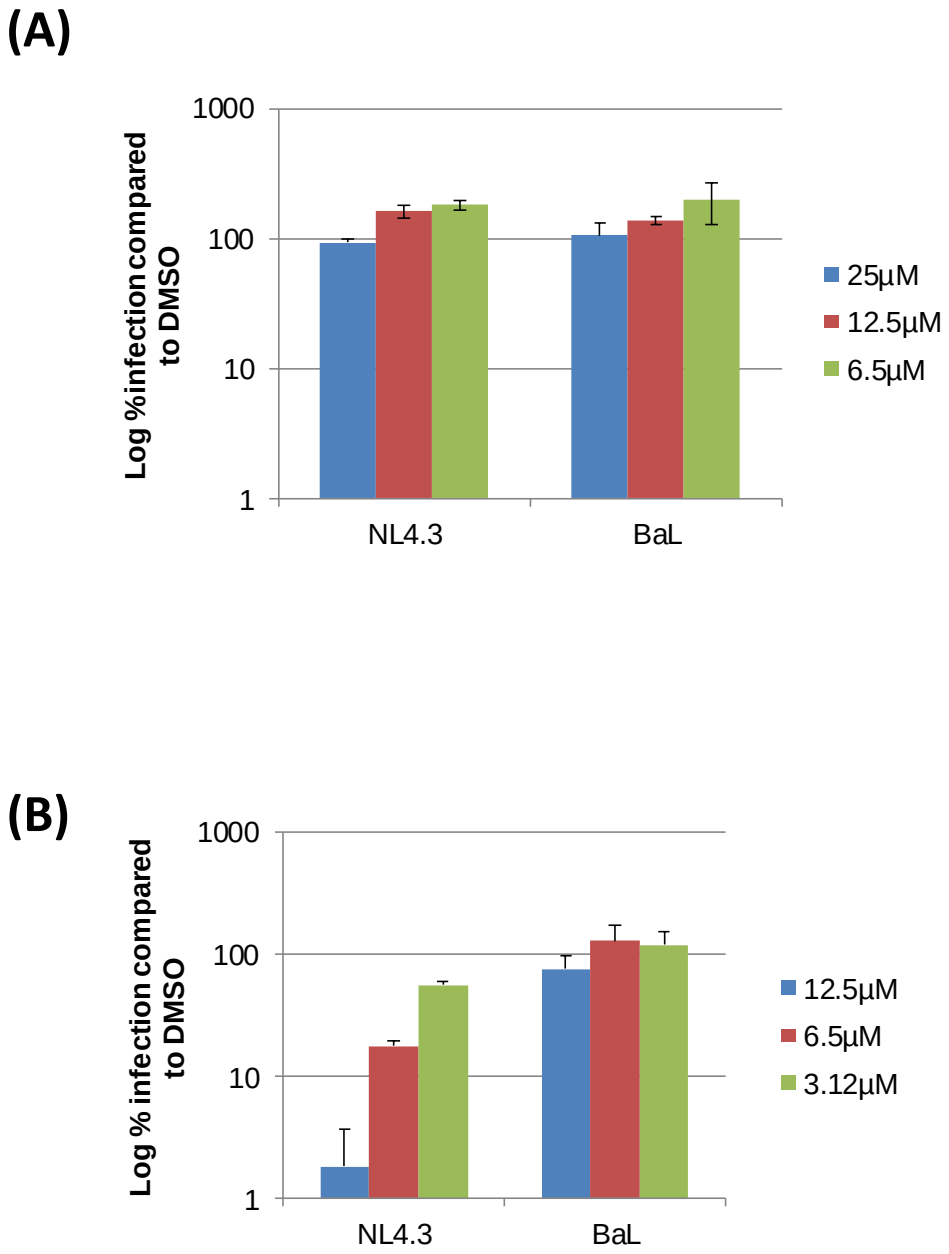

Figure 3.9. Effect of EHT and NSC treatment on HIV-1 NL4.3 and HIV-1 BaL infection in TZM-bl cells. Cells were treated for 24 hours with (A) EHT at 25, 12.5 and 6.5 µM and (B) NSC at 12.5, 6.5 and 3.1 µM, then challenged with HIV-1 NL4.3 and BaL for 48 hours and foci of infection determined. A representative of three independent experiments in triplicate is presented. Error bars represent STDEV.

3.3.4. Effect of EHT and NSC treatment on HIV-1 infection in T-cell lines.

I next investigated the effect of NSC and EHT treatment in T-cell lines, PM1 and Jurkat cells which are more relevant cell lines in HIV-1 infection since T-cells are a primary infection target of HIV-1.

Initially, the level of toxicity of EHT and NSC in PM1 and Jurkat cells was measured. Cells were incubated with EHT and NSC in serial drug dilutions from 50μM to 3μM for 48 hours and cell viability was assayed with an (3-(4,5-dimethylthiazol-2-yl)-5-(3-carboxymethoxyphenyl)-2-(4-sulfophenyl)-2H-tetrazolium, inner salt) (MTS) cytotoxic assay. In an MTS cytotoxicity assay, cell viability is proportional to the ability of cells to metabolically processing a tetrazolium salt, MTS [225].

Cytotoxicity assay of NSC in Jurkat cells (Figure 3.10A) showed that at the range of NSC concentrations assayed there was 100% cell viability compared to DMSO which suggests that the inhibitor is not toxic at these concentrations. In PM1 cells, treatment with NSC (Figure 3.10B) at concentrations higher than 25μM caused cell viability to decrease to 70% compared to DMSO. It was therefore decided to treat both Jurkat and PM1 cells with 12.5 μM, a concentration in which cell viability was of 100%.

Cell viability of Jurkat cells upon treatment with 25 μM or higher (Figure 3.10C) was of 80% compared to DMSO alone. Cell viability of PM1 cells, upon treatment with EHT from 3.125μM-12.5μM, was of 80-90% compared to DMSO (Figure 3.10D). However treatment with EHT concentrations higher than 12.5μM, caused PM1 cell viability to decrease to 60 and 40% compared to DMSO. For these reasons, it was decided to assay EHT at 12.5 μM for both cell lines.

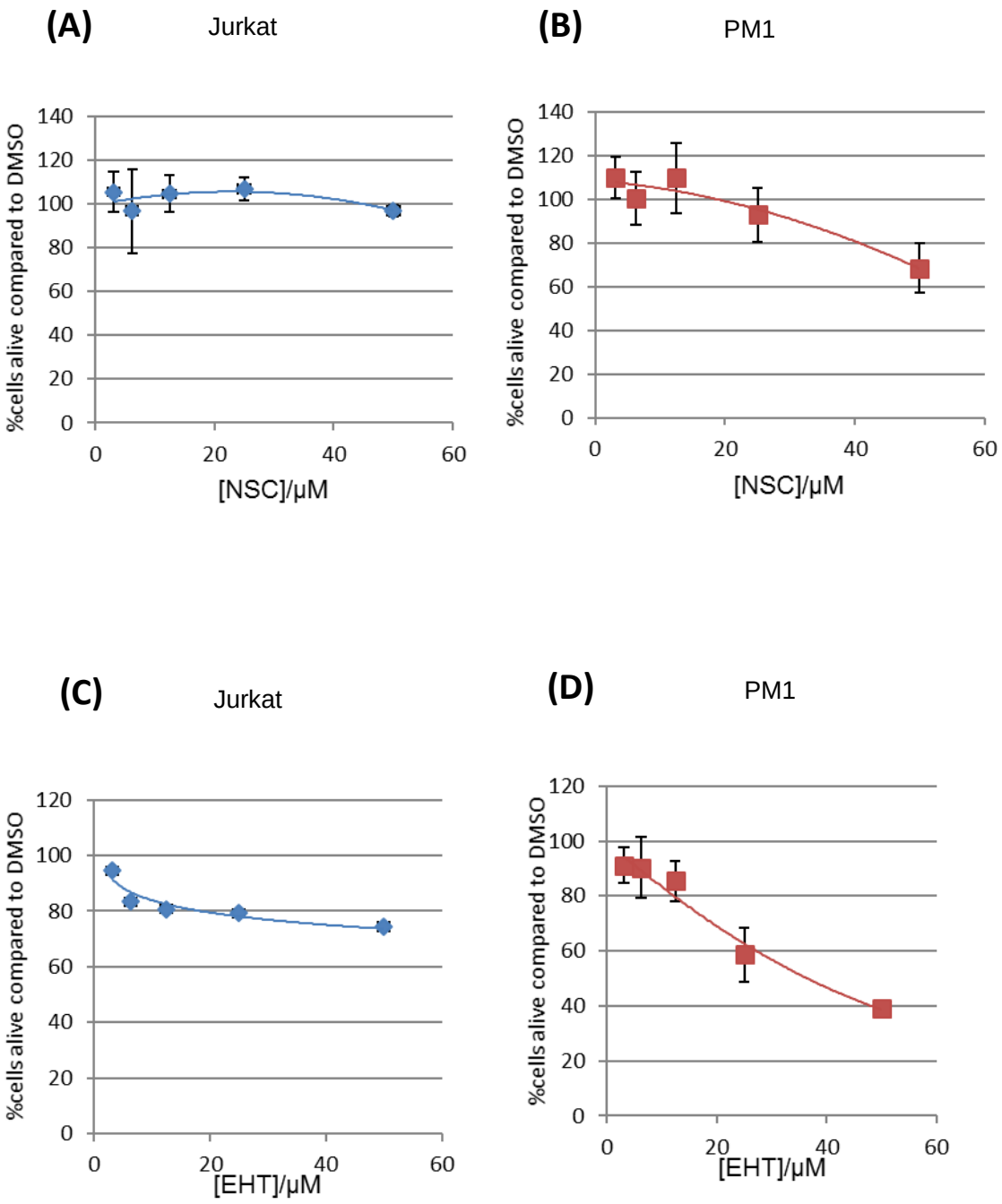

Figure 3.10. Cytotoxic profiles of NSC and EHT in Jurkats and PM1 cells. Top row, A representatitive cytotoxic profile of (A) Jurkats and (B) PM1 cells upon treatment with NSC at a range of drug concentrations from 3.1-50 μM 48 hours post-treatment. Bottom row, a representative cytotoxic profile of (C) Jurkats and (D) PM1 cells upon treatment with a range of drug concentrations from 3.1-50.0 μM, 48 hours post-treatment. Percentage of cells alive was normalised to DMSO-treated controls. Jurkats, n=3 and PM1, n=2. Per experiment each condition was done in triplicate. Error bars represent STDEV.

Having determined the concentrations of EHT and NSC which are not toxic for PM1 and Jurkat cells, I next determined the effect of these inhibitors on HIV-1 infection. Since Jurkat cells only express CXCR4 and not CCR5, only HIV-1 NL4.3 was assayed in Jurkat cells. PM1 cells express both CXCR4 and CCR5 and so, HIV-1 NL4.3 and HIV-1 BaL were assayed. Infection with HIV-1 BaL and HIV-1 NL4.3 was measured by flow cytometry since these pseudotypes express GFP (described in chapter 2, section 2.2.5.4).

PM1 cells treated with EHT for 48 hours were then challenged with HIV-1 NL4.3 or BaL. Treatment with EHT in PM1 cells increased infection with HIV-1 NL4.3 and HIV-1 BaL by 2% and 10% respectively (Figure 3.11A and 3.11B) compared to DMSO control. On the other hand, treatment of PM1 cells with NSC (Figure 3.11A and 3.11B) decreased HIV-1 NL4.3 infection by 2% and had no effect on HIV-1 BaL infection (Figure 3.11B) compared to DMSO control.

Treatment of Jurkat cells with EHT and NSC increased HIV-1 NL4.3 infection 2% and 6% respectively compared to DMSO (Figure 3.11C) control.

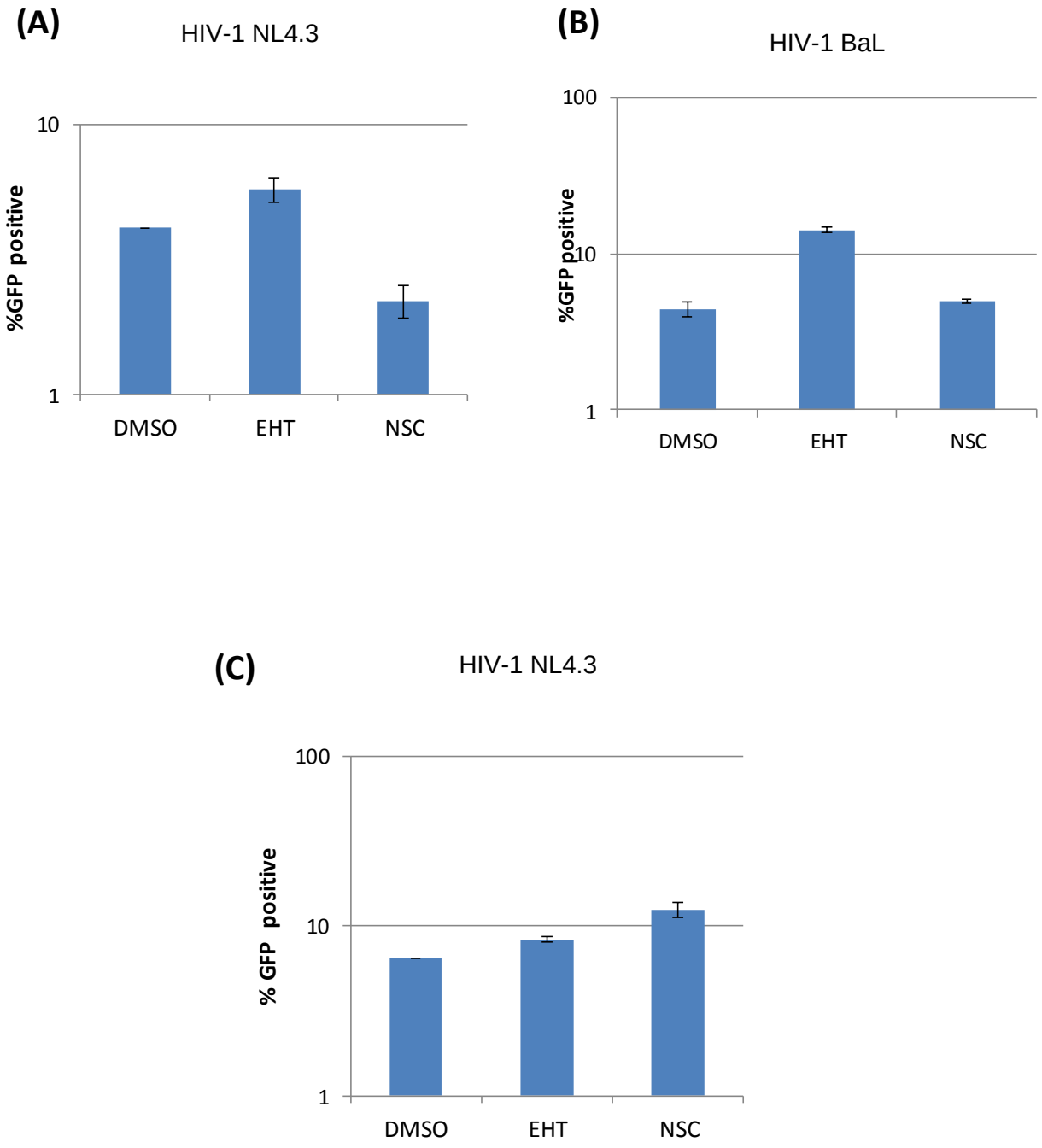

Figure 3.11. Effects of EHT and NSC treatment on HIV-1 NL4.3 and HIV-1 BaL infection in T-cell lines. PM1 cells were treated with 12.5 µM EHT and NSC for 24 hours and infected with (A) HIV-1 NL4.3 or (B) HIV-1 BaL for 48 hours. (C) Jurkat cells were treated with 12.5 µM EHT and NSC for 48 hours and infected with HIV-1 NL4.3. Flow cytometry was performed to measure the percentage of GFP-positive cells compared with DMSO treated in duplicate, N=1.

3.4. Discussion

Consistent with the requirement of Rac1 activation for HIV-1 infection [241, 255, 256, 282, 283], three independent experiments showed that treating cells with Rac1 inhibitor NSC, inhibited HIV-1 NL4.3 (X4-tropic) infection in TZM-bl cells (Figure 3.9). On the other hand, treatment with NSC had no effect on HIV-1 BaL infection. This pattern was similar upon treatment with NSC in a T-cell line, PM1 cells, although the effects were smaller than in TZM-bl cells (Figure 3.11A and 3.11B). This concurs with that of Zoughlami *et al*., who found that NSC-treated U87.CD4.CCR5 cells decreased HIV-1 HxB (X4-tropic) infection but had no effect on HIV-1 BaL (R5-tropic) infection [254]. Since, NSC targets Rac1 via its upstream regulators, Tiam1 and TrioN [279], this suggests that Tiam1 and TrioN have a role in HIV-1 infection which could be CXCR4-dependent and it could be confirmed by including other X4-tropic viruses. Importantly, it has previously been described that Rac1 inhibition causes a decrease of CXCR4 surface expression and most interestingly, Rac1 and CXCR4 are interacting partners [254]. It could therefore be that NSC treatment causes a decrease of CXCR4 which in turn decreases CXCR4 surface expression which would explain why this phenotype is observed for NL4.3 (X4-tropic) but not for HIV-1 BaL (R5-tropic). In contrast to my results and those of Zoughlami *et al*., Harmon *et al* found that NSC treatment inhibited an R5-tropic virus, HIV-1 ADA. It is possible that the opposing results could be explained by cell type differences. Harmon *et al.,* used U87 astroglioma cells whilst I used TZM-bl cells, a cervical cancer cell line, and so phenotypes could be cell-specific; however, Zoughlami et al., also employed U87 cells so it is possible that the observations made by Zoughlami *et al* and me*,* are HIV-1 BaL-specific rather than R5-specific. This could be tested by including other R5 strains such as ADA and YU2. Since sequence of V3 loops in Env determines co-receptor usage [284], an additional method to confirm these results would be by generating virus mutants with swapped V3 loops.

The step affected by Rac1 inhibition is an early step since the HIV-1 NL4.3 strain included in my experiments was a single-round infection virus which is not able to go through a full-replication cycle and is only integrated. The role of Rac1 in HIV-1 has been suggested to modulate actin rearrangements for virus entry [241, 255, 256]. It is possible that Env binds to CXCR4 and in doing so, recruits Rac1 regulators, Tiam1 and TrioN, which then mediate actin rearrangement. On the other hand, a Tiam1/TrioN-mediated Rac1 activation could also have an effect on microtubules. For instance, Rac1 regulates microtubule stabilization [266] which is required for virus pre-nuclear integration[260, 285-287]. It could therefore be that Tiam1 and TrioN activate Rac1 which in turn, have an effect on both actin rearrangements for virus entry but also, stabilize microtubules for nuclear import. Whilst discrepancies lie on the virus strains assayed, altogether, results highlight a new role for Rac1 activators, Tiam1 and TrioN in Env-mediated signalling.

Intriguingly, whilst blocking Rac1 via Tiam1 and TrioN significantly decreased HIV-1 NL4.3 infection, inhibiting Rac1 had no effect on NL4.3 nor BaL in TZM-bl. There is a possibility that EHT did not work. However, even though microtubule stability is an indirect measure of Rac1 activation, treatment with EHT caused a strong microtubule disassembly (Figure 3.8) which suggests that EHT is inhibiting Rac1 and thus, causing the expected effect on microtubule organization. EHT binds directly to Rac1 which blocks binding of Rac1 regulators [278]. A more plausible explanation could be that blocking Rac1 directly, has a strong effect that is counteracted by RhoA, since crosstalk between RhoA and Rac1 has been reported [288]. This is supported by the fact that EHT also has high affinity with Rac1b, Rac2 and Rac3 isoforms [278] and this general Rac1 inhibition might induce RhoA activation. Therefore, by inhibiting Rac1 directly, RhoA is upregulated and this has a knock on effect on Rac1 whose activity is unaffected by EHT. It could be that in Jurkats and PM1 cells, Rac1 regulation is very tightly

regulated and inhibition of Rac1 has an even stronger knock on effect that activates Rac1 and this is why an increase of NL4.3 infection is observed (Figure 3.11A and 3.11C). Another explanation could be that EHT treatment actually targets different pathways in TZM-bl cells and the T-cell lines assayed, that affect HIV-1 infection differently. Furthermore, treatment with NSC increased HIV-1 NL4.3 and BaL infection in Jurkats (Figure 3.11C), an opposing result to that observed in TZM-bl and PM1 cells; it could be that in Jurkats, Rac1 is regulated differently or that Jurkats do not express Tiam1 and TrioN and actually NSC non-specifically targets another signalling pathway that is beneficial for the virus. Another possibility could be that Jurkats do not express Rac1 and so, that the increase in NL4.3 and BaL infection is an off-target effect. It is possible that measuring the levels of expression of Rac1, TrioN and Tiam1 in all cell types could help to further understand the results.

It would therefore have been interesting to measure the activation status of Rac1 and RhoA using Raichu probes upon treatment with NSC and EHT during HIV-1 NL4.3 infection as this would have helped to understand the results. However, as shown in Figure 3.6, differences between Rac1 CA and Rac1WT were not very strong compared to what others have reported (2-fold) [274] and there was also some associated toxicity upon expression of the probes; therefore the use of this technique was discontinued. It could be that the more traditional methods to measure GTPase activity such as protein pull downs, could yield further clues to the mechanism by which HIV Env regulates Rho GTPases.

Interestingly, quantitative fluorescent imaging of three independent experiments showed that expression of the HIV-1 and HIV-2 full length CTs, significantly decreased microtubule acetylation at the single cell level (Figure 3.4). The effect of expression of the FL HIV-1 and HIV-2 gp41 CTs was stronger than the effect of the truncated CTs despite being expressed at lower levels; this suggests that

the deleted domain absent in the truncated constructs is important for mediating the observed phenotype. In addition to Rac1 [266], microtubule stability is also regulated by RhoA via the DIA signaling pathway (Figure 3.1) [264, 289]. It is possible that the FL gp41 CT binds to an activator of RhoA and sequesters it, preventing RhoA activation which in turn, destabilizes microtubules. Others have reported that the gp41 CT binds to and activates P115-RhoGEF and inhibits, viral replication [290]. Malinowsky et al, showed that expression of the gp41 full length reduces viral-cell fusion so both results concur [258]. Further studies in a stable cell line that has P115-RhoGEF knockdown followed by transient transfection of the CTs could help elucidate this phenotype; if loss of phenotype was observed in the cell line that has knockdown of P115-RhoGEF upon expression of the full length tail, this would support the hypothesis that the Env tail interacts with P115-RhoGEF. It could be confirmed doing protein pull-down assays to characterize this interaction together with confocal imaging colocalisation studies. It would also be interesting to see the effect of expression of the HIV-1 Env CT on actin structure to understand whether it might have a role in Env-mediated actin rearrangements. Altogether, these results suggest that the HIV-1 and HIV-2 Env CTs have a signaling role that triggers microtubule deacetylation; since expression of the HIV-1 Env CT has been shown to reduce virus-cell fusion [258], the Env CT and its possible interacting partners could be potential new therapeutical targets against HIV.

Results described in this chapter situate Rac1 and perhaps RhoA in a central role in HIV-1 infection and their regulation, if further confirmed, could be different depending on co-receptor usage. Various studies describe the phenotypic switch from HIV R5-tropic viruses to X4-tropic viruses, as a marker for disease progression to AIDS concomitant with a rapid CD4 T-cell depletion [291-293]. Therefore identifying the specific pathways that are activated upon CXCR4 or

CCR5 engagement could be crucial for the design of novel drugs that block the phenotypic switch, highlighting the importance of increasing the current understanding of these pathways in the HIV context. Since a role for Tiam1 and TrioN was described, I went on to investigate whether other upstream regulators of Rac1, RhoA and cdc42 might have a role in HIV-1 NL4.3 and BaL infection which is the subject of chapter 4.

3.5. Principal findings

To summarise, in this chapter the following main findings were made:

- In agreement with Malinowsky et al., expression of HIV-1 and HIV-2 FL CTs reduced tubulin acetylation significantly at the single cell level compared to control. Expression of truncated versions of HIV-1 and HIV-2 tail (with deletions at amino acids 697-859 and 697-741 respectively), resulted in less tubulin acetylation suggesting that this domain may at least partially explain the phenotype observed.
- In TZM-bl cells, treatment with Rac1 inhibitor NSC, which targets upstream regulators of Rac1, TrioN and Tiam1, inhibited 99% HIV-1 NL4.3 infection but not HIV-1 BaL compared to control. This pattern was also observed in the PM1 T-cell line.
- EHT treatment which targets Rac1 had no effect on NL4.3 or HIV-1 BaL infection in TZM-bl cells. On the other hand, EHT-treatment enhanced HIV-1 NL4.3 infection in both Jurkats and PM1 cells.

Chapter 4. Role of Rho GTPase regulators in HIV-1 infection

4.1 Introduction

The Rho family of GTPase proteins (Rho GTPases) are part of the Ras super family of GTPases of which Rac1, RhoA and cdc42 are the best characterized [294]. Since they have a pivotal role in the cell, Rho GTPases are ubiquitously expressed across species with 20 Rho GTPases identified in humans [295]. A number of studies show that Rac1, RhoA and cdc42 regulate the actin cytoskeleton which maintains cell shape, motility, and polarity [296-299]. Furthermore, RhoA and Rac1 mediate microtubule stability [264-266]. In addition to their role in the cytoskeleton, Rho GTPases also participate in other key cellular processes such as gene transcription and cell survival [300]. Rho GTPases localize to many cellular compartments including endosomes, cytosol, multivesicular bodies, actin and nuclei which reflects the many functions these proteins have in the cell [301]. Initially synthesized in the cytoplasm, their localization depends on post-translational modifications at the C-terminus such as prenylation, carboxyl methylation and AAX tripeptide proteolysis [302].

Rho GTPases weakly bind GTP and slowly hydrolyse GTP to GDP by breaking the GTP γ-phosphate bond [267]. In this manner, Rho GTPases cycle from their active GTP-bound form to their inactive GDP- form upon hydrolysis of GTP to GDP (Figure 4.1) [303]. In their active GTP-bound form, Rho GTPases can bind to downstream effectors that trigger signalling cascades [267] (for examples, see Figure 3.1). Cycling between their active and inactive forms is controlled upstream by three types of modulators: GTPase activating proteins (GAPs), guanine nucleotide exchange factors (GEFs), and guanine dissociation inhibitors (GDIs) [304]. Firstly, binding of GAPs stimulates and accelerates their hydrolytic activity, thus inactivating them [305]. On the other hand, GEFs bind to the Rho GTPase and force release of GDP , allowing GTP to bind to the Rho GTPase in an activation process [267]. Finally, since Rho GTPases are only active when

bound to the cell membrane, an additional regulation mechanism is provided by GDIs which, through interaction with the Rho GTPases, inhibit Rho GTPase membrane localization [306].

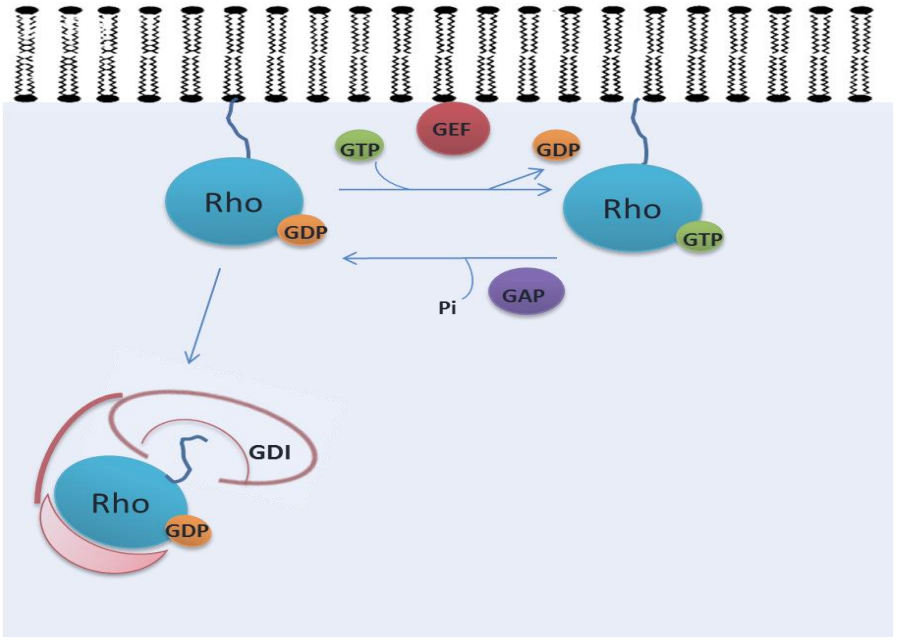

Figure 4.1. Regulation of Rho GTPases by GEFs, GAPs and GDIs. Schematic representation of the general mechanism of Rho GTPase (in blue) regulation. Rho GTPases are activated by displacement of GDP by GEFs which allows GTP to bind. Rho GTPases are inactivated by GAPs which accelerate hydrolysis of GTP to GDP with the release of inorganic phosphate (Pi). GDIs bind to the inactive form of GTPases, the GDP-bound state, preventing GTPases from binding to the membrane and thus, preventing activation. Modified from [305].

As described in chapter 3 (section 3.1), studies have suggested that the HIV Env-co-receptor interaction triggers signalling events inside the cell that aid virus infection. Briefly, HIV-1 activates Rac1 via Env-co-receptor signal transduction through activation of the Gα(q) signalling cascade [255, 256]. Moreover, the HIV-1 Env upregulates the levels of active cofilin which causes breakdown of the actin barrier [80]; cofilin is controlled upstream by cdc42, RhoA and Rac1 [231, 253]. In addition, HIV-1 has also been shown to activate RhoA via Tat in neurons in an actin-dependent mechanism [255, 307]. Recently, Wollard SM et al., showed that human brain tissues infected with HIV-1 have higher levels of activated Rac1

and that this activation is likely to be mediated by Env-CCR5 interaction [283]. The relevance of this finding lies on the fact that there are no antiretroviral targets that are able to prevent infection of the brain, one of the main latency reservoirs of HIV-1; an interesting therapeutic strategy could therefore be by targeting Rac1 activity.

In addition, results presented in chapter 3 showed that treatment with NSC which inhibits upstream regulators of Rac1, Tiam1 and TrioN, inhibited HIV-1 NL4.3 (X4-tropic) which suggests that these upstream effectors have a role in HIV-1 infection (Figure 3.9A). Interestingly, treatment with NSC had no effect on HIV-1 BaL (R5-tropic) (Figure 3.9B). There may be different signalling pathways transduced depending on the Env/co-receptor combination or virus strain. In addition, expression of the full-length Env cytoplasmic tail caused a significant decrease in microtubule acetylation which is a marker of microtubule stability (Figure 3.4); microtubule stability is controlled by Rac1 and RhoA (chapter 3, figure 3.1) [258, 264, 308]. Upon deletion of the C-terminal domain (110 amino acids) of the cytoplasmic tail, the decrease in tubulin acetylation was not significant which suggests that this domain is important for the observed phenotype. This domain has been described to be necessary for interaction of the tail with P115-RhoGEF, an upstream regulator of RhoA [290].

Both, evidence from the literature and results presented in chapter 3 suggest that Rho GTPases play a role in HIV-1 infection. However, not much is known about the role of upstream regulators of Rho GTPases in HIV-1 infection. Understanding more about these proteins could shed light onto novel therapeutic cellular targets that mutate less easily than viral targets (cellular DNA polymerases have proof-reading mechanisms whilst the HIV RT does not [309]) and are a less toxic option than targeting Rho GTPases directly since Rho GTPases are key cellular proteins. I hypothesized that GAPs and GEFs that

regulate Rho GTPases might play a positive or negative role in HIV-1 infection and that these roles might be different depending on viral co-receptor usage.

4.2 Aims:

- To determine if any of the known 145 upstream regulators of Rho GTPases have a role in HIV-1 infection.
- To determine if the role of upstream effectors of Rho-GTPases is different in NL4.3 (X4-tropic) or HIV-1 BaL (R5-tropic) infection.

4.3. Results

To identify if Rho GTPase upstream effectors affect HIV-1 BaL and HIV-1 NL4.3 infection, a siRNA screen was performed which included knockdown of the 145 known upstream regulators of Rho GTPase including GAPs and GEFs. Subsequently, a set of pre-seeded siRNAs on 96-well plates were purchased from ThermoDharmacon which included 4 single siRNAs against each of the 145 GAPs and GEFs included per well (the list of targets is included in Appendix 2 and the details of the sequences for each siRNA employed are included in the electronic version as a supplementary file).

4.3.1. Optimisation of siGLO-transfected TZM-bl cells

To optimise siRNA transfection of TZM-bl cells I tested two transfection reagents (Dharmacon reagent 1 and reagent 4). Dharmacon's siGLO-Red transfection indicator was used to determine transfection efficiency. siGLO-Red has a fluorescent red tag (557/570nm) that can be detected using a confocal or epifluorescent microscope. Transfected cells were imaged by confocal microscopy: i) to estimate the transfection efficiency using both reagents in TZM-bl cells and ii) to determine whether siGLO-Red was inside the cells as opposed to adhering to the external cell membrane. Control cells (untransfected) were cells incubated with siGLO-Red but with no added transfection reagent.

Images show that there is no red signal in the untransfected cells compared to the cells transfected with siGLO-Red and reagent 1 or reagent 4 (Figure 4.2A). Some cells transfected with siGLO-Red and reagent 1 or reagent 4 appear to have a punctuated fluorescent signal in the cells' cytoplasm and nuclei (yellow arrowheads). Quantification of cells that presented the punctuated red signal (siGLO-Red positive) versus those that did not present such staining (siGLO-Red

negative) (Figure 4.2B) showed that transfection efficiency with reagent 1 is of 70% whilst transfection efficiency with reagent 4 is of 20%.

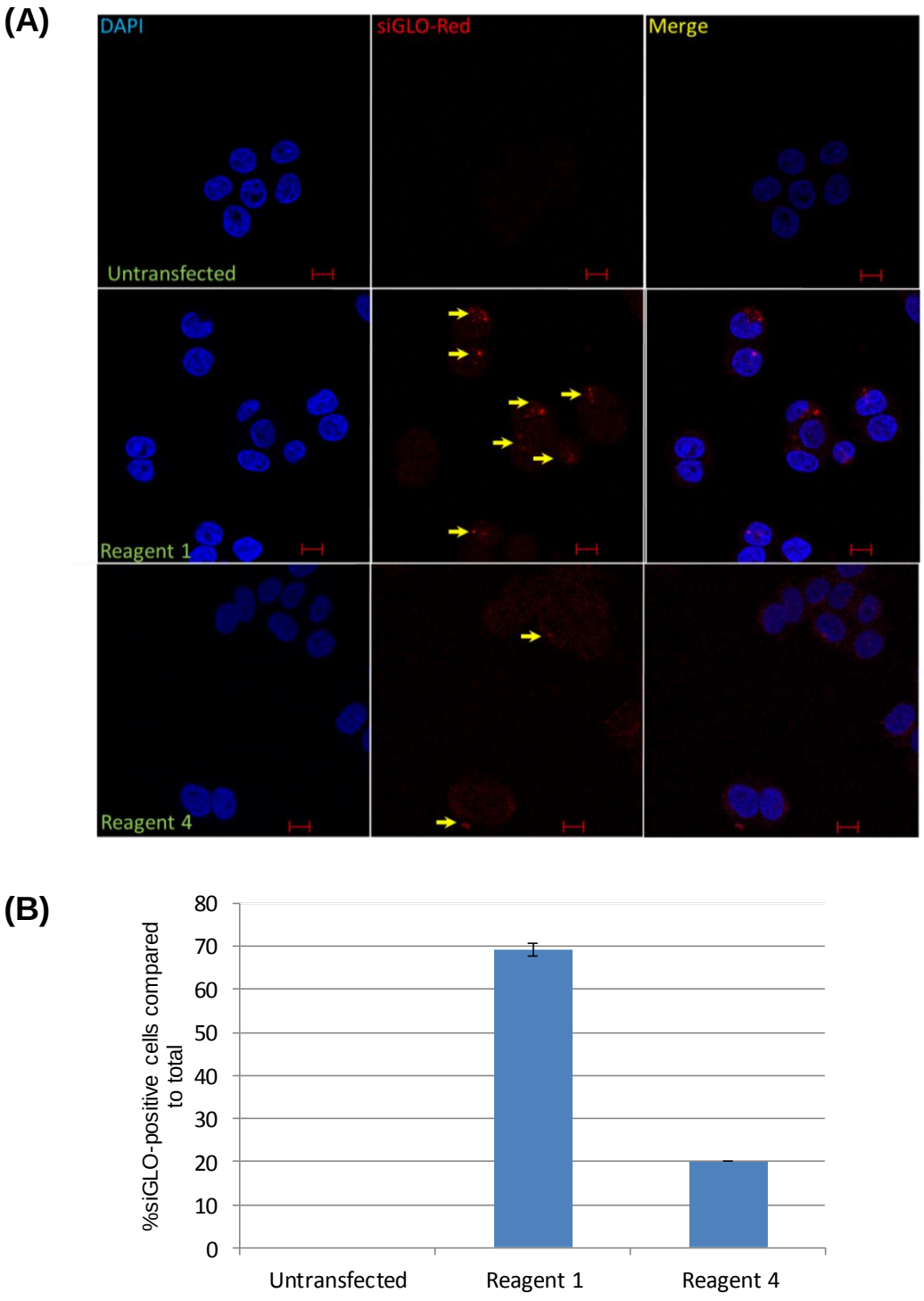

Figure 4.2. Transfection efficiency of Dharmacon reagent 1 and Dharmacon reagent 4 in TZM-bl cells. (A)TZM-bl cells were transfected with siGLO-Red using reagent 1 and reagent 4 and incubated for 48 hours, then fixed and imaged by confocal microscopy. DAPI (blue) was used to stain the nuclei. Size bar indicates 10µm. Yellow arrows indicate SiGLO-Red staining. (B) siGLO-Red positive cells compared to total cells in image. A total of 223 cells were analysed from two independent experiments.

TZM-bl cells transfected with siGLO-Red, show a punctuated red signal close to the nuclei and in the cytoplasm which is absent in the control. However, these images are not sufficient to determine whether the siRNA is internalized in the transfected cells or adhered to the cell membrane. To confirm this, z-stack confocal imaging of cells transfected with siGLO-Red was performed. Z-stack confocal imaging allows image acquisition of optical slices of a cell which provides information on the localization of fluorescent signals detected in outer and inner planes of the cells analysed.

A total of 29 optical sections of 0.3 µm in width were taken of two cells transfected with siGLO-Red; figure 4.3A shows the 29 images for the optical sections taken. As can be seen the punctuated red signal (yellow arrow) becomes into focus in the middle planes of the cell where the nuclei (DAPI) is at its brightest. As the nucleus comes out of focus in the more external planes of the cell (stacks 0-4.22 µm and stacks 8.44-9.08 µm onwards), the red signal also goes out of focus. This therefore suggests that siGLO-Red is internalized in the cell. In addition, the orthogonal view (Figure 4.3B) shows that the siGLO-Red signal is present, at the marked intersection through the XY and XZ planes that is, across the different optical slices of the cell which confirms that the siRNA is inside the cells. Altogether, evidence shows that siGLO-Red becomes internalized in the cell when transfected into TZM-bl cells with reagent 1.

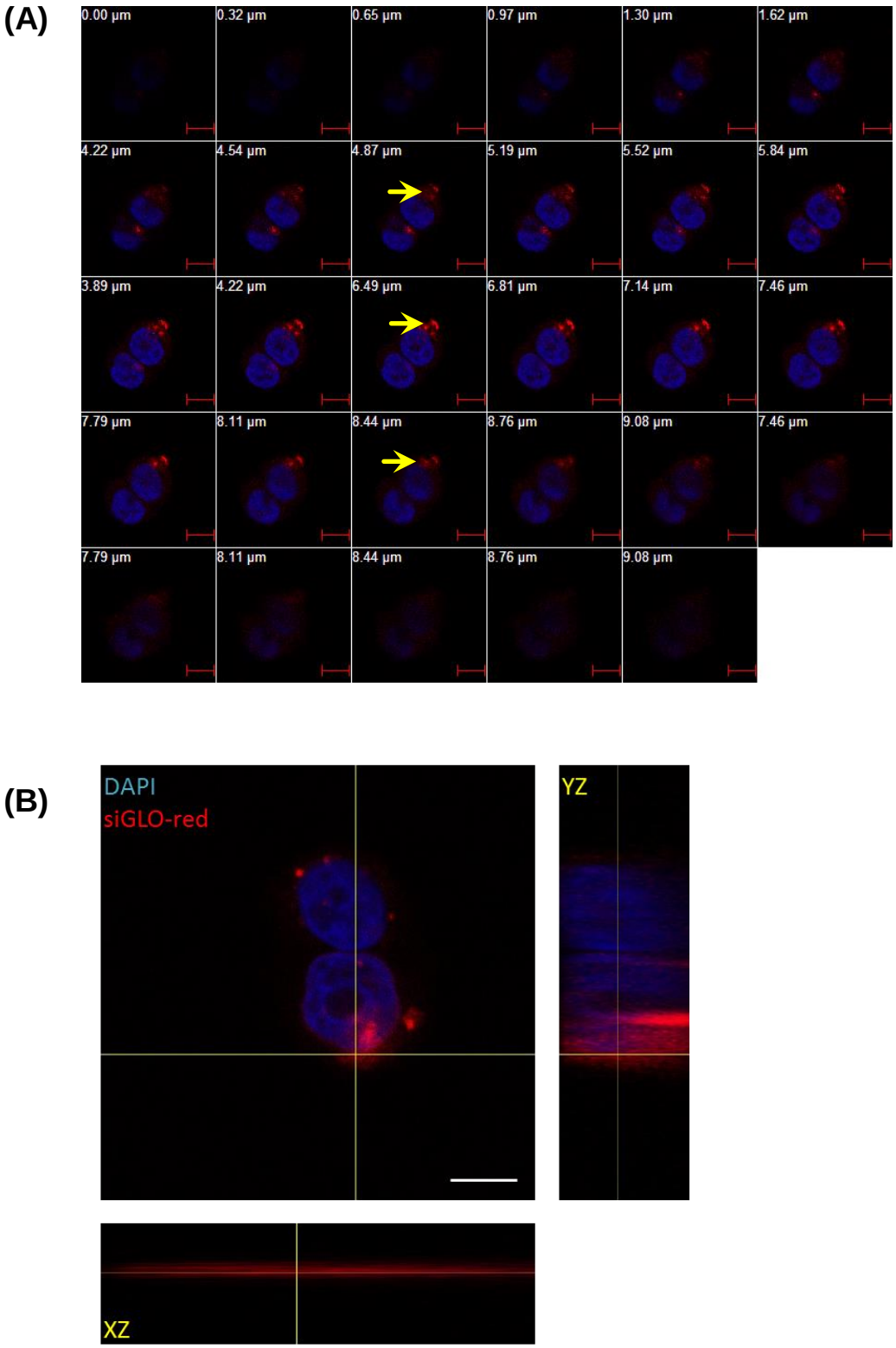

Figure 4.3. siGLO-Red is internalized in TZM-bl cells. Confocal 3D microscopy was performed of TZM-bl cells transfected with siGLO-Red and nuclei (DAPI, blue). A) Z plane confocal images of each Z-stack taken. Numbering on top left corner indicates the depth of the Z-stack; each Z-stack was of 0.32 µm. Yellow arrows indicate siGLO red. B) Orthogonal view of the red signal (punctuated staining) after transfection with siGLO-Red at the marked intersection (white lines) across the XZ and YZ planes. Size bars indicate 10µm.

4.3.2. siRNA screen of TZM-bl cells infected with HIV-1 BaL and HIV-1 NL4.3

Once the transfection conditions were optimised, the siRNA screen was performed to investigate if known GAPs and GEFs that control Rho GTPases have an effect on HIV NL4.3 (X4-tropic) or HIV-1 BaL (R5-tropic) infection. The pre-plated siRNAs were rehydrated in transfection reagent 1 and TZM-bl cells were seeded in each well of the 96-well plates (two plates per screen: one for GAPs and one for GEFs) as described in 2.2.8.2. After incubation for 48 hours, cells were infected with replication-competent HIV-1 NL4.3 (X4-tropic) and HIV-1 BaL (R5-tropic). Infection was detected by β-gal staining since TZM-bl cells have integrated β-galactosidase which is under control of the HIV-1 promoter (described in 2.2.5.3) [310]. Images of the control wells were taken using the INCell machine which includes a Nikon microscope able to take wide field images, appropriate to record virus-infected cells which after β-gal staining should present a characteristic dark blue staining. Using the images taken, quantification of virus-infected cells was performed by counting focus forming units per ml of virus added (FFU/ml).

As described at the beginning of section 4.3, each target protein was knocked down with 4 different single siRNAs against each of the 145 known GAPs and GEFs per well. siRNAs were distributed across two 96-well plates (one for GAPs and one for GEFs) per screen. Moreover, each plate included a set of negative siRNA controls which consisted of four Dharmacon ON-TARGETplus® Non-Targeting Control Pools (5 wells in total) which are not expected to interfere with HIV-1 infection. Additionally, 4 single siRNAs against CD4, CXCR4 and CCR5 each were included as positive controls for siRNA knockdown. Since CD4/CXCR4 are required for HIV-1 NL4.3 infection (X4-tropic) and CD4/CCR5

are required for HIV-1 BaL infection (R5-tropic) it is expected that down-modulation positively interferes with infection of either viruses.

At the end of the screens, cells in some wells covered approximately 80-100% of the well and had the characteristic elongated cytoplasms of TZM-bl cells, ie. had a healthy normal morphology as previously observed in the laboratory. However, in other wells, cells presented irregular monolayers, ie. cells had detached possibly due to cell death and cell morphology of the remaining cells had a round shape which normally suggests cytotoxicity. In order to exclude false positives and to be able to compare results from different wells before performing the infected cells count, each well was assessed in terms of monolayer coverage (Figure 4.4, HIV-1 NL4.3 screen and Figure 4.5 HIV-1 BaL screen). For this purpose at the time of cell fixation, each well was visualized under a light microscope and assigned a score. The score was assigned to each well depending on the percentage of cells that covered the well as observed under a light microscope (raw data in appendix 3); a score of 1 was assigned when the monolayer coverage was of over 80% and a score of 0 was assigned when the monolayer coverage was lower than 80%. Wells with a 0 score were not included in the analysis. Importantly, results show that cells from the CXCR4, CD4 and CCR5 controls included in each screen were covered 100% of the well. The 10 non-targeting controls of the BaL screen (5 per plate) also covered 100% of the well. In the NL4.3 screen, the 5 non-targeting controls of plate 1 covered 100% of the well whilst in plate 2, 3 non-targeting controls had 0% membrane integrity possibly due to contamination of those specific wells. However, since the other 7 wells of non-targeting controls presented 100% monolayer coverage, the mean control count was performed of the 7 non-targeting controls. Interestingly, some of the knockdowns such as SYDE1 or ARGHAP10 seemed to affect monolayer coverage importantly in the NL4.3 screen whilst in the BaL screen, monolayer

coverage was of 100%. It could be that NL4.3 is more cytopathic than BaL and this is why differences in cytotoxicity are seen for a same knockdown in both screens.

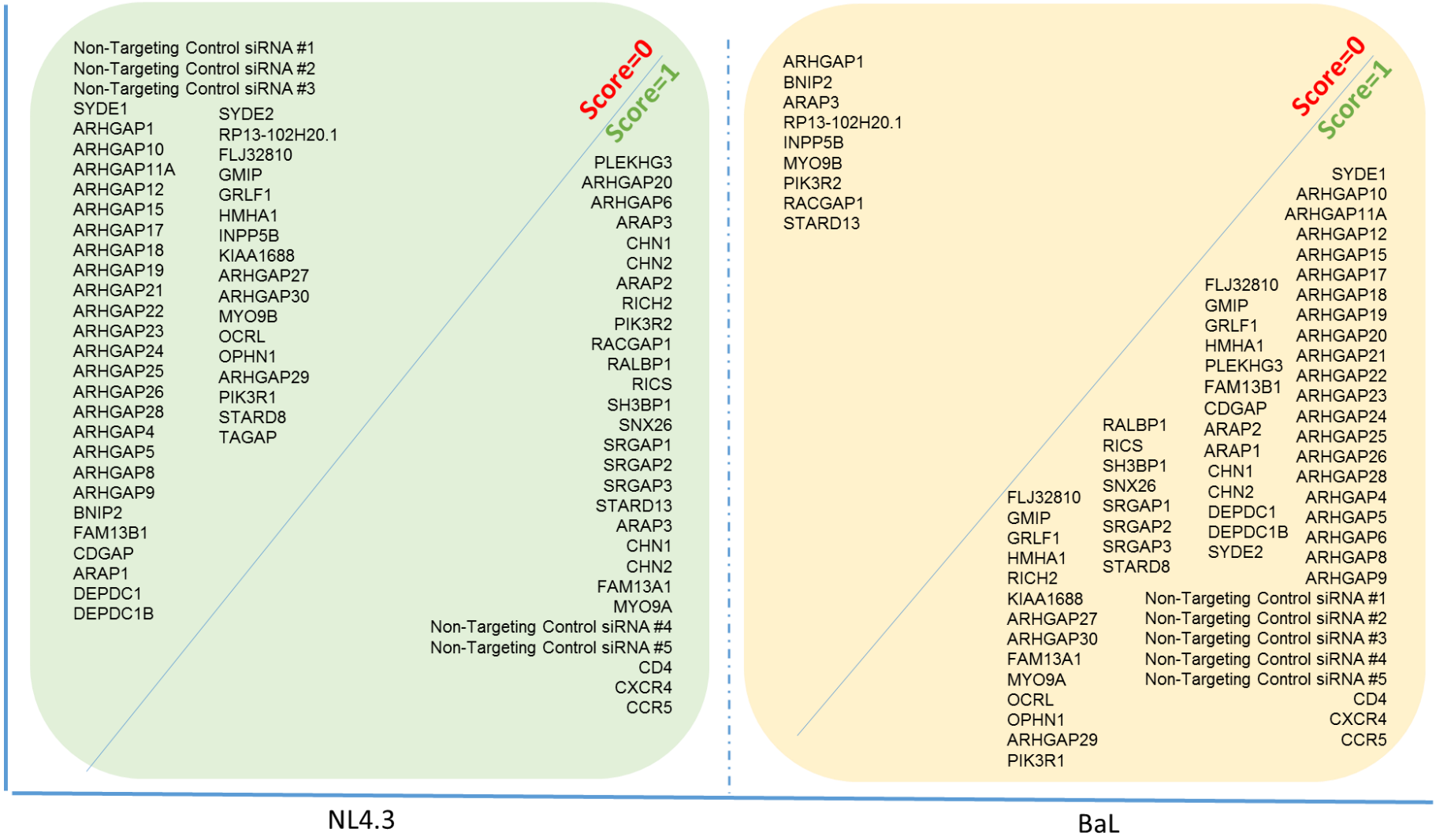

Figure 4.4. Scores (0/1) of wells after siRNA knockdown of GAPs and HIV-1 NL4.3 infection (green) and HIV-1 BaL infection (red) according to monolayer coverage of cells. Each well was assessed according to the percentage of cells that covered well (monolayer coverage) through observation with a light microscope. Wells that presented 80-100% monolayer coverage were assigned a score of 1 and cells that presented under 80% of monolayer coverage were assigned a score of 0.

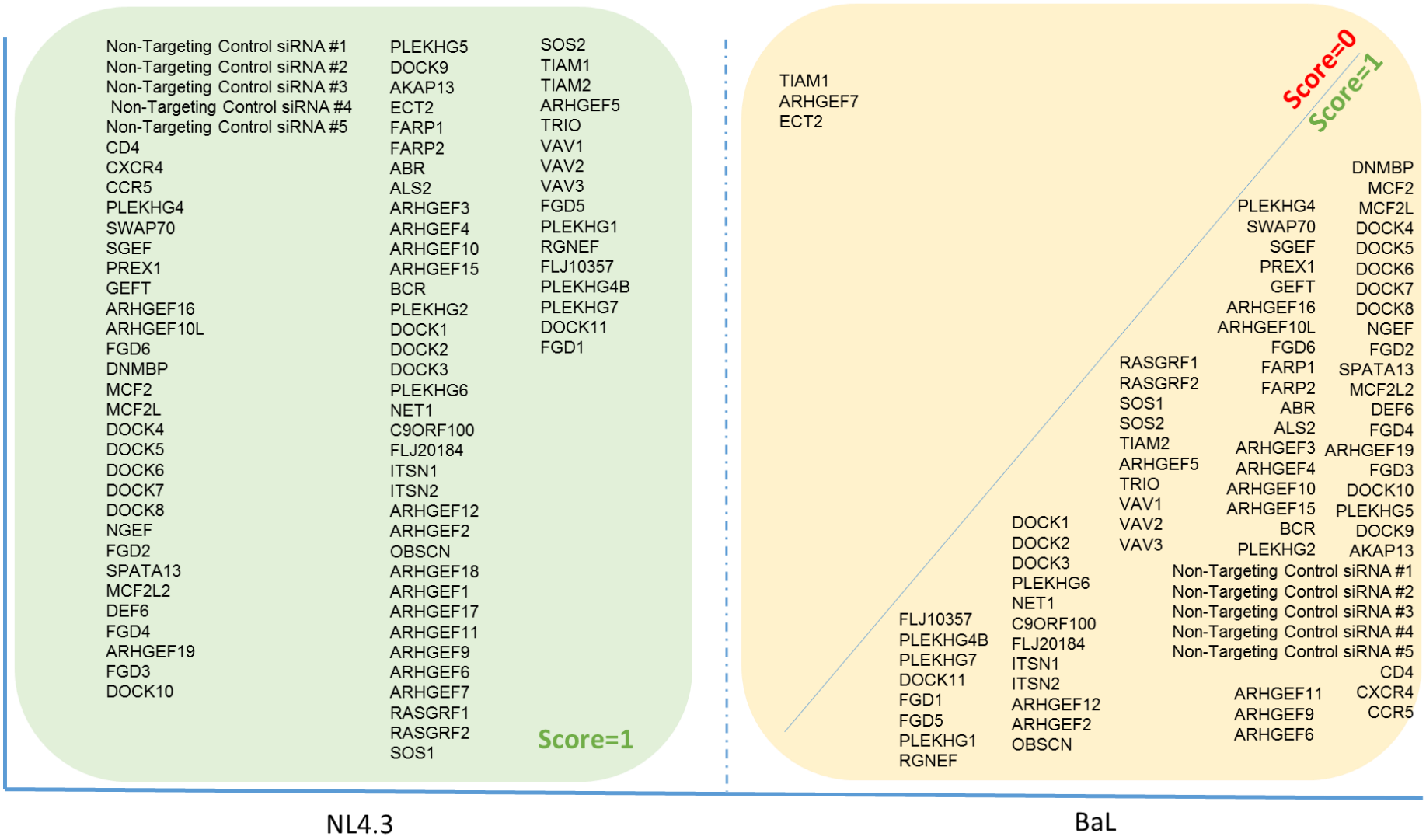

Figure 4.5. Scores (0/1) of wells after siRNA knockdown of GEFs and HIV-1 NL4.3 infection (green) and HIV-1 BaL infection (red) according to monolayer coverage of cells. Each well was assessed according to the percentage of cells that covered well (monolayer coverage) through observation with a light microscope. Wells that presented 80-100% monolayer coverage were assigned a score of 1 and cells that presented under 80% of monolayer coverage were assigned a score of 0.

Images of the control wells for the HIV-1 NL4.3 screen (Figure 4.6A, top row) show that in the CD4 and CXCR4 siRNA knockdowns, the number of HIV-1 NL4.3 foci of infection (dark β-gal staining) is lower compared to the number of infected cells in the cells alone and non-targeting siRNA controls. A decrease of foci of infection of 98% and 96% for CD4 and CXCR4 is confirmed quantitatively (Figure 4.6B) which suggests that the siRNA knockdowns are efficient. HIV-1 NL4.3 infection is unaffected by CCR5 knockdown and this is confirmed at the quantitative level whereby the number of FFU/ml of non-targeting siRNA and CCR5 are similar. This was expected since HIV-1 NL4.3 only uses CXCR4. The non-targeting and cells alone control should be similar.

Images of the control wells of the HIV-1 BaL screen show that upon knockdown of CD4 and CCR5, infection is reduced compared to cells only and non-targeting siRNA controls as expected since these two receptors are required for HIV-1 BaL (R5-tropic) entry (Figure 4.6A, bottom row). A reduction of foci of infection of 98% and 76% for CD4 and CCR5 is confirmed at the quantitative level (Figure 4.6B) suggesting that the siRNA knockdowns are efficient. HIV-1 BaL-infected cells that had CXCR4 knockdown are visually slightly higher in number to non-targeting siRNA control and cells only control and this is confirmed quantitatively. Since the primary co-receptor of HIV-1 BaL is CCR5, it was expected that knockdown of CXCR4 had no effect on infection. The fact that it is slightly higher could be due to an effect of downregulation of CXCR4 on CCR5 expression levels.

Overall the evidence presented, suggests that siRNA knockdown controls, 48 hours after transfection efficiently block HIV-1 infection as expected. Therefore, I analyzed the rest of the targets.

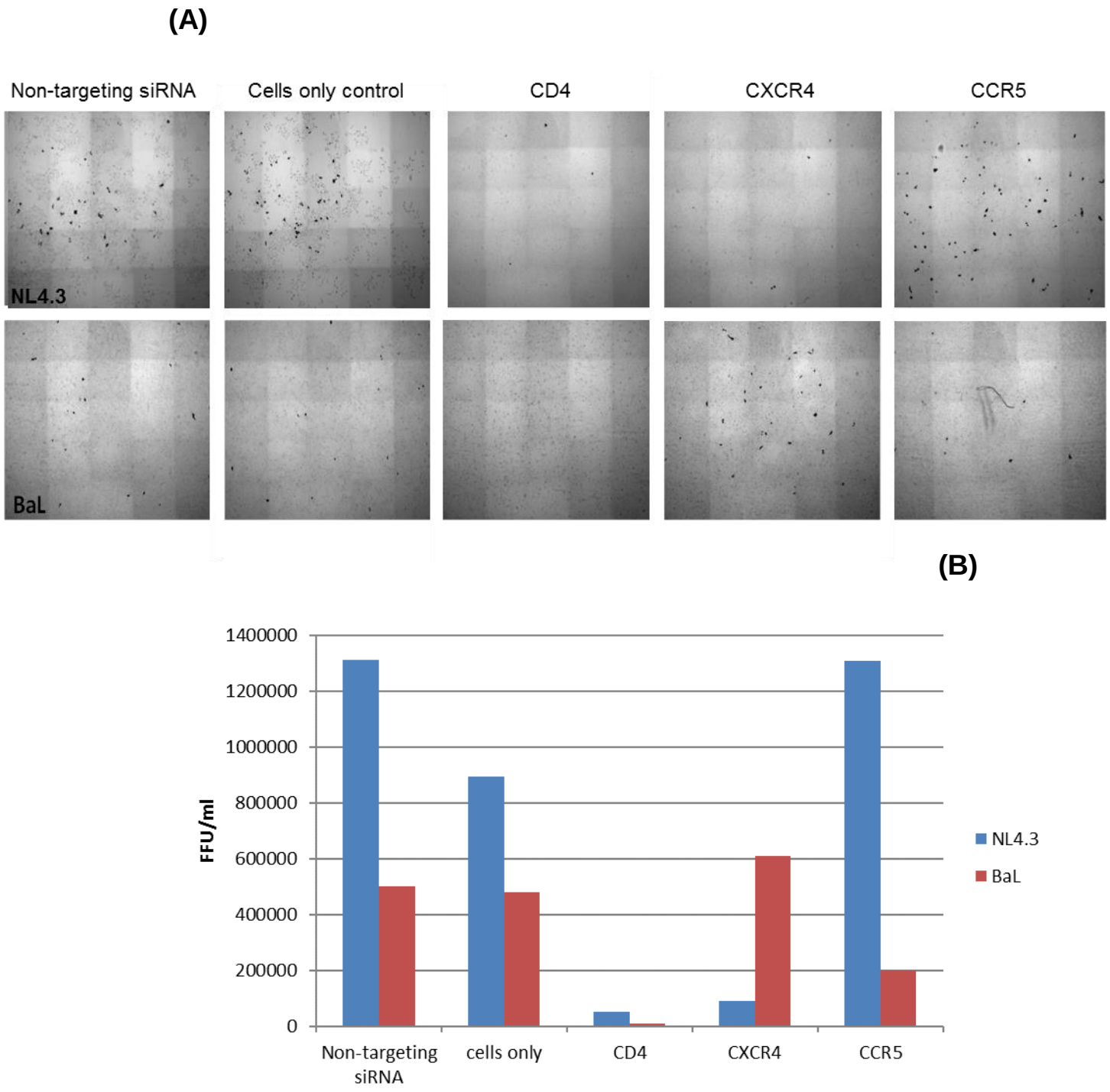

Figure 4.6. siRNA knockdown controls of HIV-1 NL4.3 and HIV-1 BaL screens. TZM-bl cells were transfected with non-targeting siRNA, anti-CD4, anti-CXCR4 and anti-CCR5 siRNA using Dharmacon transfection reagent 1 for 48 hours and infected with (A) HIV-1 NL4.3 (upper row) or BaL (bottom row) foci of infection 48 hours post infection. Cells were then fixed and infection was visualized by staining of β-galactosidase which is under the control of the HIV-1 promoter. (B) Mean number of infectious virus was calculated as focus forming units in each well containing non-targeting siRNA, cells only, anti-CD4, anti-CXCR4 and anti-CCR5 siRNA for each of the screens. N=1. FFU=Focus forming units.

In order to identify potential hits, an arbitrary threshold was established in which positive hits were those that increased or decreased infection by ±50%. Following this method, knockdown of GEFs and GAPS and subsequent infection with HIV-1 NL4.3 or HIV-1 BaL revealed a set of proteins that upon knockdown, increased or decreased infection compared to non-targeting siRNA controls Figure 4.7 and Figure4.8.

(A)

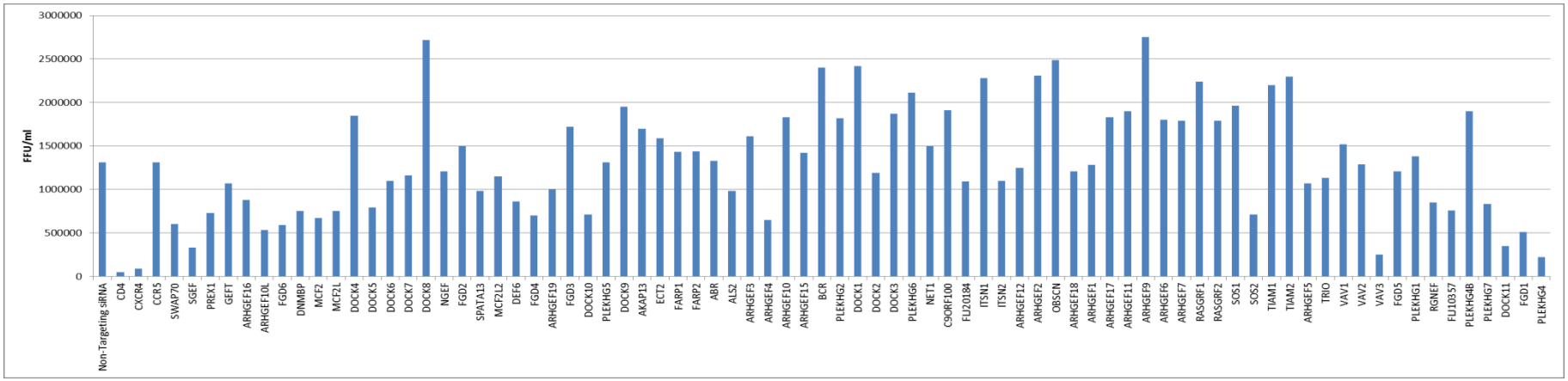

(B)

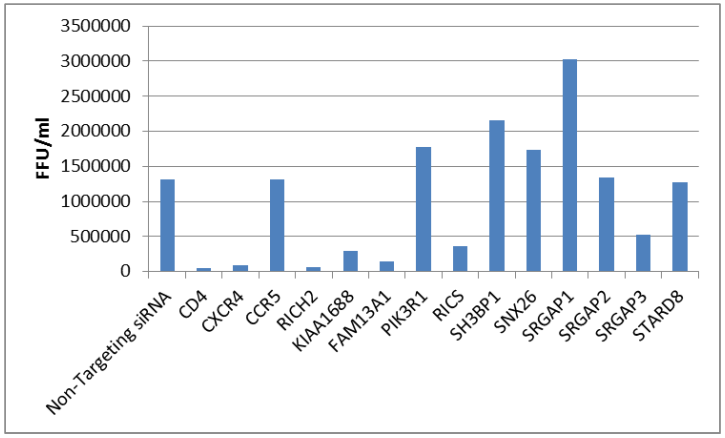

Figure 4.7. HIV-1 NL4.3 siRNA screen results. (A) Number HIV-1 NL4.3 infected cells upon siRNA knockdowns of GEFs. B) Number of HIV-1 NL4.3 infected cells upon siRNA knockdowns of GAPs hits. Infection is measured as foci of infection or focus forming units, FFU/ml. N=1.

(A)

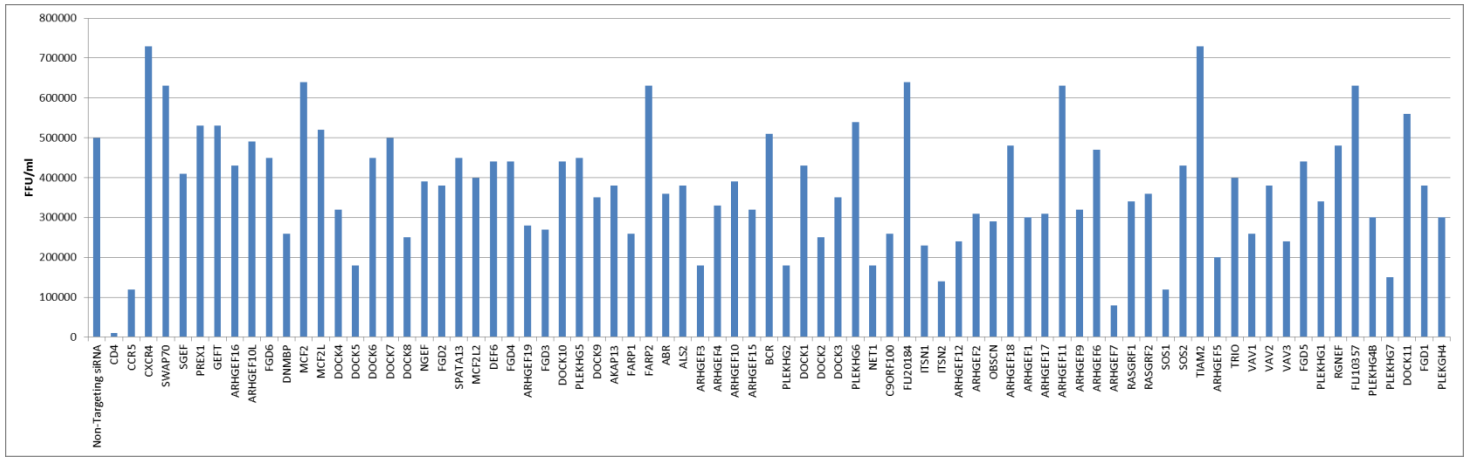

(B)

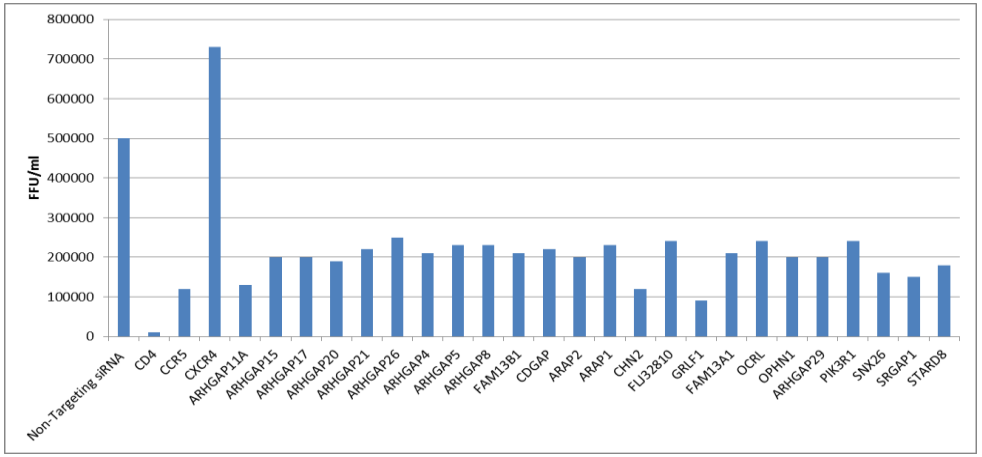

Figure 4.8. HIV-1 BaL siRNA screen results. (A) Number HIV-1 BaL infected cells upon siRNA knockdowns of GEFs. B) Number of HIV-1 BaL infected cells upon siRNA knockdowns of GAPs hits. Infection is measured as foci of infection or focus forming units FFU/ml. N=1.

In particular, knockdown of proteins found to increase infection of HIV-1 NL4.3 by 2-fold were: DOCK8, ARHGEF9 and SNX26 (Figure 4.9A and 4.9B). On the other hand, knockdown of proteins found to decrease infection by 2-fold were: SWAP70, SGEF, ARHGEF10L, FGD6, ARHGEF4, ARHGEF9, FGD1 and PLEKH7 (Figure 4.9A and 4.9B). In addition, knockdown of GAPs, RICH2, KIAA1688, FA13A1, PIK3R1, RALBP1 and SRGAP2 decreased NL4.3 infection.

(A)

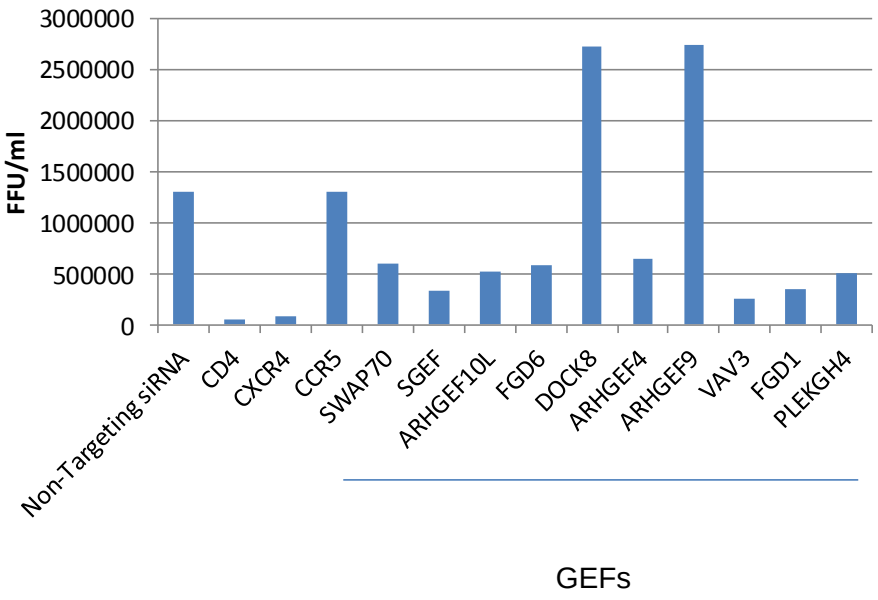

(B)

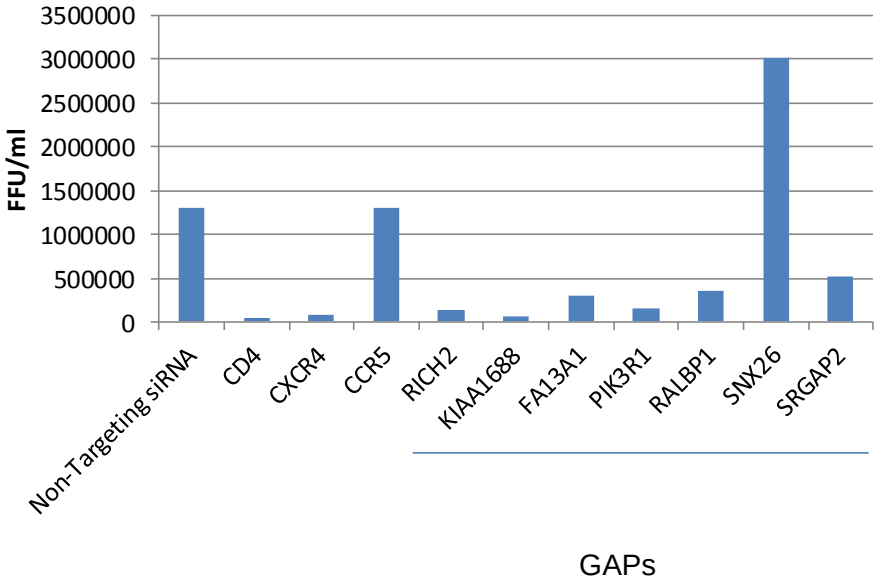

Figure 4.9. Effect of potential GEFs and GAPs on HIV-1 NL4.3 infection. (A) Number of HIV-1 NL4.3 infected cells upon siRNA knockdowns of GEFs. B) Number of HIV-1 NL4.3 infected cells upon siRNA knockdowns of GAPs hits. Infection is measured as FFU/ml. N=1

On the other hand, all the proteins identified in the HIV-1 BaL screen had a decreasing effect on HIV-1 BaL infection upon knockdown (Figure 4.10A and 4.10B). These included GEFs from the DOCK family of proteins: DOCK5, DOCK8 and DOCK2. In addition knockdown of GEFs ARHGEF3, PLEKHG2, NET1, were found to decrease infection. Two GEFs, ITNS1 and ITNS2, members of the Intersectin family of proteins were found to decrease HIV-1 Bal infection upon knockdown. In addition, ARHGEF12 and ARHGEF5 decreased HIV-1 BaL infection upon knockdown. Furthermore, SOS1, VAV3 and PLEKHG7 were also GEFs that decreased infection upon knockdown. Remarkably, a number of members from the ARHGAP family of proteins had all a decreasing effect on HIV-1 BaL infection including: ARHGAP11A, ARHGAP15, ARHGAP17, ARHGAP20, ARHGAP21, ARHGAP26, ARHGAP4, ARHGAP29, ARHGAP5, ARHGAP8. In addition, knockdown of GEFs FAM13B1, CDGAP, ARAP2, ARAP1, CHN2, FLJ32810, GRLF1, FAM13A1, OCRL, OPHN1, PIK3R1, SNX26, SRGAP1 and STARD8 were also found to decrease HIV-1 BaL infection.

Interestingly the pattern of proteins found to increase/decrease HIV-1 BaL or HIV-1 NL4.3 is different but there are also some common hits identified in both screens.

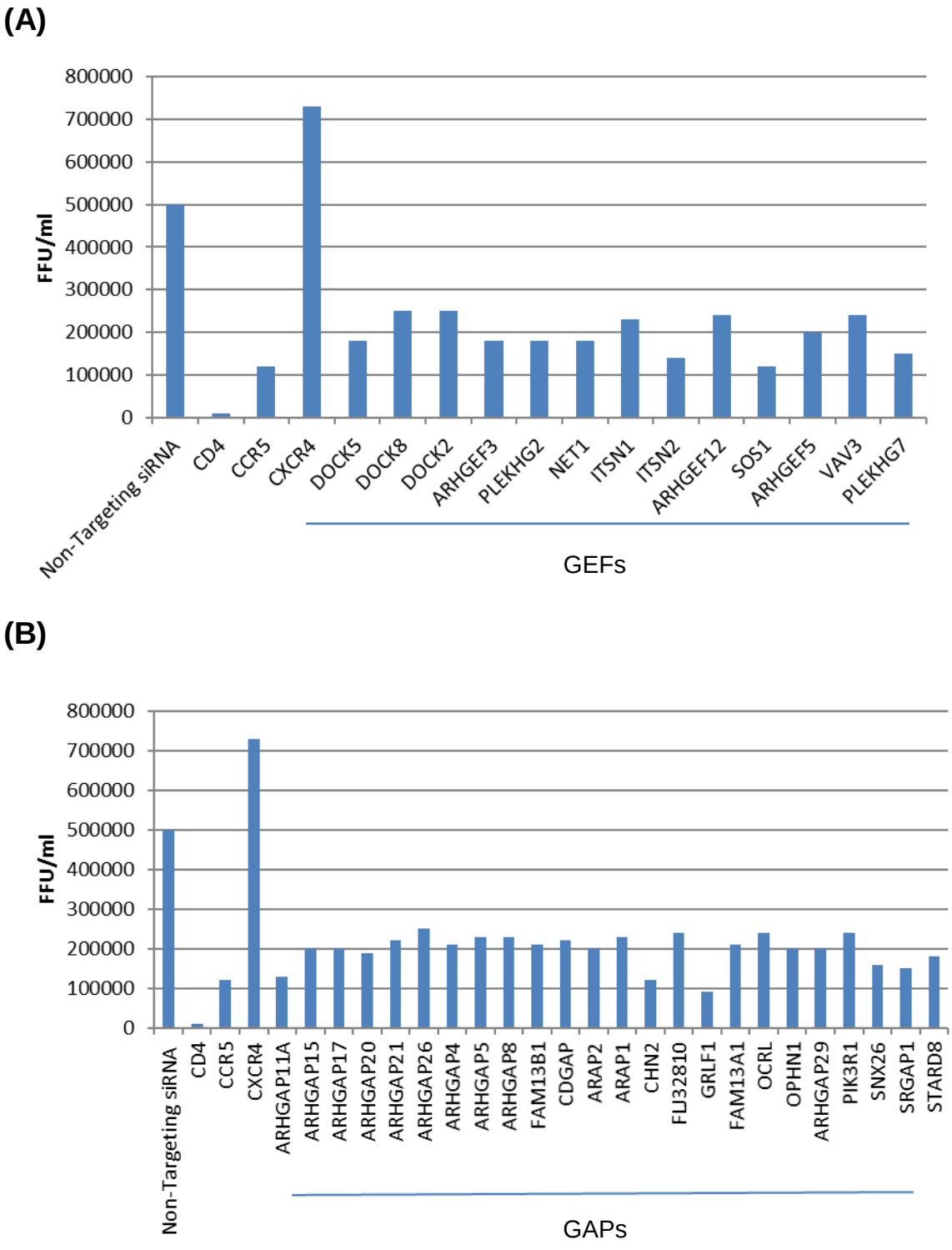

Figure 4.10. Effect of potential GAPs and GEFs on HIV-1 BaL infection. (A) Number HIV-1 BaL infected cells (FFU/ml) upon siRNA knockdowns of GAP hits. B) Number of HIV-1 BaL infected cells upon siRNA knockdowns of GEFs hits. N=1. Infection is measured as FFU/ml.

4.4 Discussion

At early stages of infection, HIV-1 Env interacts with a main receptor, CD4 and a co-receptor, CXCR4 or CCR5 [48]. These interactions result in 1) access into the cell and 2) signalling events [80, 232, 242, 255, 283, 311, 312], that change the cell's environment for replication advantage. The first objective has been well characterized in an effort to develop inhibitors which block viral entry and so, viral infection [313]. These efforts have contributed to the development of entry inhibitors which are widely used as part of the HAART drug regime such as maraviroc [139, 313], a CCR5 antagonist or fuzeon, a gp41 fusion peptide [131]. However, Env signaling and its downstream consequences for HIV-1 infection is one of the aspect of HIV biology that it is still not well understood.

Results presented in chapter 3 suggested that upstream effectors that control Rac1, Tiam1 and TrioN, have a role in HIV-1 infection since, treatment with NSC, an inhibitor designed to inhibit these proteins, reduced HIV-1 NL4.3 infection (Figure 3.9). Interestingly, treatment with NSC had no effect on HIV-1 BaL infection. I therefore hypothesized: i)that there could be other upstream regulators of Rho GTPases that may be involved in HIV-1 infection and 2)that it could be that there are differences between signaling events elicited by the Env protein of an X4-tropic virus (HIV-1 NL4.3) and an R5-tropic virus (HIV-1 BaL). Screening of 145 GAPs and GEFs that regulate Rho GTPases identified 31 proteins in total which can be divided into three classes: 1) proteins that had a 2-fold effect on HIV-1 NL4.3 infection, 2) proteins that had a 2-fold effect on HIV-1 BaL infection and 3) proteins that had a 2-fold effect on both HIV-1 NL4.3 and BaL infection (Figure 4.11A). To identify signalling pathways involved, each hit was searched in PubMed, NCBI Gene and UniProt EMBL databases (Figure 4.11B and 4.11C).

(A)

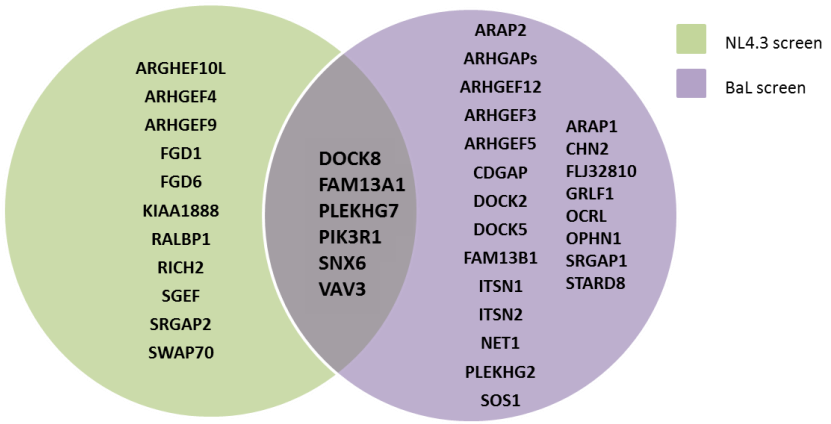

(B)

Protein	GAP/GEF	Effect on HIV-1 NL4.3 infection	Target Rho-GTPase	References
SWAP70	GEF	Decrease	RhoA	[314]
SGEF	GEF	Decrease	Rho G	[315]
ARHGEF10L	GEF	Decrease	RhoA, RhoC and RhoB	[316]
FGD6	GEF	Decrease		
DOCK8	GEF	Increase	Rac1 and Cdc42	[317]
ARHGEF4	GEF	Decrease	Rac1 and cdc42	[318, 319]
ARHGEF9	GEF	Increase	Cdc42	[320]
VAV3	GEF	Decrease	Rac1	[321]
FGD1	GEF	Decrease	Unknown	
PLEKGH4	GEF	Decrease	Unknown	
RICH2	GAP	Decrease	Cdc42	[322]
KIAA1688	GAP	Decrease	Unknown	
FA13A1	GAP	Decrease	Unknown	
PIK3R1	GAP	Decrease	Rac1	[323]
RALBP1	GAP	Decrease	Ral	[324]
SNX26	GAP	Increase	Unknown	
SRGAP2	GAP	Decrease	Unknown	

(C)

Protein	GAP/GEF	Effect on HIV-1 BaL infection	Target Rho-GTPase	References
DOCK5	GEF	Decrease	Rac1	[325]
DOCK8	GEF	Decrease	Rac1	[326]
DOCK2	GEF	Decrease	Rac1	[325]
ARHGEF3	GEF	Decrease	RhoA	[327]
PLEKHG2	GEF	Decrease	Rac1 and Cdc42	[328]
NET1	GEF	Decrease	RhoA	[329]
ITSN1	GEF	Decrease	Cdc42	[330]
ITSN2	GEF	Decrease	Cdc42	[331]
ARHGEF12	GEF	Decrease	RhoA	[332]
SOS1	GEF	Decrease	Rac1	[319]
ARHGEF5	GEF	Decrease	RhoA	[333]
VAV3	GEF	Decrease	Rac1	[321]
PLEKHG7	GEF	Decrease	Unknown	
ARHGAP family of proteins	GAP	Decrease	RhoA	[334]
FAM13B1	GAP	Decrease	Unknown	
CDGAP	GAP	Decrease	Cdc42	[335]
ARAP2	GAP	Decrease	Rac1	[336]
ARAP1	GAP	Decrease	RhoA	[337]
CHN2	GAP	Decrease	Unknown	
FLJ32810	GAP	Decrease	Unknown	
GRLF1	GAP	Decrease	RhoA	[338]
FAM13A1	GAP	Decrease	Unknown	
OCRL	GAP	Decrease	Rac1	[339]
OPHN1	GAP	Decrease	RhoA, Cdc42 and Rac1	[340]
PIK3R1	GAP	Decrease	Rac1	[323]
SNX26	GAP	Decrease	Unknown	
SRGAP1	GAP	Decrease	Rac1	[341]
STARD8	GAP	Decrease	Unknown	

Figure 4.11. (A) Summary of GAPs and GEFs hits identified in siRNA upon HIV-1 NL4.3 and HIV-1 BaL infection. (B) HIV-1 NL4.3 and (C) HIV-1 BaL hits are organized based on an increase or decrease effect on infection upon knockdown and on the basis of Rho GTPase known target. A database search was done using PubMed, NCBI Gene and UniProt EMBL to identify the Rho GTPase target of each hit and references are included.

The screen was performed, having previously optimized the best transfection conditions in TZM-bl cells by trialling the efficiency of two different transfection reagents (Figure 4.2) and after confirmation that the siRNA was internalized at the chosen conditions (Figure 4.3). In the screens performed, each GAP and GEF protein was knocked down with 4 single siRNAs per well. In addition, 5 non-targeting siRNAs per plate were included and 4 single siRNAs per target against CD4, CXCR4 and CCR5 were included in each plate. Although Western-Blot analysis of the knockdowns was not performed, siRNA knockdowns against CD4, CXCR4 and CCR5 proved to be efficient robustly across the 4 plates since there was a decrease of HIV-1 NL4.3 infection upon knockdown of CD4 and upon knockdown of CXCR4 and a decrease of HIV-1 BaL infection upon knockdown of CD4 and upon knockdown of CCR5 as expected (Figure 4.6).

Results support the first hypothesis formulated in this chapter: that GAPs and GEFs not previously described for HIV, may have a role in HIV-1 infection since upon knockdown of these genes the levels of infection are altered compared to controls. In fact, the majority of proteins that had an effect on HIV-1 NL4.3 or BaL infection are different. These results therefore also support the second hypothesis formulated: that it could be that the signal transduction pathways elicited by the Env protein of HIV-1 NL4.3 (X4-tropic) and HIV-1 BaL (R5-tropic) are different. Interestingly, DOCK8, PIK3R1, PLEHGH7, FAM13A, VAV3 and SNX6 were found to have effects on both HIV-1 NL4.3 and BaL infection which also suggests that there are common signalling pathways triggered by both HIV-1 virus strains. Unfortunately the Rho-GTPase target for PLEHGH7, FAM13A and SNX6 is unknown so further conclusions cannot be made.

Knockdown of the GEF protein DOCK8, inhibited HIV-1 BaL infection. From a mechanistic point of view, HIV-1 BaL inhibition of infection by knockdown of DOCK8 is reasonable. DOCK8 is an activator of Rac1 [342] and HIV-1 Env has

been shown to activate Rac1 to rearrange the actin cytoskeleton for cell entry [254-256]; therefore it would be expected that targeting Rac1 activation causes a decrease in infection since actin is not depolymerised, preventing efficient HIV internalization. Supporting this rationale, other members of the DOCK family, DOCK2 and DOCK5, also decreased BaL infection since they also activate Rac1 [325]. In particular, DOCK2 has been shown to form a complex with HIV-1 Nef that activates Rac1 and this in turn, inhibits T-cell chemotaxis [282] ; it could therefore be that knocking down DOCK2 prevents Nef-DOCK2 activation of Rac1. Intriguingly, knockdown of DOCK8 results in enhancement of HIV-1 NL4.3 as opposed to the decreasing observation of HIV-1 BaL infection. An explanation could be that knock down of DOCK8 affects an additional pathway to Rac1 activation that is important for HIV-1 NL4.3 infection. For instance, DOCK8 has also been shown to target cdc42 activation [343] and so, it is possible that this pathway is involved in HIV-1 NL4.3 infection specifically.

The role of Rac1 activation in HIV-1 infection is further supported by the fact that knockdown of all of the GEF hits identified in both screens (ARHGEF4, VAV3, PLEKHG2, SOS1..) that activate Rac1 (Figure 4.9A and 4.9B) have a decreasing effect on HIV-1 BaL and HIV-1 NL4.3 infection; other than the identified common hit DOCK8, all of the other GEFs identified are different suggesting that this pathway could be differentially regulated by NL4.3 and BaL Env proteins through engagement of CCR5 or CXCR4. It would be interesting to further confirm this with other R5/X4 strains to understand whether this differential regulation is X4/R5-tropic specific or only strain-specific.

Cdc42 is upstream of LIMK1 which inactivates cofilin by phosphorylation [231]. On the other hand, Env signaling via CXCR4 activates cofilin which allows HIV to overcome cortical actin restriction [80]; It would therefore be expected that knockdown of cdc42 activators, enhances HIV-1 NL4.3 infection and knockdown

of inactivators, decreases HIV-1 NL4.3 infection. Following this rationale, knockdown of ARHGEF9, an activator of cdc42, increased HIV-1 NL4.3 infection and knockdown of RICH2, an inactivator of cdc42 decreased HIV-1 NL4.3. It could be that the reason behind why HIV-1 patients have active levels of cofilin upregulated [252], is due to an Env-triggered activation of cdc42 that is through viral regulation of ARHGEF9 or RICH2 and so, understanding further this pathway may enlighten the road to novel therapeutic targets that block the aberrant Env-triggered cofilin activation. Unexpectedly, knockdown of an activator of cdc42, FDG6, decreased HIV-1 NL4.3 infection. This protein has been shown to associate with filamin [344] which in turn, is required for actin-dependent CXCR4 clustering to aid virus entry [79], so it could that knockdown of FDG6 affects this pathway negatively.

In the HIV-1 BaL screen a different set of cdc42 regulators were identified suggesting that HIV-1 BaL and HIV-1 NL4.3 Env, trigger different cdc42 signalling pathways. The differences are not only in the proteins identified but possibly also in the mechanism. For instance, whilst knockdown of cdc42 activator ARHGEF9 increased NL4.3 infection, knockdown of cdc42 activators, ITSN1 and ITSN2, decreased HIV-1 BaL infection. Apart from their role in signaling via cdc42 activation [330, 331], intersectins have been shown to have a role in clathrin and caveolin-mediated endocytosis as scaffold proteins [345]. HIV-1 has also been shown to enter the cell via endocytosis [76]. Interestingly, knockdown of two proteins from the Intersectin family of proteins, ITSN1 and ITSN2, were found to decrease HIV-1 BaL infection. It would therefore be interesting to further characterize this phenotype by comparison with a virus pseudotyped with Vesicular Stomatitis Virus (VSV-G) Env, a virus that enters cells via endocytosis [346]; this would contribute to understand whether upon knockdown of ITSN1 and ITSN2, the endocytic pathway or the cdc42 signalling pathway is affected.

The role of RhoA in the HIV context is complex. Firstly, RhoA activation increases microtubule stability via mDIA [264] and stathmin [265, 266] which is required for efficient nuclear import of the HIV-1 preintegration complex [286, 287]. On the other hand, RhoA is also involved in actin reorganization through the ROCK-LIMK-cofilin [347] pathway which HIV subverts to overcome cortical actin restriction upon entry [80]. Therefore, RhoA activation might negatively or positively influence HIV-1 replication. In the screen it was observed that no matter whether the protein identified was an activator or inactivator of RhoA, the effect upon knockdown is a decreasing effect which might reflect these complexities. Interestingly, even though RhoA has these multiple roles that affect HIV-1 replication, only one RhoA GEF, SWAP70, was identified in the NL4.3 screen as opposed to a number of RhoA GAPs and GEFs identified in the BaL screen, suggesting that RhoA might play a more central role in BaL infection than in NL4.3.

There is no evidence for the role of GTPases other than Rac1, RhoA and cdc42 in HIV-1 infection. Interestingly, knockdown of SGEF, a GEF that regulates RhoG and RALBP1, a GAP that regulates RaI respectively, decreased HIV-1 NL4.3 which could suggest a novel role for these GTPases in HIV-1 replication.

Finally, whilst inhibiting Tiam1 and TrioN via treatment with NSC, inhibited HIV-1 NL4.3 (chapter 3), I observed that knockdown of Tiam1 increased NL4.3 infection (Appendix 4) and knockdown of TriO caused a small decrease of HIV-1 NL4.3 infection ; the decrease/increase observed did not reach 2-fold and this is why they are not included in the main body of the chapter but as part of the appendices; however, since chapter 3 had experiments that included these proteins I deemed appropriate to comment them. The differences observed between siRNA and inhibitor phenotypes could be explained possibly by a difference in the viruses employed in both assays; whilst in the inhibitor

experiments, the viruses employed were single-round infection viruses, viruses employed in the screen were full-replication competent viruses. It could therefore be that early stages of HIV infection, present in the single round assay are affected by NSC treatment. This possibility could be confirmed by including full-replication viruses in the inhibitor assays. It is also possible that whilst the siRNA specifically targeted Tiam1 or Trio, the Tiam1/TrioN combination that NSC targets, affects negatively NL4.3 virus replication.

Altogether these results, if further confirmed by assaying other X4 and R5-tropic viruses, shed light on the differential signalling pathways activated upon different HIV Env-receptor engagement. Their importance in infection could yield novel therapeutic targets.

4.5 Principal findings

The following findings have been described:

- Knockdown of 39 proteins encoding Rho-GTPase regulators had an effect on HIV-1 BaL or HIV-1 NL4.3 suggesting that Rho-GTPase regulators play a role in HIV-1 infection.
- Importantly, the set of proteins identified in the BaL and HIV NL4.3 screens were majorly different which suggests differences in the signaling pattern elicited by HIV-1 BaL and HIV-1 NL4.3 viruses.
- All the activators of Rac1 identified in the screen had a decreasing effect on both HIV-1 BaL and NL4.3 infection highlighting the importance of Rac1 activation on HIV-1 infection and a possible novel role of these proteins in HIV-1 replication.
- Interestingly, three members of the DOCK family inhibited HIV-1 BaL infection which could suggest a new role of these proteins with therapeutic potential.

Chapter 5. HIV-1 antiviral activity of PAF1

5.1 Introduction

As reviewed in chapter 1 (section 1.10.9) Liu. et al., showed that upon knockdown of PAF1, there is an increase of HIV-1 early viral transcripts within two hours of infection [158]. As previously discussed the majority of the known cellular functions of PAF1 are mostly involved in control of transcription and gene expression (Chapter 1, section 1.10.9). Interestingly the effects of PAF1c knockdown, enhanced viral reverse transcription, manifest within an hour of viral challenge. I hypothesised 3 different models of how PAF1 could be blocking HIV-1. Firstly, PAF1 could be restricting HIV-1 infection through its known nuclear functions. Secondly, PAF's action may shuttle from the nucleus to the cytoplasm [348] upon detection of incoming virus. This hypothesis is reasonable since HIV restriction occurs at a very early stage of infection prior to integration [158]. A third model, is an indirect mechanism by which upon HIV-1 entry, an unidentified protein signals to PAF1 which triggers effects of PAF1 from the nuclei resulting in expression of inflammatory genes. I therefore tested for evidence to support any of these three models.

5.2 Aims

The proposed aims for this chapter are:

- To understand whether the nuclear localisation of PAF1 is required for HIV-1 infection.
- To investigate whether PAF1 changes its cellular localisation upon HIV-1 infection.
- To understand whether HIV-1 counteracts PAF1.

5.3 Results

5.3.1 Quantitation of PAF1 mean integrated density in nuclei and cytoplasm

To analyse PAF1 levels in nuclei and cytoplasm, the periphery of each cell was drawn using the free-hand drawing application of ImageJ MBF. This selection or region of interest (ROI) is defined as the total amount of PAF1 per cell. DAPI staining defines the limit of the nuclei (Figure 5.1). Since staining of PAF1 is stronger in the nuclei than in the cytoplasm, the nuclei were purposely drawn larger than their actual size. This is to prevent high intensity readouts from the nuclei being attributed to the cytoplasm. The cytoplasmic regions are defined as the difference between total and nuclear regions. An intensity threshold was set according to the staining in which black pixels correspond to background and red pixels correspond to foreground (or pixels to be analysed). The same intensity threshold was applied across each experiment. Integrated density levels of the thresholded images (corrected total fluorescence) were then determined for each cell in total, nuclear and cytoplasmic regions and mean integrated density levels were calculated.

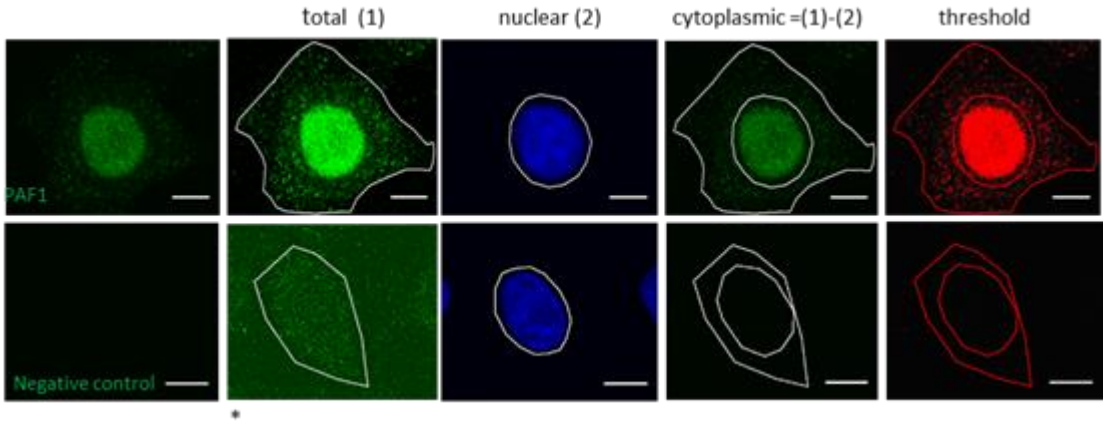

Figure 5.1. Example of the method of quantification of integrated density levels of PAF1. ROIs are selected (white lines) for the whole cell's contour (total), nuclear regions are selected using DAPI and cytoplasmic regions are defined as the difference between total and nuclear. Equal thresholds (red) in the green channel are set for all images analysed. Scale bar represents 10 µm. *Since the staining was not very strong in the cytoplasm, contrast is increased to be able to visualise the cell's periphery.

5.3.2. Characterisation of PAF1 cellular localisation.

Immunostaining was performed to visualise where endogenous PAF1 was located in HeLa-CD4+ cells. Confocal images (Figure 5.2) show that PAF1 is localised mainly in the nuclei as shown by co-localisation with DAPI. The staining is continuous throughout the nucleus which suggests that PAF1 is present in all compartments of the nuclei, including the nucleoli; In addition, images also show that PAF1 is present in the cytoplasm. The cytoplasmic staining is weaker than in the nuclei, indicating that PAF1 is considerably less abundant in the cytoplasm; both these results are in agreement with previously published data by Zhu et al., who report a strong signal of PAF1 throughout the nuclei and a weak signal in the cytoplasm of HeLa cells [196]. Importantly, there is no observable fluorescent signal in cells stained with the secondary antibody alone in either cellular compartment.

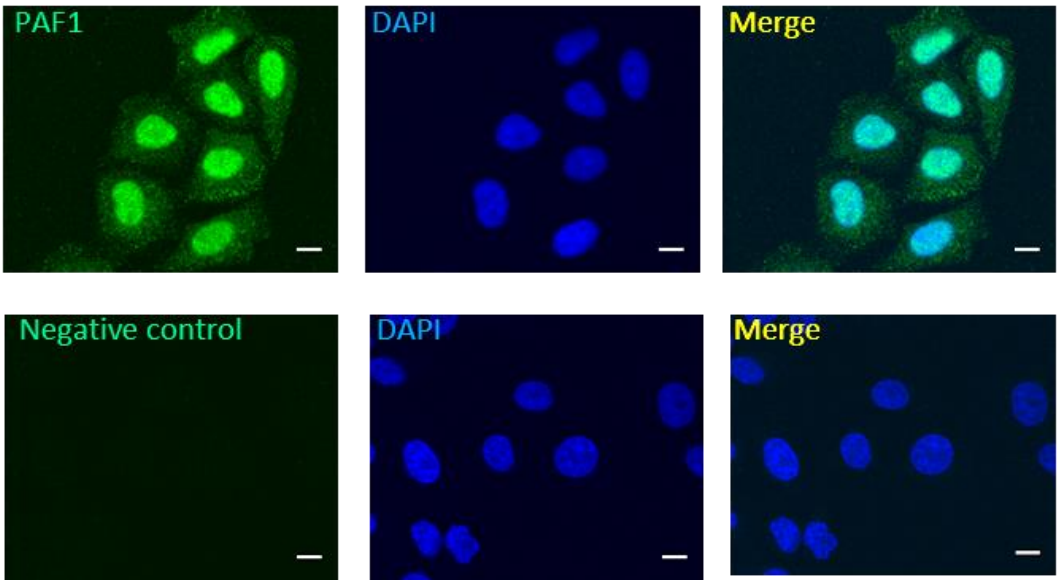

Figure 5.2. Endogenous PAF1 in Hela-CD4+ cells. Example of confocal images of HeLa-CD4+ cells stained for PAF1 (green). DAPI (blue) was used to visualise nuclei followed by anti-rabbit 488 secondary antibody, which was also used alone as negative control. Size bars represent 10µm.

Quantification of mean integrated density was determined for total, nuclear and cytoplasmic regions of 120 cells from three independent experiments were

performed as described in section 5.3.1. Treatment with secondary antibody alone was included as a control. Importantly, the signal detected in negative control cells was found to be negligible compared to total PAF1 staining (Figure 5.3A). Concordant with what was observed in the confocal images, quantitative image analysis showed that PAF1 is mainly localised in the nuclei (80%) and to a lesser extent in the cytoplasm (20%) (Figure 5.3B and 5.3C).

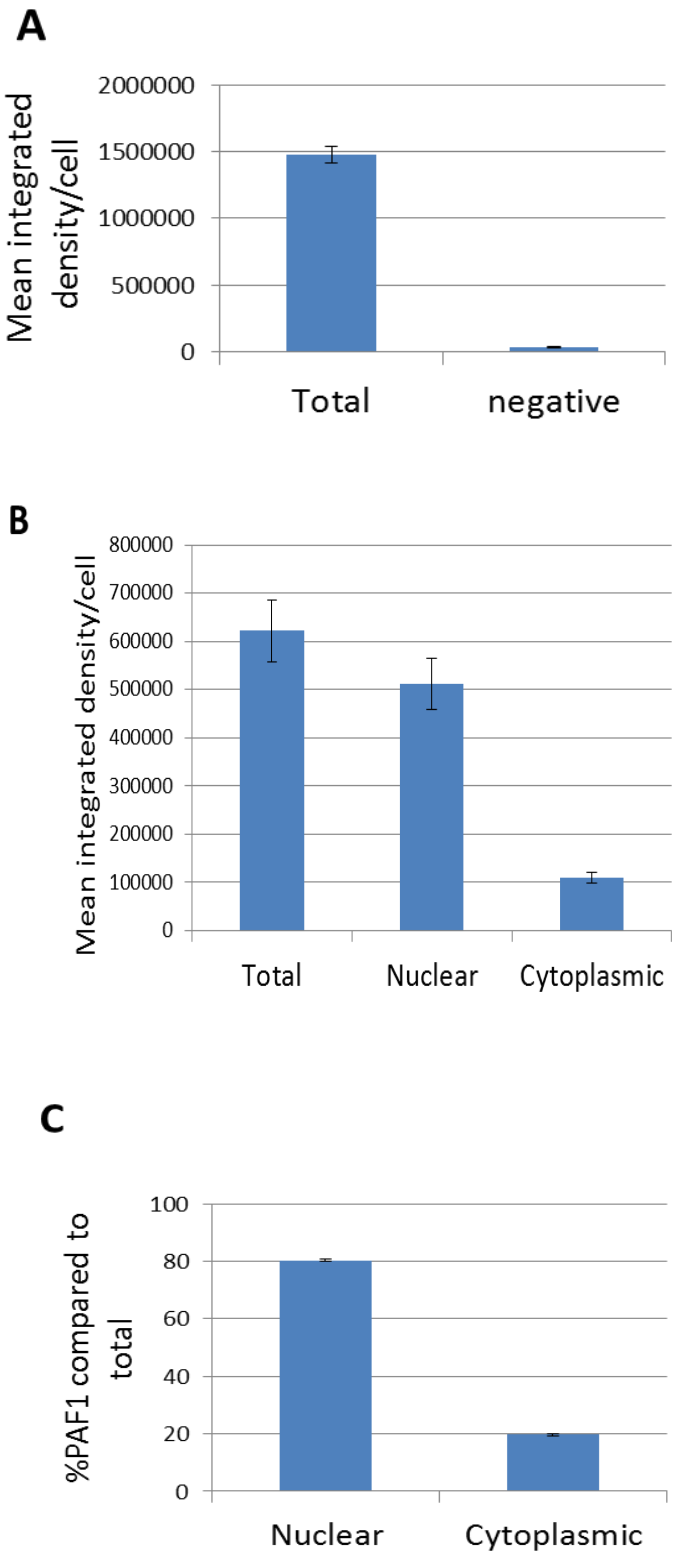

Figure 5.3. Endogenous PAF1 is expressed in nuclei and cytoplasm of HeLa-CD4+ cells. A. Mean integrated density quantification of endogenous PAF1 immunostaining in total HeLa-CD4+ cells stained for PAF1 and with secondary antibody (negative) alone. B. Mean integrated density quantification of endogenous PAF1 immunostaining in total, nuclear and cytoplasmic regions of HeLa-CD4+ cells. C. Mean percentage of PAF1 in nuclear and cytoplasmic regions compared to total. Data is representative of three

independent experiments. A total of 40 cells were analysed per experiment. Error bars represent SEM.

To visualise more accurately the cellular distribution of endogenous PAF1, a confocal z-stack of a HeLa-CD4+ cell stained for endogenous PAF1 was performed. For this purpose, a total of 33 confocal optical sections with a width of 1µm each were taken. In the orthogonal view of the PAF1 confocal z-stack, a representative optical slice is shown (Figure 5.4A). At the marked intersection, PAF1 is present in the cross section through the XY and XZ planes, that is, across the different optical slices of the cell. Analysis of the integrated density of PAF1 in each optical slice was performed to make a more accurate measurement of the amount of PAF1 in the cytoplasm and nuclei in the different sections of the cell. Figure 5.4B shows the quantification of the PAF1 fluorescent signal in nuclei and cytoplasm across different optical slices. The fluorescent signal intensity (integrated density, y-axis) is measured in each optical slice where each optical slice is 1µm in width. Results show that PAF1 is more abundant in the nuclei than in the cytoplasm across the optical slices. Maximum integrated density in nuclear and cytoplasmic compartments is present in the mid planes of the cell. Image acquisition was therefore performed in all experiments by focusing on the mid planes of the cell to ensure maximum fluorescent signal of both compartments was recorded.

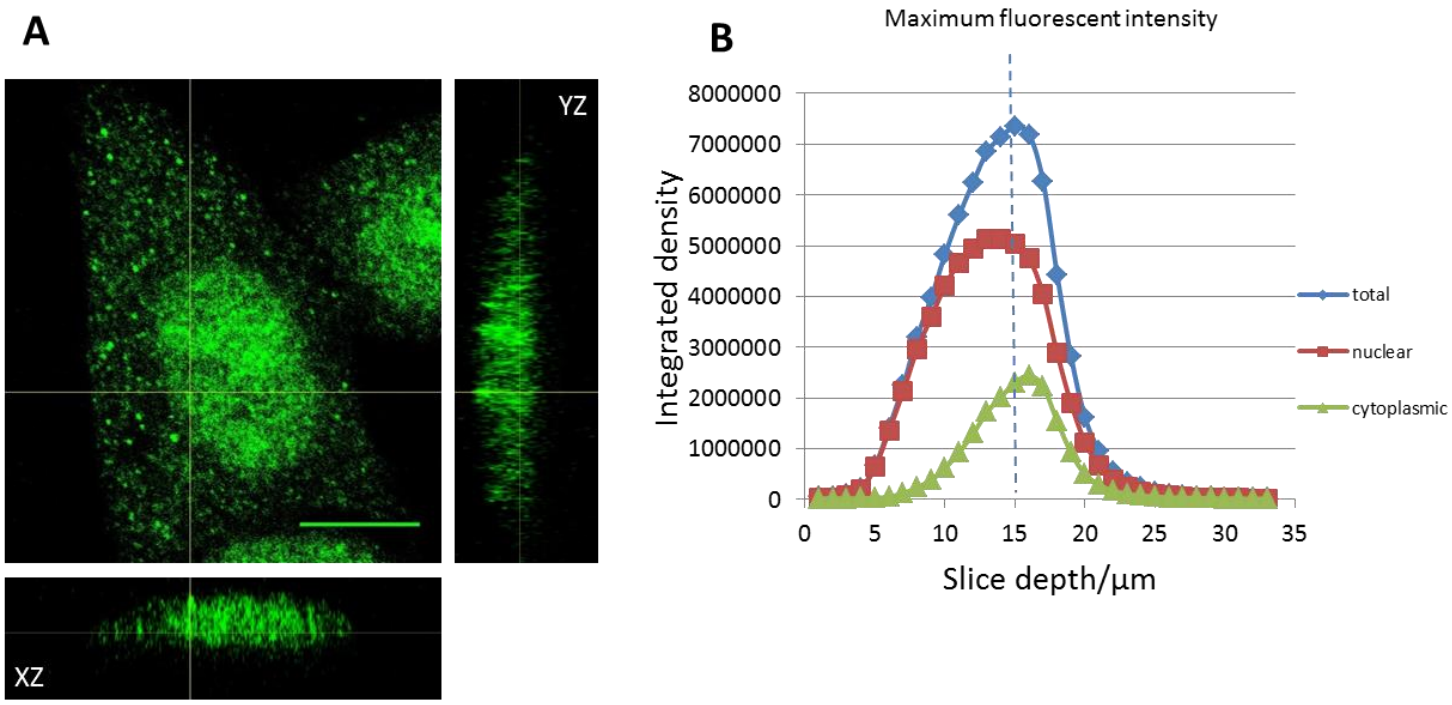

Figure 5.4. Endogenous PAF1 is present in nuclei and cytoplasm throughout the cell's volume. A. Orthogonal view of a Z-stack confocal image of a HeLa-CD4+ cell immunostained for PAF1, scale bar represents 10 µm. B. Integrated density levels of PAF1 measured for each optical slice in total, nuclear and cytoplasmic regions.

To confirm the presence of PAF1 in the cytoplasm, HeLa-CD4+ cells were fractionated by sucrose gradient centrifugation to purify the nuclear and cytoplasmic fractions (method in section 2.2.2). Since GAPDH and Histone3 are found mainly in the cytoplasm and in the nuclei respectively [349, 350], they were included as controls to assess the purity of the cytoplasmic and nuclear fractions respectively. Protein concentration was calculated by BCA reagent assay (see Methods 2.2.10). Equal amounts of protein were loaded in each lane. Western-Blot analysis shows that GAPDH (expected size of 36 kDa) (the original Western-Blot is included in Appendix 4) is absent in the nuclear fraction and that Histone3 (expected size of 15 kDa) is absent in the cytoplasmic fraction, suggesting that the fractions were relatively pure (Figure 5.5A). In both cytoplasmic and nuclear

fractions a band of approximately 80 kDa can be observed, which is the expected size of PAF1. This suggests that PAF1 is located in the nuclei and in the cytoplasm specifically. Additionally, a band around 60 kDa was also detected which again could possibly be a degradation product according to manufacturers. Densitometric analysis of the PAF1 bands (method in section 2.2.10) shows that PAF1 is localised 80% in the nuclei and 20% in the cytoplasm, a result which correlates with the single cell analysis data (Figure 5.5B). Altogether, both quantitative confocal imaging and cellular fractionation results suggest that endogenous PAF1 is localised in the cytoplasm and nucleus of HeLa-CD4+ cells. This is in agreement with Moniaux et al., who showed that were fractionated and Western-Blot analysis showed that PAF1 was present in both the nuclear and cytoplasmic compartments of Panc1 cells [351].

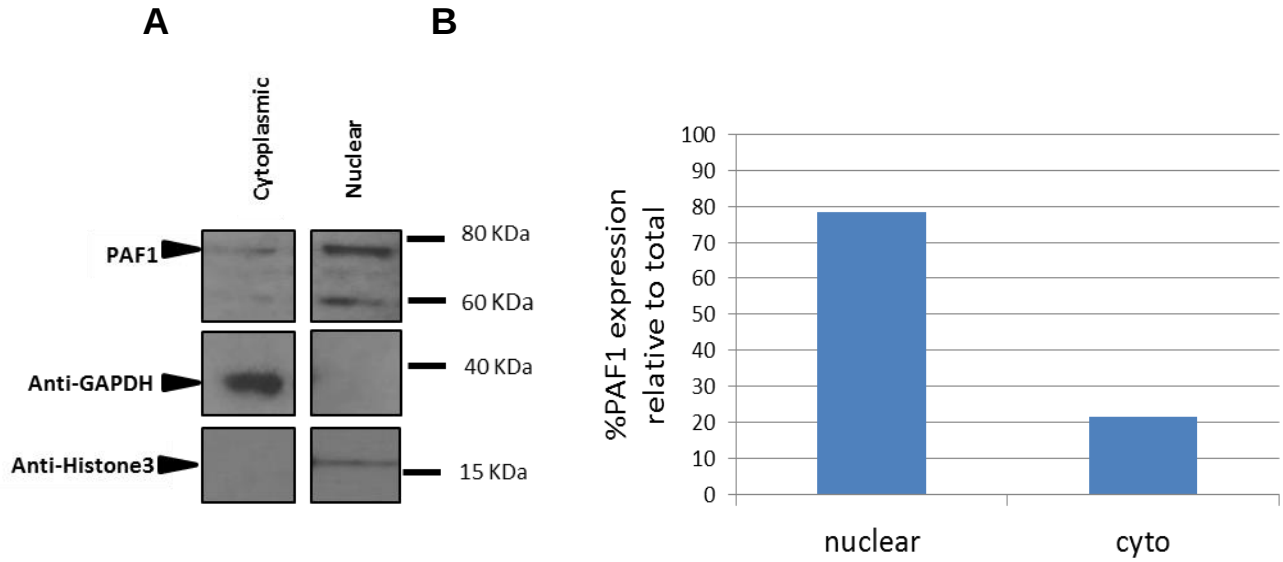

Figure 5.5. Endogenous PAF1 is present in nuclear and cytoplasmic fractions of HeLa-CD4+ cells. A. Western blot analysis of PAF1 expression levels in nuclear and cytoplasmic fractions of HeLa-CD4+ cells. GAPDH and histone3 were included to monitor cytoplasmic and nuclear fraction purity respectively. B. Western-Blot densitometric analysis of PAF1 bands in nuclear and cytoplasmic fractions compared to total. The percentage of PAF1 in nuclear and cytoplasmic fractions compared to total was calculated by densitometry analysis using ImageJ MBF software.

5.3.3 siRNA knockdown of endogenous PAF1 results in a decrease of PAF1 in the nuclei and cytoplasm of HeLa-CD4+ cells.

The specificity of the PAF1 antibody was tested. HeLa-CD4+ cells were treated with 10nM of a control non-targeting siRNA, cyclophilin B (CB) control, and siRNA specific for PAF1 for 72 hours (method in section 2.2.9.3). Cells were then fixed and stained for endogenous PAF1 and DAPI was used to visualise nuclei. Confocal images (Figure 5.6A) show that the fluorescent signal in PAF1-siRNA knockdown cells is strongly decreased compared to CB control cells. Importantly, there is no detectable fluorescent signal in the green channel in cells incubated with anti-rabbit488 secondary antibody only. These results confirm the specificity of the antibody. As can be seen, the PAF1 siRNA knockdown effect is variable from cell to cell; some cells present a strong downregulation evidenced by a steep decrease of fluorescent signal especially in the nucleus (cells marked with arrowheads) whilst other cells have a more modest decrease in fluorescent signal which suggests that the knockdown was not 100% efficient. This result is in agreement with Western-Blot analysis of cell lysates (Figure 5.6B) that had been treated with siRNA against PAF1 whereby the levels of PAF1 are the lowest in the PAF1 knockdown cells (as expected) compared to cells only and CB control but PAF1 can still be detected. Western-Blot analysis (method in section 2.2.10). using the PAF1 antibody detects three bands: a band of approximately 80 kDa, which is the expected size of PAF1, a band at around 60 kDa, which has been described by the manufacturers as a possible degradation product, and a band at around 160 kDa. Nevertheless, even though the siRNA knockdown was only a 50-70% efficient, confocal images and Western-Blot analysis show a decrease in the levels of PAF1 which support the notion that the antibody is specific.

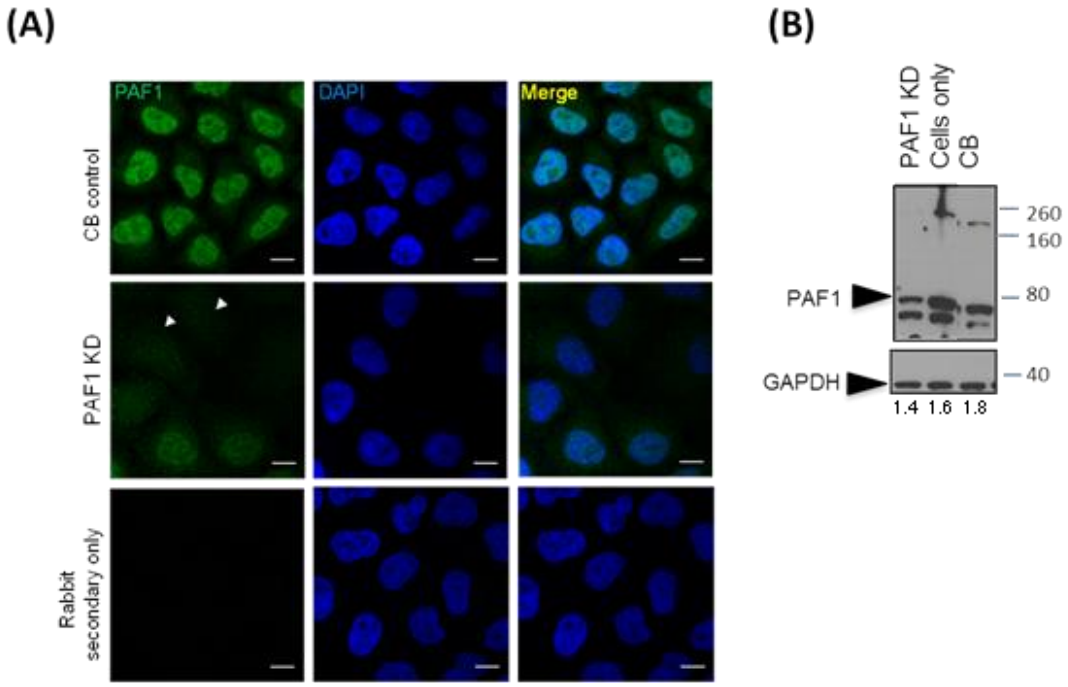

5.6. PAF1 siRNA knockdown downregulates PAF1 protein levels. Cells were treated with siRNA against CB (control) and PAF1 for 72 hours. HeLa-CD4+ cells were then fixed and stained for endogenous PAF1. A. Example of confocal images of HeLa-CD4+ cells stained for PAF1 (green) after treatment with siRNA against CB and PAF1 (PAF1 KD). DAPI (blue) was used to visualise nuclei. Anti-rabbit 488 secondary antibody was used as negative control. Arrow heads indicate cells with a strong decrease of PAF1 expression levels. Scale bar represents 10 µm. B. Western-Blot analysis of cell lysates from cells treated with siRNA against PAF1 (PAF1 KD) and CB. Number represents the ratio of PAF1 (band at ~80kDa) normalised to GAPDH. Cells only control was also included. CB= Cyclophillin B.

To characterise whether the decrease of PAF1 upon knockdown occurs in total cells and nuclear and cytoplasmic compartments, ie. whether the staining is specific, quantification of the integrated density levels of PAF1 in knockdown cells was performed compared to CB control.

Confocal zoom images (Figure 5.7A) of single cells treated with CB and PAF1 siRNA show that there is a strong decrease of the fluorescent signal of PAF1 in the nucleus. The fluorescent signal of an immunostain can vary in different experiments. To compare results of different experiments and to analyse them statistically, integrated density levels of CB control and siRNA knockdown cells were normalised to average CB control integrated density (Figure 5.7B) in each

experiment. Results from three experiments show that there is a decrease of 60% of total PAF1 upon PAF1 siRNA knockdown compared to CB control at the single cell level.

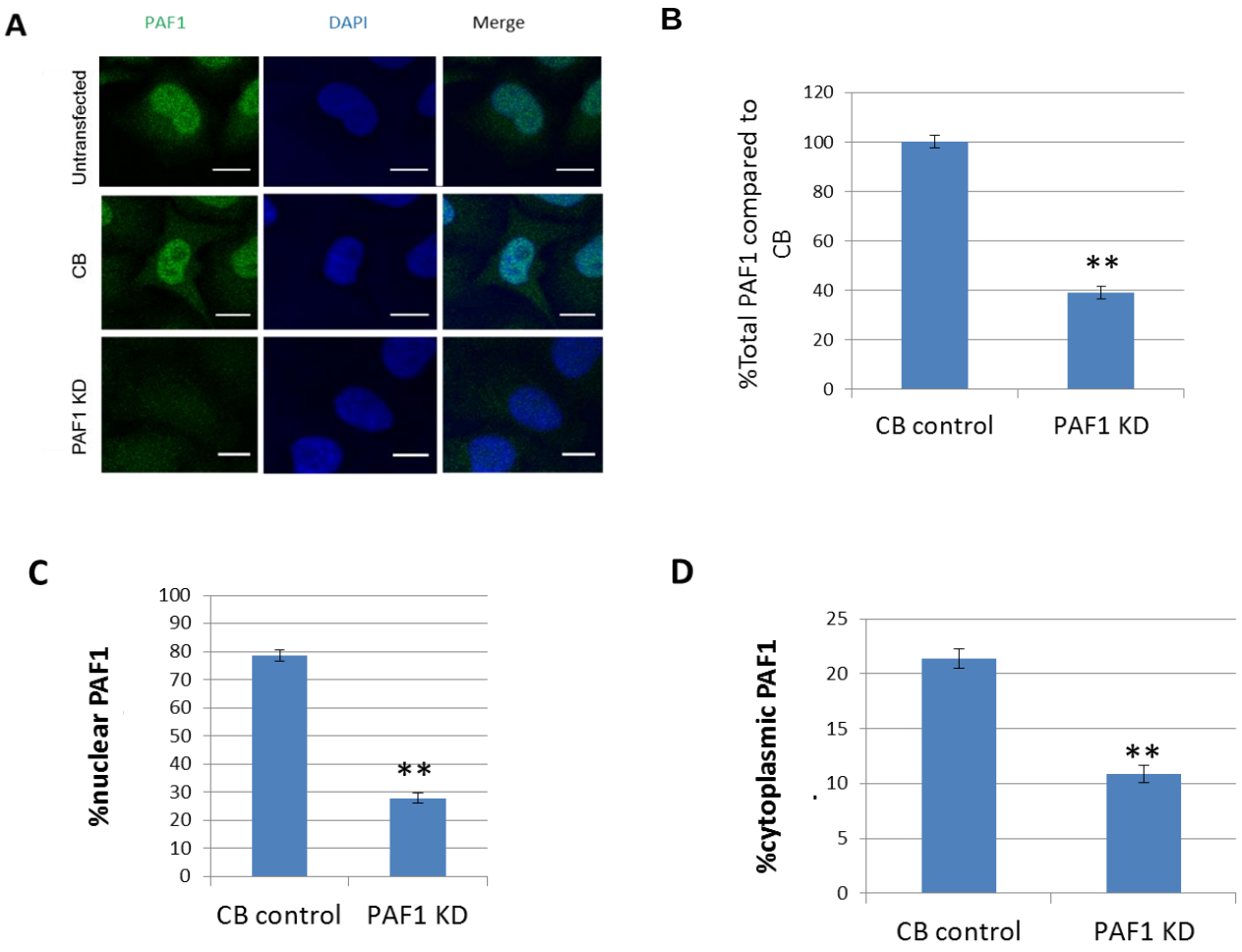

Figure 5.7. Effect of PAF1 siRNA knockdown on total, nuclear and cytoplasmic endogenous PAF1 levels. Cells were treated with siRNA against cyclophillin B (control) and PAF1 for 72 hours. HeLa-CD4+ cells were then fixed and stained for endogenous PAF1. A. Example of confocal images of a HeLa-CD4+ cells stained for PAF1 (green). DAPI (blue) was used to visualise nuclei after treatment with siRNA against CB and PAF1. B. Total endogenous PAF1 integrated density levels. C. Nuclear mean percentage of PAF1 in CB and PAF1-siRNA treated cells compared to CB control. D. Cytoplasmic PAF1 in siRNA- to PAF treated cells compared to CB control. Data is representative of three independent experiments. A total of 220 cells were analysed. Scale bar represents 10 µm. Error bars represent SEM. Significance was assessed by Wilcoxon Man-Whitney test ,**P<0.01. Error bars represent SEM. Size bars represent 10µm.

Having confirmed by Western-Blot (Figure 5.6B) and at the single cell level (Figure 5.7B), that upon siRNA knockdown, total PAF1 protein levels are

downregulated, the next step was to understand if there is a loss of PAF1 fluorescent signal in the cytoplasm as well as the nucleus whether the cytoplasmic and/or nuclear staining is specific. A decrease of PAF1 in the cytoplasm and nuclei of PAF1 knockdown cells compared to CB control is observable (Figure 5.7B) but the decrease in the cytoplasm is less convincing visually possibly because cytoplasmic PAF1 is already low in CB control cells. So, quantitative analysis was performed of each cell compartment. Mean integrated density levels were measured in nuclei and cytoplasm and normalised to the average CB control (Figure 5.7C and Figure 5.7D). Results show that both nuclear and cytoplasmic PAF1 levels are reduced more than 50% upon PAF1 knockdown compared to CB control. Since there is a loss of the fluorescent signal in the nuclei and in the cytoplasm upon knockdown of PAF1, this suggests that PAF1 is reduced by equal amounts in both cellular compartments.

5.3.4 Effect of overexpression of murine PAF1 constructs on HIV-1 infection.

In 2013, Kim et al., generated a series of murine PAF1 (mPAF1) constructs with the aim of understanding the functional domains that are involved in its role in the transcriptional repression of genes induced by interleukin 1β (IL-1β) [352]. These constructs were kindly provided by Kim et al., A schematic representation of these constructs (Figure (5.8A) shows that murine wild type PAF1 (mPAF1WT) is 535 amino acids in length, the mPAF1ΔNLS deletion mutant has a deletion of amino acids 255-284 and the deletion mutant that abrogates its chromatin binding function has a deletion of amino acids 285-355 (mPAF1(Δ285-355). Sequence alignment of the murine and human PAF1 sequences was performed by ClustalW2 software to understand how conserved the NLS and chromatin binding regions are (Figure 5.8B). Results show that the nuclear localisation signal and chromatin binding domain described by Kim.N. et al. in the murine model is 100% conserved in human PAF1. They could therefore, be useful tools

to further understand the relationship between the HIV-1 antiviral function and cellular localisation of PAF1.

To confirm the cellular localisation in HeLa-CD4+ cells of the murine constructs, HeLa-CD4+ cells were fixed and stained 24-hours post-transfection with the PAF1 murine constructs. Since the constructs have a Myc-tag, cells were stained for Myc for epifluorescent imaging. Images show that mPAF1WT and mPAF1Δ(285-355) are located mostly in the nuclei (Figure 5.8C and Figure 5.8D). On the other hand, mPAF1ΔNLS is located mostly in the cytoplasm of HeLa-CD4+ cells as expected.

To study the effect of overexpressing these constructs on HIV-1 infection, transfection of mPAF1WT, mPAF1ΔNLS and mPAF1(Δ285-355) was performed 24 hours prior to HIV-1 89.6 viral challenge, alongside Myc-empty vector as control. Focus forming units or foci of infection (FFU) were quantified (method described in 2.2.5.5). Results show that overexpression of mPAF1WT results in a 20% reduction in infection (Figure 5.8E). Similarly, overexpression of mPAF1ΔNLS also decreased HIV-1 infection by 20%. However, overexpression of mPAF1(Δ285-355) which is impaired for chromatin binding decreased infection by 40%. Overexpression of mPAF1(Δ285-355) restricts HIV-1 infection better than mPAF1WT and mPAF1ΔNLS, suggesting that a nuclear function of PAF1 is responsible for its antiviral activity.

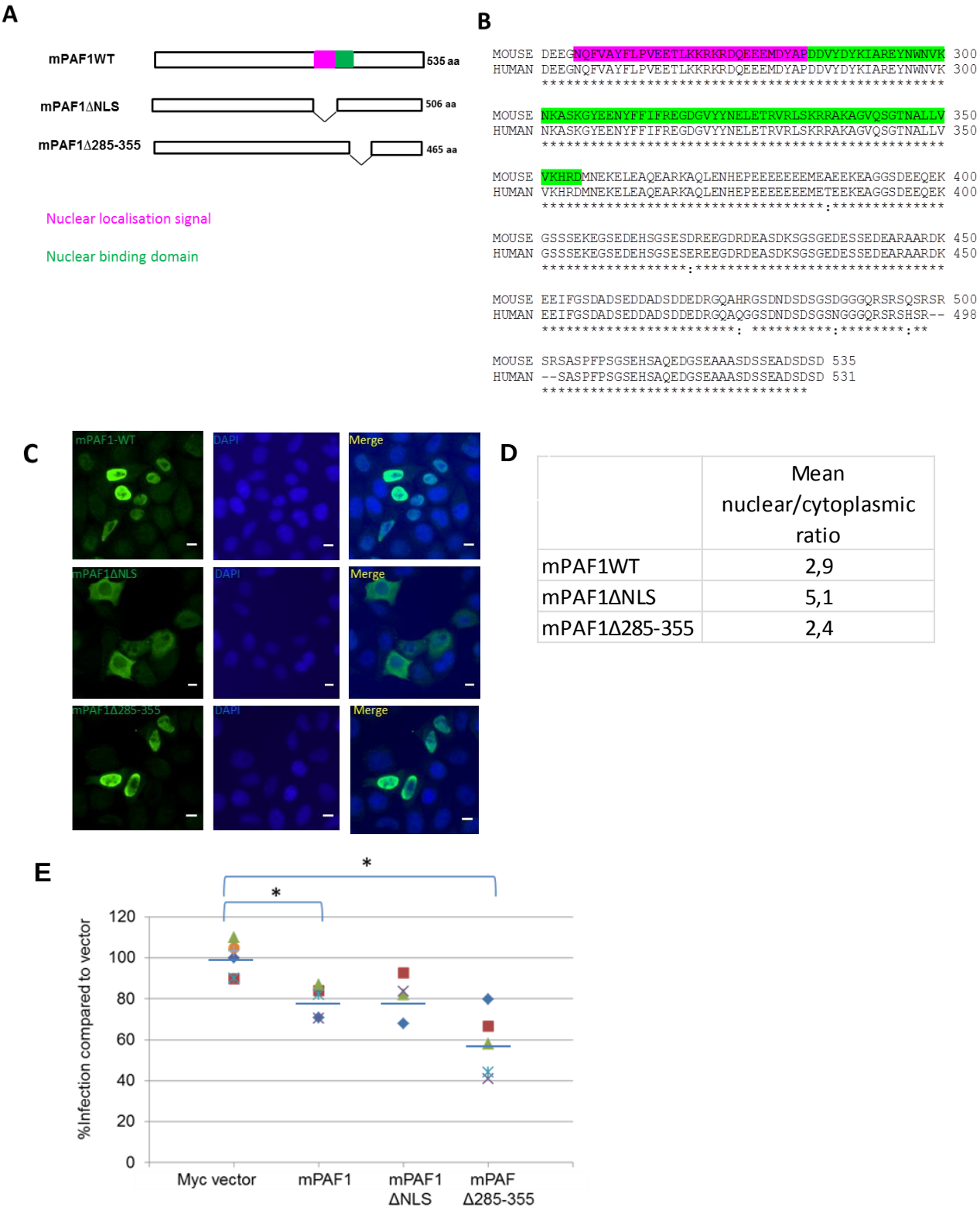

Figure 5.8. Effect of overexpression of murine PAF1 constructs. A. Schematic diagram of wild type mPAF1, mPAF1ΔNLS and mPAF1Δ285-355. B. Sequence alignment (ClustalW2) of the murine nuclear localisation signal and chromatin binding domain with the human PAF1 sequence. C. Localisation of wild type mPAF1, mPAF1ΔNLS and mPAF1Δ285-355 in HeLa-CD4+ cells. Cells were transfected for 24 hours and subsequently fixed and stained for anti-Myc. Untransfected cells were stained with anti-Myc as negative control. D. Mean nuclear/cytoplasmic ratio of cells expressing wild type mPAF1, mPAF1ΔNLS and mPAF1Δ285-355. (E) Effect of overexpression of wild type mPAF1, mPAF1ΔNLS and mPAF1Δ285-355 upon HIV-1 89.6 infection. Cells were transfected with Myc-vector, wild type mPAF1, mPAF1ΔNLS and mPAF1Δ285-355. After 24 hours, cells were challenged with HIV-1 89.6 for 48-hours. FFU were quantified. Data is representative of three independent experiments. Significance was assessed by Wilcoxon Man-Whitney test ,**P<0.01.

5.3.4 Effect of HIV-1 viral challenge on PAF1 expression levels at early stages of infection.

To determine if PAF1 expression is altered after viral challenge, HeLa-CD4+ cells were incubated with replication-competent HIV-1 89.6 (obtained from the Centre for AIDS Research (NIBSC, UK)) at a MOI of 1, for 30 minutes, 1 and 6 hours then fixed and stained for PAF1. To identify infected cells, cells were stained for HIV-1 CA (method in 2.2.9.3). Cells were also lysed for Western-Blot densitometry analysis (methods in section 2.2.10). Confocal images (Figure 5.9A) show the initial basal level of endogenous PAF1 in uninfected HeLa-CD4+ cells with a negative signal in the CA red channel. Within 30 minutes after viral challenge, there is a decrease in endogenous PAF1 compared to unchallenged cells as seen by a reduction in fluorescent signal in the green PAF1. Levels of PAF1 at one hour post-infection are similar to unchallenged cells. At 6 hours post-infection, endogenous PAF1 fluorescent signal is stronger than in uninfected cells. CA staining is characterised by a punctuated particle-like morphology that accumulates at the cell's membrane and in the cytoplasm and gets stronger over time. As previously observed in the lab, Western-Blot analysis of lysates from cells infected for 30 minutes, 1 hour and 6 hours (Figure 5.9B) show that there is a downregulation of PAF1 within 30 minutes of infection compared to uninfected, similar to observations made by confocal imaging. Protein levels of PAF1 increase at 1 hour post-infection compared to the levels of PAF1 at 30 minutes post-infection; however, at 1 hour post infection, PAF1 levels are lower than uninfected. At 6 hours post-infection there is a strong increase of PAF1 protein expression levels compared to uninfected.

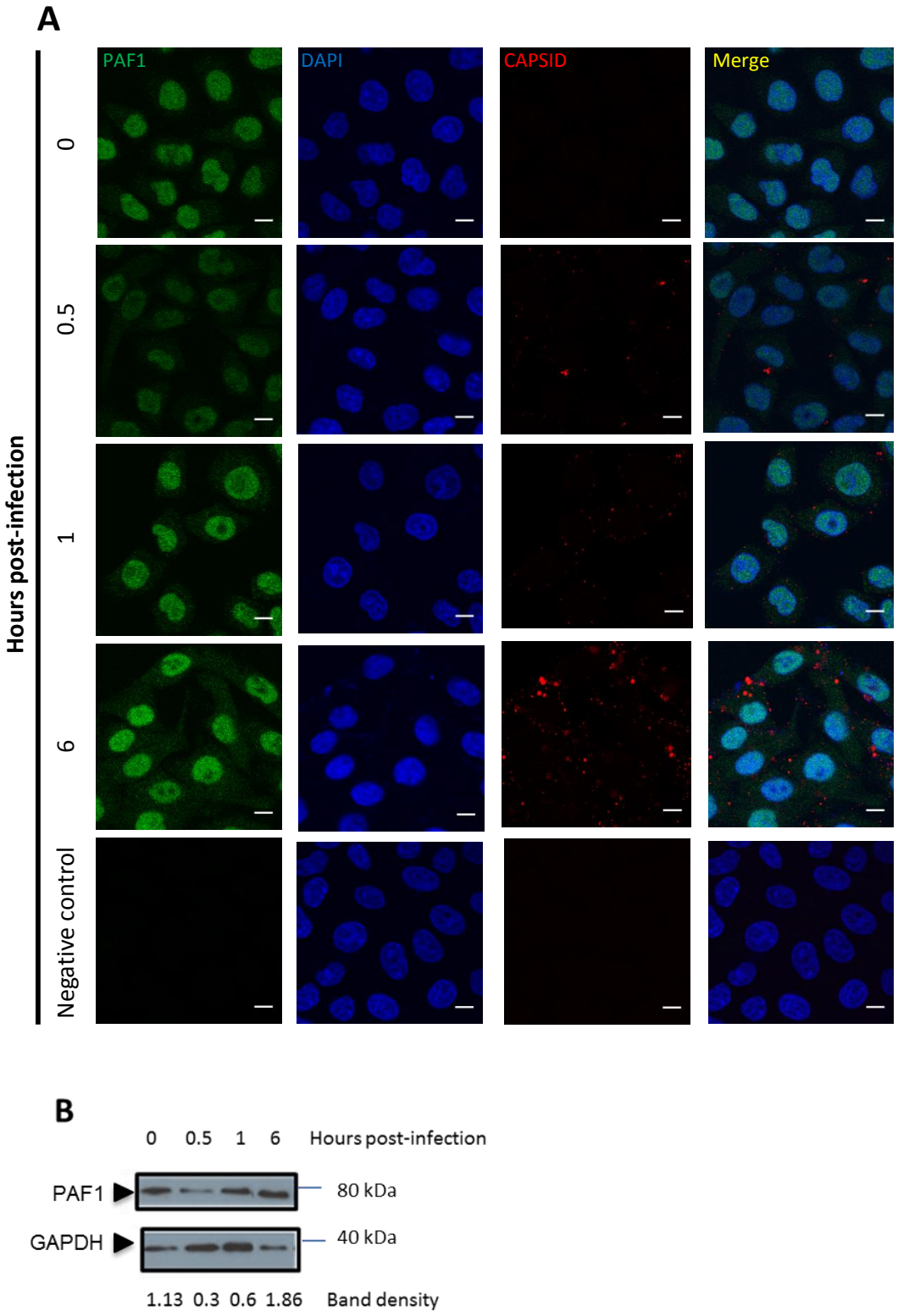

Figure 5.9. PAF1 is downregulated during early stages of HIV-1 infection. HeLa-CD4+ cells were challenged with HIV-1 89.6 for 0.5, 1 and 6 hours. A. Example of confocal images of HeLa-CD4+ cells stained for PAF1 (green) and HIV-1CA (red) N=3. DAPI was used to visualise nuclei. Anti-rabbit Alexa 488 and anti-mouse Alexa 555 secondary antibodies were used as negative controls. Scale bars represent 10 µm. B. Western-Blot analysis of the levels of PAF1 in HeLa-CD4+ cells at 0, 0.5, 1 and 6 hours post-infection N=1. Proportional band density (was measured using ImageJ MBF software.

Having observed that there is a change in the expression levels of PAF1 upon different time points of infection, I next quantified these changes at the single cell level as described in 2.2.9.3. As can be seen in figure 5.9A, not all cells are infected at 30 minutes and 1 hour of virus incubation. To analyse only the cells that were infected, a quantification method of infection was established using CA as a marker of infection. This method was established to distinguish between cells with internalised CA and cells that are negative for CA and also to quantify the number of cells infected per field of view taken at the different time points.

In this quantification method (Figure 5.10A) endogenous PAF1 staining is used to mark the cell's periphery. In the CA image, a threshold was set to exclude possible background pixels or CA aggregates. With this threshold, only CA particles that are within an area of 0.17-2.61 μm^2 are included as positive. The threshold was kept constant across each experiment; using the set thresholds a mask was generated showing the CA particles that fall within the set parameters. Figure 5.10A shows an example of the method from an image of an endogenous PAF1 staining infected for 1 hour. Initially, the contour of the four cells was selected using the PAF1 staining to delimit the cell. Particle analysis in ImageJ MBF was performed and the ROIs were overlaid and the particles detected. In the image analysed, 3 out of 4 cells (75%) have detected internalised CA. Longer challenge times with virus should increase the number of CA particles detected because more time is allowed for virus to enter cells. Figure 5.10B shows an example of endogenous PAF1 immunostaining at 0, 0.5, 1 and 6 hours post challenge with a multiplicity of infection (MOI) of 0.1. MOI is the ratio of infectious HIV-1 particles per cell which is quantified for every virus stock produced by *in situ* p24 immunostaining (see section 2.2.5.3 for method). As can be observed in the mask showing the cells selected and particles detected by this method, no CA particles are detected in the unchallenged control. On the other hand, the

number of detected particles in each challenge time point increases with time. Figure 5.10C shows the mean percentage of cells with intracellular CA each time point of three independent experiments at an MOI of 0.1. Within 30 minutes of virus incubation, 50% of the cells contain CA. Percentage of intracellular CA increases to 80% upon one hour of virus incubation and within 6 hours of virus incubation, 100% cells have intracellular CA. Since the number of cells with internalised CA increases with time robustly across experiments this suggests that this method of detection is valid. In addition, infecting with a higher MOI, should increase the number of CA particles detected by the designed quantification method. Figure 5.10D shows the percentage of cells with internalised CA detected at 0, 0.5, 1 and 6 hours post infection with an MOI of 0.1 and 1. Results show that, 30 minutes post-infection, the percentage of cells with intracellular CA with an MOI of 1 is two times higher than the percentage of cells with intracellular CA with an MOI of 0.1. Altogether, these results further validate the quantification method described, as a measure of internalised CA.

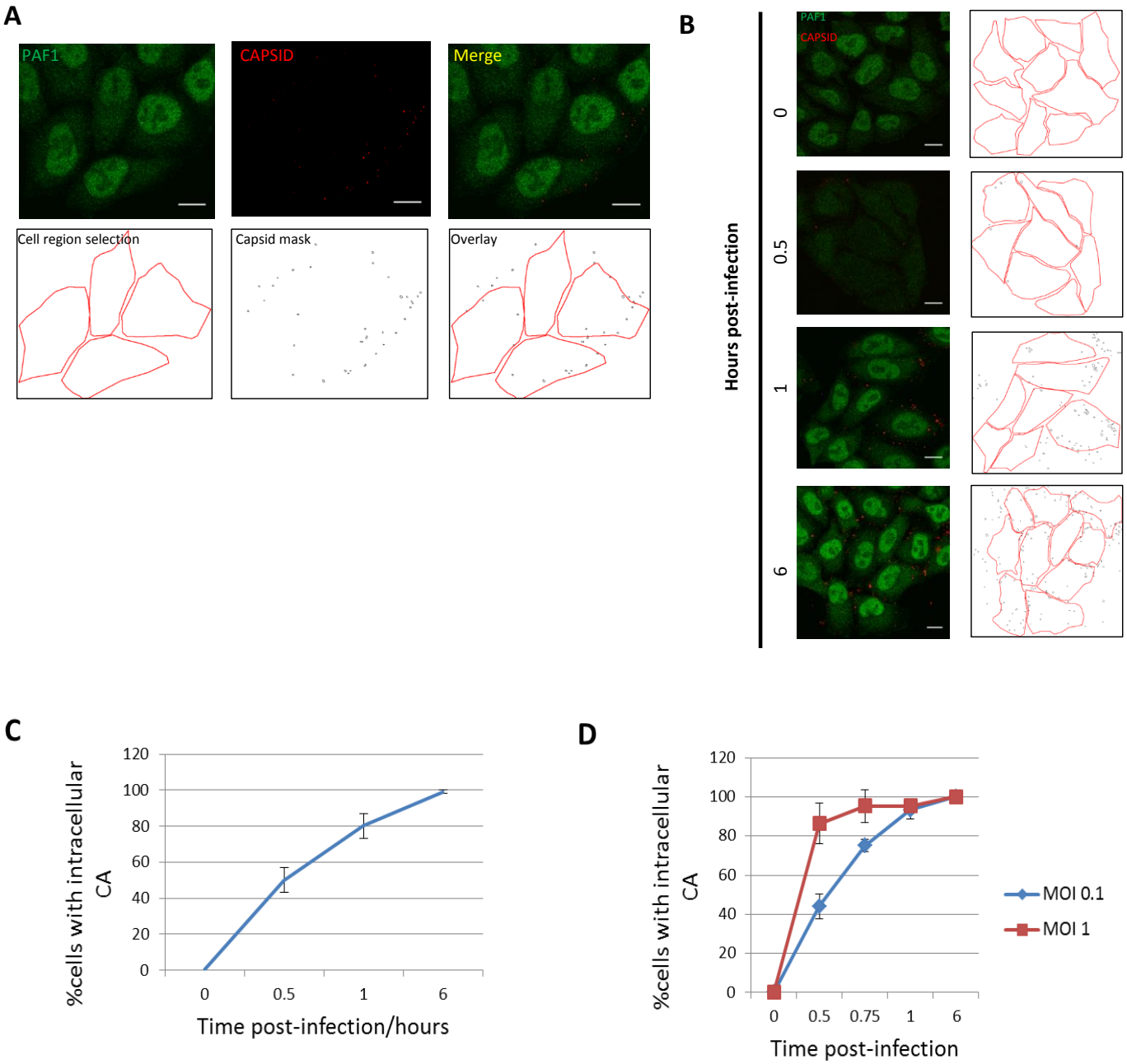

Figure 5.10. Intracellular CA levels upon incubation with HIV-1 89.6 for 0, 0.5, 1 and 6 hours by quantitative confocal imaging. A. Method of quantification of CA particles. Top: Endogenous PAF1 (green), HIV-1 CA (red) and merged confocal images of HeLaHeLa-CD4+cellsinfected with HIV-1 89.6 for 1 hour. Bottom: cell selection mask (left), CA mask showing CAs detected (centre) and overlay mask of CAs detected in the selected cell regions (right). B. Confocal images of endogenous PAF1 (green) at different time points of infection (left column) and their corresponding masks generated (right column). Scale bars represent 10 µm. C. Mean percentage infection at 0, 0.5, 1 and 6 hours post-infection. Data is representative of three independent experiments. D. Mean percentage HIV-1 infection of HeLa-CD4+ cells infected for 0, 0.5, 1 and 6 hours with MOIs of 0.1 and 1, n=1.

Using this method to define cells that have or not intracellular CA, the integrated density levels of PAF1 in infected cells were analysed at the different time points of infection. A total of 320 cells were analysed from three independent experiments. Total mean integrated density levels for each cell were measured and mean percentage PAF1 was calculated compared to uninfected cells. Results show that there is a significant decrease of PAF1 (40%) at 30 minutes after viral challenge compared to uninfected (Figure 5.11A). At one hour post-infection, PAF1 expression levels are 110% expression levels in uninfected cells. At 6 hours post infection, integrated density levels of PAF1 are 1.8 fold higher than basal PAF1 levels in uninfected cells. Altogether, these results suggest that PAF1 is downregulated within 30 minutes of infection and that PAF1 expression levels then recover at one hour post-infection, increasing to levels higher than basal at 6 hours post-infection.

Earlier I proposed a nuclear role in the mechanism for PAF1 restriction of HIV-1. I investigated if there was a change in localisation of PAF1 between the nucleus and cytoplasm, at different times of infection. PAF1 expression levels were analysed by quantitative confocal imaging as performed in the earlier studies presented in this chapter. consistent with what was observed by eye in 5.9A, the levels of PAF1 expression decrease within 30 minutes of infection, are similar within one hour of infection and are higher than uninfected PAF1 basal levels within 6 hours of infection (Figure 5.11A). In addition and similarly to what was previously observed (Figure 5.3C), results show that initially, in unchallenged cells, PAF1 localises 78% in the nuclei and 22% in the cytoplasm as previously observed (Figure 5.11B) . Upon 30 minutes of infection, there is a small but significant change ($p>0.05$ as analysed by Wilcoxon Man-Whitney test) in PAF1 distribution in which 72% of PAF1 localises in the nuclei and 28% localises in the cytoplasm. At one hour post infection, levels of PAF1 in nuclei and cytoplasm are

similar to unchallenged cells where PAF1 is present 76% in the nuclei and 24% in the cytoplasm. At 6 hours post infection 72% of PAF1 is present in the nuclei and 28% is present in the cytoplasm (p=0.041). These results suggest that although small, there are changes in the cellular distribution of PAF1 upon infection.

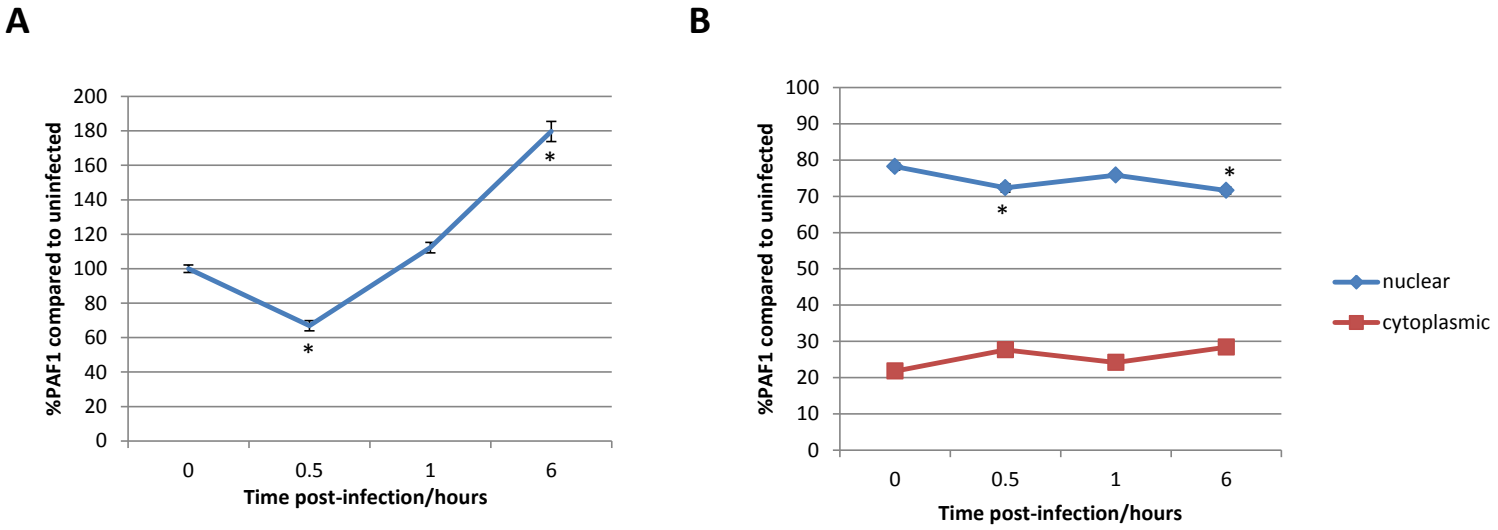

Figure 5.11. Effect of HIV-1 challenge on total, nuclear and cytoplasmic PAF1 expression levels. A. Percentage of total PAF1 expression levels compared to uninfected in cells infected for 0, 0.5, 1 and 6 hours. Mean integrated density levels per cell were normalised to mean average integrated density levels in uninfected cells. B. Nuclear and cytoplasmic mean percentage PAF1 expression levels at 0, 0.5, 1 and 6 hours post-infection compared to uninfected. 320 cells were analysed in total. Data is representative of three independent experiments. Error bars represent SEM. Significance was assessed by Wilcoxon Man-Whitney test *P<0.05

5.3.5. HIV-1 requires viral entry to downregulate PAF1.

PAF1 is downregulated within 30 minutes of HIV-1 infection as previously observed by confocal imaging and Western-Blot. To further investigate whether HIV infection might require entry to downregulate PAF1, HeLa-CD4+ cells were treated for 1 hour with anti-CD4 antibody prior to challenge with HIV-1 89.6 for 30 minutes and 1 hour. Cells were then fixed and stained for endogenous PAF1 and HIV-1 CA.

Initially, to understand whether the anti-CD4 antibody is effective at blocking virus entry, CA quantification of confocal images (Figure 5.12A) was performed and the mean percentage of cells with detected intracellular CA for each time point was calculated as described in figure 5.10. Quantification of intracellular CA (figure 5.12B) shows that that at 30 minutes of challenge, 40% of cells have intracellular CA whilst in anti-CD4+-treated cells only 20% of cells have detectable CA. At 1 hour post challenge, 50% of untreated cells have intracellular CA whilst 25% of anti-CD4+ treated cells have intracellular CA. This therefore suggests that anti-CD4+ treatment partially decreases internalised CA levels by 2-fold compared to untreated.

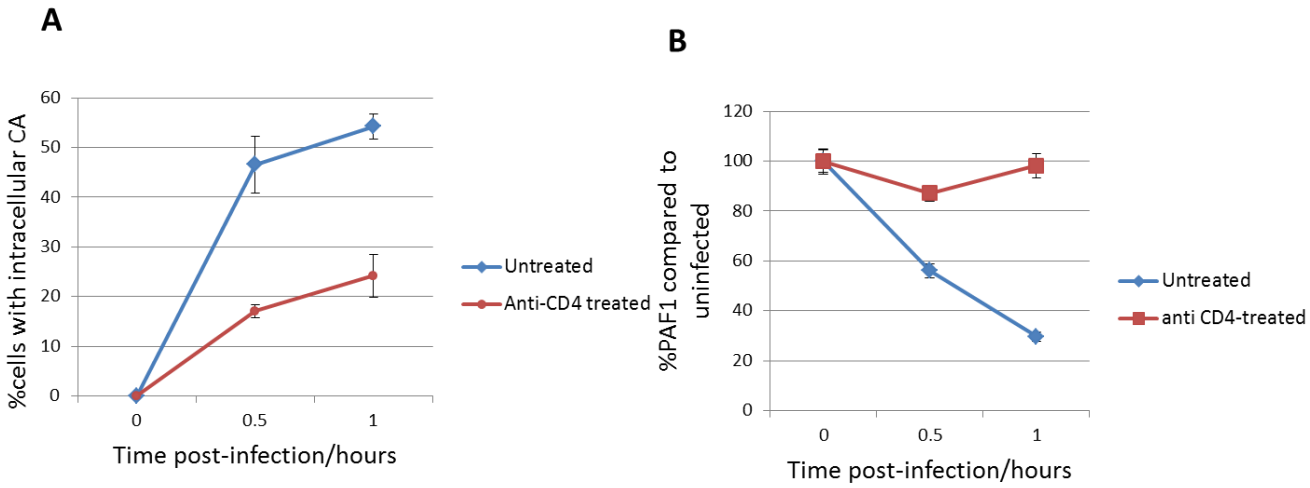

Figure 5.12. Effect of anti-CD4+ treatment on PAF1 downregulation by HIV-1 in Hela-CD4+ cells. A..Mean percentage intracellular HIV-1 89.6 capsid in untreated and anti-CD4+ treated cells per field taken. B. Mean percentage total PAF1 integrated density levels normalised to uninfected in DMSO and anti-CD4+ treated cells, infected for 30 minutes and 1 hour with HIV-1 89.6, N=1. Error bars represent SEM.MOI=0.6.

Confocal images of control untreated cells, show that there is a decrease of PAF1 within 30 minutes of infection as previously characterised and that PAF1 further decreases within one hour of challenge compared to uninfected (Figure 5.13). On the other hand, in anti-CD4 treated cells, the decrease in PAF1

expression within 30 minutes is less strong than the decrease observed in untreated cells. Having confirmed that treatment with anti-CD4+ decreases viral entry, quantification of PAF1 integrated density levels was performed in cells, treated/untreated with anti-CD4 and challenged with HIV-1 for 30 minutes and one hour (Figure 5.13B). In untreated cells, there is a decrease of PAF1 of 40% compared to uninfected. In contrast, in cells treated with anti-CD4+ there is a decrease of only 15% of total PAF1, 30 minutes post-infection compared to unchallenged cells. One hour post-infection, levels of PAF1 in anti-CD4-treated cells, are similar to the levels of PAF1 in uninfected cells. Therefore, downregulation of PAF1 is stronger in untreated cells than in cells treated with anti-CD4 in which, there is less incoming virus compared to untreated. These results suggest that downregulation of PAF1 requires HIV-1 virus entry.

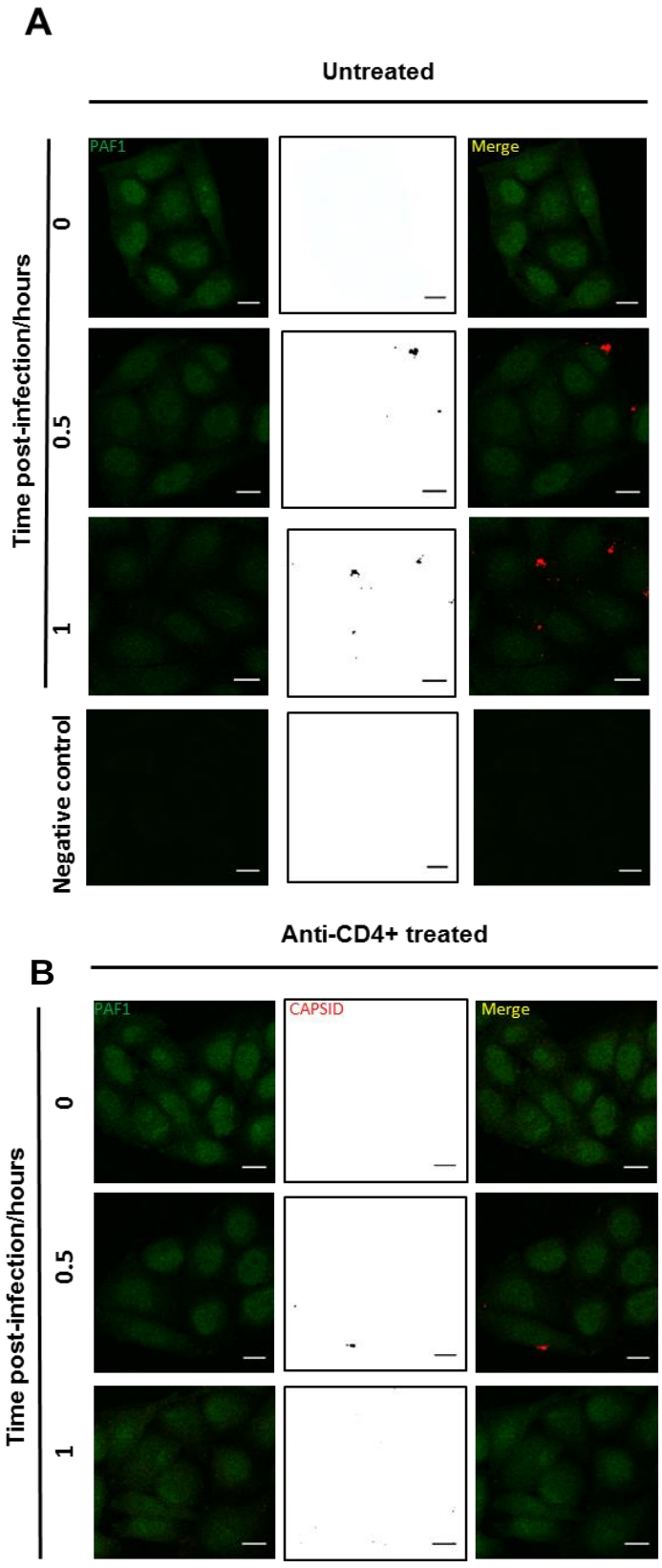

Figure 5.13. Effect of HIV-1 challenge on PAF1 on untreated/anti-CD4-treated cells. A. Confocal images of untreated cells infected with HIV-1 89.6 for 0, 0.5 and 1 hour stained for endogenous PAF1 (green) and HIV-1 CA (red). Anti-rabbit 488 and anti-mouse 555 secondary antibodies were used as negative controls. B. Confocal images of cells pre-treated with anti-CD4+ for one hour before infection with HIV-1 89.6 for 0, 0.5 and 1 hour stained for endogenous PAF1 (green) and HIV-1 CA (red). Capsid is represented in white/black scale for ease of view. N=1. Scale bars represent 10 µm.

5.4 Discussion

Since PAF1 restriction of HIV-1 occurs at a very early stage of infection [158], I hypothesised that PAF1 could be acting via one or two of three mechanisms to inhibit HIV-1 infection: i) from the nuclei, ii)from the cytoplasm upon detection of incoming virus, iii) through an indirect mechanism via a signalling molecule in the cytoplasm that then signals to nuclear PAF1.

After confirming the specificity of the PAF1 antibody by siRNA knockdown (Figure 5.3), quantitative image analysis of three independent experiments showed that 80% of PAF1 is located in the nuclei whilst 20% PAF1 is located in the cytoplasm (Figure 5.5); this result was confirmed by cellular fractionation (Figure 5.7). The presence of PAF1 mainly in the nuclei but also in the cytoplasm is concordant with other studies performed in different cell lines [196, 353, 354]. It would be interesting to siRNA knockdown other components of the PAF1c complex such as SKI8 [198] which has been shown to shuttle between the cytoplasm and the nuclei, to see if upon knockdown, PAF1 expression is lost in the cytoplasm. This would be a strategy to show that SKI8 might be involved in the localisation of PAF1 in the cytoplasm. The presence of PAF1 in the nucleoli (Figure 5.4) was expected since, apart from the nuclear functions described, in yeast, PAF1 also binds ribosomal RNA and influences the rate of RNA pol I, involved in ribosome biogenesis which takes place in the nucleoli [355, 356]. In addition, yeast PAF1 has a role in 3' end formation of snoRNAs) through interaction with Nrd1 and Nab3 [208]. Altogether, results show that PAF1 is located in the nuclei and cytoplasm which does not exclude any of the initial hypothesis formulated.

However, overexpression of the PAF1ΔNLS mutant has a similar effect to overexpression of mPAF1WT which inhibits 20% HIV-1 replication (Figure 5.8D). This suggests that having more PAF1 in the cytoplasm does not inhibit more efficiently HIV-1 replication; therefore its restriction function might not be exerted

from the cytoplasm but rather from the nucleus. Interestingly, overexpression of mPAF1Δ285-355, the mutant that affects the chromatin binding ability of PAF1 and that was found to be mainly nuclear (Figure 5.8C), restricts 40% of HIV-1 infection, two times more potently than mPAF1wt. This suggests that PAF1 might restrict HIV-1 through a function that is nuclear but not necessarily through chromatin binding. Additionally, it could be that overexpression of the mPAF1Δ285-355 changes the PAF1c stoichiometry and releases other components which may have a function in restricting HIV-1. For instance, Liu *et al.,* showed that the individual components of the PAF1c also restrict HIV-1 infection [158]. Overall the evidence presented suggests that PAF1 could be acting from the nuclei rather than from the cytoplasm.

Results show that overexpression of mPAF1wt reduced HIV-1 infection by 20% whilst overexpression of a PAF1 human construct, inhibits over 50% infection suggesting that human PAF1 is more potent [158]. This could be due to a low transfection efficiency of the murine construct (Figure 5.8C). On the other hand, a Clustal W2 sequence alignment was performed and it showed that murine and human PAF1 differ in 5 amino acid residues which are all concentrated in the C-terminal domain of PAF1 (Figure 5.8A). These substitutions of for example a non-polar residue such as Alanine for a polar residue such as Threonine (in position 386) are quite significant in molecular terms. It could be therefore, that these five amino acid changes in the murine and human PAF1 versions affect the PAF1 HIV antiviral potency. It has been reported that the C-terminal domain of human PAF1 (residues 376-531), where these key amino acids are located, is a region involved in H3 binding [202] which might be important for HIV-1 restriction; this would favour a model whereby PAF1 could be restricting HIV-1 from the nuclei through regulation of H3 modifications and gene expression. In fact Marazzi et

al., showed that PAF1 directly interacts with H3 [29] which together with my results would further support a nuclear role of PAF1 in HIV-1 restriction.

Confocal imaging and Western-Blot analysis of cell lysates supported the observation that challenge of cells with HIV-1 89.6 caused a decrease of 40% total endogenous PAF1 levels (Figure 5.9). These results suggest that PAF1 is a restriction factor that HIV-1 counteracts. Downregulation occurs within 30 minutes of virus challenge. It could be that the rapid down regulation is in fact mediated by Env signalling. Further studies with a VSV-G pseudotyped virus could help to test this. Alternatively, it could be that gp120 activates an indirect signalling pathway which in turn, results in PAF1 degradation. For example, gp120 has been shown to upregulate the macrophage colony-stimulating factor (M-CSF) which induces activation of pro-apoptotic pathways to avoid macrophage death [357]. However, Env signalling mediation is unlikely because the decrease in PAF1 expression is not as strong in cells treated with CD4+ than in untreated cells (Figure 5.13) which suggests that to downregulate PAF1, HIV-1 needs to be inside of cells. The CD4 observation better supports a model in which the very rapid downregulation of PAF1 could be mediated by a protein that enters the cell with HIV, a protein that is enclosed in the virus particle. It is known that upon viral assembly and release, HIV particles take up passively, a series of cellular proteins, mainly glycoproteins which are membrane-bound [358]. It could be that the HIV-1 viral particle enters with a cellular protein that upon entry, sequesters PAF1 and downregulates it. For example, the HIV particle is known to sequester ubiquitin[359]; ubiquitin ligase targets proteins to degradation pathways [360]. HIV-1 is also known to incorporate members of the endocytic pathway such as Rab5a [361] or clathrin [362] which could also target rapidly PAF1 for degradation. It could be that instead of a cellular protein, HIV utilises an

accessory viral protein to downregulate PAF1. For example Vpu counteracts tetherin by binding to it and targeting it to a lysosomal degradation pathway [171].

Analysis of nuclear and cytoplasmic levels of PAF1 at the different time points, suggest that there is a significant change of the levels of PAF1 at these compartments (8%). Although significant, these changes are very small to conclude that it is the virus that actually changes PAF1 localisation, especially since PAF1 subcellular localisation depends on cell cycle [37]. Live cell imaging experiments with synchronised cells expressing a fluorescently-labelled PAF1 construct and subsequent viral challenge could help understand better the spatio-temporal changes of PAF1.

A hurdle to current antiretroviral therapies is the ability of HIV-1 to rapidly mutate due to its high error-prone reverse transcriptase. On average, every three cycles of replication, an error is introduced in the HIV genome [363]. As a consequence, resistance to current treatments has been reported [364-366]. In addition, current treatments available are combination drug regimes that aim to inhibit multiple viral targets and limit resistance but pose toxicity problems [367, 368]. From a therapeutic point of view, targeting early stages of HIV viral infection is advantageous because it decreases the chances of mutagenic evolution during reverse transcription and of establishment of latency [369]. Liu *et al*,, showed that restriction of HIV-1 resulting from the action of PAF1 occurs in steps prior to integration [158] therefore investigating further the mechanism of PAF1 is interesting from the therapeutical point of view.

5.5 Principal findings

To summarise, in this chapter the following findings were described:

- Endogenous PAF1 is located in the cytoplasm and nuclei.

- Overexpression experiments with murine PAF1 mutants suggest that PAF1 exerts its antiviral function from the nucleus and this nuclear function might not require chromatin binding.

- On the other hand HIV-1 counteracts PAF1 by downregulating PAF1 upon 30 minutes of viral challenge suggesting that early events in viral replication need to be protected.

6. General discussion

6.1 HIV-1 Env signalling significance and possible mechanisms

Since viruses have small genomes compared to multicellular organisms, in order to survive and economise their genomes, virus proteins often have multiple functions. For instance, the viral envelope serves various purposes for the virus. Firstly, viral envelope proteins are antagonists of cellular receptors and so, it is via the envelope protein that viruses recognise and bind to cellular receptors in order to gain access into the cell. Secondly, numerous studies have described that viral envelope proteins also serve the virus to evade the immune response[370]. Some examples of viral glycoproteins that modulate the immune response include: Herpes Simplex virus type 1 glycoprotein C [370], Ebola virus glycoprotein [371, 372] or the Hepatitis C Virus E1/E2 glycoproteins [373] to name a few. In addition to entry and immune evasion, binding of viral glycoproteins can mediate signalling events that modulate the cell's environment [374, 375]. In chapter 3 and 4, I aimed to increase the current knowledge in HIV-1 Env signalling pathways.

Microtubules are one of the major components of the cytoskeleton and perform crucial cellular functions including cell migration, cell polarization and vesicle transport [376]. Stable microtubule subsets are highly post-translationally modified (by for example, tyrosination and acetylation [377]) whilst less stable microtubule subsets have reduced post-translational modifications, are highly dynamic and explore the cells environment in a "search and capture" mode [287]. McDonald et al., described in 2002 that HIV-1 hijacks the microtubule network in order to traffic the reverse transcription complex from the cytoplasm to the nuclei [260]; Since then, more recent studies have revealed a physical interaction between the viral capsid and microtubule-associated protein 1A (MAP1A) required for efficient nuclear translocation [285] and requirement of microtubules and dynein, a microtubule-associated protein that pulls cargo along the

microtubules in the cell [378] during uncoating [261, 262]. In addition, HIV-1 has been shown to induce stable microtubules via a microtubule end-binding protein 1 regulator, Kif4, [287]. Interestingly, induction of microtubule acetylation has also been shown to be induced by Env gp120 incubation [263]. These observations would support a requirement for stable microtubules to which the pre-integration complex binds to in order to not only shuttle to the nuclei but also protect the viral DNA from cytoplasmic degradation [261]. In contrast, I found that expression of the Env cytoplasmic gp41 domain decreases microtubule acetylation, possibly via a not yet described, signalling mechanism. Malinowsky et al., showed that microtubule deacetylation by gp41 CT expression, decreases virus-cell fusion [258]. This result would suggest that the gp41 CT signals solely to negatively affect virus replication. However, it could be that microtubule deacetylation, has an additional function that was not measured in the virus-cell fusion assay performed by Malinowsky et al.,that positively affects virus replication. This would lead to a model in which both microtubule stabilisation and destabilisation occur. It could be that initially, right after the Env cytoplasmic domain is inserted in the cytoplasm, the gp41 destabilises the microtubules by deacetylation in order to increase the subset of dynamic microtubules which through their search and capture dynamic, search and capture incoming HIV-1 particles from the plasma membrane. Interestingly, Vaccinia virus has been shown to increase the dynamics of microtubules by reducing the levels of acetylation of peripheral microtubules which enhances the frequency at which the microtubules reach the cell cortex; the mechanism involves inhibition of RhoA by the vaccinia virus protein F11L [379]. My results also showed that to decrease microtubule acetylation, the full length cytoplasmic tail is required because expression of the truncated versions had a weaker effect on tubulin acetylation. It is therefore possible that the deleted portion of the tail involves a domain like that of vaccinia F11L which interacts with a protein that results in RhoA inhibition and triggers

microtubule destabilisation. Zhang et al., described that the C-terminal domain of the cytoplasmic tail that includes the deleted portion of the truncated version, interacts with P115-RhoGEF, an activator of RhoA. It would therefore be interesting to investigate whether knockdown of P115-RhoGEF abolishes the microtubule deacetylation observed upon CT expression as well as to measure by live cell imaging whether there is more incoming virus in CT-expressing cells.

Destabilisation (as reported in the present thesis) and stabilisation of microtubules (as shown in the literature) could both be exerted through different mechanisms and for different functions that benefit viral replication. Therefore, a model by which the cytoplasmic tail signals to decrease microtubule stability and facilitate virus capture from the membrane, is not exclusive with a model whereby microtubule stability is then required for shuttling of the pre-integration complex to the nuclei (Figure 6.1).

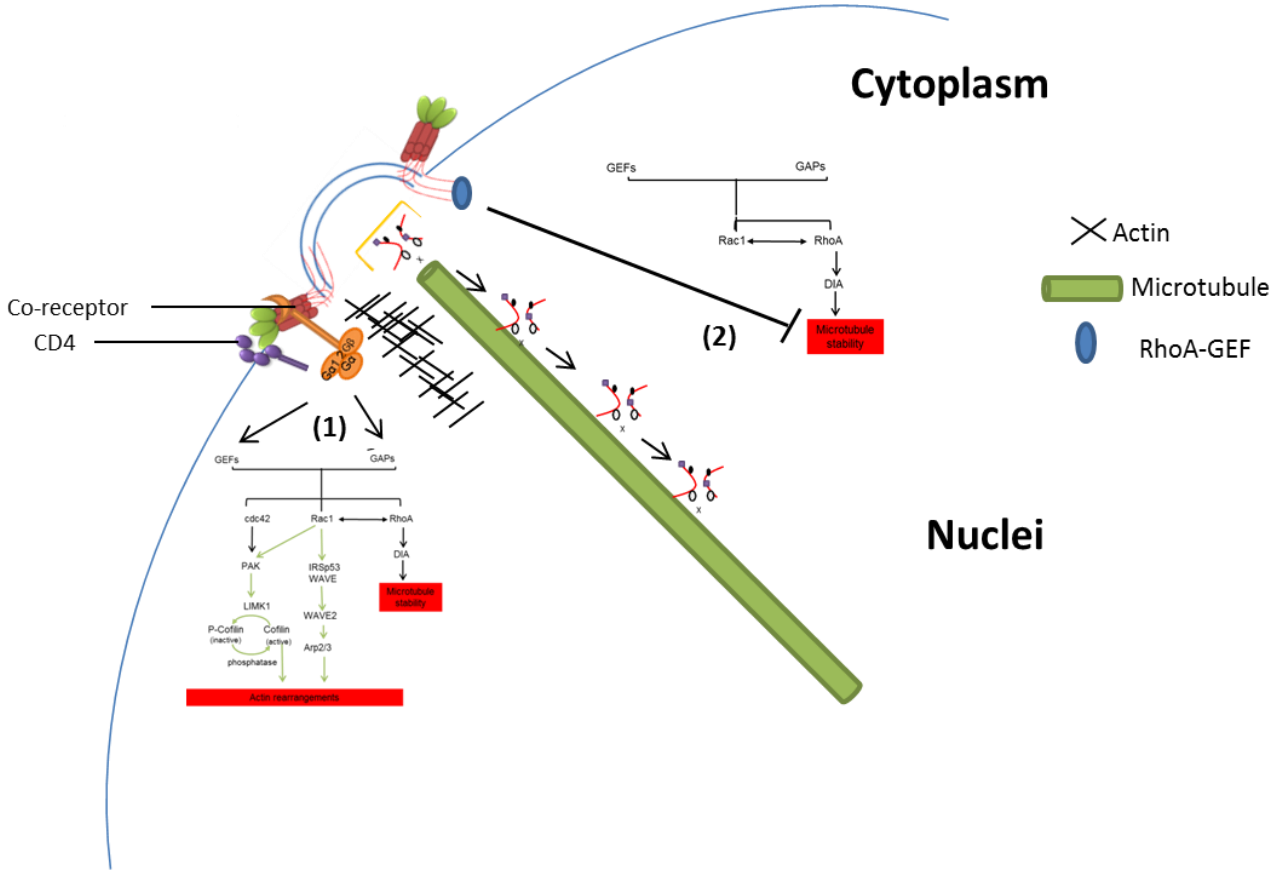

Figure 6.1. Model of possible Env signalling in HIV-1 infection through Rho-GTPases. This model includes two mechanisms that are not exclusive as a result of my results and those of others [254-256, 283]. In (1), the Env protein binds to CD4 and CXCR4 which triggers activation of downstream Gα1,2 protein. This in turn, activates and signals to GAPs and GEFs that activate Rac1, cdc42 and RhoA; this then, triggers activation of cofilin to break down the actin barrier and stabilise microtubules for shuttling the pre-integration complex to the nuclei. In (2), the Env cytoplasmic tail could hijack a Rho-GEF that activates Rac1 or RhoA and trigger the observed microtubule destabilisation via inactivation of either or both Rac1 or RhoA. The objective of this destabilisation could be to increase the microtubules instability and promote the search and capture of incoming virus from the membrane cortex.

RhoA is a known regulator of microtubule dynamics via the RhoA-DIA pathway [264] and of actin polymerisation through the ROCK-LIMK1-cofilin pathway [347]. The role of RhoA in HIV-1 infection has not been described even though HIV requires stable microtubules early in infection [260, 261, 287] and overcomes cortical actin restriction for entry via Env-triggered cofilin activation [80]. It is also known that RhoA and Rac1 can regulate each other [272]. Rac1 is involved in

actin polymerisation by PAK-LIMK1 [231] and in microtubule stability via stathmin [266]. Env activation of Rac1 has been described [254-256, 283]. Both the mutual Rac1-RhoA regulation together with the fact that both Rac1 and RhoA control functions that affect negatively (actin polymerisation) and positively (microtubule stabilisation) HIV replication, suggest that the role of RhoA and Rac1 in HIV is complex. This is possibly why, results from the screen did not show a uniform conclusion as to whether knocking down an activator or inactivator of for example RhoA had a positive or negative effect on HIV infection. However, independently of being an activator or inactivator of RhoA, knockdown of RhoA upstream regulators caused an inhibition effect on HIV-1 replication especially for HIV-1 BaL and in the case of Rac1, knockdown of identified activators of Rac1 majorly caused inhibition of HIV-1 infection. Their multiple relevant functions in HIV makes both Rac1 and RhoA interesting therapeutical targets and so, it is therefore important to further confirm and understand the role of the upstream effectors identified.

The screen also revealed a novel role for upstream regulators of cdc42 in HIV-1 infection, not previously characterised which were different depending on the HIV-1 virus strain assayed. Since cdc42 is upstream of cofilin, known to be activated through Env-signalling via CXCR4 [80, 252], it would be interesting to understand further the consequences of knockdown of specific GAPs and GEFs that control cdc42 upon infection to understand whether Env-mediated cofilin activation is triggered specifically via these proteins upon receptor engagement.

Taking into account the array of GAPs and GEFs that showed an effect specifically on NL4.3 and BaL, one question is whether at the physiological levels of expression of Env in HIV-1 infected patients, these signalling pathways are relevant since it is possible that the levels of expression in *in vitro* models are much higher than in patients [242, 380]. As argued by Wu et al., much of the

reservoirs of HIV-1 are found in lymphatic tissue and so, it is difficult to measure based only on plasma viral load[242]. However, a study performed by Melar et al., suggested that at physiological levels Env is able to trigger signalling events [381].

Targeting GEFs and GAPs offers an advantage over targeting for example, actin or the actual Rho GTPases: they are oftenly tissue-specific [382]; it would therefore be interesting to evaluate whether these proteins are expressed specifically in T-cells and/or macrophages. Understanding further the differences in signalling events upon infection by X4 and R5-tropic viruses, could be determinant in finding novel therapies that aim to target the co-receptor usage switch from R5 to X4 that has been described previous to AIDS development [292] and which are more strain-specific.

6.2. The role of PAF1 in HIV-1 infection

Since its discovery, as part of the PAF1 complex [189, 190], increasing evidence on the role of PAF1 has revealed multiple nuclear functions. For instance, PAF1 is found associated with nuclear proteins that control transcription initiation [187], transcription elongation [189, 203, 383] and post-transcriptional processing of mRNA [206-208]. In addition to these functions, PAF1 also has an additional nuclear role in gene regulation which is regulation of histone modifications [212, 384, 385]. However, PAF1 has also been shown to be expressed in the cell's cytoplasm [196, 351] and its role in the cytoplasm has not been described. My results showed that PAF1 localises mainly in the nuclei and to a lesser extent in the cytoplasm, which agrees with the evidence so far, regarding its localisation. In addition, PAF1 has been described to have a role not only in HIV-1 infection [158, 209] but also in adenovirus [210, 386] and influenza virus infection [212]. Both Marazzi I et al., and Fonseca et al., describe a role of PAF1 in influenza and

adenovirus infection that involves the recruitment of PAF1 for viral transcriptional activation, ie. a positive role for the virus. Liu.L et al., described a novel role of PAF1 that restricts HIV-1 virus infection at a step post-entry but previous to integration, ie. a negative or inhibiting role against the virus [158]. Therefore, the PAF1 mechanisms described for influenza virus or adenovirus are different to the mechanism of PAF1 in HIV-1 restriction. However, the Marazzi et al. study described that whilst influenza virus infection elicits a strong upregulation of a number of genes that include inflammatory and immune response genes, in PAF1 knockdown cells the response was reduced, suggesting that PAF1 is involved in upregulation of possible antiviral genes against influenza virus [212]. It is possible that PAF1 also regulates transcription of antiviral genes upon HIV-1 infection. For instance, results of the overexpression of murine cytoplasmic PAF1 (PAF1ΔNLS) had a similar effect on HIV-1 89.6 infection compared to PAFWT, suggesting that the role is not a cytoplasmic but a nuclear role. Interestingly, overexpression of a PAF1 mutant that is not able to bind to chromatin, decreased infection more potently than the murine wild-type PAF1 suggesting that the role of PAF1 in infection could be a nuclear role that is not directly related to chromatin binding. For instance, to regulate histone methylation, PAF1 binds to chromohelicase DNA-binding protein I[385]; it could be that to exert its antiviral function against HIV-1, PAF1 regulates gene expression by control of DNA methylation via other proteins such as chromohelicase DNA-binding protein as mediators thus, avoiding the chromatin binding function.

Interestingly, upon 30 minutes of incubation with HIV-1, PAF1 is downregulated and the levels of PAF1 recover to basal levels within one hour. This rapid counteraction of PAF1 by HIV-1 supports a model (Figure 6.2) whereby HIV-1 enters into the cell with a protein that targets PAF1 for degradation.

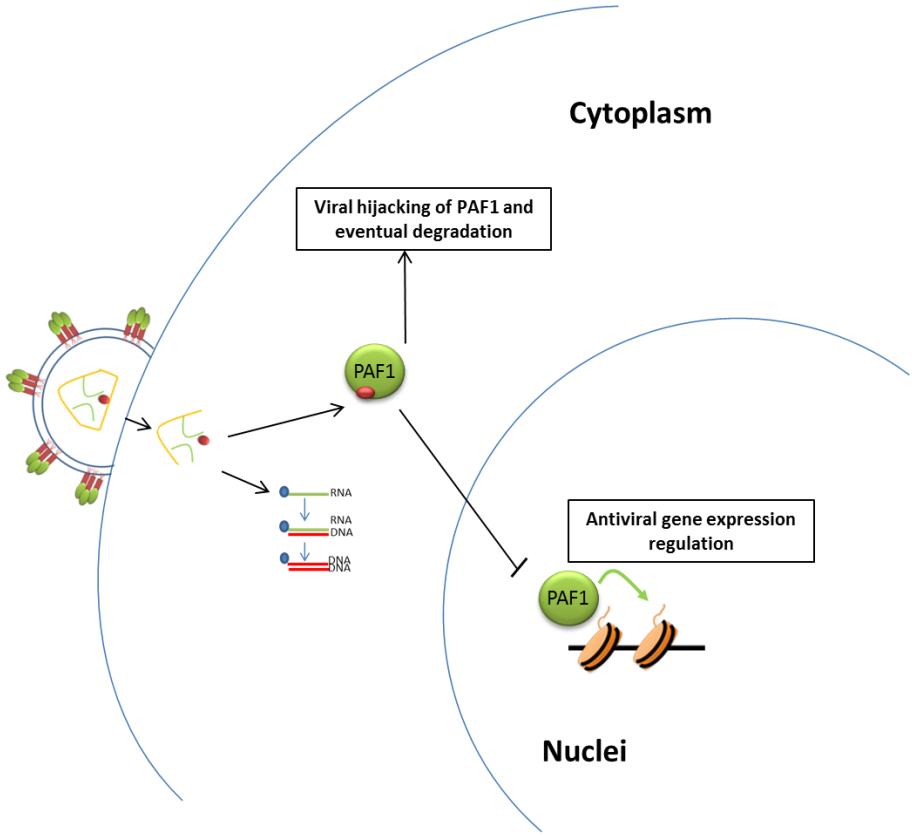

Figure 6.2. Model of possible mechanism by which HIV-1 counteracts PAF1 and PAF1 restricts HIV-1. In the proposed model, PAF1 has a nuclear role that does not involve chromatin binding but that could possibly involve gene expression regulation. On the other hand, HIV-1 counteracts PAF1 early in infection in a step previous to reverse transcription that could involve a protein (in red) that the virus releases upon uncoating.

Results from the final experiment, support this model since the downregulation effect was less prominent in cells that had been treated with CD4 (and as a consequence had less internalised capsid) than in untreated cells. Counteraction of restriction factors by HIV-1 has previously been described. For example, tetherin is counteracted by Vpu which targets tetherin to an ER-associated and lysosomal degradation pathway [170, 171]. The influenza virus NS1 protein has a histone mimic domain that is able to bind to PAF1 [212]. It would be interesting to investigate whether any of the accessory proteins of HIV-1 has a similar histone mimic domain that could enable PAF1 binding. The HIV-1 restriction factor, SAMHD1 is downregulated by SIV-encoded Vpx [177, 178]. Interestingly, SAMHD1 restricts HIV-1 through a cytoplasmic function but actually is

downregulated in the nuclei by Vpx [179]. It could be that, oppositely to SAMHD1, since PAF1 is degraded so fast upon viral challenge, it is degraded in the cytoplasm although it has a nuclear antiviral function.

As to how the effect of PAF1 could translate to a patient situation it is worth mentioning that PAF1 is expressed in primary human T-cells, monocytes and macrophages and that it also acts to neutralise HIV-2 and SIV isolates which highlights its physiological relevance not only in the HIV-1 context but also as a broad-acting antiretroviral. Since PAF1 is involved in crucial cellular functions, it could be that the major therapeutical benefits arise from its mechanism and the possible other proteins implicated rather than as a direct target, which is why further characterisation of this mechanism is required.

Chapter 7. Appendices

Appendix 1. Statement of originality

I, Ana Guerrero Alonso, confirm that the research included within this thesis is my own work or that where it has been carried out in collaboration with, or supported by others, that this is duly acknowledged below and my contribution indicated. Previously published material is also acknowledged below.

I attest that I have exercised reasonable care to ensure that the work is original, and does not to the best of my knowledge break any UK law, infringe any third party's copyright or other Intellectual Property Right, or contain any confidential material.

I accept that the College has the right to use plagiarism detection software to check the electronic version of the thesis.

I confirm that this thesis has not been previously submitted for the award of a degree by this or any other university.

The copyright of this thesis rests with the author and no quotation from it or information derived from it may be published without the prior written consent of the author.

Details of collaboration and publications:

The murine PAF1 constructs employed in chapter 5 were kindly obtained from Yoo JH's lab. I very much acknowledge their contribution to my thesis.

This thesis was funded by the Medical Research Council, UK.

Signature: Ana Guerrero Alonso

Date: 20/03/15

Appendix 2. List of GEFs and GAPs included in siRNA screen (chapter 4)

	GEF/GAP	Gene name
1	GEF	SWAP70
2	GEF	SGEF
3	GEF	PREX1
4	GEF	GEFT
5	GEF	ARHGEF10
6	GEF	FLJ10521
7	GEF	FGD6
8	GEF	DNMBP
9	GEF	MCF2
10	GEF	MCF2L
11	GEF	DOCK4
12	GEF	DOCK5
13	GEF	DOCK6
14	GEF	DOCK7
15	GEF	DOCK8
16	GEF	NGEF
17	GEF	FGD2
18	GEF	SPATA13
19	GEF	MCF2L2
20	GEF	DEF6
21	GEF	FGD4
22	GEF	ARHGEF19
23	GEF	FGD3
24	GEF	DOCK10
25	GEF	PLEKHG5
26	GEF	DOCK9
27	GEF	AKAP13
28	GEF	LOC351864
29	GEF	ECT2
30	GEF	FARP1
31	GEF	FARP2
32	GEF	ABR
33	GEF	ALS2
34	GEF	ARHGEF3
35	GEF	ARHGEF4
36	GEF	ARHGEF10
37	GEF	ARHGEF15

38	GEF	BCR
39	GEF	PLEKHG2
40	GEF	DOCK1
41	GEF	DOCK2
42	GEF	DOCK3
43	GEF	FLJ10665
44	GEF	NET1
45	GEF	C9ORF100
46	GEF	FLJ20148
47	GEF	ITSN1
48	GEF	ITSN2
49	GEF	ARHGEF12
50	GEF	ARHGEF2
51	GEF	KIAA1639
52	GEF	ARHGEF18
53	GEF	ARHGEF1
54	GEF	ARHGEF17
55	GEF	ARHEGF11
56	GEF	ARHGEF9
57	GEF	ARHGEF6
58	GEF	ARHGEF7
59	GEF	RASGRF1
60	GEF	RASGRF2
61	GEF	SOS1
62	GEF	SOS2
63	GEF	TIAM1
64	GEF	TIAM2
65	GEF	ARHEGF5
66	GEF	TRIO
67	GEF	VAV1
68	GEF	VAV2
69	GEF	VAV3
70	GEF	FGD5
71	GEF	PLEKHG1
72	GEF	RGNEF
73	GEF	FLJ10357
74	GEF	PLEKHG4B
75	GEF	PLEKHG7
76	GEF	DOCK11
77	GEF	FGD1
78	GEF	KALRN

79	GEF	PLEKHG4
80	GEF	PLEKHG3
81	GAP	7H3
82	GAP	ARHGAP1
83	GAP	ARHGAP10
84	GAP	ARHGAP11A
85	GAP	ARHGAP12
86	GAP	ARHGAP15
87	GAP	ARHGAP17
88	GAP	ARHGAP18
89	GAP	ARHGAP19
90	GAP	ARHGAP20
91	GAP	ARHGAP21
91	GAP	ARHGAP22
93	GAP	ARHGAP23
94	GAP	ARHGAP24
95	GAP	ARHGAP25
96	GAP	ARHGAP26
97	GAP	ARHGAP28
98	GAP	ARHGAP4
99	GAP	ARHGAP5
100	GAP	ARHGAP6
101	GAP	ARHGAP8
102	GAP	ARHGAP9
103	GAP	BNIP2
104	GAP	C5ORF5
105	GAP	CDGAP
106	GAP	CENTD1
107	GAP	CENTD2
108	GAP	CENTD3
109	GAP	CHN1
110	GAP	CHN2
111	GAP	DEPDC1
112	GAP	DEPDC1B
113	GAP	DLC1
114	GAP	FKSG42
115	GAP	FLJ13815
116	GAP	FLJ30058
117	GAP	37 FLJ32810
118	GAP	GMIP
119	GAP	GRLF1

120	GAP	HA-1
121	GAP	INPP5B
122	GAP	KIAA0672
123	GAP	KIAA1688
124	GAP	LOC201176
125	GAP	LOC257106
126	GAP	LOC389211
127	GAP	MYO9A
128	GAP	MYO9B
129	GAP	OCRL
130	GAP	OPHN1
131	GAP	PARG1
132	GAP	PIK3R1
133	GAP	PIK3R2
134	GAP	RACGAP1
135	GAP	RALBP1
136	GAP	RICS
137	GAP	SH3BP1
138	GAP	SNX26
139	GAP	SRGAP1
140	GAP	SRGAP2
142	GAP	SRGAP3
143	GAP	STARD13
144	GAP	STARD8
145	GAP	TAGAP

Appendix 3. Observed monolayer coverage after siRNA knockdown and HIV-1 NL4.3 and BaL infection (raw data)

(A) Observed cell monolayer coverage in each well after GEFs siRNA knockdown and HIV-1 NL4.3 infection.

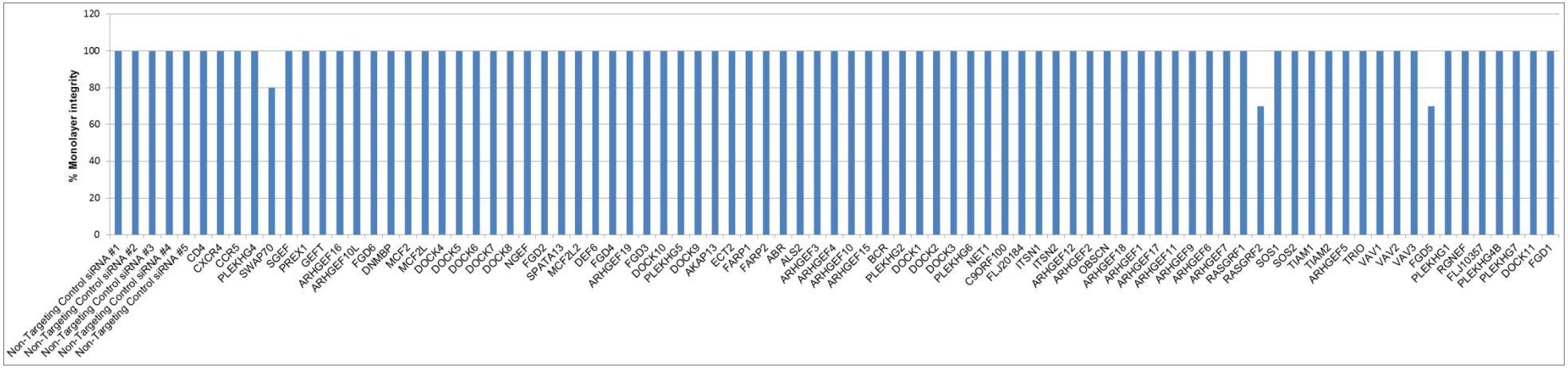

(B) Observed cell monolayer coverage in each well after GEFs siRNA knockdown and HIV-1 BaL infection.

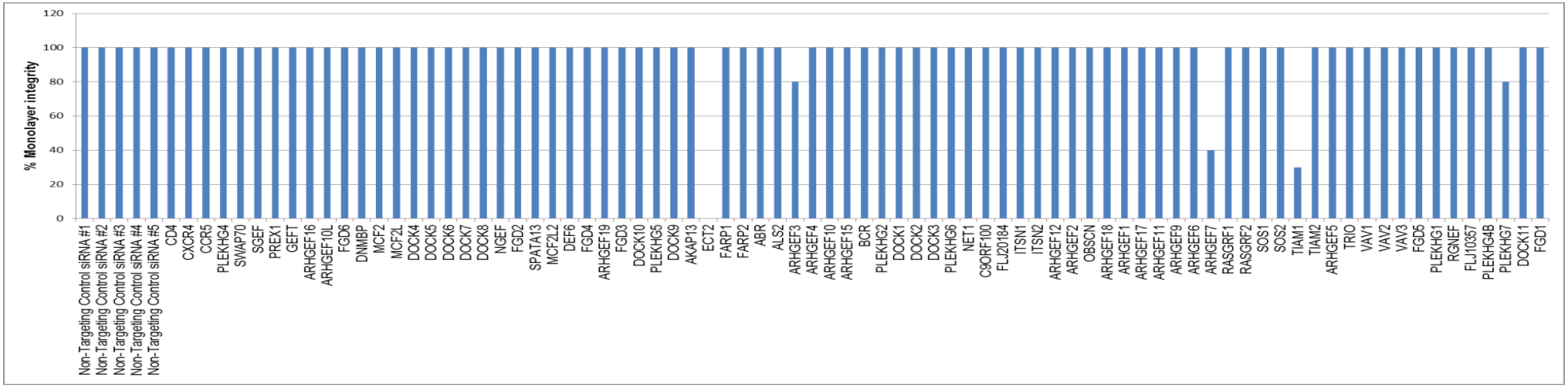

(C) Observed cell monolayer coverage in each well after GAPs siRNA knockdown and HIV-1 NL4.3 infection.

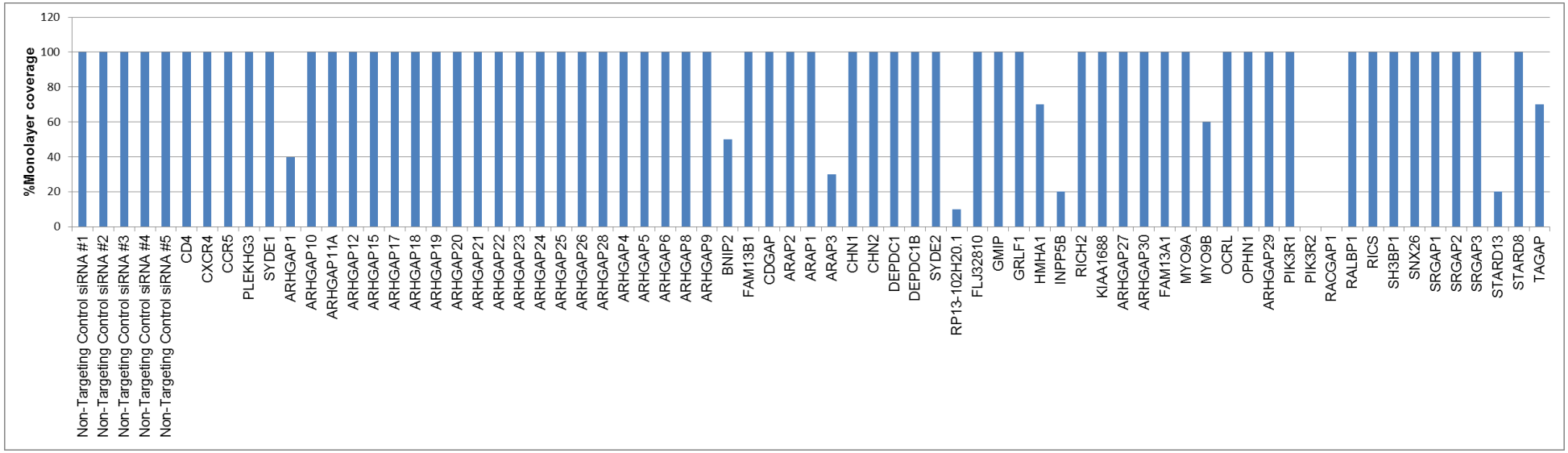

(D) Observed cell monolayer coverage in each well after GAPs siRNA knockdown and HIV-1 BaL infection.

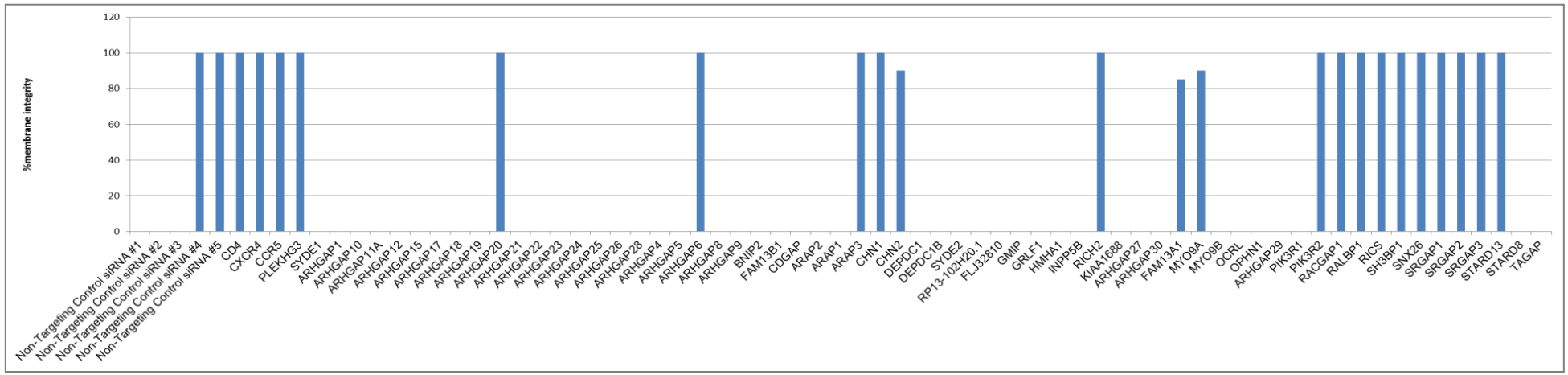

Appendix 4.Western-Blot of the cellular fractionation of PAF1

Hela-CD4+ cells were treated with 0.1% NP40 in PBS for 1 and 4 minutes. Cells were fractionated into nuclear (Nuc) and cytoplasmic (Cyto) fractions and PAF1, GAPDH (cytoplasmic marker) and histone 3 (nuclear marker) were analysed by Western-Blot.

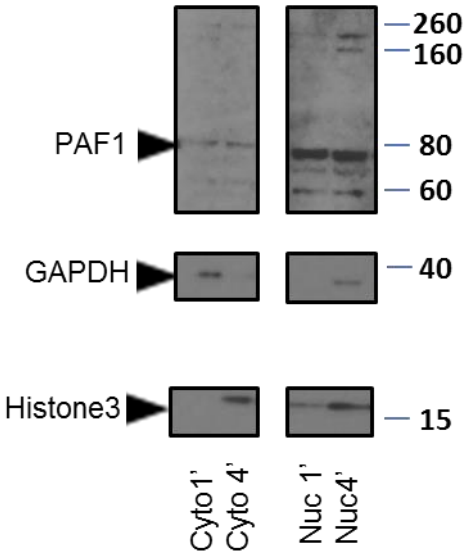

Appendix 5. PAF1 staining quantification repeats

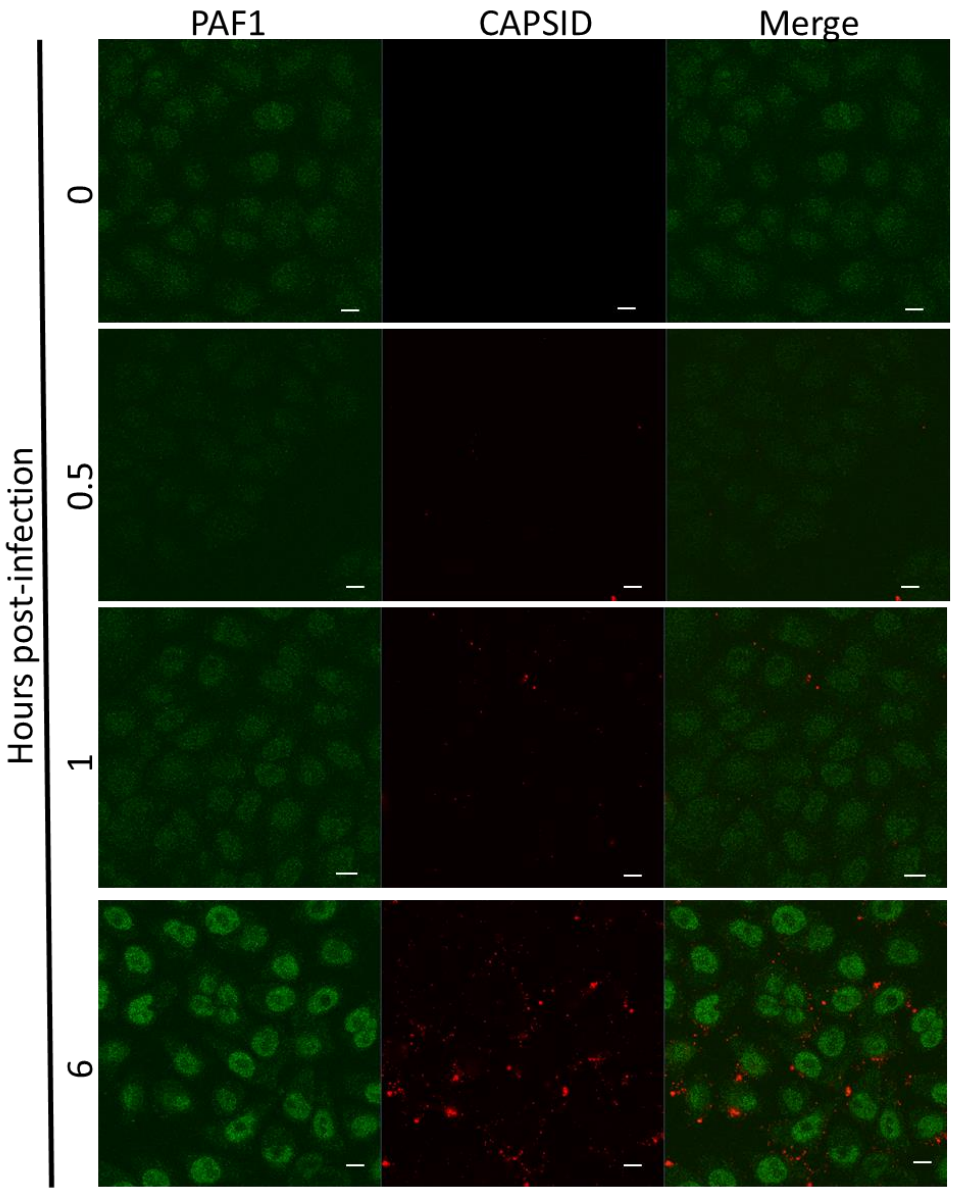

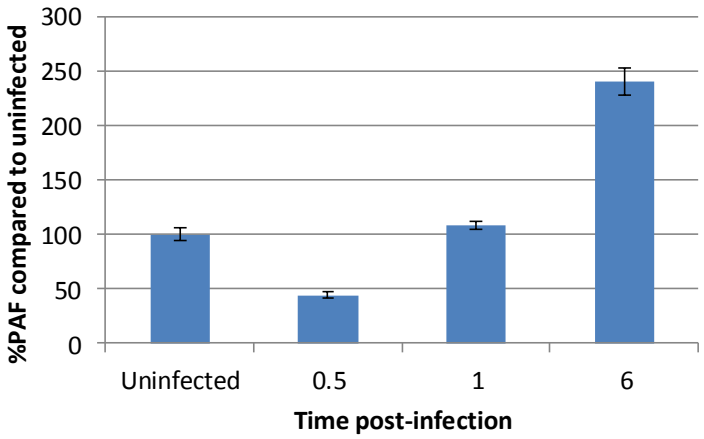

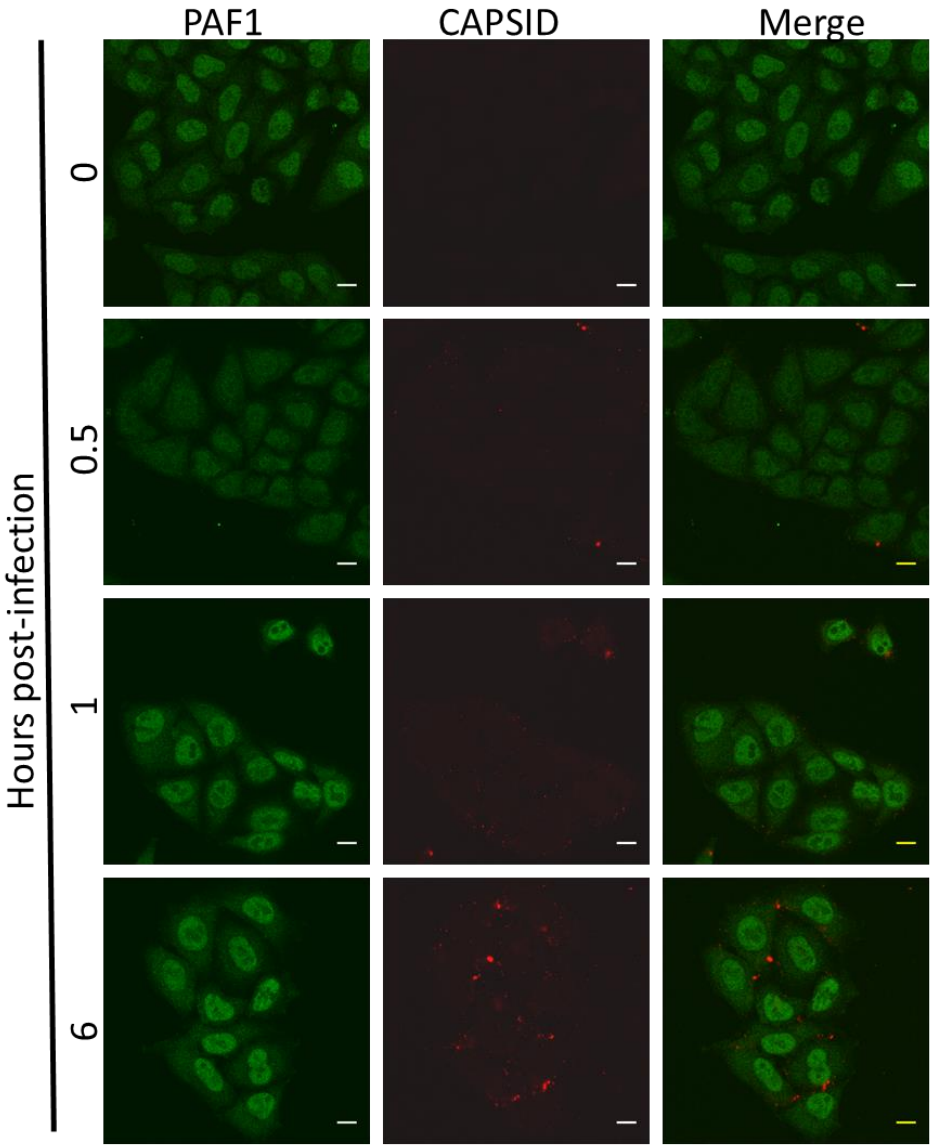
PAF1
CAPSID
Merge
Hours post-infection
0
0.5
1
6

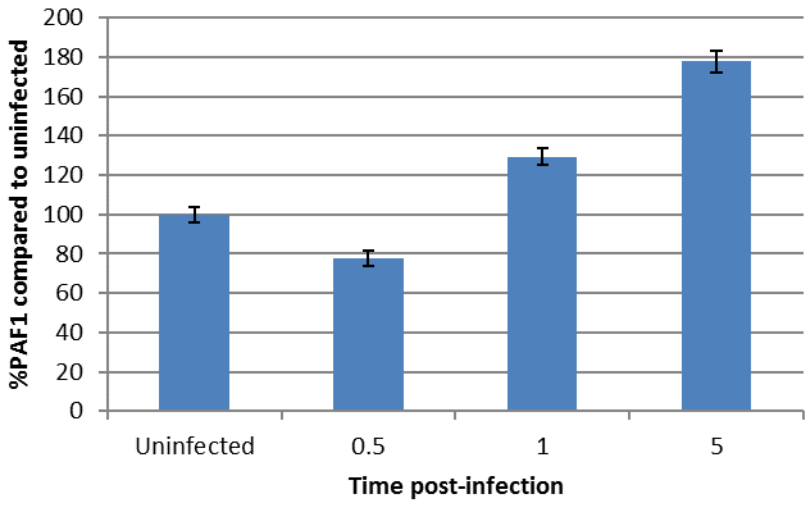
%PAF1 compared to uninfected
200
180
160
140
120
100
80
60
40
20
0
Uninfected
0.5
1
5
Time post-infection

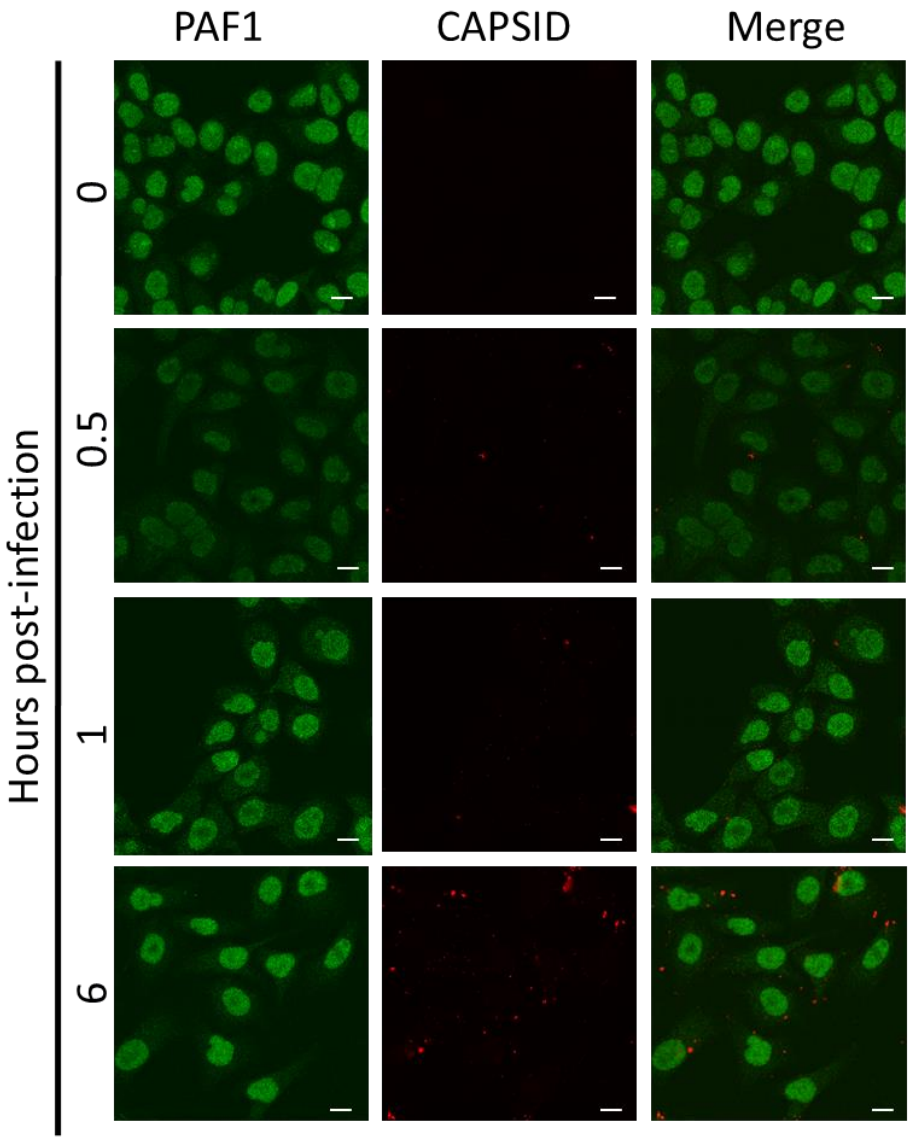
PAF1
CAPSID
Merge
Hours post-infection
0
0.5
1
6

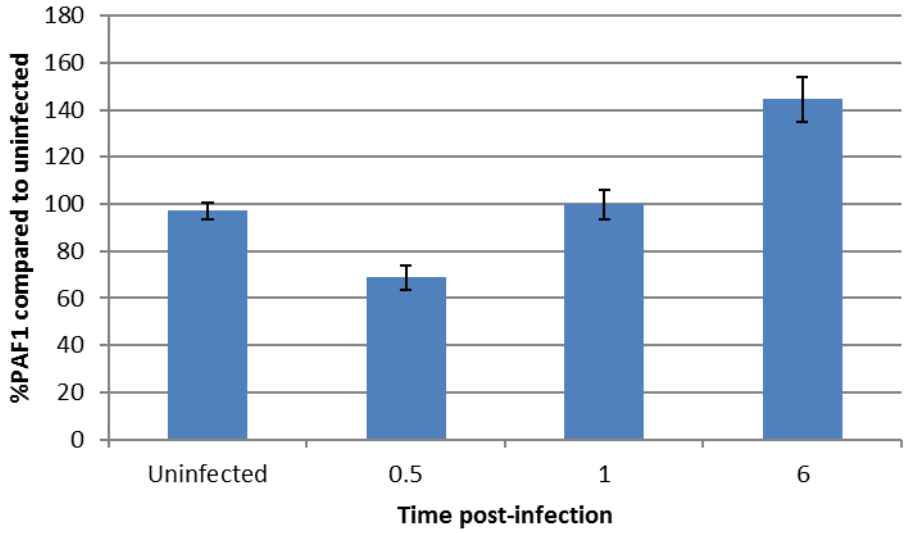
180
160
140
120
100
80
60
40
20
0
%PAF1 compared to uninfected
Uninfected
0.5
1
6
Time post-infection

Chapter 8. Bibliography

1. Lechevalier, H., *Dmitri Iosifovich Ivanovski (1864–-1920)*. 1972, *Bacteriological Reviews*. p. 135—45. .
2. Baltimore, D., *RNA-dependent DNA polymerase in virions of RNA tumour viruses.* Nature, 1970. **226**(5252): p. 1209-11.
3. Baltimore, D., *Expression of animal virus genomes.* Bacteriol Rev, 1971. **35**(3): p. 235-41.
4. Sharma, P., et al., *Novel drug delivery approaches on antiviral and antiretroviral agents.* J Adv Pharm Technol Res, 2012. **3**(3): p. 147-59.
5. Fauquet, C., Mayo, MA, Maniloff, J, Desselberger, U, and Ball, LA, *Classification and Nomenclature of Viruses, 8th ICTV Report of the International Committee on Taxonomy of Viruses*. 2005, Elsevier/Academic Press: Elsevier/Academic Press. p. 1259.
6. Weiss, R.A., *Retrovirus classification and cell interactions.* J Antimicrob Chemother, 1996. **37 Suppl B**: p. 1-11.
7. Weiss, R.A., *The discovery of endogenous retroviruses.* Retrovirology, 2006. **3**: p. 67.
8. Tazi, J., et al., *Alternative splicing: regulation of HIV-1 multiplication as a target for therapeutic action.* FEBS J, 2010. **277**(4): p. 867-76.
9. M, K.D. and H.P. M, *Fields Virology*. 2013, Lippincott Williams & Wilkins: Philadelphia, PA, USA.
10. Sharp, P.M. and B.H. Hahn, *Origins of HIV and the AIDS pandemic.* Cold Spring Harb Perspect Med, 2011. **1**(1): p. a006841.
11. Ward, M.J., et al., *Estimating the rate of intersubtype recombination in early HIV-1 group M strains.* J Virol, 2013. **87**(4): p. 1967-73.
12. Lepa, A. and A.K. Siwicki, *Retroviruses of wild and cultured fish.* Pol J Vet Sci, 2011. **14**(4): p. 703-9.
13. Affranchino, J.L. and S.A. González, *Understanding the process of envelope glycoprotein incorporation into virions in simian and feline immunodeficiency viruses.* Viruses, 2014. **6**(1): p. 264-83.
14. Herrmann-Hoesing, L.M., *Diagnostic assays used to control small ruminant lentiviruses.* J Vet Diagn Invest, 2010. **22**(6): p. 843-55.
15. Payne, L.N. and V. Nair, *The long view: 40 years of avian leukosis research.* Avian Pathol, 2012. **41**(1): p. 11-9.
16. Gallo, R.C., et al., *Isolation of human T-cell leukemia virus in acquired immune deficiency syndrome (AIDS).* Science, 1983. **220**(4599): p. 865-7.
17. Barré-Sinoussi, F., et al., *Isolation of a T-lymphotropic retrovirus from a patient at risk for acquired immune deficiency syndrome (AIDS).* Science, 1983. **220**(4599): p. 868-71.
18. Popovic, M., et al., *Detection, isolation, and continuous production of cytopathic retroviruses (HTLV-III) from patients with AIDS and pre-AIDS.* Science, 1984. **224**(4648): p. 497-500.
19. Clavel, F., et al., *Isolation of a new human retrovirus from West African patients with AIDS.* Science, 1986. **233**(4761): p. 343-6.
20. Clavel, F., et al., *Human immunodeficiency virus type 2 infection associated with AIDS in West Africa.* N Engl J Med, 1987. **316**(19): p. 1180-5.
21. Peeters, M., et al., *Risk to human health from a plethora of simian immunodeficiency viruses in primate bushmeat.* Emerg Infect Dis, 2002. **8**(5): p. 451-7.
22. Santoro, M.M. and C.F. Perno, *HIV-1 Genetic Variability and Clinical Implications.* ISRN Microbiol, 2013. **2013**: p. 481314.
23. Arts, E.J. and D.J. Hazuda, *HIV-1 antiretroviral drug therapy.* Cold Spring Harb Perspect Med, 2012. **2**(4): p. a007161.

24. Temin, H.M., *Retrovirus variation and reverse transcription: abnormal strand transfers result in retrovirus genetic variation.* Proc Natl Acad Sci U S A, 1993. **90**(15): p. 6900-3.
25. Buonaguro, L., M.L. Tornesello, and F.M. Buonaguro, *Human immunodeficiency virus type 1 subtype distribution in the worldwide epidemic: pathogenetic and therapeutic implications.* J Virol, 2007. **81**(19): p. 10209-19.
26. Michael, N.L., *Host genetic influences on HIV-1 pathogenesis.* Curr Opin Immunol, 1999. **11**(4): p. 466-74.
27. Fisher, A.G., et al., *Biologically diverse molecular variants within a single HIV-1 isolate.* Nature, 1988. **334**(6181): p. 444-7.
28. Troyer, R.M., et al., *Variable fitness impact of HIV-1 escape mutations to cytotoxic T lymphocyte (CTL) response.* PLoS Pathog, 2009. **5**(4): p. e1000365.
29. Hemelaar, J., et al., *Global and regional distribution of HIV-1 genetic subtypes and recombinants in 2004.* AIDS, 2006. **20**(16): p. W13-23.
30. Kannangai, R., S. David, and G. Sridharan, *Human immunodeficiency virus type-2-A milder, kinder virus: an update.* Indian J Med Microbiol, 2012. **30**(1): p. 6-15.
31. Blattner, W., R.C. Gallo, and H.M. Temin, *HIV causes AIDS.* Science, 1988. **241**(4865): p. 515-6.
32. Ward, J.W., et al., *Transmission of human immunodeficiency virus (HIV) by blood transfusions screened as negative for HIV antibody.* N Engl J Med, 1988. **318**(8): p. 473-8.
33. Schiffner, T., Q.J. Sattentau, and C.J. Duncan, *Cell-to-cell spread of HIV-1 and evasion of neutralizing antibodies.* Vaccine, 2013. **31**(49): p. 5789-97.
34. Tobin, N.H. and G.M. Aldrovandi, *Immunology of pediatric HIV infection.* Immunol Rev, 2013. **254**(1): p. 143-69.
35. McCormack, S.A. and B.M. Best, *Protecting the Fetus Against HIV Infection: A Systematic Review of Placental Transfer of Antiretrovirals.* Clin Pharmacokinet, 2014.
36. Park, J.W., et al., *Ten years of experience in the prevention of mother-to-child human immunodeficiency virus transmission in a university teaching hospital.* Korean J Pediatr, 2014. **57**(3): p. 117-24.
37. Gottlieb, M.S., *Pneumocystis pneumonia--Los Angeles. 1981.* Am J Public Health, 2006. **96**(6): p. 980-1; discussion 982-3.
38. Organisation, W.H., *WHO CASE DEFINITIONS OF HIV FOR SURVEILLANCE AND REVISED CLINICAL STAGING AND IMMUNOLOGICAL CLASSIFICATION OF HIV-RELATED DISEASE IN ADULTS AND CHILDREN* 2007: WHO Press.
39. Gupta, V. and S. Gupta, *Laboratory markers associated with progression of HIV infection.* Indian J Med Microbiol, 2004. **22**(1): p. 7-15.
40. Hofmann, B., et al., *Serum beta 2-microglobulin level increases in HIV infection: relation to seroconversion, CD4 T-cell fall and prognosis.* AIDS, 1990. **4**(3): p. 207-14.
41. Murr, C., et al., *Neopterin as a marker for immune system activation.* Curr Drug Metab, 2002. **3**(2): p. 175-87.
42. Dranoff, G., *Cytokines in cancer pathogenesis and cancer therapy.* Nat Rev Cancer, 2004. **4**(1): p. 11-22.
43. Lifson, J.D., et al., *AIDS retrovirus induced cytopathology: giant cell formation and involvement of CD4 antigen.* Science, 1986. **232**(4754): p. 1123-7.
44. Alkhatib, G., et al., *CC CKR5: a RANTES, MIP-1alpha, MIP-1beta receptor as a fusion cofactor for macrophage-tropic HIV-1.* Science, 1996. **272**(5270): p. 1955-8.
45. Deng, H., et al., *Identification of a major co-receptor for primary isolates of HIV-1.* Nature, 1996. **381**(6584): p. 661-6.

46. Feng, Y., et al., *HIV-1 entry cofactor: functional cDNA cloning of a seven-transmembrane, G protein-coupled receptor.* Science, 1996. **272**(5263): p. 872-7.
47. Clapham, P.R. and A. McKnight, *HIV-1 receptors and cell tropism.* Br Med Bull, 2001. **58**: p. 43-59.
48. Dittmar, M.T., et al., *HIV-1 tropism and co-receptor use.* Nature, 1997. **385**(6616): p. 495-6.
49. Rowland-Jones, S.L., *HIV: The deadly passenger in dendritic cells.* Curr Biol, 1999. **9**(7): p. R248-50.
50. Nottet, H.S. and H.E. Gendelman, *Unraveling the neuroimmune mechanisms for the HIV-1-associated cognitive/motor complex.* Immunol Today, 1995. **16**(9): p. 441-8.
51. Wilkie, F.L., et al., *Cognitive Effects of HIV-1 Infection.* CNS Spectr, 2000. **5**(5): p. 33-51.
52. Moore, M.D. and W.S. Hu, *HIV-1 RNA dimerization: It takes two to tango.* AIDS Rev, 2009. **11**(2): p. 91-102.
53. Moore, M.D., et al., *Dimer initiation signal of human immunodeficiency virus type 1: its role in partner selection during RNA copackaging and its effects on recombination.* J Virol, 2007. **81**(8): p. 4002-11.
54. Pettit, S.C., et al., *Ordered processing of the human immunodeficiency virus type 1 GagPol precursor is influenced by the context of the embedded viral protease.* J Virol, 2005. **79**(16): p. 10601-7.
55. Jacks, T., et al., *Characterization of ribosomal frameshifting in HIV-1 gag-pol expression.* Nature, 1988. **331**(6153): p. 280-3.
56. Freed, E.O., *HIV-1 replication.* Somat Cell Mol Genet, 2001. **26**(1-6): p. 13-33.
57. Dayton, A.I., et al., *The trans-activator gene of the human T cell lymphotropic virus type III is required for replication.* Cell, 1986. **44**(6): p. 941-7.
58. Fisher, A.G., et al., *The trans-activator gene of HTLV-III is essential for virus replication.* Nature, 1986. **320**(6060): p. 367-71.
59. Pollard, V.W. and M.H. Malim, *The HIV-1 Rev protein.* Annu Rev Microbiol, 1998. **52**: p. 491-532.
60. Lever, A., et al., *Identification of a sequence required for efficient packaging of human immunodeficiency virus type 1 RNA into virions.* J Virol, 1989. **63**(9): p. 4085-7.
61. Lundquist, C.A., et al., *Nef-Mediated Downregulation of CD4 Enhances Human Immunodeficiency Virus Type 1 Replication in Primary T Lymphocytes.* Journal of Virology, 2002. **76**(9): p. 4625-4633.
62. Blagoveshchenskaya, A.D., et al., *HIV-1 Nef downregulates MHC-I by a PACS-1- and PI3K-regulated ARF6 endocytic pathway.* Cell, 2002. **111**(6): p. 853-66.
63. Collette, Y., et al., *Physical and functional interaction of Nef with Lck. HIV-1 Nef-induced T-cell signaling defects.* J Biol Chem, 1996. **271**(11): p. 6333-41.
64. Coates, K. and M. Harris, *The human immunodeficiency virus type 1 Nef protein functions as a protein kinase C substrate in vitro.* J Gen Virol, 1995. **76 (Pt 4)**: p. 837-44.
65. Coates, K., et al., *Analysis of the interactions between Nef and cellular proteins.* Res Virol, 1997. **148**(1): p. 68-70.
66. Kogan, M. and J. Rappaport, *HIV-1 accessory protein Vpr: relevance in the pathogenesis of HIV and potential for therapeutic intervention.* Retrovirology, 2011. **8**: p. 25.
67. Ayinde, D., et al., *Limelight on two HIV/SIV accessory proteins in macrophage infection: is Vpx overshadowing Vpr?* Retrovirology, 2010. **7**: p. 35.
68. González, M.E., *Vpu Protein: The Viroporin Encoded by HIV-1.* Viruses, 2015. **7**(8): p. 4352-68.

69. Neil, S.J., T. Zang, and P.D. Bieniasz, *Tetherin inhibits retrovirus release and is antagonized by HIV-1 Vpu.* Nature, 2008. **451**(7177): p. 425-30.
70. Aldrovandi, G.M. and J.A. Zack, *Replication and pathogenicity of human immunodeficiency virus type 1 accessory gene mutants in SCID-hu mice.* J Virol, 1996. **70**(3): p. 1505-11.
71. Jamieson, B.D., et al., *Requirement of human immunodeficiency virus type 1 nef for in vivo replication and pathogenicity.* J Virol, 1994. **68**(6): p. 3478-85.
72. Stopak, K., et al., *HIV-1 Vif blocks the antiviral activity of APOBEC3G by impairing both its translation and intracellular stability.* Mol Cell, 2003. **12**(3): p. 591-601.
73. Wang, X., et al., *Interactions between HIV-1 Vif and human ElonginB-ElonginC are important for CBF-β binding to Vif.* Retrovirology, 2013. **10**: p. 94.
74. Gallaher, W.R., *Detection of a fusion peptide sequence in the transmembrane protein of human immunodeficiency virus.* Cell, 1987. **50**(3): p. 327-8.
75. Matthews, T.J., et al., *Interaction between the human T-cell lymphotropic virus type IIIB envelope glycoprotein gp120 and the surface antigen CD4: role of carbohydrate in binding and cell fusion.* Proc Natl Acad Sci U S A, 1987. **84**(15): p. 5424-8.
76. Miyauchi, K., et al., *HIV enters cells via endocytosis and dynamin-dependent fusion with endosomes.* Cell, 2009. **137**(3): p. 433-44.
77. Iyengar, S., J.E. Hildreth, and D.H. Schwartz, *Actin-dependent receptor colocalization required for human immunodeficiency virus entry into host cells.* J Virol, 1998. **72**(6): p. 5251-5.
78. Konig, R. and W. Zhou, *Signal transduction in T helper cells: CD4 coreceptors exert complex regulatory effects on T cell activation and function.* Curr Issues Mol Biol, 2004. **6**(1): p. 1-15.
79. Jiménez-Baranda, S., et al., *Filamin-A regulates actin-dependent clustering of HIV receptors.* Nat Cell Biol, 2007. **9**(7): p. 838-46.
80. Yoder, A., et al., *HIV envelope-CXCR4 signaling activates cofilin to overcome cortical actin restriction in resting CD4 T cells.* Cell, 2008. **134**(5): p. 782-92.
81. Engelman, A. and P. Cherepanov, *The structural biology of HIV-1: mechanistic and therapeutic insights.* Nat Rev Microbiol, 2012. **10**(4): p. 279-90.
82. Matreyek, K.A. and A. Engelman, *Viral and cellular requirements for the nuclear entry of retroviral preintegration nucleoprotein complexes.* Viruses, 2013. **5**(10): p. 2483-511.
83. Sundquist, W.I. and H.G. Kräusslich, *HIV-1 assembly, budding, and maturation.* Cold Spring Harb Perspect Med, 2012. **2**(7): p. a006924.
84. Frankel, A.D. and J.A. Young, *HIV-1: fifteen proteins and an RNA.* Annu Rev Biochem, 1998. **67**: p. 1-25.
85. Samson, M., et al., *Resistance to HIV-1 infection in caucasian individuals bearing mutant alleles of the CCR-5 chemokine receptor gene.* Nature, 1996. **382**(6593): p. 722-5.
86. Zhu, P., et al., *Electron tomography analysis of envelope glycoprotein trimers on HIV and simian immunodeficiency virus virions.* Proc Natl Acad Sci U S A, 2003. **100**(26): p. 15812-7.
87. Postler, T.S. and R.C. Desrosiers, *The tale of the long tail: the cytoplasmic domain of HIV-1 gp41.* J Virol, 2013. **87**(1): p. 2-15.
88. Douglas, N.W., G.H. Munro, and R.S. Daniels, *HIV/SIV glycoproteins: structure-function relationships.* J Mol Biol, 1997. **273**(1): p. 122-49.
89. Liu, J., et al., *Molecular architecture of native HIV-1 gp120 trimers.* Nature, 2008. **455**(7209): p. 109-13.

90. Liu, J., *Structure of the HIV-1 gp41 Membrane-Proximal Ectodomain Region in a Putative Prefusion Conformation†,‡ - Biochemistry (ACS Publications).* (Web): February 18, 2009.
91. Rizzuto, C.D., et al., *A conserved HIV gp120 glycoprotein structure involved in chemokine receptor binding.* Science, 1998. **280**(5371): p. 1949-53.
92. Buzon, V., et al., *Crystal structure of HIV-1 gp41 including both fusion peptide and membrane proximal external regions.* PLoS Pathog, 2010. **6**(5): p. e1000880.
93. Teixeira, C., et al., *Viral surface glycoproteins, gp120 and gp41, as potential drug targets against HIV-1: brief overview one quarter of a century past the approval of zidovudine, the first anti-retroviral drug.* Eur J Med Chem, 2011. **46**(4): p. 979-92.
94. Tomkowicz, B. and R.G. Collman, *HIV-1 entry inhibitors: closing the front door.* Expert Opin Ther Targets, 2004. **8**(2): p. 65-78.
95. Ambrose, Z. and C. Aiken, *HIV-1 uncoating: connection to nuclear entry and regulation by host proteins.* Virology, 2014. **454-455**: p. 371-9.
96. Braaten, D., E.K. Franke, and J. Luban, *Cyclophilin A is required for an early step in the life cycle of human immunodeficiency virus type 1 before the initiation of reverse transcription.* J Virol, 1996. **70**(6): p. 3551-60.
97. Ptak, R.G., et al., *Inhibition of human immunodeficiency virus type 1 replication in human cells by Debio-025, a novel cyclophilin binding agent.* Antimicrob Agents Chemother, 2008. **52**(4): p. 1302-17.
98. Hulme, A.E., O. Perez, and T.J. Hope, *Complementary assays reveal a relationship between HIV-1 uncoating and reverse transcription.* Proc Natl Acad Sci U S A, 2011. **108**(24): p. 9975-80.
99. Xu, H., et al., *Evidence for biphasic uncoating during HIV-1 infection from a novel imaging assay.* Retrovirology, 2013. **10**: p. 70.
100. Shin, M.K., J. Lee, and W.S. Ryu, *A novel cis-acting element facilitates minus-strand DNA synthesis during reverse transcription of the hepatitis B virus genome.* J Virol, 2004. **78**(12): p. 6252-62.
101. Sarafianos, S.G., et al., *Structure and function of HIV-1 reverse transcriptase: molecular mechanisms of polymerization and inhibition.* J Mol Biol, 2009. **385**(3): p. 693-713.
102. Fassati, A., et al., *Nuclear import of HIV-1 intracellular reverse transcription complexes is mediated by importin 7.* EMBO J, 2003. **22**(14): p. 3675-85.
103. Gallay, P., et al., *Role of the karyopherin pathway in human immunodeficiency virus type 1 nuclear import.* J Virol, 1996. **70**(2): p. 1027-32.
104. Christ, F., et al., *Transportin-SR2 imports HIV into the nucleus.* Curr Biol, 2008. **18**(16): p. 1192-202.
105. Ebina, H., et al., *Role of Nup98 in nuclear entry of human immunodeficiency virus type 1 cDNA.* Microbes Infect, 2004. **6**(8): p. 715-24.
106. König, R., et al., *Global analysis of host-pathogen interactions that regulate early-stage HIV-1 replication.* Cell, 2008. **135**(1): p. 49-60.
107. Engelman, A. and P. Cherepanov, *The lentiviral integrase binding protein LEDGF/p75 and HIV-1 replication.* PLoS Pathog, 2008. **4**(3): p. e1000046.
108. Rittner, K., et al., *The human immunodeficiency virus long terminal repeat includes a specialised initiator element which is required for Tat-responsive transcription.* J Mol Biol, 1995. **248**(3): p. 562-80.
109. Karn, J. and C.M. Stoltzfus, *Transcriptional and posttranscriptional regulation of HIV-1 gene expression.* Cold Spring Harb Perspect Med, 2012. **2**(2): p. a006916.
110. Liu, J., et al., *Specific NF-kappa B subunits act in concert with Tat to stimulate human immunodeficiency virus type 1 transcription.* J Virol, 1992. **66**(6): p. 3883-7.

111. Sodroski, J., et al., *Location of the trans-activating region on the genome of human T-cell lymphotropic virus type III.* Science, 1985. **229**(4708): p. 74-7.
112. Berkhout, B., R.H. Silverman, and K.T. Jeang, *Tat trans-activates the human immunodeficiency virus through a nascent RNA target.* Cell, 1989. **59**(2): p. 273-82.
113. Wei, P., et al., *A novel CDK9-associated C-type cyclin interacts directly with HIV-1 Tat and mediates its high-affinity, loop-specific binding to TAR RNA.* Cell, 1998. **92**(4): p. 451-62.
114. Tahirov, T.H., et al., *Crystal structure of HIV-1 Tat complexed with human P-TEFb.* Nature, 2010. **465**(7299): p. 747-51.
115. Marshall, N.F. and D.H. Price, *Purification of P-TEFb, a transcription factor required for the transition into productive elongation.* J Biol Chem, 1995. **270**(21): p. 12335-8.
116. Malim, M.H., et al., *The HIV-1 rev trans-activator acts through a structured target sequence to activate nuclear export of unspliced viral mRNA.* Nature, 1989. **338**(6212): p. 254-7.
117. Rausch, J.W. and S.F. Le Grice, *HIV Rev Assembly on the Rev Response Element (RRE): A Structural Perspective.* Viruses, 2015. **7**(6): p. 3053-75.
118. Adamson, C.S., K. Salzwedel, and E.O. Freed, *Virus maturation as a new HIV-1 therapeutic target.* Expert Opin Ther Targets, 2009. **13**(8): p. 895-908.
119. Kieffer, C., et al., *Two distinct modes of ESCRT-III recognition are required for VPS4 functions in lysosomal protein targeting and HIV-1 budding.* Dev Cell, 2008. **15**(1): p. 62-73.
120. Morita, E., et al., *Identification of human MVB12 proteins as ESCRT-I subunits that function in HIV budding.* Cell Host Microbe, 2007. **2**(1): p. 41-53.
121. Morita, E., et al., *ESCRT-III protein requirements for HIV-1 budding.* Cell Host Microbe, 2011. **9**(3): p. 235-42.
122. Cambiano, V., et al., *Antiretroviral therapy for prevention of HIV transmission: implications for Europe.* Euro Surveill, 2013. **18**(48): p. 20647.
123. Ensoli, B., et al., *Challenges in HIV Vaccine Research for Treatment and Prevention.* Front Immunol, 2014. **5**: p. 417.
124. LaBonte, J., J. Lebbos, and P. Kirkpatrick, *Enfuvirtide.* Nat Rev Drug Discov, 2003. **2**(5): p. 345-346.
125. Young, F.E., *The role of the FDA in the effort against AIDS.* Public Health Rep, 1988. **103**(3): p. 242-5.
126. Mitsuya, H., et al., *3'-Azido-3'-deoxythymidine (BW A509U): an antiviral agent that inhibits the infectivity and cytopathic effect of human T-lymphotropic virus type III/lymphadenopathy-associated virus in vitro.* Proc Natl Acad Sci U S A, 1985. **82**(20): p. 7096-100.
127. de Béthune, M.P., *Non-nucleoside reverse transcriptase inhibitors (NNRTIs), their discovery, development, and use in the treatment of HIV-1 infection: a review of the last 20 years (1989-2009).* Antiviral Res, 2010. **85**(1): p. 75-90.
128. Ivetac, A. and J.A. McCammon, *ELUCIDATING THE INHIBITION MECHANISM OF HIV-1 NON-NUCLEOSIDE REVERSE TRANSCRIPTASE INHIBITORS THROUGH MULTI-COPY MOLECULAR DYNAMICS SIMULATIONS.* Journal of molecular biology, 2009. **388**(3): p. 644-658.
129. Lin, P.F., et al., *A small molecule HIV-1 inhibitor that targets the HIV-1 envelope and inhibits CD4 receptor binding.* Proc Natl Acad Sci U S A, 2003. **100**(19): p. 11013-8.
130. Reimann, K.A., et al., *A humanized form of a CD4-specific monoclonal antibody exhibits decreased antigenicity and prolonged plasma half-life in rhesus monkeys*

while retaining its unique biological and antiviral properties. AIDS Res Hum Retroviruses, 1997. **13**(11): p. 933-43.
131. Wild, C., et al., *The inhibitory activity of an HIV type 1 peptide correlates with its ability to interact with a leucine zipper structure.* AIDS Res Hum Retroviruses, 1995. **11**(3): p. 323-5.
132. Bayes, M., X. Rabasseda, and J.R. Prous, *Gateways to clinical trials.* Methods Find Exp Clin Pharmacol, 2003. **25**(4): p. 317-40.
133. Koh, Y., K.A. Matreyek, and A. Engelman, *Differential sensitivities of retroviruses to integrase strand transfer inhibitors.* J Virol, 2011. **85**(7): p. 3677-82.
134. Fantauzzi, A. and I. Mezzaroma, *Dolutegravir: clinical efficacy and role in HIV therapy.* Ther Adv Chronic Dis, 2014. **5**(4): p. 164-77.
135. Liedtke, M.D., et al., *Long-term efficacy and safety of raltegravir in the management of HIV infection.* Infect Drug Resist, 2014. **7**: p. 73-84.
136. Cottrell, M.L., T. Hadzic, and A.D. Kashuba, *Clinical pharmacokinetic, pharmacodynamic and drug-interaction profile of the integrase inhibitor dolutegravir.* Clin Pharmacokinet, 2013. **52**(11): p. 981-94.
137. Kräusslich, H.G., et al., *Activity of purified biosynthetic proteinase of human immunodeficiency virus on natural substrates and synthetic peptides.* Proc Natl Acad Sci U S A, 1989. **86**(3): p. 807-11.
138. Kohl, N.E., et al., *Active human immunodeficiency virus protease is required for viral infectivity.* Proc Natl Acad Sci U S A, 1988. **85**(13): p. 4686-90.
139. De Clercq, E., *Anti-HIV drugs: 25 compounds approved within 25 years after the discovery of HIV.* Int J Antimicrob Agents, 2009. **33**(4): p. 307-20.
140. Esser, M.T., et al., *Cyanovirin-N binds to gp120 to interfere with CD4-dependent human immunodeficiency virus type 1 virion binding, fusion, and infectivity but does not affect the CD4 binding site on gp120 or soluble CD4-induced conformational changes in gp120.* J Virol, 1999. **73**(5): p. 4360-71.
141. Delany-Moretlwe Sinead, S.E., Myer Landon, Ahmed Khatija, Nkala Busi, Maboa Rebone, Gama Cynthia, Sibiya Sydney, Sebe Modulakgotla, Brumskine William, Bekker Linda-Gail, Nchabeleng Maposhane, Lombard Carl, Gray Glenda, Rees Helen, *FACTS 001: Characteristics of Participants Enrolled in a Phase III Randomised Controlled Trial of Tenofovir Gel for Prevention of HIV-1 and HSV-2*. 2014, AIDS research and Human Retroviruses. p. 281-A282. .
142. Nel, A., et al., *Baseline Characteristics of HIV-negative Women Enrolled into the Ring Study - A Clinical Trial of the Dapivirine Vaginal Ring for HIV-1 Prevention.* AIDS Res Hum Retroviruses, 2014. **30 Suppl 1**: p. A289.
143. Auvert, B., et al., *Randomized, controlled intervention trial of male circumcision for reduction of HIV infection risk: the ANRS 1265 Trial.* PLoS Med, 2005. **2**(11): p. e298.
144. Bailey, R.C., et al., *Male circumcision for HIV prevention in young men in Kisumu, Kenya: a randomised controlled trial.* Lancet, 2007. **369**(9562): p. 643-56.
145. Gray, R.H., et al., *Male circumcision for HIV prevention in men in Rakai, Uganda: a randomised trial.* Lancet, 2007. **369**(9562): p. 657-66.
146. Jayathunge, P.H., et al., *Male Circumcision and HIV Transmission; What Do We Know?* Open AIDS J, 2014. **8**: p. 31-44.
147. Fisher, A.K., Y. Voronin, and R. Jefferys, *Therapeutic HIV vaccines: prior setbacks, current advances, and future prospects.* Vaccine, 2014. **32**(43): p. 5540-5.
148. Ahlers, J.D., *All eyes on the next generation of HIV vaccines: strategies for inducing a broadly neutralizing antibody response.* Discov Med, 2014. **17**(94): p. 187-99.

149. Flynn, N.M., et al., *Placebo-controlled phase 3 trial of a recombinant glycoprotein 120 vaccine to prevent HIV-1 infection.* J Infect Dis, 2005. **191**(5): p. 654-65.
150. Pitisuttithum, P., et al., *Randomized, double-blind, placebo-controlled efficacy trial of a bivalent recombinant glycoprotein 120 HIV-1 vaccine among injection drug users in Bangkok, Thailand.* J Infect Dis, 2006. **194**(12): p. 1661-71.
151. Priddy, F.H., et al., *Safety and immunogenicity of a replication-incompetent adenovirus type 5 HIV-1 clade B gag/pol/nef vaccine in healthy adults.* Clin Infect Dis, 2008. **46**(11): p. 1769-81.
152. Esparza, J., *A brief history of the global effort to develop a preventive HIV vaccine.* Vaccine, 2013. **31**(35): p. 3502-18.
153. Catanzaro, A.T., et al., *Phase 1 safety and immunogenicity evaluation of a multiclade HIV-1 candidate vaccine delivered by a replication-defective recombinant adenovirus vector.* J Infect Dis, 2006. **194**(12): p. 1638-49.
154. Rerks-Ngarm, S., et al., *Vaccination with ALVAC and AIDSVAX to prevent HIV-1 infection in Thailand.* N Engl J Med, 2009. **361**(23): p. 2209-20.
155. Lazarus, E.M., et al., *Uptake of Genital Mucosal Sampling in HVTN 097, a Phase 1b HIV Vaccine Trial in South Africa.* PLoS One, 2014. **9**(11): p. e112303.
156. *Executive Summary of the Global Update on the Health Sector Response to HIV, 2014*. 2014, © World Health Organization 2014.
157. Lilly, F. and T. Pincus, *Genetic Control Of Murine Viral Leukemogenesis*, in *Advances in Cancer Research*, S.W.a.A.H. George Kleln, Editor. 1973, Academic Press. p. 231-277.
158. Liu, L., et al., *A whole genome screen for HIV restriction factors.* Retrovirology, 2011. **8**: p. 94.
159. von Schwedler, U., et al., *Vif is crucial for human immunodeficiency virus type 1 proviral DNA synthesis in infected cells.* J Virol, 1993. **67**(8): p. 4945-55.
160. Gabuzda, D.H., et al., *Role of vif in replication of human immunodeficiency virus type 1 in CD4+ T lymphocytes.* J Virol, 1992. **66**(11): p. 6489-95.
161. Simon, J.H. and M.H. Malim, *The human immunodeficiency virus type 1 Vif protein modulates the postpenetration stability of viral nucleoprotein complexes.* J Virol, 1996. **70**(8): p. 5297-305.
162. Mangeat, B., et al., *Broad antiretroviral defence by human APOBEC3G through lethal editing of nascent reverse transcripts.* Nature, 2003. **424**(6944): p. 99-103.
163. Harris, R.S., et al., *DNA deamination mediates innate immunity to retroviral infection.* Cell, 2003. **113**(6): p. 803-9.
164. Bishop, K.N., et al., *APOBEC-mediated editing of viral RNA.* Science, 2004. **305**(5684): p. 645.
165. Stremlau, M., et al., *The cytoplasmic body component TRIM5alpha restricts HIV-1 infection in Old World monkeys.* Nature, 2004. **427**(6977): p. 848-53.
166. Sayah, D.M., et al., *Cyclophilin A retrotransposition into TRIM5 explains owl monkey resistance to HIV-1.* Nature, 2004. **430**(6999): p. 569-73.
167. Keckesova, Z., L.M. Ylinen, and G.J. Towers, *The human and African green monkey TRIM5alpha genes encode Ref1 and Lv1 retroviral restriction factor activities.* Proc Natl Acad Sci U S A, 2004. **101**(29): p. 10780-5.
168. Allouch, A., et al., *The TRIM family protein KAP1 inhibits HIV-1 integration.* Cell Host Microbe, 2011. **9**(6): p. 484-95.
169. Hammonds, J., et al., *Immunoelectron microscopic evidence for Tetherin/BST2 as the physical bridge between HIV-1 virions and the plasma membrane.* PLoS Pathog, 2010. **6**(2): p. e1000749.

170. Mangeat, B., et al., *HIV-1 Vpu neutralizes the antiviral factor Tetherin/BST-2 by binding it and directing its beta-TrCP2-dependent degradation.* PLoS Pathog, 2009. **5**(9): p. e1000574.
171. Iwabu, Y., et al., *HIV-1 accessory protein Vpu internalizes cell-surface BST-2/tetherin through transmembrane interactions leading to lysosomes.* J Biol Chem, 2009. **284**(50): p. 35060-72.
172. Yin, X., et al., *Equine tetherin blocks retrovirus release and its activity is antagonized by equine infectious anemia virus envelope protein.* J Virol, 2014. **88**(2): p. 1259-70.
173. Xu, F., et al., *Tetherin inhibits prototypic foamy virus release.* Virol J, 2011. **8**: p. 198.
174. Kaletsky, R.L., et al., *Tetherin-mediated restriction of filovirus budding is antagonized by the Ebola glycoprotein.* Proc Natl Acad Sci U S A, 2009. **106**(8): p. 2886-91.
175. Alexaki, A., Y. Liu, and B. Wigdahl, *Cellular reservoirs of HIV-1 and their role in viral persistence.* Curr HIV Res, 2008. **6**(5): p. 388-400.
176. Hrecka, K., et al., *Vpx relieves inhibition of HIV-1 infection of macrophages mediated by the SAMHD1 protein.* Nature, 2011. **474**(7353): p. 658-61.
177. Lahouassa, H., et al., *SAMHD1 restricts the replication of human immunodeficiency virus type 1 by depleting the intracellular pool of deoxynucleoside triphosphates.* Nat Immunol, 2012. **13**(3): p. 223-8.
178. Goldstone, D.C., et al., *HIV-1 restriction factor SAMHD1 is a deoxynucleoside triphosphate triphosphohydrolase.* Nature, 2011. **480**(7377): p. 379-82.
179. Brandariz-Nuñez, A., et al., *Role of SAMHD1 nuclear localization in restriction of HIV-1 and SIVmac.* Retrovirology, 2012. **9**: p. 49.
180. Cribier, A., et al., *Phosphorylation of SAMHD1 by cyclin A2/CDK1 regulates its restriction activity toward HIV-1.* Cell Rep, 2013. **3**(4): p. 1036-43.
181. Zhang, J., D.T. Scadden, and C.S. Crumpacker, *Primitive hematopoietic cells resist HIV-1 infection via p21.* J Clin Invest, 2007. **117**(2): p. 473-81.
182. Allouch, A., et al., *p21-mediated RNR2 repression restricts HIV-1 replication in macrophages by inhibiting dNTP biosynthesis pathway.* Proc Natl Acad Sci U S A, 2013. **110**(42): p. E3997-4006.
183. Goujon, C., et al., *Human MX2 is an interferon-induced post-entry inhibitor of HIV-1 infection.* Nature, 2013. **502**(7472): p. 559-62.
184. Liu, Z., et al., *The interferon-inducible MxB protein inhibits HIV-1 infection.* Cell Host Microbe, 2013. **14**(4): p. 398-410.
185. Fricke, T., et al., *MxB binds to the HIV-1 core and prevents the uncoating process of HIV-1.* Retrovirology, 2014. **11**: p. 68.
186. Marno, K.M., et al., *Novel restriction factor RNA-associated early-stage anti-viral factor (REAF) inhibits human and simian immunodeficiency viruses.* Retrovirology, 2014. **11**: p. 3.
187. Akhtar, M.S., et al., *TFIIH kinase places bivalent marks on the carboxy-terminal domain of RNA polymerase II.* Mol Cell, 2009. **34**(3): p. 387-93.
188. Wood, A. and A. Shilatifard, *Bur1/Bur2 and the Ctk complex in yeast: the split personality of mammalian P-TEFb.* Cell Cycle, 2006. **5**(10): p. 1066-8.
189. Shi, X., et al., *Paf1p, an RNA polymerase II-associated factor in Saccharomyces cerevisiae, may have both positive and negative roles in transcription.* Mol Cell Biol, 1996. **16**(2): p. 669-76.
190. Wade, P.A., et al., *A novel collection of accessory factors associated with yeast RNA polymerase II.* Protein Expr Purif, 1996. **8**(1): p. 85-90.
191. Mueller, C.L. and J.A. Jaehning, *Ctr9, Rtf1, and Leo1 are components of the Paf1/RNA polymerase II complex.* Mol Cell Biol, 2002. **22**(7): p. 1971-80.

192. Koch, C., et al., *A role for Ctr9p and Paf1p in the regulation G1 cyclin expression in yeast.* Nucleic Acids Res, 1999. **27**(10): p. 2126-34.
193. Costa, P.J. and K.M. Arndt, *Synthetic lethal interactions suggest a role for the Saccharomyces cerevisiae Rtf1 protein in transcription elongation.* Genetics, 2000. **156**(2): p. 535-47.
194. Stolinski, L.A., D.M. Eisenmann, and K.M. Arndt, *Identification of RTF1, a novel gene important for TATA site selection by TATA box-binding protein in Saccharomyces cerevisiae.* Mol Cell Biol, 1997. **17**(8): p. 4490-500.
195. Jaehning, J.A., *The Paf1 complex: platform or player in RNA polymerase II transcription?* Biochim Biophys Acta, 2010. **1799**(5-6): p. 379-88.
196. Zhu, B., et al., *The human PAF complex coordinates transcription with events downstream of RNA synthesis.* Genes Dev, 2005. **19**(14): p. 1668-73.
197. Brown, J.T., X. Bai, and A.W. Johnson, *The yeast antiviral proteins Ski2p, Ski3p, and Ski8p exist as a complex in vivo.* RNA, 2000. **6**(3): p. 449-57.
198. Halbach, F., et al., *The yeast ski complex: crystal structure and RNA channeling to the exosome complex.* Cell, 2013. **154**(4): p. 814-26.
199. Amrich, C.G., et al., *Cdc73 subunit of Paf1 complex contains C-terminal Ras-like domain that promotes association of Paf1 complex with chromatin.* J Biol Chem, 2012. **287**(14): p. 10863-75.
200. Warner, M.H., K.L. Roinick, and K.M. Arndt, *Rtf1 is a multifunctional component of the Paf1 complex that regulates gene expression by directing cotranscriptional histone modification.* Mol Cell Biol, 2007. **27**(17): p. 6103-15.
201. de Jong, R.N., et al., *Structure and DNA binding of the human Rtf1 Plus3 domain.* Structure, 2008. **16**(1): p. 149-59.
202. Chu, X., et al., *Structural insights into Paf1 complex assembly and histone binding.* Nucleic Acids Res, 2013. **41**(22): p. 10619-29.
203. Squazzo, S.L., et al., *The Paf1 complex physically and functionally associates with transcription elongation factors in vivo.* EMBO J, 2002. **21**(7): p. 1764-74.
204. Pavri, R., et al., *Histone H2B monoubiquitination functions cooperatively with FACT to regulate elongation by RNA polymerase II.* Cell, 2006. **125**(4): p. 703-17.
205. Rozenblatt-Rosen, O., et al., *The tumor suppressor Cdc73 functionally associates with CPSF and CstF 3' mRNA processing factors.* Proc Natl Acad Sci U S A, 2009. **106**(3): p. 755-60.
206. Mueller, C.L., et al., *The Paf1 complex has functions independent of actively transcribing RNA polymerase II.* Mol Cell, 2004. **14**(4): p. 447-56.
207. Farber, L.J., et al., *The tumor suppressor parafibromin is required for posttranscriptional processing of histone mRNA.* Mol Carcinog, 2010. **49**(3): p. 215-23.
208. Sheldon, K.E., D.M. Mauger, and K.M. Arndt, *A Requirement for the Saccharomyces cerevisiae Paf1 complex in snoRNA 3' end formation.* Mol Cell, 2005. **20**(2): p. 225-36.
209. Sobhian, B., et al., *HIV-1 Tat assembles a multifunctional transcription elongation complex and stably associates with the 7SK snRNP.* Mol Cell, 2010. **38**(3): p. 439-51.
210. Fonseca, G.J., et al., *Viral retasking of hBre1/RNF20 to recruit hPaf1 for transcriptional activation.* PLoS Pathog, 2013. **9**(6): p. e1003411.
211. Fonseca, G.J., M.J. Cohen, and J.S. Mymryk, *Adenovirus E1A Recruits the Human Paf1 Complex To Enhance Transcriptional Elongation.* J Virol, 2014. **88**(10): p. 5630-7.
212. Marazzi, I., et al., *Suppression of the antiviral response by an influenza histone mimic.* Nature, 2012. **483**(7390): p. 428-33.

213. Raposo, R.A., et al., *Effects of cellular activation on anti-HIV-1 restriction factor expression profile in primary cells.* J Virol, 2013. **87**(21): p. 11924-9.
214. Blankson, J.N., et al., *Isolation and characterization of replication-competent human immunodeficiency virus type 1 from a subset of elite suppressors.* J Virol, 2007. **81**(5): p. 2508-18.
215. Zaunders, J. and D. van Bockel, *Innate and Adaptive Immunity in Long-Term Non-Progression in HIV Disease.* Front Immunol, 2013. **4**: p. 95.
216. Abdel-Mohsen, M., et al., *Expression profile of host restriction factors in HIV-1 elite controllers.* Retrovirology, 2013. **10**: p. 106.
217. Taylor, R.G., D.C. Walker, and R.R. McInnes, *E. coli host strains significantly affect the quality of small scale plasmid DNA preparations used for sequencing.* Nucleic Acids Res, 1993. **21**(7): p. 1677-8.
218. Clavel, F. and P. Charneau, *Fusion from without directed by human immunodeficiency virus particles.* J Virol, 1994. **68**(2): p. 1179-85.
219. Derdeyn, C.A., et al., *Sensitivity of Human Immunodeficiency Virus Type 1 to the Fusion Inhibitor T-20 Is Modulated by Coreceptor Specificity Defined by the V3 Loop of gp120.* Journal of Virology, 2012. **74**(18): p. 8358-8367.
220. DuBridge, R.B., et al., *Analysis of mutation in human cells by using an Epstein-Barr virus shuttle system.* Mol Cell Biol, 1987. **7**(1): p. 379-87.
221. Chesebro, B., et al., *Use of a new CD4-positive HeLa cell clone for direct quantitation of infectious human immunodeficiency virus from blood cells of AIDS patients.* J Infect Dis, 1991. **163**(1): p. 64-70.
222. Schneider, U., H.U. Schwenk, and G. Bornkamm, *Characterization of EBV-genome negative "null" and "T" cell lines derived from children with acute lymphoblastic leukemia and leukemic transformed non-Hodgkin lymphoma.* International Journal of Cancer, 2012. **19**(5): p. 621-626.
223. Lusso, P., et al., *Growth of macrophage-tropic and primary human immunodeficiency virus type 1 (HIV-1) isolates in a unique CD4+ T-cell clone (PM1): failure to downregulate CD4 and to interfere with cell-line-tropic HIV-1.* J Virol, 1995. **69**(6): p. 3712-20.
224. Genois, N., G.A. Robichaud, and M.J. Tremblay, *Mono Mac 1: a new in vitro model system to study HIV-1 infection in human cells of the mononuclear phagocyte series.* J Leukoc Biol, 2000. **68**(6): p. 854-64.
225. Cory, A.H., et al., *Use of an aqueous soluble tetrazolium/formazan assay for cell growth assays in culture.* Cancer Commun, 1991. **3**(7): p. 207-12.
226. Neumann, T., et al., *T20-insensitive HIV-1 from naive patients exhibits high viral fitness in a novel dual-color competition assay on primary cells.* Virology, 2005. **333**(2): p. 251-62.
227. Horwitz, J.P., et al., *SUBSTRATES FOR CYTOCHEMICAL DEMONSTRATION OF ENZYME ACTIVITY. I. SOME SUBSTITUTED 3-INDOLYL-BETA-D-GLYCOPYRANOSIDES.* J Med Chem, 1964. **7**: p. 574-5.
228. Nakamura, T., et al., *Analysis of the spatiotemporal activation of rho GTPases using Raichu probes.* Methods Enzymol, 2006. **406**: p. 315-32.
229. Roszik, J., J. Szöllosi, and G. Vereb, *AccPbFRET: an ImageJ plugin for semi-automatic, fully corrected analysis of acceptor photobleaching FRET images.* BMC Bioinformatics, 2008. **9**: p. 346.
230. Cocchi, F., et al., *Identification of RANTES, MIP-1 alpha, and MIP-1 beta as the major HIV-suppressive factors produced by CD8+ T cells.* Science, 1995. **270**(5243): p. 1811-5.
231. Yang, N., et al., *Cofilin phosphorylation by LIM-kinase 1 and its role in Rac-mediated actin reorganization.* Nature, 1998. **393**(6687): p. 809-12.

232. Vorster, P.J., et al., *LIM kinase 1 modulates cortical actin and CXCR4 cycling and is activated by HIV-1 to initiate viral infection.* J Biol Chem, 2011. **286**(14): p. 12554-64.
233. Nobes, C.D. and A. Hall, *Rho, rac, and cdc42 GTPases regulate the assembly of multimolecular focal complexes associated with actin stress fibers, lamellipodia, and filopodia.* Cell, 1995. **81**(1): p. 53-62.
234. Koretzky, G.A., et al., *Tyrosine phosphatase CD45 is required for T-cell antigen receptor and CD2-mediated activation of a protein tyrosine kinase and interleukin 2 production.* Proc Natl Acad Sci U S A, 1991. **88**(6): p. 2037-41.
235. Waterman, P.M., et al., *The inositol 5-phosphatase SHIP-1 and adaptors Dok-1 and 2 play central roles in CD4-mediated inhibitory signaling.* Immunol Lett, 2012. **143**(1): p. 122-30.
236. Juszczak, R.J., et al., *Effect of human immunodeficiency virus gp120 glycoprotein on the association of the protein tyrosine kinase p56lck with CD4 in human T lymphocytes.* J Biol Chem, 1991. **266**(17): p. 11176-83.
237. Cefai, D., et al., *Internalization of HIV glycoprotein gp120 is associated with down-modulation of membrane CD4 and p56lck together with impairment of T cell activation.* J Immunol, 1992. **149**(1): p. 285-94.
238. Jabado, N., et al., *Interaction of HIV gp120 and anti-CD4 antibodies with the CD4 molecule on human CD4+ T cells inhibits the binding activity of NF-AT, NF-kappa B and AP-1, three nuclear factors regulating interleukin-2 gene enhancer activity.* Eur J Immunol, 1994. **24**(11): p. 2646-52.
239. Zimmermann, K., et al., *The Orientation of HIV-1 gp120 Binding to the CD4 Receptor Differentially Modulates CD4+ T Cell Activation.* J Immunol, 2014.
240. Hofmann, B., et al., *Human immunodeficiency virus proteins induce the inhibitory cAMP/protein kinase A pathway in normal lymphocytes.* Proc Natl Acad Sci U S A, 1993. **90**(14): p. 6676-80.
241. Harmon, B., N. Campbell, and L. Ratner, *Role of Abl kinase and the Wave2 signaling complex in HIV-1 entry at a post-hemifusion step.* PLoS Pathog, 2010. **6**(6): p. e1000956.
242. Wu, Y. and A. Yoder, *Chemokine coreceptor signaling in HIV-1 infection and pathogenesis.* PLoS Pathog, 2009. **5**(12): p. e1000520.
243. Lodowski, D.T. and K. Palczewski, *Chemokine receptors and other G protein-coupled receptors.* Curr Opin HIV AIDS, 2009. **4**(2): p. 88-95.
244. Takeda, S., et al., *Identification of G protein-coupled receptor genes from the human genome sequence.* FEBS Lett, 2002. **520**(1-3): p. 97-101.
245. Oldham, W.M. and H.E. Hamm, *Heterotrimeric G protein activation by G-protein-coupled receptors.* Nat Rev Mol Cell Biol, 2008. **9**(1): p. 60-71.
246. Cattaneo, F., et al., *Cell-Surface Receptors Transactivation Mediated by G Protein-Coupled Receptors.* Int J Mol Sci, 2014. **15**(11): p. 19700-19728.
247. Wu, L., et al., *Interaction of chemokine receptor CCR5 with its ligands: multiple domains for HIV-1 gp120 binding and a single domain for chemokine binding.* J Exp Med, 1997. **186**(8): p. 1373-81.
248. Bleul, C.C., et al., *The lymphocyte chemoattractant SDF-1 is a ligand for LESTR/fusin and blocks HIV-1 entry.* Nature, 1996. **382**(6594): p. 829-33.
249. McKnight, A., et al., *A broad range of chemokine receptors are used by primary isolates of human immunodeficiency virus type 2 as coreceptors with CD4.* J Virol, 1998. **72**(5): p. 4065-71.
250. Weissman, D., et al., *Macrophage-tropic HIV and SIV envelope proteins induce a signal through the CCR5 chemokine receptor.* Nature, 1997. **389**(6654): p. 981-5.
251. Seror, C., et al., *Extracellular ATP acts on P2Y2 purinergic receptors to facilitate HIV-1 infection.* J Exp Med, 2011. **208**(9): p. 1823-34.

252. Wu, Y., et al., *Cofilin activation in peripheral CD4 T cells of HIV-1 infected patients: a pilot study.* Retrovirology, 2008. **5**: p. 95.
253. Sumi, T., et al., *Cofilin phosphorylation and actin cytoskeletal dynamics regulated by rho- and Cdc42-activated LIM-kinase 2.* J Cell Biol, 1999. **147**(7): p. 1519-32.
254. Zoughlami, Y., et al., *Regulation of CXCR4 conformation by the small GTPase Rac1: implications for HIV infection.* Blood, 2012. **119**(9): p. 2024-32.
255. Pontow, S.E., et al., *Actin cytoskeletal reorganizations and coreceptor-mediated activation of rac during human immunodeficiency virus-induced cell fusion.* J Virol, 2004. **78**(13): p. 7138-47.
256. Harmon, B. and L. Ratner, *Induction of the Galpha(q) signaling cascade by the human immunodeficiency virus envelope is required for virus entry.* J Virol, 2008. **82**(18): p. 9191-205.
257. Rowell, J.F., P.E. Stanhope, and R.F. Siliciano, *Endocytosis of endogenously synthesized HIV-1 envelope protein. Mechanism and role in processing for association with class II MHC.* J Immunol, 1995. **155**(1): p. 473-88.
258. Malinowsky, K., J. Luksza, and M.T. Dittmar, *Susceptibility to virus-cell fusion at the plasma membrane is reduced through expression of HIV gp41 cytoplasmic domains.* Virology, 2008. **376**(1): p. 69-78.
259. Perdiz, D., et al., *The ins and outs of tubulin acetylation: more than just a post-translational modification?* Cell Signal, 2011. **23**(5): p. 763-71.
260. McDonald, D., et al., *Visualization of the intracellular behavior of HIV in living cells.* J Cell Biol, 2002. **159**(3): p. 441-52.
261. Lukic, Z., et al., *HIV-1 uncoating is facilitated by dynein and kinesin 1.* J Virol, 2014. **88**(23): p. 13613-25.
262. Pawlica, P. and L. Berthoux, *Cytoplasmic dynein promotes HIV-1 uncoating.* Viruses, 2014. **6**(11): p. 4195-211.
263. Valenzuela-Fernández, A., et al., *Histone deacetylase 6 regulates human immunodeficiency virus type 1 infection.* Mol Biol Cell, 2005. **16**(11): p. 5445-54.
264. Palazzo, A.F., et al., *mDia mediates Rho-regulated formation and orientation of stable microtubules.* Nat Cell Biol, 2001. **3**(8): p. 723-9.
265. Daub, H., et al., *Rac/Cdc42 and p65PAK regulate the microtubule-destabilizing protein stathmin through phosphorylation at serine 16.* J Biol Chem, 2001. **276**(3): p. 1677-80.
266. Wittmann, T., G.M. Bokoch, and C.M. Waterman-Storer, *Regulation of microtubule destabilizing activity of Op18/stathmin downstream of Rac1.* J Biol Chem, 2004. **279**(7): p. 6196-203.
267. Cherfils, J. and M. Zeghouf, *Regulation of small GTPases by GEFs, GAPs, and GDIs.* Physiol Rev, 2013. **93**(1): p. 269-309.
268. Howes, S.C., et al., *Effects of tubulin acetylation and tubulin acetyltransferase binding on microtubule structure.* Mol Biol Cell, 2014. **25**(2): p. 257-66.
269. Westermann, S. and K. Weber, *Post-translational modifications regulate microtubule function.* Nat Rev Mol Cell Biol, 2003. **4**(12): p. 938-47.
270. Wen, Y., et al., *EB1 and APC bind to mDia to stabilize microtubules downstream of Rho and promote cell migration.* Nat Cell Biol, 2004. **6**(9): p. 820-30.
271. Mistry, S.J. and G.F. Atweh, *Role of stathmin in the regulation of the mitotic spindle: potential applications in cancer therapy.* Mt Sinai J Med, 2002. **69**(5): p. 299-304.
272. Chauhan, B.K., et al., *Balanced Rac1 and RhoA activities regulate cell shape and drive invagination morphogenesis in epithelia.* Proc Natl Acad Sci U S A, 2011. **108**(45): p. 18289-94.
273. Dong, C. and G. Wu, *G-protein-coupled receptor interaction with small GTPases.* Methods Enzymol, 2013. **522**: p. 97-108.

274. Itoh, R.E., et al., *Activation of rac and cdc42 video imaged by fluorescent resonance energy transfer-based single-molecule probes in the membrane of living cells.* Mol Cell Biol, 2002. **22**(18): p. 6582-91.
275. Pertz, O., *Spatio-temporal Rho GTPase signaling - where are we now?* J Cell Sci, 2010. **123**(Pt 11): p. 1841-50.
276. Aoki, K., T. Nakamura, and M. Matsuda, *Spatio-temporal regulation of Rac1 and Cdc42 activity during nerve growth factor-induced neurite outgrowth in PC12 cells.* J Biol Chem, 2004. **279**(1): p. 713-9.
277. Day, R.N. and D.W. Piston, *Spying on the hidden lives of proteins.* Nat Biotechnol, 1999. **17**(5): p. 425-6.
278. Shutes, A., et al., *Specificity and mechanism of action of EHT 1864, a novel small molecule inhibitor of Rac family small GTPases.* J Biol Chem, 2007. **282**(49): p. 35666-78.
279. Gao, Y., et al., *Rational design and characterization of a Rac GTPase-specific small molecule inhibitor.* Proc Natl Acad Sci U S A, 2004. **101**(20): p. 7618-23.
280. Elias, B.C., et al., *Polyamine-dependent activation of Rac1 is stimulated by focal adhesion-mediated Tiam1 activation.* Cell Adh Migr, 2010. **4**(3): p. 419-30.
281. Ellenbroek, S.I., S. Iden, and J.G. Collard, *The Rac activator Tiam1 is required for polarized protrusional outgrowth of primary astrocytes by affecting the organization of the microtubule network.* Small GTPases, 2012. **3**(1): p. 4-14.
282. Janardhan, A., et al., *HIV-1 Nef binds the DOCK2-ELMO1 complex to activate rac and inhibit lymphocyte chemotaxis.* PLoS Biol, 2004. **2**(1): p. E6.
283. Woollard, S.M., et al., *HIV-1 induces cytoskeletal alterations and Rac1 activation during monocyte-blood-brain barrier interactions: modulatory role of CCR5.* Retrovirology, 2014. **11**: p. 20.
284. Hwang, S.S., et al., *Identification of the envelope V3 loop as the primary determinant of cell tropism in HIV-1.* Science, 1991. **253**(5015): p. 71-4.
285. Fernandez, J., et al., *Microtubule-Associated Proteins 1 (MAP1) Promote Human Immunodeficiency Virus Type I (HIV-1) Intracytoplasmic Routing to the Nucleus.* J Biol Chem, 2014.
286. Gallo, D.E. and T.J. Hope, *Knockdown of MAP4 and DNAL1 produces a post-fusion and pre-nuclear translocation impairment in HIV-1 replication.* Virology, 2012. **422**(1): p. 13-21.
287. Sabo, Y., et al., *HIV-1 induces the formation of stable microtubules to enhance early infection.* Cell Host Microbe, 2013. **14**(5): p. 535-46.
288. Kim, D., et al., *MicroRNA-34a modulates cytoskeletal dynamics through regulating RhoA/Rac1 crosstalk in chondroblasts.* Journal of Biological Chemistry, 2012.
289. Destaing, O., et al., *A novel Rho-mDia2-HDAC6 pathway controls podosome patterning through microtubule acetylation in osteoclasts.* J Cell Sci, 2005. **118**(Pt 13): p. 2901-11.
290. Zhang, H., et al., *Functional interaction between the cytoplasmic leucine-zipper domain of HIV-1 gp41 and p115-RhoGEF.* Curr Biol, 1999. **9**(21): p. 1271-4.
291. Schuitemaker, H., et al., *Biological phenotype of human immunodeficiency virus type 1 clones at different stages of infection: progression of disease is associated with a shift from monocytotropic to T-cell-tropic virus population.* J Virol, 1992. **66**(3): p. 1354-60.
292. Hedskog, C., et al., *Longitudinal ultradeep characterization of HIV type 1 R5 and X4 subpopulations in patients followed from primary infection to coreceptor switch.* AIDS Res Hum Retroviruses, 2013. **29**(9): p. 1237-44.

293. Mild, M., et al., *Differences in molecular evolution between switch (R5 to R5X4/X4-tropic) and non-switch (R5-tropic only) HIV-1 populations during infection.* Infect Genet Evol, 2010. **10**(3): p. 356-64.
294. Wennerberg, K., K.L. Rossman, and C.J. Der, *The Ras superfamily at a glance.* Journal of Cell Science, 2005. **118**(5): p. 843-846.
295. Van Aelst, L. and C. D'Souza-Schorey, *Rho GTPases and signaling networks.* Genes Dev, 1997. **11**(18): p. 2295-322.
296. Ridley, A.J. and A. Hall, *Distinct patterns of actin organization regulated by the small GTP-binding proteins Rac and Rho.* Cold Spring Harb Symp Quant Biol, 1992. **57**: p. 661-71.
297. Ridley, A.J., et al., *The small GTP-binding protein rac regulates growth factor-induced membrane ruffling.* Cell, 1992. **70**(3): p. 401-10.
298. Ridley, A.J. and A. Hall, *The small GTP-binding protein rho regulates the assembly of focal adhesions and actin stress fibers in response to growth factors.* Cell, 1992. **70**(3): p. 389-99.
299. Dominguez, R. and K.C. Holmes, *Actin structure and function.* Annu Rev Biophys, 2011. **40**: p. 169-86.
300. Cook, D.R., K.L. Rossman, and C.J. Der, *Rho guanine nucleotide exchange factors: regulators of Rho GTPase activity in development and disease.* Oncogene, 2014. **33**(31): p. 4021-35.
301. Michaelson, D., et al., *Differential localization of Rho GTPases in live cells: regulation by hypervariable regions and RhoGDI binding.* J Cell Biol, 2001. **152**(1): p. 111-26.
302. Clarke, S., *Protein isoprenylation and methylation at carboxyl-terminal cysteine residues.* Annu Rev Biochem, 1992. **61**: p. 355-86.
303. H, L., et al., *Biochemistry*. 2000, W.H.Freeman: New York.
304. Garcia-Mata, R., E. Boulter, and K. Burridge, *The 'invisible hand': regulation of RHO GTPases by RHOGDIs.* Nat Rev Mol Cell Biol, 2011. **12**(8): p. 493-504.
305. Etienne-Manneville, S. and A. Hall, *Rho GTPases in cell biology.* Nature, 2002. **420**(6916): p. 629-35.
306. Moon, S.Y. and Y. Zheng, *Rho GTPase-activating proteins in cell regulation.* Trends Cell Biol, 2003. **13**(1): p. 13-22.
307. Krogh, K.A., E. Lyddon, and S.A. Thayer, *HIV-1 Tat activates a RhoA signaling pathway to reduce NMDA-evoked calcium responses in hippocampal neurons via an actin-dependent mechanism.* J Neurochem, 2014.
308. Cernuda-Morollón, E., et al., *Rac activation by the T-cell receptor inhibits T cell migration.* PLoS One, 2010. **5**(8): p. e12393.
309. Bebenek, K., et al., *Error-prone polymerization by HIV-1 reverse transcriptase. Contribution of template-primer misalignment, miscoding, and termination probability to mutational hot spots.* J Biol Chem, 1993. **268**(14): p. 10324-34.
310. Platt, E.J., et al., *Evidence that ecotropic murine leukemia virus contamination in TZM-bl cells does not affect the outcome of neutralizing antibody assays with human immunodeficiency virus type 1.* J Virol, 2009. **83**(16): p. 8289-92.
311. Pontow, S., et al., *Antiviral activity of a Rac GEF inhibitor characterized with a sensitive HIV/SIV fusion assay.* Virology, 2007. **368**(1): p. 1-6.
312. Nikolic, D.S., et al., *HIV-1 activates Cdc42 and induces membrane extensions in immature dendritic cells to facilitate cell-to-cell virus propagation.* Blood, 2011. **118**(18): p. 4841-52.
313. Haqqani, A.A. and J.C. Tilton, *Entry inhibitors and their use in the treatment of HIV-1 infection.* Antiviral Res, 2013. **98**(2): p. 158-70.

314. Xu, X., et al., *Swap70b is required for convergent and extension cell movement during zebrafish gastrulation linking Wnt11 signalling and RhoA effector function.* Dev Biol, 2014. **386**(1): p. 191-203.
315. Ellerbroek, S.M., et al., *SGEF, a RhoG guanine nucleotide exchange factor that stimulates macropinocytosis.* Mol Biol Cell, 2004. **15**(7): p. 3309-19.
316. Winkler, S., et al., *GrinchGEF--a novel Rho-specific guanine nucleotide exchange factor.* Biochem Biophys Res Commun, 2005. **335**(4): p. 1280-6.
317. Gadea, G. and A. Blangy, *Dock-family exchange factors in cell migration and disease.* Eur J Cell Biol, 2014.
318. Cheng, H.T., et al., *Association of Asef and Cdc42 expression to tubular injury in diseased human kidney.* J Investig Med, 2013. **61**(7): p. 1097-103.
319. Itoh, R.E., et al., *Phosphorylation and activation of the Rac1 and Cdc42 GEF Asef in A431 cells stimulated by EGF.* J Cell Sci, 2008. **121**(Pt 16): p. 2635-42.
320. Grosskreutz, Y., et al., *Identification of a gephyrin-binding motif in the GDP/GTP exchange factor collybistin.* Biol Chem, 2001. **382**(10): p. 1455-62.
321. Pan, D., et al., *P-Rex and Vav Rac-GEFs in platelets control leukocyte recruitment to sites of inflammation.* Blood, 2014.
322. Raynaud, F., et al., *Rho-GTPase-activating protein interacting with Cdc-42-interacting protein 4 homolog 2 (Rich2): a new Ras-related C3 botulinum toxin substrate 1 (Rac1) GTPase-activating protein that controls dendritic spine morphogenesis.* J Biol Chem, 2014. **289**(5): p. 2600-9.
323. Tourette, C., et al., *A large scale Huntingtin protein interaction network implicates Rho GTPase signaling pathways in Huntington disease.* J Biol Chem, 2014. **289**(10): p. 6709-26.
324. Yan, C., et al., *Discovery and characterization of small molecules that target the GTPase Ral.* Nature, 2014. **515**(7527): p. 443-7.
325. Watanabe, M., et al., *DOCK2 and DOCK5 act additively in neutrophils to regulate chemotaxis, superoxide production, and extracellular trap formation.* J Immunol, 2014. **193**(11): p. 5660-7.
326. Nishikimi, A., et al., *Immune regulatory functions of DOCK family proteins in health and disease.* Exp Cell Res, 2013. **319**(15): p. 2343-9.
327. Mullin, B.H., et al., *Influence of ARHGEF3 and RHOA knockdown on ACTA2 and other genes in osteoblasts and osteoclasts.* PLoS One, 2014. **9**(5): p. e98116.
328. Runne, C. and S. Chen, *PLEKHG2 promotes heterotrimeric G protein βγ-stimulated lymphocyte migration via Rac and Cdc42 activation and actin polymerization.* Mol Cell Biol, 2013. **33**(21): p. 4294-307.
329. Menon, S., et al., *Rho GTPase-independent regulation of mitotic progression by the RhoGEF Net1.* Mol Biol Cell, 2013. **24**(17): p. 2655-67.
330. Humphries, A.C., S.K. Donnelly, and M. Way, *Cdc42 and the Rho GEF intersectin-1 collaborate with Nck to promote N-WASP-dependent actin polymerisation.* J Cell Sci, 2014. **127**(Pt 3): p. 673-85.
331. Rodriguez-Fraticelli, A.E., et al., *The Cdc42 GEF Intersectin 2 controls mitotic spindle orientation to form the lumen during epithelial morphogenesis.* J Cell Biol, 2010. **189**(4): p. 725-38.
332. Lessey-Morillon, E.C., et al., *The RhoA guanine nucleotide exchange factor, LARG, mediates ICAM-1-dependent mechanotransduction in endothelial cells to stimulate transendothelial migration.* J Immunol, 2014. **192**(7): p. 3390-8.
333. Kuroiwa, M., et al., *The guanine nucleotide exchange factor Arhgef5 plays crucial roles in Src-induced podosome formation.* J Cell Sci, 2011. **124**(Pt 10): p. 1726-38.
334. Yeung, C.Y., et al., *Arhgap28 is a RhoGAP that inactivates RhoA and downregulates stress fibers.* PLoS One, 2014. **9**(9): p. e107036.

335. Karimzadeh, F., et al., *A stretch of polybasic residues mediates Cdc42 GTPase-activating protein (CdGAP) binding to phosphatidylinositol 3,4,5-trisphosphate and regulates its GAP activity.* J Biol Chem, 2012. **287**(23): p. 19610-21.
336. Chen, P.W., et al., *ARAP2 signals through Arf6 and Rac1 to control focal adhesion morphology.* J Biol Chem, 2013. **288**(8): p. 5849-60.
337. Miyata, M., et al., *Regulation by afadin of cyclical activation and inactivation of Rap1, Rac1, and RhoA small G proteins at leading edges of moving NIH3T3 cells.* J Biol Chem, 2009. **284**(36): p. 24595-609.
338. Arthur, W.T. and K. Burridge, *RhoA inactivation by p190RhoGAP regulates cell spreading and migration by promoting membrane protrusion and polarity.* Mol Biol Cell, 2001. **12**(9): p. 2711-20.
339. Faucherre, A., et al., *Lowe syndrome protein OCRL1 interacts with Rac GTPase in the trans-Golgi network.* Hum Mol Genet, 2003. **12**(19): p. 2449-56.
340. Fotinos, A., et al., *Loss of Oligophrenin1 leads to uncontrolled Rho activation and increased thrombus formation in mice.* J Thromb Haemost, 2014.
341. Yamazaki, D., et al., *srGAP1 regulates lamellipodial dynamics and cell migratory behavior by modulating Rac1 activity.* Mol Biol Cell, 2013. **24**(21): p. 3393-405.
342. Wang, S.J., et al., *CD147 promotes Src-dependent activation of Rac1 signaling through STAT3/DOCK8 during the motility of hepatocellular carcinoma cells.* Oncotarget, 2014.
343. Harada, Y., et al., *DOCK8 is a Cdc42 activator critical for interstitial dendritic cell migration during immune responses.* Blood, 2012. **119**(19): p. 4451-61.
344. Steenblock, C., et al., *The Cdc42 guanine nucleotide exchange factor FGD6 coordinates cell polarity and endosomal membrane recycling in osteoclasts.* J Biol Chem, 2014. **289**(26): p. 18347-59.
345. Gubar, O., et al., *Intersectin: The Crossroad between Vesicle Exocytosis and Endocytosis.* Front Endocrinol (Lausanne), 2013. **4**: p. 109.
346. Sun, X., et al., *Role of clathrin-mediated endocytosis during vesicular stomatitis virus entry into host cells.* Virology, 2005. **338**(1): p. 53-60.
347. Maekawa, M., et al., *Signaling from Rho to the actin cytoskeleton through protein kinases ROCK and LIM-kinase.* Science, 1999. **285**(5429): p. 895-8.
348. Hahn, M.A. and D.J. Marsh, *Identification of a functional bipartite nuclear localization signal in the tumor suppressor parafibromin.* Oncogene, 2005. **24**(41): p. 6241-8.
349. Schmitz, H.D., C. Dutiné, and J. Bereiter-Hahn, *Exportin 1-independent nuclear export of GAPDH.* Cell Biol Int, 2003. **27**(7): p. 511-7.
350. Müller, S. and G. Almouzni, *A network of players in H3 histone variant deposition and maintenance at centromeres.* Biochim Biophys Acta, 2014. **1839**(3): p. 241-50.
351. Moniaux, N., et al., *The human RNA polymerase II-associated factor 1 (hPaf1): a new regulator of cell-cycle progression.* PLoS One, 2009. **4**(9): p. e7077.
352. Kim, N., et al., *IL-1β-specific recruitment of GCN5 histone acetyltransferase induces the release of PAF1 from chromatin for the de-repression of inflammatory response genes.* Nucleic Acids Res, 2013. **41**(8): p. 4495-506.
353. Woodard, G.E., et al., *Parafibromin, product of the hyperparathyroidism-jaw tumor syndrome gene HRPT2, regulates cyclin D1/PRAD1 expression.* Oncogene, 2005. **24**(7): p. 1272-6.
354. Moniaux, N., et al., *The human homologue of the RNA polymerase II-associated factor 1 (hPaf1), localized on the 19q13 amplicon, is associated with tumorigenesis.* Oncogene, 2006. **25**(23): p. 3247-57.

355. Zhang, Y., et al., *The Paf1 complex is required for efficient transcription elongation by RNA polymerase I.* Proc Natl Acad Sci U S A, 2009. **106**(7): p. 2153-8.
356. Zhang, Y., et al., *The RNA polymerase-associated factor 1 complex (Paf1C) directly increases the elongation rate of RNA polymerase I and is required for efficient regulation of rRNA synthesis.* J Biol Chem, 2010. **285**(19): p. 14152-9.
357. Swingler, S., et al., *Apoptotic Killing of HIV-1–Infected Macrophages Is Subverted by the Viral Envelope Glycoprotein.* PLoS Pathog, 2007. **3**(9): p. e134.
358. Fortin, J.F., et al., *Host-derived ICAM-1 glycoproteins incorporated on human immunodeficiency virus type 1 are biologically active and enhance viral infectivity.* J Virol, 1997. **71**(5): p. 3588-96.
359. Amit, I., et al., *Tal, a Tsg101-specific E3 ubiquitin ligase, regulates receptor endocytosis and retrovirus budding.* Genes Dev, 2004. **18**(14): p. 1737-52.
360. d'Azzo, A., A. Bongiovanni, and T. Nastasi, *E3 ubiquitin ligases as regulators of membrane protein trafficking and degradation.* Traffic, 2005. **6**(6): p. 429-41.
361. Chertova, E., et al., *Proteomic and biochemical analysis of purified human immunodeficiency virus type 1 produced from infected monocyte-derived macrophages.* J Virol, 2006. **80**(18): p. 9039-52.
362. Popov, S., et al., *Human immunodeficiency virus type 1 and related primate lentiviruses engage clathrin through Gag-Pol or Gag.* J Virol, 2011. **85**(8): p. 3792-801.
363. Gao, F., et al., *Unselected mutations in the human immunodeficiency virus type 1 genome are mostly nonsynonymous and often deleterious.* J Virol, 2004. **78**(5): p. 2426-33.
364. Guo, W., et al., *Impact of Y181C and/or H221Y mutation patterns of HIV-1 reverse transcriptase on phenotypic resistance to available non-nucleoside and nucleoside inhibitors in China.* BMC Infect Dis, 2014. **14**(1): p. 237.
365. Basson, A.E., et al., *Impact of Drug Resistance-Associated Amino Acid Changes in HIV-1 Subtype C on Susceptibility to Newer Nonnucleoside Reverse Transcriptase Inhibitors.* Antimicrob Agents Chemother, 2015. **59**(2): p. 960-71.
366. Xu, H.T., et al., *Effects of the W153L substitution in HIV reverse transcriptase on viral replication and drug resistance to multiple categories of reverse transcriptase inhibitors.* Antimicrob Agents Chemother, 2014. **58**(8): p. 4515-26.
367. Saison, J., et al., *Fatal cumulative toxicities of HAART in a stable, AIDS-free, HIV-infected patient.* BMJ Case Reports, 2012. **2012**.
368. Bouvin-Pley, M., et al., *Drift of the HIV-1 envelope glycoprotein gp120 toward increased neutralization resistance over the course of the epidemic: a comprehensive study using the most potent and broadly neutralizing monoclonal antibodies.* J Virol, 2014.
369. Chan, E., G.J. Towers, and W. Qasim, *Gene therapy strategies to exploit TRIM derived restriction factors against HIV-1.* Viruses, 2014. **6**(1): p. 243-63.
370. Hook, L.M., et al., *Herpes simplex virus type 1 and 2 glycoprotein C prevents complement-mediated neutralization induced by natural immunoglobulin M antibody.* J Virol, 2006. **80**(8): p. 4038-46.
371. Francica, J.R., et al., *Steric shielding of surface epitopes and impaired immune recognition induced by the ebola virus glycoprotein.* PLoS Pathog, 2010. **6**(9): p. e1001098.
372. Reynard, O., et al., *Ebolavirus glycoprotein GP masks both its own epitopes and the presence of cellular surface proteins.* J Virol, 2009. **83**(18): p. 9596-601.
373. Crotta, S., et al., *Inhibition of natural killer cells through engagement of CD81 by the major hepatitis C virus envelope protein.* J Exp Med, 2002. **195**(1): p. 35-41.

374. Zhao, L.J., et al., *Mitogen-activated protein kinase signalling pathways triggered by the hepatitis C virus envelope protein E2: implications for the prevention of infection.* Cell Prolif, 2007. **40**(4): p. 508-21.
375. Beaufils, P., et al., *The (YXXL/I)2 signalling motif found in the cytoplasmic segments of the bovine leukaemia virus envelope protein and Epstein-Barr virus latent membrane protein 2A can elicit early and late lymphocyte activation events.* EMBO J, 1993. **12**(13): p. 5105-12.
376. Watanabe, T., J. Noritake, and K. Kaibuchi, *Regulation of microtubules in cell migration.* Trends Cell Biol, 2005. **15**(2): p. 76-83.
377. Janke, C. and J.C. Bulinski, *Post-translational regulation of the microtubule cytoskeleton: mechanisms and functions.* Nat Rev Mol Cell Biol, 2011. **12**(12): p. 773-86.
378. Pavin, N. and I.M. Tolić-Nørrelykke, *Dynein, microtubule and cargo: a ménage à trois.* Biochem Soc Trans, 2013. **41**(6): p. 1731-5.
379. Arakawa, Y., J.V. Cordeiro, and M. Way, *F11L-mediated inhibition of RhoA-mDia signaling stimulates microtubule dynamics during vaccinia virus infection.* Cell Host Microbe, 2007. **1**(3): p. 213-26.
380. Klasse, P.J. and J.P. Moore, *Is there enough gp120 in the body fluids of HIV-1-infected individuals to have biologically significant effects?* Virology, 2004. **323**(1): p. 1-8.
381. Melar, M., D.E. Ott, and T.J. Hope, *Physiological levels of virion-associated human immunodeficiency virus type 1 envelope induce coreceptor-dependent calcium flux.* J Virol, 2007. **81**(4): p. 1773-85.
382. Spear, M., J. Guo, and Y. Wu, *Novel anti-HIV therapeutics targeting chemokine receptors and actin regulatory pathways.* Immunol Rev, 2013. **256**(1): p. 300-12.
383. Wier, A.D., et al., *Structural basis for Spt5-mediated recruitment of the Paf1 complex to chromatin.* Proc Natl Acad Sci U S A, 2013. **110**(43): p. 17290-5.
384. Rozenblatt-Rosen, O., et al., *The parafibromin tumor suppressor protein is part of a human Paf1 complex.* Mol Cell Biol, 2005. **25**(2): p. 612-20.
385. Dey, P., et al., *Human RNA polymerase II-association factor 1 (hPaf1/PD2) regulates histone methylation and chromatin remodeling in pancreatic cancer.* PLoS One, 2011. **6**(10): p. e26926.
386. Fonseca, G.J., et al., *Adenovirus evasion of interferon-mediated innate immunity by direct antagonism of a cellular histone posttranslational modification.* Cell Host Microbe, 2012. **11**(6): p. 597-606.